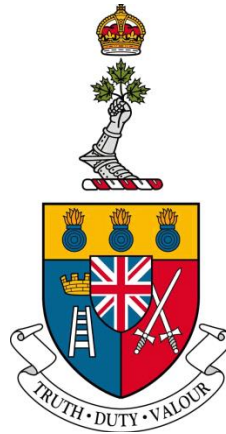


An Ultracapacitive Energy Storage System for a Future Integrated Power System Warship

Un système de stockage d'énergie ultracapacitive pour un système intégré de production
du futur navire de guerre



A Thesis Submitted to the Division of Graduate Studies
of the Royal Military College of Canada
by

Warner A Shillington
Lieutenant-Commander

In Partial Fulfilment of the Requirements for the Degree of
Master's of Applied Science in Electrical Engineering

September, 2016

©This thesis may be used within the Department of National Defence but copyright for open
publication remains the property of the author

ABSTRACT

Land transportation vehicles are currently shifting to hybrid or battery power systems in order to reduce fuel consumption and optimize efficiency. The emerging technology of ultracapacitors is playing a key role in such vehicles by offering energy storage and surge capability. Those same technologies can be applied to the changing naval environment of Integrated Power System (IPS) ships.

Both civilian and military vessels are moving towards IPS constructs where all prime movers turn generators, propulsion is provided through Alternating Current (AC) or Direct Current (DC) machines, and these propulsion motors, as well as auxiliary, ancillary and hotel loads will all feed off one power grid.

Conventional naval ships are designed with backup systems to maintain operational capabilities for short periods when power generation equipment capability is lost. With Electrical Power Generation and Distribution (EPG&D) and propulsion systems delinked, conventional warships can still maneuver in the event of a blackout. In addition, a loss of propulsion has no impact on the EPG&D system and thus other vital safe-at-sea equipment, such as internal and external communications and navigational radars, as well as combat equipment, all remain operational.

In an IPS warship, however, a loss of power generation capability will render all ship systems inoperable including propulsion. In this state, a warship is extremely vulnerable not only to combat threats but also to navigational hazards. This risk can be mitigated by having a backup power system that is able to meet electric demand long enough for operators to restore power generation capability.

Ships' generators often use speed droop to ensure balanced loading between power sources. A ship-wide Ultracapacitive Energy Storage (UCES) System that is responsive to frequency changes can seamlessly integrate with an isolated EPG&D system. In doing so, this UCES would significantly increase blackout redundancy, risk mitigating future IPS warship operations, while decreasing fuel consumption and increasing operational endurance. By using MATLAB's Simulink for system modelling, this thesis provides a proof of concept for integrating a UCES system into future IPS warships.

RÉSUMÉ

Les véhicules de transport terrestres se tournent présentement vers les systèmes hybrides ou à batteries pour réduire la consommation de carburant et augmenter l'efficacité. La technologie émergence des ultracondensateurs joue un rôle clé dans ces véhicules en offrant une capacité de stockage d'énergie et une capacité d'intensification. Ces mêmes technologies peuvent être appliquées au monde changeant des navires au mode de système intégré de production (SIP).

Les vaisseaux civils et militaires se tournent vers les SIP où les moteurs primaires tournent des générateurs, la propulsion est fournie par des machines à courant alternatifs ou continus et ces moteurs à propulsions, en plus des charges auxiliaires (primaires et secondaires) et de la gestion domestiques, vont être approvisionnés d'un seul réseau électrique.

Les navires conventionnels sont conçus avec des systèmes de réserve pour maintenir leur capacité opérationnelle durant les courtes périodes de temps où la capacité de génération de courant est perdue. Parce que les systèmes de génération et distribution de courant et les systèmes de propulsions sont séparés, les navires de guerre conventionnels peuvent manœuvrer lors de pannes de courant. De plus, un mal fonctionnement des systèmes de propulsion n'a pas d'impact sur les systèmes électriques, et l'équipement vital de sécurité comme les systèmes de communication internes et externes, les radars de navigation et l'équipement de combat demeurent opérationnels.

Cependant, dans un navire de guerre SIP, une perte de courant rend tous les systèmes inopérables, incluant les systèmes de propulsion. Dans cet état, un navire de guerre est très vulnérable aux dangers du combat et de la navigation. Ce risque peut être mitigé en ayant un système de réserve capable de rencontrer la demande en électricité jusqu'à ce que les opérateurs puissent réparer le système de génération de puissance électrique.

Les génératrices des navires utilisent souvent un écart permanent de tours pour s'assurer que les charges sont balancées entre les sources de puissance. Un système de stockage d'énergie ultra capacitive répondant aux changements de fréquence peut s'intégrer avec un système isolé de génération et distribution de courant. De ce fait, ce système de stockage augmenterait la redondance lors de pertes de courant, mitigerait les risques envers les opérations des navires SIP, améliorerait les économies de carburant et augmenterait l'endurance opérationnelle. En utilisant MATLAB Simulink pour la modélisation du système, cette thèse fournit une validation du principe d'intégration d'un système de stockage d'énergie ultra capacitive dans un futur navire SIP.

TABLE OF CONTENTS

ABSTRACT	II
RÉSUMÉ	III
TABLE OF CONTENTS	IV
LIST OF TABLES	VII
LIST OF FIGURES	VIII
LIST OF EQUATIONS	IX
LIST OF SYMBOLS, ABBREVIATIONS AND ACRONYMS	X
CHAPTER 1 : INTRODUCTION – THE NEED FOR UCES IN IPS WARSHIPS	1
1.1 : THE BENEFITS OF ELECTRIC PROPULSION	1
1.1.1 : <i>Equipment Savings</i>	2
1.1.2 : <i>Fuel Savings</i>	2
1.1.3 : <i>Smaller Spaces and Increased Survivability</i>	3
1.2 : A CURRENT IPS WARSHIP	3
1.3 : A UCES FOR AN IPS WARSHIP	5
CHAPTER 2 : LITERATURE REVIEW	7
2.1 : WARSHIP BACK-UP SYSTEMS	7
2.1.1 : <i>Small Scale UPS</i>	7
2.1.2 : <i>High Pressure Compressed Air (HP Air)</i>	8
2.1.3 : <i>Low Pressure Compressed Air (LP Air)</i>	8
2.1.4 : <i>Emergency Fuel System</i>	8
2.1.5 : <i>Controllable Reversible Pitch Propellers (CRPP)</i>	9
2.1.6 : <i>Steering</i>	9
2.1.7 : <i>Emergency Lighting</i>	9
2.1.8 : <i>Diesel Driven Fire Pumps</i>	9
2.1.9 : <i>The necessity of system redundancies</i>	9
2.2 : CAUSES OF BLACKOUTS AT SEA	10
2.3 : ENERGY STORAGE IN UTILITY SYSTEMS	11
2.3.1 : <i>Pumped Hydro Electric Storage</i>	12
2.3.2 : <i>Compressed Air Energy Storage</i>	13
2.3.3 : <i>Batteries</i>	13
2.3.4 : <i>Flywheels</i>	14
2.3.5 : <i>Super Magnetic Energy Storage (SMES)</i>	14
2.3.6 : <i>Supercapacitors</i>	14
2.3.7 : <i>An analysis of the leading technologies for future warship ESSs</i>	15
2.4 : OTHER HIGH POWER ULTRACAPACITOR APPLICATIONS	18
2.4.1 : <i>Load Levelling - Hydraulic Mining Shovels</i>	18
2.4.2 : <i>General Load Levelling - Regenerative Braking and Acceleration Assistance</i>	19
2.4.3 : <i>UCES as a replacement for BESS: The Chariot E-bus</i>	21
2.4.4 : <i>Synopsis of Other High Power Applications</i>	22
2.4.5 : <i>Control Schemes in Supercapacitor Applications</i>	22
2.5 : CONCLUSION.....	23
CHAPTER 3 : MODEL ENVIRONMENT - A UCES FIT FOR A SHIP	24

3.1 : POWER EXPECTATIONS FOR UCES INTEGRATION INTO AN IPS WARSHIP	24
3.2 : SIZE LIMITATIONS OF THE UCES	26
3.3 : THE ULTRACAPACITOR MODULE	27
3.3.1 : <i>The Aowei Industries ultracapacitor bus</i>	27
3.3.2 : <i>Theoretical module based on Skeleton Technologies' components</i>	28
3.3.3 : <i>Charge balancing – a manufacturers' problem</i>	30
3.3.4 : <i>Module Construction</i>	31
3.4 : CONCLUSION	32
CHAPTER 4 : MODEL DESCRIPTION.....	33
4.1 : SYSTEM OVERVIEW	33
4.2 : SYSTEM ASSUMPTIONS	34
4.3 : SYNCHRONOUS GENERATOR.....	35
4.4 : GENERATOR SPEED DROOP CONTROLLER	36
4.5 : SHIP'S LOAD	38
4.6 : VOLTAGE TRANSFORMER AND THREE PHASE RECTIFIER.....	39
4.7 : CHARGING CIRCUITRY	39
4.7.1 : <i>Module Load Controller</i>	40
4.7.2 : <i>Charge Limiting Rheostat</i>	42
4.7.3 : <i>Charging Module</i>	44
4.8 : ULTRACAPACITOR MODULE	46
4.8.1 : <i>Simulink's Supercapacitor Object</i>	46
4.8.2 : <i>Ultracapacitor Module Implementation</i>	48
4.9 : DISCHARGE CIRCUITRY	49
4.9.1 : <i>Discharge Controller</i>	50
4.9.2 : <i>Controlled Inverter</i>	52
CHAPTER 5 : METHOD AND RESULTS	56
5.1 : INTRODUCTION.....	56
5.2 : SIMULINK SIMULATION PARAMETERS.....	56
5.3 : SYSTEM SIMULATION METHODS AND RESULTS	58
5.3.1 : <i>Module Charging under a Static Load</i>	58
5.3.2 : <i>Module Discharging to a Static Load</i>	65
5.3.3 : <i>Load Changes during charging operations</i>	68
5.3.4 : <i>Load Changes during Discharging Operations</i>	71
5.3.5 : <i>Generator to UCES handovers</i>	73
CHAPTER 6 : CONCLUSION.....	77
6.1 : FUTURE MODELLING RECOMMENDATIONS	77
6.1.1 : <i>Simulation Software</i>	77
6.1.2 : <i>Polling Distinction</i>	78
6.1.3 : <i>Charge Limiting Rheostat</i>	78
6.1.4 : <i>Improved Buck Chopper performance</i>	78
6.1.5 : <i>Commercial Components</i>	79
6.1.6 : <i>Realism</i>	79
6.1.7 : <i>Paralleling</i>	79
6.2 : IPS WARSHIPS ARE THE FUTURE.....	80
CHAPTER 7 : REFERENCES	81
APPENDIX A : ADDITIONAL CHARGING SYSTEM RESULTS	85
APPENDIX A.1 : CHARGING RESULTS WITH A 1 MW STATIC LOAD	86
APPENDIX A.2 : CHARGING RESULTS WITH A 2 MW STATIC LOAD	88

APPENDIX A.3 : CHARGING RESULTS WITH A 3 MW STATIC LOAD	90
APPENDIX A.4 : CHARGING RESULTS WITH A 4 MW STATIC LOAD	92
APPENDIX A.5 : CHARGING RESULTS WITH A 5 MW STATIC LOAD	94
APPENDIX A.6 : CHARGING RESULTS WITH A 6 MW STATIC LOAD	96
APPENDIX A.7 : CHARGING RESULTS WITH A 7 MW STATIC LOAD	98
APPENDIX A.8 : CHARGING RESULTS WITH AN 8 MW STATIC LOAD	100
APPENDIX A.9 : CHARGING RESULTS WITH A 9 MW STATIC LOAD	102
APPENDIX A.10 : CHARGING RESULTS WITH A 10 MW STATIC LOAD	104
APPENDIX A.11 : CHARGING RESULTS WITH AN 11 MW STATIC LOAD	106
APPENDIX B : ADDITIONAL DISCHARGE SYSTEM RESULTS.....	108
APPENDIX B.1 : DISCHARGE RESULTS POWERING A 1MW STATIC LOAD	108
APPENDIX B.2 : DISCHARGE RESULTS POWERING A 2MW STATIC LOAD	110
APPENDIX B.3 : DISCHARGE RESULTS POWERING A 3MW STATIC LOAD	112
APPENDIX B.4 : DISCHARGE RESULTS POWERING A 4MW STATIC LOAD	114
APPENDIX B.5 : DISCHARGE RESULTS POWERING A 5MW STATIC LOAD	116
APPENDIX B.6 : DISCHARGE RESULTS POWERING A 6MW STATIC LOAD	118
APPENDIX B.7 : DISCHARGE RESULTS POWERING A 7MW STATIC LOAD	120
APPENDIX B.8 : DISCHARGE RESULTS POWERING AN 8MW STATIC LOAD	122
APPENDIX B.9 : DISCHARGE RESULTS POWERING A 9MW STATIC LOAD	124
APPENDIX B.10 : DISCHARGE RESULTS POWERING A 10MW STATIC LOAD	126
APPENDIX B.11 : DISCHARGE RESULTS POWERING AN 11MW STATIC LOAD	128
APPENDIX B.12 : DISCHARGE RESULTS POWERING A 12MW STATIC LOAD	130
APPENDIX B.13 : DISCHARGE RESULTS POWERING A 13MW STATIC LOAD	132
APPENDIX B.14 : DISCHARGE RESULTS POWERING A 14MW STATIC LOAD	134
APPENDIX B.15 : DISCHARGE RESULTS POWERING A 15MW STATIC LOAD	136

LIST OF TABLES

Table 1 - ESS comparison for warship integration based upon a 30MW demand	16
Table 2 - Current Commerical and Experimental Ultracapacitors	17
Table 3 - Aowei Industries High voltage ultracapacitor module	28
Table 4 - Skeleton Technologies SPA2100 Details	29
Table 5 - Theoretical ultracapacitor module used in the simulation	30
Table 6 - Rheostat Resistance Given the Module Load Signal	44
Table 7 - UCES Charging Under Static Load Conditions	61
Table 8 - UCES Discharge Endurance	67

LIST OF FIGURES

Figure 1 - Type 45 Propulsion System	4
Figure 2 - Distributed Generation with ESS	11
Figure 3 - ESS over demand protection and frequency regulation assist [17]	11
Figure 4 - Power Profile of Current ESS Technologies	12
Figure 5 - A Generic Electrochemical Double Layer Ultracapacitor [20]	14
Figure 6 - Hybrid Hydraulic Mining Shovel Power System with UCES [28]	19
Figure 7 - Generalized Traction System for Regenerative Braking [20]	20
Figure 8 - ESS assist with vehicle performance [20].....	21
Figure 9 - Power Speed Curve of a Typical Frigate Sized Vessel	24
Figure 10 - Conceptual IPS Warship	25
Figure 11 - Model environment for the UCES system	26
Figure 12 - Charge Balancing Arrangements: Passive resistance, Controlled resistance, DC/DC converters, and Zener diodes [42]	31
Figure 13 - Top level system model in Simulink.....	33
Figure 14 - Top level view of Generator	35
Figure 15 - Bottom level view of the Generator	36
Figure 16 - Generator Speed Droop Controller	37
Figure 17 - Ship's loads	38
Figure 18 - Top level view of Charging Controller and Power Electronics	40
Figure 19 - Bottom Level View of the Module Load Controller	41
Figure 20 - Bottom Level View of the Charge Limiting Rheostat.....	43
Figure 21 - Mid-level view of the Charging Module	45
Figure 22 - Buck Chopper	45
Figure 23 - Ultracapacitor Measurements	48
Figure 24 - Top level view of Discharge Circuitry	50
Figure 25 - Bottom Level View of Discharge Controller	51
Figure 26 – Mid-Level View of the Controlled Inverter.....	52
Figure 27 - Bottom Level View of Ideal Switch Inverter	53
Figure 28 - UCES Discharge in Discrete Mode.....	57
Figure 29 - UCES Discharge in Continuous Mode.....	57
Figure 30 - Generator Data for UCES Charging at 1 MW Load	59
Figure 31 - Ultracapacitor Charge Data at 1 MW Load.....	60
Figure 32 - Generator Data for UCES Charging at 2 MW Load	62
Figure 33 - Ultracapacitor Charge Data at 2 MW Load Step Time 10 μ s.....	63
Figure 34 - Ultracapacitor Charge Data at 2 MW Load Step Time 10 ms.....	64
Figure 35 - UCES Discharge to a 9 MW Load.....	65
Figure 36 - UCES Discharge Data to a 9 MW Load	66
Figure 37 - Charging Operations with a 3MW to 12 MW increase at 5 seconds	69
Figure 38 - Discharging Operations with a 15 to 1 MW load decrease at 2 seconds	72
Figure 39 - Generator to UCES Handover at 3MW Demand	74
Figure 40 - UCES to Generator Handover at 6MW Demand	75

LIST OF EQUATIONS

Ultracapacitor Capacitance(1)	15
DC Losses(2)	28
Capacitance of a Module (3)	29
ESR of a Module (4)	29
Ideal Sinusoidal Voltage Equation (5).....	36
Generator Speed Droop (6)	37
Three-phase to DC voltage (7)	39
Buck Chopper Voltage Output (8)	45
Charge Equation (9)	46
Simulink Ultracapacitor Voltage (10)	47
Electrostatic capacitance(11).....	47
Ultracapacitor Voltage Output (12).....	47
State of Charge (13)	48
Inverter Voltage Output(14).....	53

LIST OF SYMBOLS, ABBREVIATIONS AND ACRONYMS

AC	Alternating Current
BESS	Battery Energy Storage System(s)
CODLOG	Combined Diesel Electric or Gas (Turbine)
CRPP	Controllable Reversible Pitch Propellers
DC	Direct Current
DDFP	Diesel-Driven Fire Pump
DG	Diesel Generator
EDLC	Electric Double-Layer Capacitor
EPG&D	Electrical Power Generation and Distribution
ESR	Equivalent Series Resistance
EST.	Estimated
ESS	Energy Storage System(s)
HMCS	Her Majesty's Canadian Ship
HP	High Pressure (Air)
IPS	Integrated Power System
LP	Low Pressure (Air)
MDFP	Motor-Driven Fire Pump
MLO	Main Lube Oil
PF	Power Factor
PI	Proportional Integrative
pu	Per Unit
PWM	Pulse-Width Modulation
RAS	Replenishment-at-Sea
RCN	Royal Canadian Navy
rms	Root Mean Square
RN	Royal Navy (United Kingdom)
rpm	Revolutions per Minute
SIP	système intégré de production
SMES	Super Magnetic Energy Storage
SOC	State of Charge
UCES	Ultracapacitor Energy Storage System
UK	United Kingdom
UPS	Uninterruptable Power Supply (or Supplies)
VAC	Volts Alternating Current
VDC	Volts Direct Current
VAR	Volt-Amps Reactive

CHAPTER 1 : INTRODUCTION – THE NEED FOR UCES IN IPS WARSHIPS

Integrated Power System (IPS) Warships offer tremendous advantages over their conventional counter parts. This includes equipment savings, maintenance reduction, fuel savings, and fewer geographical restrictions on equipment placement, the latter having a large impact on hull integrity and survivability.

Despite all these advantages, the future of electric warships is at risk. Blackout risks associated with previous IPS warships are leading some navies to pursue hybrid vessels over purely electric propulsion plants. The Royal Navy's (RN) Type 45 illustrates some of the risk associated with an IPS warship. Subsequently, the United Kingdom (UK) has been developing the hybrid Type 26 Global Combat Ship, which is expected to begin construction in 2016 [1].

Yet, the risk associated with all electric ships can be reduced in the same fashion that the utility grids are mitigating blackout risks from distributed power generation. Energy Storage Systems (ESS) provide an ability to maintain power during power generation gaps. If applied to an IPS warship, a fast responding and sufficiently powerful ESS could span a gap between generator failure and the time it takes to emergency start another generator. This would give an IPS warship the ability to remain fully operational throughout a loss of power generation capability. As such an ESS is critical to the success of future IPS warships.

Due to their high efficiency and long lifecycles, ultracapacitors are well suited to provide the energy storage solution to an IPS warship.

To demonstrate the need for an Ultracapacitor Energy Storage System (UCES) in future IPS warships, this chapter will examine the advantageous offered by electric propulsion; the dangers associated with electric propulsion using the RN's Type 45 as an example; and substantiate the suitability of ultracapacitors as means of providing blackout protection for an electric ship.

1.1 : The Benefits of Electric Propulsion

Warships contain a tremendous amount of equipment to support propulsion operations. This equipment is often considerably more complex than its civilian marine equivalents due to the need for redundancy and survivability in combat environments. With every piece of additional equipment come additional procurement, spares, and maintenance costs. Future IPS warships can be extremely beneficial by reducing equipment, creating fuel savings, and increasing survivability by removing geographical restrictions on equipment placement.

1.1.1 : Equipment Savings

Conventional warships have distinct Electrical Power Generation and Distribution (EPG&D) and propulsion systems. These two systems can often operate independently of one another - the propulsion side remains functional during a blackout through multiple redundancies that are discussed in section 2.1.

However the isolated mechanical propulsion plant requires a plethora of equipment that is superfluous in an IPS warship. The equipment savings that can be realized by moving to electrically propelled warship includes, but is not limited to,

- a) Propulsion Engines – Separate prime movers for EPG&D and propulsion can be combined into engine generator sets that can provide electrical power for both propulsion and all other loads.
- b) Transmission – Massive marine gearboxes are required to convert the high speed low torque power produced by the engines and convert it to high torque low speed rotational power for use by the ship's propellers. In an IPS warship, this can be replaced by electrical cable run to a speed controlled electric machine.
- c) Main Lube Oil (MLO) – A large system on its own, it is designed to lubricate the aforementioned transmission components. This system is not required in an IPS setting.
- d) Controllable Reversible Pitch Propeller (CRPP) – This complex hydraulic system is designed to allow for better engine loading and permit astern movements while maintain the same direction of shaft rotation. This system is not needed in an IPS construct where electric machines drive the propellers.
- e) Shaftlines – These large mechanical power transmitters often penetrate through multiple bulkheads to deliver power from the transmission system to the propellers themselves. They are not required in an IPS environment as the electric motors can easily be co-located next to the propellers they drive.
- f) Steering – Not directly eliminated by electric propulsion, the rudder style steering system can be easily replaced if an azimuthing pod or Z-drive arrangement is incorporated into the IPS warship design.

In addition, the removal of all this unnecessary equipment also provides savings in future maintenance and labour costs. Although an IPS warship would require large electric machines to drive the propellers, something not required in conventional warships, the long term cost saving in equipment and maintenance should be significant. But that is not the only benefit.

1.1.2 : Fuel Savings

IPS warships also impart considerable fuel savings by reducing the number of running engines required in conventional or even hybrid ships and by allowing the generator coupled engines to operate continuously at their optimum speeds.

Conventional warships often run multiple generator sets and propulsion engines in order to provide blackout protection and propulsion redundancy. This is often performed even when one engine or generator set could satisfy the demand. For example, if the ship is in a potential dangerous scenario: special sea duty or action stations.

As engines all consume power to run their ancillary equipment and overcome losses, even when no power output is achieved, the reduction in the number of running engines will almost always impart fuel savings. So naturally by combining prime movers, an IPS ship can provide an instant fuel savings by running only one or two engines, as opposed to the two to four required in conventional ships.

But with a large ESS, an IPS warship can do even better. If an ESS can provide adequate power to the ship long enough for the crew to emergency start a running engine, then there would never be a need to run redundant engines simply to mitigate risk. Since warships spend many hours running redundant engines when coming in or out of harbour, navigating close to land, performing Replenishment At Sea (RAS) or any other hazard operation, the fuel savings potential offered by an IPS warship through the elimination of this redundant engine operation is immense.

1.1.3: Smaller Spaces and Increased Survivability

Finally, the removal of all the equipment listed in section 1.1.1 has a tertiary benefit. On a conventional or hybrid warship, the engines must be co-located and aligned with the transmission, which in turn must be co-located and aligned with the shaftline, which in turn must be affixed to the propellers.

This co-location of equipment demands large open engine rooms and numerous bulkhead penetrations to allow the long shaftlines to penetrate to the propellers. But an IPS warship doesn't need any of that. The generator sets can be isolated from each other, and simply need to be connected electrically to a switchboard and electric machines. This provides geographical freedom to place equipment in an ideal layout to maximize ship stability while increasing flood and fire protection.

So if IPS warships provide all these benefits, then why are they at risk?

1.2 : A Current IPS Warship

Although IPS warships have been proposed since 1995 [2], the Royal Canadian Navy (RCN) currently has no major surface combat ship designed with electric propulsion. However, the Royal Navy (RN) does.

The RN's Type 45 was one of a few emerging platforms touted as the future of electric warships. As seen in the basic layout in Figure 1, the destroyer features two 25MW Rolls Royce, Northrup Grumman WR21 advanced cycle Gas Turbines for main power and two Wartsila Diesel Generators (DG) for standby or harbour use [2].

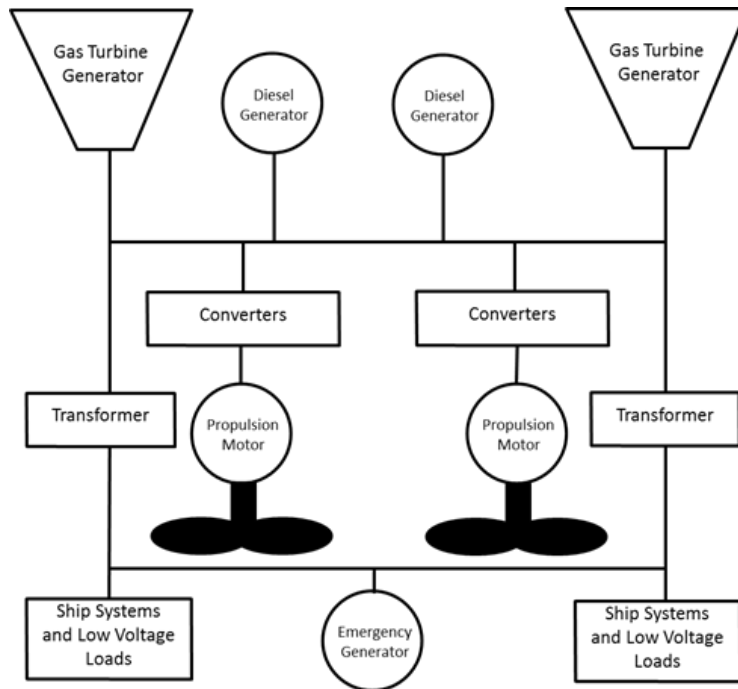


Figure 1 - Type 45 Propulsion System

Yet, there is a lack of bulk power storage integrated into the system. The net effect is that the ship is unable to maintain propulsion in the event of a blackout, forcing sailors to manage the precarious scenario colloquially described as a “combat drift” until generation can be restored. As the RN moves forward, their next generation of ship (the Type 26 frigate) is intended to have a hybrid Combined Diesel Electric or Gas (CODLOG) propulsion system where power generation is provided by diesel generators. At low speeds the power generation system will drive electric machines, but high power propulsion demands will be satisfied by gas turbines providing mechanical energy to the propellers [3].

The Type 26 hybrid is a move away from the concepts of IPS where a few generators can supply all the ships power requirements (including propulsion). However, an IPS vessel has fewer systems, which reduces procurement, maintenance, and fuel costs, while increasing flexibility [4].

So why, then, is the RN shifting away from the IPS design seen in the Type 45? One argument is that due to the lack of propulsion redundancy, the UK has been forced to operate the type 45 in a conservative manner, i.e., away from confined waters and navigational hazards for fear of a blackout and loss of ship control at an inopportune moment.

Warships cannot be choosy about their operational scenarios. But mitigating risk is a tenet of every good Captain and Engineering Officer. And, an ESS incorporated into an IPS ship would certainly help to mitigate that risk.

1.3 : A UCES for an IPS Warship

As seen above, IPS offers distinct advantages for ships but must be risk mitigated with an ESS to ensure future success. However, prior to selecting an energy storage medium, the risk and the role of that ESS should be better defined.

One of the real risks to IPS warships is a loss of power generation equipment. Although ships possess multiple engines, they cannot always and should not always be run just to mitigate blackout risks. Assuming another generator set would be available, but not running when a ship blacks out, then an ESS only needs to be capable of maintaining IPS ship operations long enough for crews to emergency start and bring online a redundant generator.

The literature review in chapter 2 provides a comprehensive analysis of the different storage mediums – the details of which will not be repeated in this introduction. However, the summary is that Battery Energy Storage Systems (BESS) or UCES are the most suited to warship integration.

Due to the short duration requirement, UCES provides numerous advantages over batteries in this application. This is because they can be efficiently charged, but more importantly, discharged quickly and efficiently, allowing them to output high power over short periods; and, they offer improved lifecycle behaviour over batteries while their solid state construction reduces risk in a moving and damage prone environment.

In addition, as the technology matures, ultracapacitors are expected to be capable of delivering this amount of power over increasingly longer durations. Nevertheless, ultracapacitors are currently capable of providing an IPS warship with a few minutes of power, which is long enough for crews to emergency start another generator or disengage from a dangerous scenario.

This introduction has delineated the problem. IPS warships offer numerous advantages through the equipment reduction, fuel savings, and the potential for increased survivability through better equipment layout. However, they do introduce a significant new risk. A blackout on an IPS warship would be detrimental as it would render all ship systems inoperable. To mitigate this risk and ensure IPS warship success, these future ships will need a large ESS capable of bridging the gap between the loss and return of power generation capability.

As a developing technology, ultracapacitors are well suited to fit this short duration role in a harsh marine and combat environment. As such, future IPS warships need an ESS capable of providing ship-wide backup power in order to succeed.

The chapters to follow provide the necessary background information for, the description of, and the results of the shipboard UCES proof of concept that was modelled and simulated in MATLAB's Simulink.

Chapter 2 provides a literature review that outlines some of the technical investment in current shipboard backup systems, an analysis of the causes of shipboard blackouts, an analysis of ESS used in utility systems, and a review of other high power applications for ultracapacitors.

Since the future IPS warships in which this thesis's UCES model will reside in are not currently defined, Chapter 3 outlines the generic shipboard environment for which the proof of concept was intended to operate within. Chapter 4 provides the technical description of UCES model, while chapter 5 provides outlines the testing methods and results of the simulation. Finally, Chapter 6 provides a conclusion that focuses of future recommendations to improvement subsequent shipboard UCES models.

Together, these chapters generate the argument for the real implementation of backup ultracapacitive power system in future IPS warships.

CHAPTER 2 : LITERATURE REVIEW

The following chapter provides pertinent background information on warships and ultracapacitors. The first section outlines the current investment in backup systems in conventional ships, while the second section describes ways in which a vessel may succumb to a loss of electrical power generation capability. Both of these sections in turn justify the investment in large scale energy storage for future vessels.

The third section compares storage mediums and concludes that UCES will be the best option to provide this energy redundancy to a future vessel. Finally, the fourth section analyzes other applications where ultracapacitors have been used for energy storage.

2.1 : Warship Back-up Systems

Any energy storage system capable of delivering power in the megawatt range comes at a significant price; however, the technical complexity and cost currently being invested in warships backups system demonstrates the necessity of a ship-wide Uninterruptable Power Supply (UPS). This section will provide background information on current conventional warship redundancies; discuss the causes and frequency of blackouts at sea; demonstrate current ESS practices on IPS ships; and, conclude with a discussion on utility system level ESSs and their suitability for naval integration.

In a conventional warship, energy storage methods vary greatly from system to system and even ship to ship. A Halifax Class frigate for example, uses no less than eight unique systems to maintain essential propulsion and damage control systems during a blackout. This section will briefly discuss these systems and their advantages and disadvantages.

2.1.1: Small Scale UPS

Ship-wide control and monitoring systems maintain functionality during a blackout via battery backed up UPS. The systems work well but are limited in capacity to 1 or 2 KW or KVA rating. They provide both power conditioning (120 Volts Alternating Current (VAC) and/or 28 Volts Direct Current (VDC) output) and backup power via lead acid gel cell batteries connected in a 72VDC configuration [5].

The lead acid battery offers the lowest cost solution to battery storage, while the gel cell provides a spill and hydrogen off gas resistant environment. The gel cell does not provide the same ease of the wet cell in predicting premature failure, whereas the former's condition can be predicted by its specific gravity [6].

2.1.2: High Pressure Compressed Air (HP Air)

In the event of a blackout, the main engines of Halifax class ship are unaffected. However the main gearing still requires lubrication. The MLO pumps, normally electrically driven, are driven by an air turbine supplied by stored air within the High Pressure (HP) air system at 207 bar. This backup system works well and can react quickly to loss of electrical power by opening a single valve to allow air to flow to the turbine, which then drives the same shaft that the electric motor would normally turn via an overrunning clutch [7].

The HP air backup system advantages are quick response time (relative to the requirement), ease of monitoring system charge/readiness status via pressure sensors, and complete independence from the EPG&D system. The disadvantages are the explosion risk of high pressure air vessels during a fire; dieseling risk if oil entrainment occurs; risk to personnel if the system is damaged; high noise during operation; tight tolerances and high maintenance; and, dependence on the UPS backed up control and Low Pressure (LP) air systems to send a signal to initiate the air turbine start sequence and provide the motive force to actuate the pneumatically operated valve. In addition, the system may ice up due to the natural temperature drop of a gas during expansion. If used for long periods without external heating, components exposed to the pressure drop may freeze.

2.1.3: Low Pressure Compressed Air (LP Air)

The LP air system provides motive force to actuate pneumatically-operated valves throughout the ship. Although the LP air compressors trip during a blackout, the large air receivers contain enough residual air to allow operators to control ship operations for a few minutes – this time varies greatly upon valve usage [8]. There is also an HP to LP Air cross connect to increase the LP air reserve.

While 7 bar LP air is considerably safer to personnel than 207 bar HP air and does not have the same risk of icing as HP air, it poses little potential to do work and therefore has low power density.

2.1.4: Emergency Fuel System

While fuel pumps are in operation, a portion of the flow is diverted to an emergency fuel tank, which is located a few decks above the fuel main. This header tank is essentially a potential energy reserve of fuel. During a blackout, the emergency fuel tank maintains pressure on the fuel main, ensuring a constant supply of fuel is available to the main engines and generators until power is restored or the tank is depleted [9].

The greatest asset of this potential energy storage system is its seamless operation. Although operators must ensure some valve reconfiguration takes place, this is only done to maximize endurance. The pressure on the fuel main never drops during a blackout, as it is always under a head pressure provided by the emergency fuel tank. The disadvantage is that, like Pumped Hydraulic Electric Storage (PHES), the energy density is extremely low. Regardless, the system only needs to provide approximately 1 bar pressure to the engines, which have their own engine-driven fuel pumps.

2.1.5: Controllable Reversible Pitch Propellers (CRPP)

Although technically not a storage system, an entirely separate subsystem exists within the CRPP system to provide hydraulic pressure when the normal motor drive pumps fail during a blackout. This separate pump system is driven by belts off the main shaft lines. The system clutches in automatically in the event of pressure drop [10].

As it is not a true ESS, the advantages and disadvantages will not be discussed; however, it does reflect a means of recovering kinetic energy and is yet another redundant system built into the Halifax class.

2.1.6: Steering

When enabled, the steering system runs a separate pump set to “charge” hydraulic receivers. These receivers contain a gas bladder that compresses under hydraulic pressure. This distinct subsystem is hydraulically isolated from the remainder of the steering system and maintains its potential energy charge until required. In the event of the blackout, the subsystem can be activated to center the rudder to a neutral position.

Although the system is effective, it adds considerable technical complexity and maintenance for a “one-time use” feature.

2.1.7: Emergency Lighting

Numerous lights throughout the ship are fitted with backup battery packs. These packs of “D” cell batteries maintain lighting without interruption during a blackout, but require five year life cycling [5].

2.1.8: Diesel Driven Fire Pumps

While the firemain is normally supplied via Motor-Driven Fire Pumps (MDFPs), separate Diesel-Driven Fire Pumps (DDFPs) exist to maintain damage control capability during a blackout. The diesel to the DDFPs is provided by co-located day tanks, which are normally isolated from the remainder of the fuel system. These days tank can be thought of as stored chemical energy [11].

These fire pumps are extremely effective and can operate for many hours in the dead ship condition, allowing the crew to focus on saving the ship when all other capability has been lost.

2.1.9: The necessity of system redundancies

Although every vessel is slightly different, this section used a Halifax class frigate as an example to describe how complex, evolved, and different these backup systems are on a warship; however, this level of technical complexity is often a burden, not an asset. Different systems require more unique skill sets for maintainers to be familiar with, more unique spares to be carried onboard to rectify equipment failures and support maintenance, and simply more ways in which system failure can occur.

Despite the complexities, these redundancies are essential in maintaining warship capability during a blackout. The high costs associated with these systems can be easily offset against a single incident that could significantly damage or sink a ship. And, in a moving corrosion prone environment, an experienced sailor should expect and accept that generators will fail for a number of reasons.

2.2 : Causes of Blackouts at Sea

A loss of power generation capability is a common occurrence in a naval environment and without sufficient energy storage solutions this will lead to blackout. While a number of different articles such as [12] and [13] propose theories and algorithms to maximize engine effectiveness, combustion engine efficiency is always maximized at or near full load. As such, the number of running generators should be reduced, which increases the load on the remaining generator(s), to minimize maintenance and fuel costs. However, the chance of blacking out is increased if generators are heavily loaded. Hence, there are competing requirements between operational redundancy and cost.

If conducting single or heavily loaded generation operation a ship-wide blackout can occur from the failure of a single generator, which can easily be triggered by, but not limited to,

- a) Fuel problems;
- b) Air intake restrictions;
- c) Excessive water intake from sea state or adverse weather conditions;
- d) Sensor malfunction leading to engine trip;
- e) Operator error;
- f) Maintainer error;
- g) Catastrophic engine failure;
- h) Minor engine failure leading to a trip condition being met;
- i) Loss of vital auxiliary services such as sea water cooling;
- j) Fire;
- k) Certain switchboard faults, such as the generator isolation breaker tripping open;
- l) Electrical transmission line failure;
- m) Flood; and,
- n) Battle damage.

As the fishing vessel *American Dynasty* demonstrated when she slammed into the alongside Her Majesty's Canadian Ship (HMCS) WINNIPEG, a blackout at an inopportune moment can be catastrophic [14].

The point to note is that blackouts occur at sea on a routine basis. A vessel that is not prepared for a loss of power generation capability poses a considerable risk to both itself and other ships. So what is being done to mitigate blackout risks on current IPS warships?

2.3 : Energy Storage in Utility Systems

Like ships, the utility level power grid is also undergoing significant change. Since vessels also have high power demands, some of the technologies and lessons learned from the smart grid could be applied to IPS warships. One key fact is that “approximately 20% of generation capacity exists to meet peak demand 5% of the time [15].” On warships, this is even worse, where significant extra power generation capacity is not only available but often kept running in case of a single generator failure. In the smart grid, bulk ESS are being proposed and implemented, in order to reduce capacity losses, regulate the power from variable sources or changing loads, and reduce the probability of blackout.

In Figure 2, variable power generation sources provide power to local loads and the main grid. If generation is plentiful, an ESS system absorbs excess power [16].

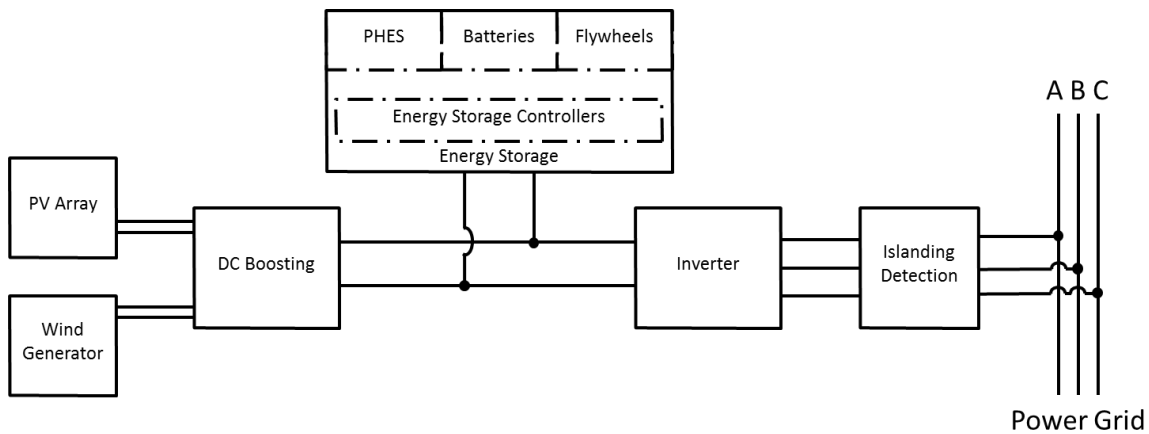


Figure 2 - Distributed Generation with ESS

Not only does this provide added protection against blackout, but as shown in Figure 3 this power can then be released over periods where generation capacity cannot meet demand [17].

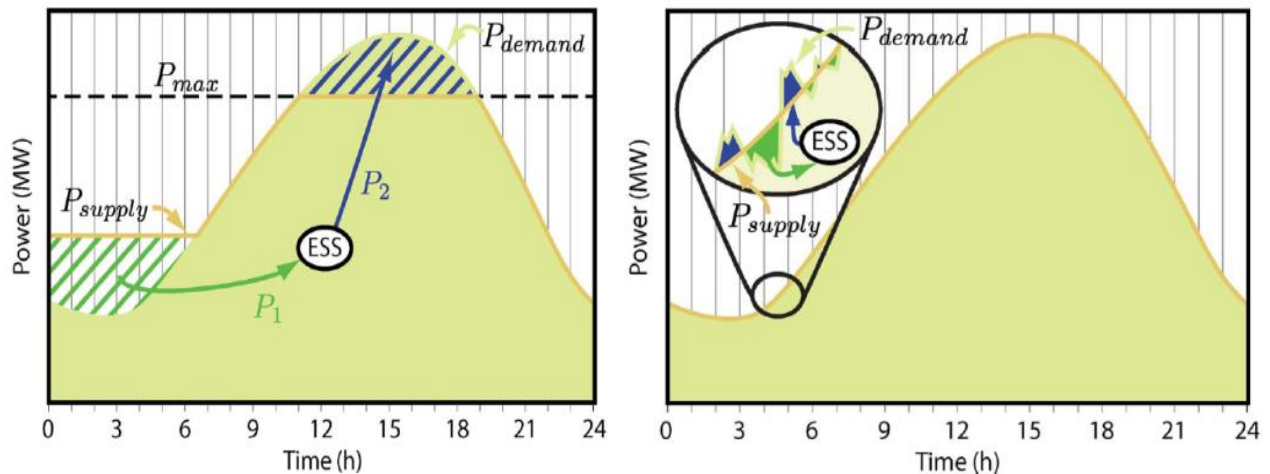


Figure 3 - ESS over demand protection and frequency regulation assist [17]

The application of Figure 3 to naval operation is significant. With an ESS able to provide supplement power, a future IPS warship could significantly reduce the risk of overloading a running generator. Not only would this ESS provide blackout protection, but also a short sprint capability could be achieved without the need for running an additional generator. If the ESS is capable of responding quickly it can be used to accommodate small and short fluctuations in demand. Again, this would provide another level of blackout protection allowing generators to be run near full load without risk of overload. This rapid response ESS would also help to regulate EPG&D system frequency, alleviating that requirement from the power generation equipment. A breakdown of current ESS technology is shown in Figure 4.

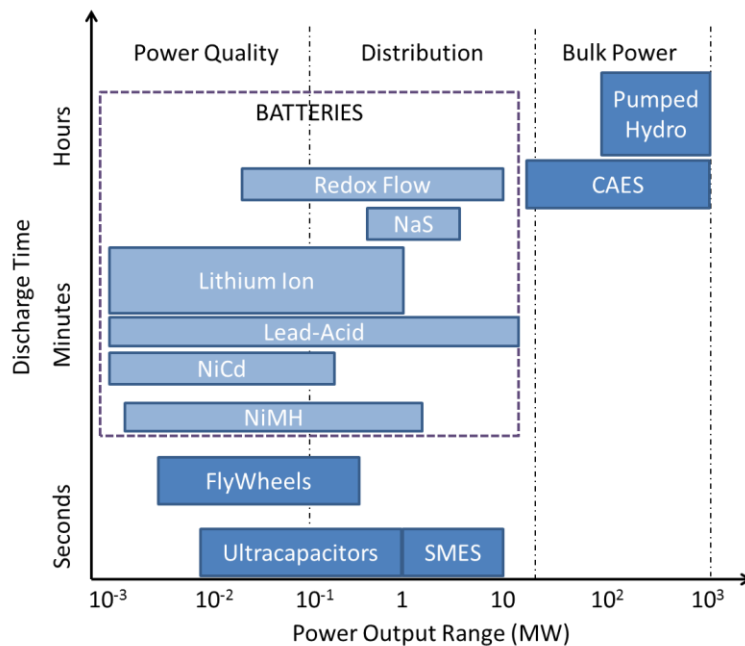


Figure 4 - Power Profile of Current ESS Technologies

To realize which, if any, of these smart grid ESSs are suitable for warships, they are briefly analyzed below.

2.3.1: Pumped Hydro Electric Storage

Pumped Hydro Electric Storage is currently the most plentiful bulk ESS in the utility system used on land. Due to its large size and low power density, it is not a viable option for high power demands within a ship.

2.3.2: Compressed Air Energy Storage

Compressed Air Energy Storage is a promising technology which offers considerably higher power density over PHES. Traditional systems are considered diabatic as waste heat of compression is absorbed and discarded via heat exchangers. Adiabatic systems remove and store the heat from compression stages, which is later applied to reheat the air between expansion stages during power generation [18]. This negates the need for an external heat source at expansion, but does significantly increase technical complexity and requires a large capacity latent heat storage medium.

The safety risks associated with HP air and the space required for storage do not make it a viable option for high power demands in a confined space, such as a warship.

2.3.3: Batteries

Chemical cells in various forms have long been used throughout warships for energy storage. In an IPS environment, they could provide electrical energy directly to the distribution system. They can also be geographically dispersed which increases ESS survivability during a damage control incident. Some considerations for battery selection are power density and energy density, cost, chemical hazards within the ship, reliability, life cycle and maintenance requirements, off gassing, and charge/discharge periods.

While Sodium-Sulfur (NaS) batteries offer high power output and high energy capacity these devices suffer from significant safety concerns. Metallic sodium, for instance, ignites with water making it an extreme hazard in a marine environment [16].

While batteries vary greatly in their capacity and power output, they are all generally marred by a relatively low number of lifecycles when compared to other ESS technology. Reduction-oxidation (Redox), otherwise known as Flow Batteries, are a promising technology that exhibit better lifecycle behaviour but require pumping systems to maintain flow of the externally stored electrolytes through the electrodes. Their efficiencies range from 50-80%, making them less than ideal for larger storage applications [17]. While the energy densities of Redox batteries vary greatly they are generally less than lithium ion.

Although lead acid has been used for many years in submarines these cells suffers from hydrogen off gassing, the most promising battery technology for marine integration remains lithium ion due to its high energy capacity.

2.3.4: Flywheels

These kinetic energy devices have been used for frequency regulation in gyro buses since the 1950s. Their charge and discharge rates are limited by the motor/generator coupled to the device. They suffer from high self-discharge due to frictional losses, and have many components which limit the maximum operational speed (energy storage capacity): bearings, electrical machine limits, and centripetal force limits of fly wheel material. While composite materials and vacuum containment systems may reduce these limitations and losses, currently-constructed fly wheels have an upper energy storage capacity around 25 kWh [16], which is well below the needs of a warship.

2.3.5: Super Magnetic Energy Storage (SMES)

Super Magnetic Energy Storage (SMES) systems are Direct Current (DC) devices, comprising of superconductive material coiled into a solenoid or toroid configuration, which can store massive amounts of power for discharge over small time periods. They have quick response time and can improve power quality in the correct power electronic structure. The significant drawback is cost and technical complexity. These costs are due mainly to the refrigeration system required to keep a superconductive material at superconductive temperatures (approximately 200°K for high temperature superconductors), as well as the price of the power electronics to support the device [19].

For navy ships, where a refrigeration system could easily be brought offline due to combat, SMES may not yet be a prudent solution to an emergency use ESS. In addition, the high costs of the system are somewhat prohibitive.

2.3.6: Ultracapacitors

Ultracapacitors are in many ways similar to traditional capacitors. However they sport much higher capacitances and can hold significantly more energy. As seen in Figure 5, they feature a positive and negative electrode that functions like a traditional electrostatic capacitor.

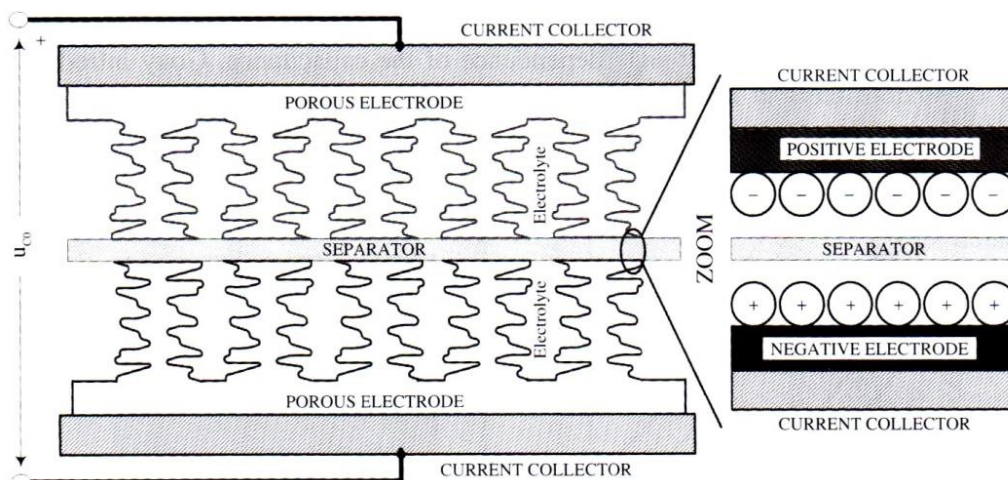


Figure 5 - A Generic Electrochemical Double Layer Ultracapacitor [20]

Additionally, this electrostatic layer is covered by a porous material usually consisting of a carbon formation: activated carbon, graphene, or carbon nanotubes. This diffused layer is immersed in an electrolyte and includes a separator. When charged, a portion of the total capacitance comes from the electrostatic effect; however, a significant portion of the capacitance also comes from the diffused layer, where charge is stored in the porous electrode. An ultracapacitor's capacitance can be described by the voltage dependent equation:

$$C(v) = C_0 + k_c V \quad (1)$$

where $C(v)$ is the ultracapacitor's capacitance;
 C_0 is electrostatic capacitance;
 k_c is the diffused layer coefficient; and,
 V is internal voltage [20].

Unlike a traditional capacitor though, the electrolyte experiences breakdown at higher voltages. As such, an individual cell is normally limited to a voltage of no more than 2-3V. In order to produce useful voltages, the cells have to be combined in series. The voltage across the series must also be well regulated to ensure an individual cell does not experience an overvoltage condition.

Ultracapacitors should also be charged under steady DC conditions, as increasing frequency diminishes their total capacitance. In addition, their energy density is currently only about a fraction of lithium-ion batteries; however, the technology is trending towards significantly increased energy storage capacity in the near future.

Despite these drawbacks, ultracapacitors have significant advantages for warship integration. Due to their high power density, ultracapacitors are a good fit for short interval, high demand applications. Their solid state construction, long life cycle, and graceful degradation make them ideal for a moving, damage-prone environment of a warship. In addition, their ideal thermal operating conditions are well aligned with sea surface temperatures.

2.3.7: An analysis of the leading technologies for future warship ESSs

As shown in section 2.1, there is currently a myriad of different backup ESSs invested into major warships. These systems create added demand on operators and maintainers, supply systems, and management. Although navies are moving towards IPS warships, these ships have not been built with ESSs capable of maintaining propulsion power during a blackout, which is a common occurrence at sea.

While the utility system is currently implementing alternative ESS, some are not feasible for ship integration either due to size, safety, or system survivability concerns in marine or combat environments. Table 1 outlines a comparison of the current ESS technology and comments on their suitability for IPS warship integration.

Table 1 - ESS comparison for warship integration based upon a 30MW demand

ESS Type	Warship Integration Risks	Est. Life [cycles]	Energy Density [Wh/kg]	Power Density [W/kg]	Storage Mass for 30 MW [T] of Power	Storage Mass for 30MW-min [T] of Energy	Reference
Pumped Hydro Electric Storage	Ship stability	N/A	Height dependent		Impractical for warship integration		
Super Magnetic Energy Storage	Electric discharge, complex refrigeration system	Near infinite	1-10 Est.	4000-40000 Est.	Impractical for warship integration with current Technology		[19]
Compressed Air Energy Storage	Fire, explosion	N/A	2-5*	*	*	100-250*	[18]
Flywheels	High inertial moment	10 ⁶	Maximum capacity estimated at 25 kWh or 1.5 MW-min				[16]
Batteries: Lead-acid	Chemical, electric discharge, explosion	200-2000	20-35	25	1200	14-25	[20]
Batteries: lithium-ion	Chemical, electric discharge	500-2000	100-200	360	83.33	2.5-5	[20]
Ultracapacitors: Model SCHE3500	Electric discharge	10 ⁶	10.1	26000	1.15	49.5	[21]

* - varies with operating pressure

The columns in Table 1 provide a comparison of the different ESS types by examining their risks to warship integration; the estimated service life in lifecycles; their energy density and power density; the mass in tons required to provide 30MW of power based upon the power density; the mass in tons required to provide a 30MW-min based upon the energy density; and, the references from which this data was gathered.

The 30MW and 30MW-min columns were based upon the assumption that a frigate or destroyer at full power would consume 30MW. Thus they provide a prediction of the mass required to deliver 30MW and to provide that full power to the ship for a minute during a blackout.

The comparison removes PHES and SMES technology immediately due to their unsuitability for a marine application. The storage of energy through movement of water would create extreme instability. A PHES would easily capsize a ship well before it produced any amount of suitable energy storage. SEMS cryogenic requirement demand a level of technological refinement that is too difficult to maintain in marine and combat environments.

CAESS provides a wide range of energy and power densities based upon the operating pressure. This increased pressure provides increased capacity but also increases risk. Under high pressure conditions, a ship would still need 100 tons of compressed air storage to provide a 30MW-min.

Flywheels, on the other hand, have many mechanical or materials consideration that limit their energy storage capacity to around 25kWh or 1.5 MW-min. This is insufficient for a ship-wide backup system.

The comparison changes once lead-acid and lithium ion batteries are analyzed. A short duration ESS based upon lithium-ion batteries would be limited by the amount of power it could deliver, not by the amount of energy it could store. Although 2.5 tons of high capacity lithium ion batteries could store 30MW-min of energy, a system would need 83 tons of batteries to achieve an output of 30MW. Commercially available ultracapacitors, on the other hand, could easily deliver adequate power. The design constraint with an Ultracapacitor Energy Storage (UCES) system would be the amount of energy it could store, rather than the power it could deliver.

The risk and lifecycle columns of Table 1 reveal that ultracapacitors offers significant advantages over BESS both in reduced risk and significantly longer service life. In addition, a UCES also has the potential for significantly increased capacity as ultracapacitor technology matures. Table 2 compares a current commercially available unit with results from experimental ultracapacitors.

Table 2 - Current Commercial and Experimental Ultracapacitors

Production Method	Ultracapacitor Model	Energy Density [Wh/kg]	Power Density [W/kg]	Storage Mass for a 30MW-min [T]	Reference
Commercial	SCHE3500	10.1	26,000	49.5	[21]
Experimental	Graphene EDLC	30.51	15,340	17	[22]
Experimental	Carbon Nanotube EDLC	35	N/A	14	[23]
Experimental	Carbon Nanotube with Ruthenium Oxide	74	N/A	6.8	[24]
Experimental	Chemically Reduced Graphene	143.7	2,800	3.5	[25]

For example, a 50 ton UPS based upon a current commercially available ultracapacitor might only provide one minute of full power to a destroyer or frigate during a blackout. However, if some of the leading edge high energy experimental capacitors become commercially available at the next equipment life cycle, this UPS capability could be extended to ten or more minutes of full power operation by simply swapping out capacitor banks.

Reference [20] notes that the energy density of ultracapacitors are expected to increase by a factor of 10 in the near future. This is supported by the proven energy densities of experimental ultracapacitors as shown in Table 2.

In conclusion, as warships evolve to IPS constructs, there is a significant need for large power ESSs to fill the operational void created by a loss of power generation capability. A large scale, ship-wide UPS based upon the emerging technologies of ultracapacitors can create a viable solution.

2.4 : Other High Power Ultracapacitor Applications

Although ultracapacitors have not seen much headway in marine applications, they have been introduced with good results in a variety of other transport fields. This includes regenerative braking and acceleration assistance in hybrid buses, automobiles, and rail cars; high cranking current for engine starting; backups for opening aircraft doors; power regulation in wind turbines [20] [26]; load leveling in hybrid hydraulic mining shovels; and, short term ESS to fill the gap between power failure and backup generator starting [27].

As numerous applications already exist for ultracapacitors, the scope within this section will be limited to a few examples to provide the general context: the hydraulic mining shovel as a specific load leveling example; regenerative braking as a general load levelling example; and, the Chariot E-bus as a larger scale UCES system.

2.4.1: Load Levelling - Hydraulic Mining Shovels

The work presented in [28] illustrates a power balancing application of ultracapacitors. While not a backup power system per se, the integration of ultracapacitors with diesel power vehicles has analogous applications in a marine environment.

By nature, a hydraulic mining shovel requires peak power during shovelling operations and then very little throughout the rest of its cycle. Diesel engines are slow to respond to power changes - one reason why gas turbines are preferred for warship main engines – and they are highly inefficient during transitions. By mating the system to a hybrid diesel-electric drive, the load on the engine can be leveled, as power surges are moderated by the ultracapacitors.

The arrangement in Figure 6 draws many parallels to a shipboard EPG&D system where DGs provide power to an Alternating Current (AC) (vice the DC one below) distribution main feeding motor-driven hydraulic pumps and meeting auxiliary power demands.

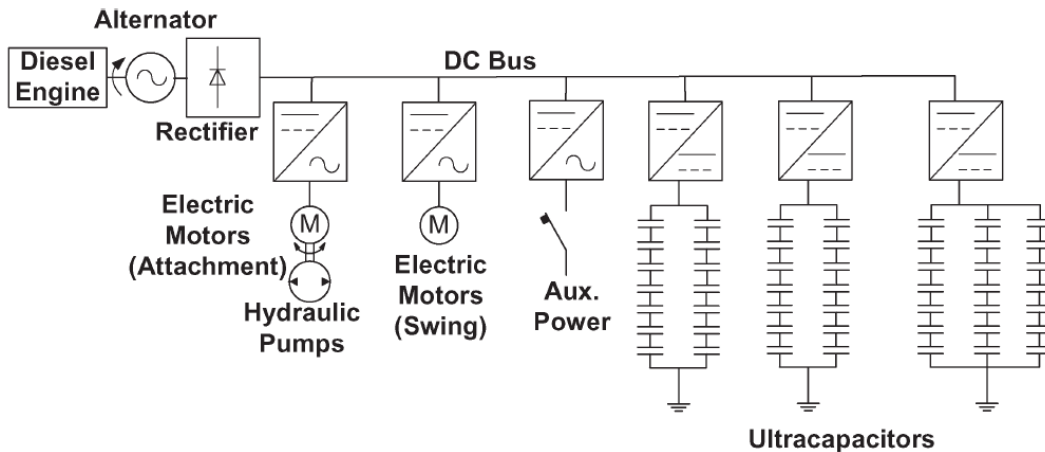


Figure 6 - Hybrid Hydraulic Mining Shovel Power System with UCES [28]

The 2.25 MW UCES illustrated above provides considerable power smoothing qualities. This reduced engine peak demand by 35%, and improved engine loading by 25%. If redesigned, the same hydraulic mining shovel needs could be met by a lower rated diesel engine, and that diesel engine could be operated at more efficient power levels.

This system demonstrates two direct benefits for naval UCES integration. Firstly, engine generator sets could be designed to meet steady state power requirements as opposed to peak transient demands. Secondly, the practice of running extra engines in precarious scenarios to provide redundancy in case one was to fail could be eliminated. These benefits would include procurement, maintenance, and fuel costs [29].

2.4.2: General Load Levelling - Regenerative Braking and Acceleration Assistance

Another efficiency increasing application of ultracapacitors is through regenerative braking systems. A regenerative braking system can be applied to almost all electrically propelled vehicles, but it requires a storage medium capable of quickly absorbing the high powers produced during braking. Battery packs are often unable to do so due to their lower power densities. As such, an UCES is the superior choice.

Figure 7 demonstrates a generalized system that could be applied to almost any traction vehicle.

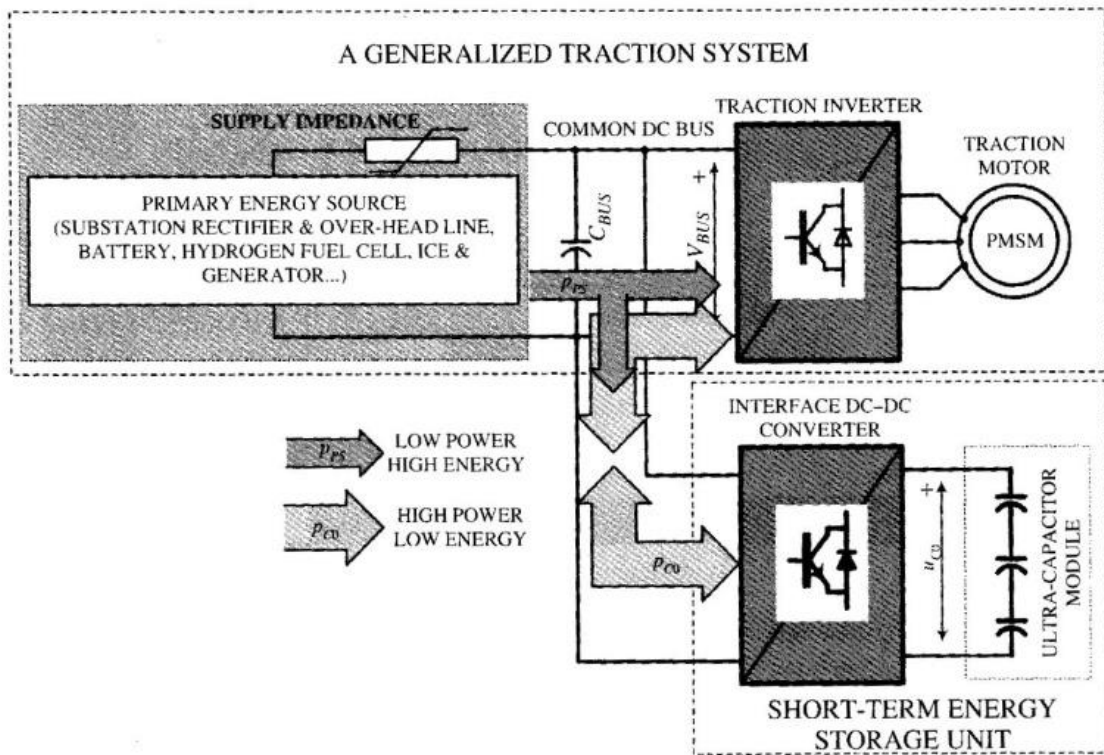


Figure 7 - Generalized Traction System for Regenerative Braking [20]

Although a traction system and regenerative braking has little application to a marine application, the generalized system design shown in the figure above has an analogous application to an IPS warship. The block labelled Primary Energy Source is analogous to ship's generator, with the inverter and traction motor representing a ship's main propulsion motor. The short-term energy storage unit could be used as a ship-wide UPS as opposed to an energy recovery unit.

Figure 8 illustrates the role of these energy recover systems from a power and vehicle state perspective.

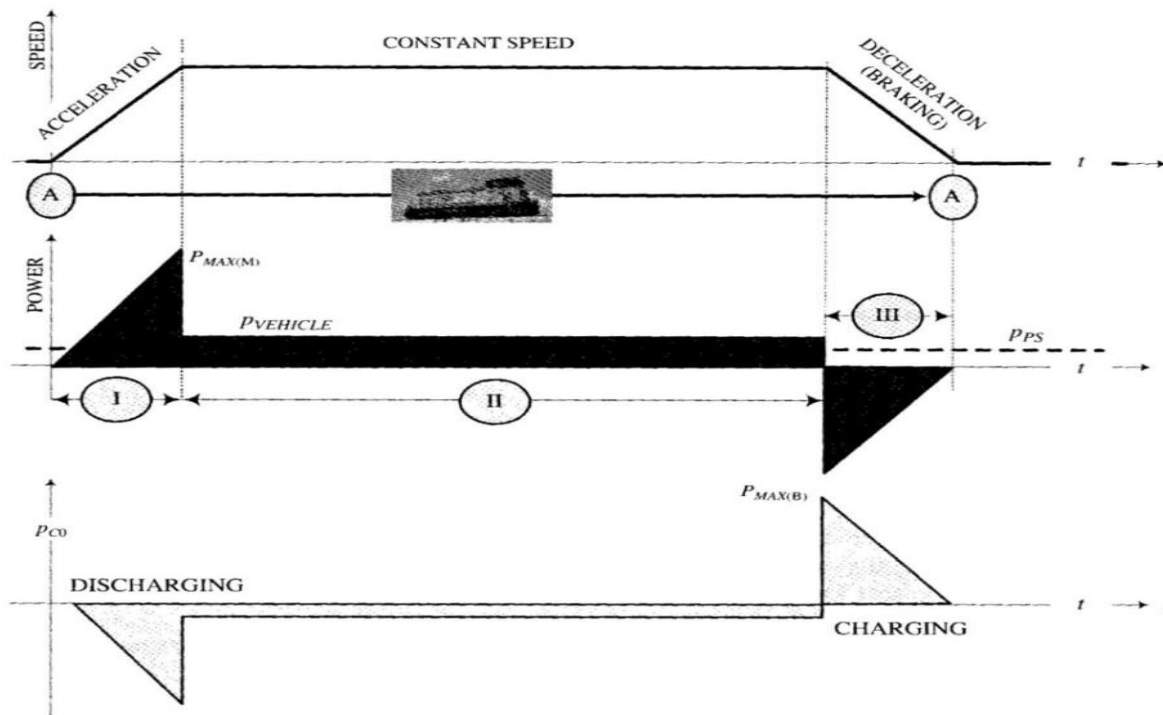


Figure 8 - ESS assist with vehicle performance [20]

Since considerable energy is consumed during vehicle acceleration and discarded when braking, these regenerative systems boast considerable savings when used in city driving. In an urban setting, reference [30] found that the integration of a basic regenerative braking system into a small automobile increased efficiency by 51.7%. Again, this is a basic example of load leveling but it does draw parallels to ship systems. For example, a short sprint or a large transitory load such as starting of a large induction motor could be regulated by an ESS in much the same way acceleration or compensated for in the figures above.

2.4.3: UCES as a replacement for BESS: The Chariot E-bus

Since 2006, the city of Shanghai has been operating buses powered by ultracapacitors and battery banks. These buses draw upon the energy stored in ultracapacitors banks for transits between stops where they are then recharged via overhead charging stations. The ultracapacitor banks provide sufficient power for 3 miles; however, for longer distances, there are reserve battery banks which extend the range to 15 miles – there is no internal combustion engine [31], [32].

Aowei industries website [32] provides specifics details on the ultracapacitor banks being used. The ESS weighs in at 1450 kg, which is just under 10% of the overall weight of the vehicle at 16,000 kg. As a comparison the warship projected UCES would make up 3% of the overall mass of a 5,000 ton frigate.

As expected, ultracapacitor technology has improved and in 2014, a bus powered exclusively by Aowei ultracapacitors was released under the name Chariot E-bus. This bus has a range of 20km, which is sufficient for it to complete its route and recharge at the station in 3 to 5 minutes [33].

The Chariot E-bus application demonstrates that a stand-alone UCES is a viable operation for short term operation between power sources. In addition, they can be more cost effective than BESSs, as battery banks would require a number of replacements during the vehicle lifespan [34].

2.4.4: Synopsis of Other High Power Applications

This section has demonstrated that UCES are beginning to see implementation in land-based transport with much success. They can reduce engine power requirements by offering load leveling, improve engine performance and fuel efficiency, offer energy recover abilities, and even replace BESS in some domains. While ultracapacitor research with respect to naval integration has traditionally been focused on surge power to support future rail gun and laser weaponry [35], UCES has proven its ability to act as a short term ESS. An UCES can easily provide adequate power during a short gap in power generation capability aboard a warship.

2.4.5: Control Schemes in Ultracapacitor Applications

What this section has also shown is the arrangement of power electronics typically associated with a UCES. Due to their requirement to be charged by DC currents, ultracapacitors typically feature bidirectional DC/DC converters such as those seen in Figure 6 and Figure 7 and references [20] and [26].

Future warship integration, however, will likely require that an UCES is coupled to synchronous AC generator. As such, control schemes with AC networks should also be analyzed. Reference [29] describes ultracapacitors in a three phase arrangement with AC power being supplied by a generator, while [36] describes a UCES designed for distribution grid integration.

Both of these references use similar power electronics to charge and discharge the ultracapacitors. The charging scheme has the generator developed AC power or AC main power rectified by PWM converter and passed through bidirectional DC/DC converter to charge the ultracapacitors. During discharge, the ultracapacitors diminishing DC voltage is regulated by the DC converter and inverted through a PWM inverter back to the system main voltage.

This arrangement of AC/DC converters coupled with DC/DC converters is the typical arrangement in which power electronics and ultracapacitors are combined with AC networks.

2.5: Conclusion

This literature review has shown the immense cost and complexity associated with conventional warship backup systems. Since survivability and redundancy are intrinsic to naval design, future warships can also be expected to have significant investment into their back up systems. However, a single ship-wide back up system offers some significant advantages in easing the complexity and high maintenance costs associated with maintaining a myriad of small independent systems.

Making an electric back up system is logical for a future IPS warship, as the greatest risk to such a vessel is from a loss of power generation capability. A blackout, as shown, can occur for many reasons. Although navies can try to reduce the number of blackouts a ship experiences, they will never be eliminated entirely.

As such, energy storage sufficient to span a loss of power generation capability is a prudent investment. While utility grids present many different methods to store energy, only BESS and UCES are suitable for marine applications - with the latter being the preferred option.

Although ultracapacitors have not been used as a large scale storage medium in warships, their use in other high power applications demonstrates their suitability for short period high demand scenarios. As such, this literature review has provided the pertinent background details that characterize the need for UCES in future IPS warships. In addition, the review also analyzed the typical arrangement of power electronics to support such a system.

However, the size and capacity of such a system will vary greatly depending upon the warship for which the UCES is being designed. Therefore the environment in which the UCES will operate must be established.

CHAPTER 3 : MODEL ENVIRONMENT - A UCES FIT FOR A SHIP

Prior to characterizing the model components and displaying the results of the proof of concept, the characteristics of the storage medium the model was designed to operate with must be shown. The power expectations and size limitations were key factors in the selection of a theoretical ultracapacitor module based upon commercially available components. The following chapter will demonstrate the researched decisions that led to the UCES selection.

3.1 : Power expectations for UCES integration into an IPS Warship

As a Marine Systems Engineering Officer in the RCN, the author designed the model with consideration of the power requirements expected of a possible future IPS warship. The Canadian navy's future platform for a major surface ship will likely be a destroyer or frigate; however, more important than the classification is the displacement size and length of the vessel. Given the parameters of the Halifax class, one would expect a future RCN IPS vessel to be in the order of 5000 tons displacement with a length of 450 ft.

Power requirements for such a vessel are based largely upon propulsion demands, as other ship's loads, usually 1 +/- 0.5 MWs, make up only a fraction of the overall demand. As specific warship hull power curves are classified, Figure 9 shows a power speed curve for a typical hull around 450 foot and 5000 tons displacement.

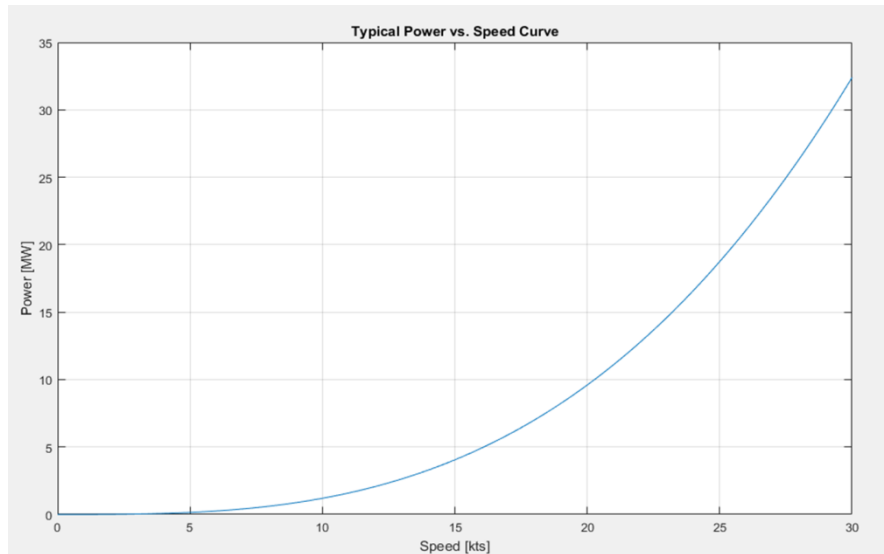


Figure 9 - Power Speed Curve of a Typical Frigate Sized Vessel

As seen above, the ship power requirements become increasingly prohibitive with speed. Assuming a 1MW static draw for all other equipment, an IPS vessel with a maximum power output of 30MW would have 29 MW remaining available for propulsion loads. This equates to approximately 27-29 kts, which is a reasonable assumption for a ship's top speed.

For redundancy, the IPS model ship was assumed to have a similar electrical layout to the Halifax Class [5] with four 15 MW generators providing power. In order to easily meet paralleling requirements, the UCES should be equally sized to a generator and should also be able to deliver 15 MW of power. Figure 10 demonstrates the author's conceptual IPS warship.

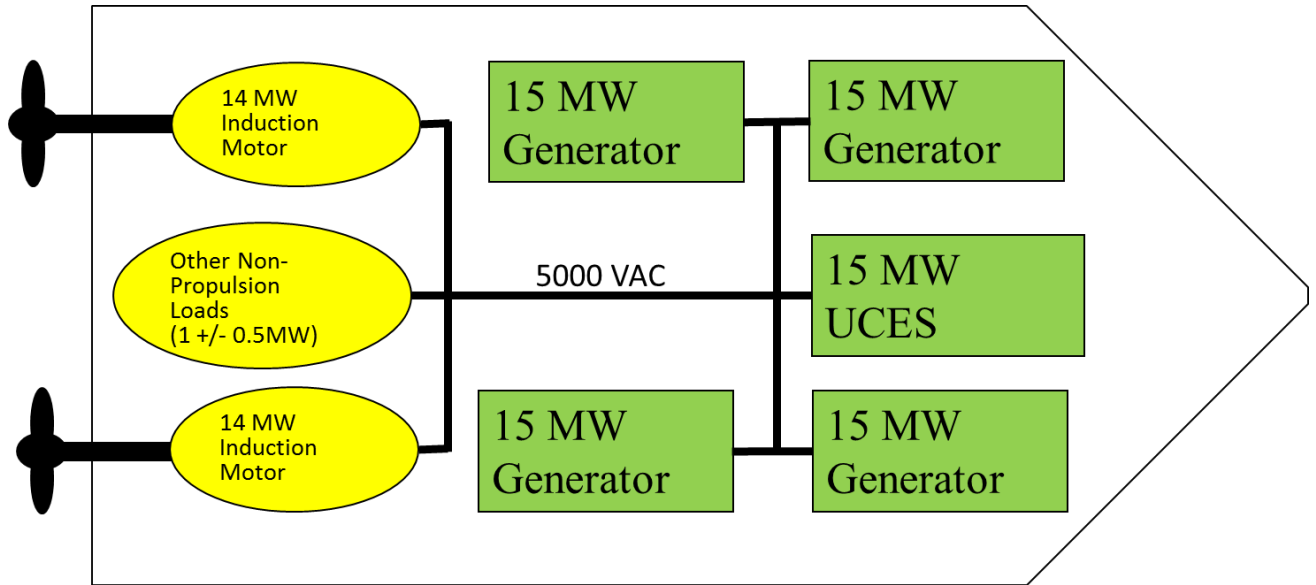


Figure 10 - Conceptual IPS Warship

Also shown in the figure above is the system voltage at 5000 VAC (Root Mean Square (rms) phase-to-neutral), 3 phase, 60 Hz, which was an estimate based upon an interview with RCN experts [37].

However, the modelling of induction motors and multiple generators would add needless complexity. Figure 11 shows the conceptual IPS model further reduced to a single generator with a single variable load and an ESS. This created a model environment that provided the necessary loading and generator requirements without any extraneous details. This allowed the simulation to be focused mainly on the design of the UCES rather than an EPG&D system as a whole.

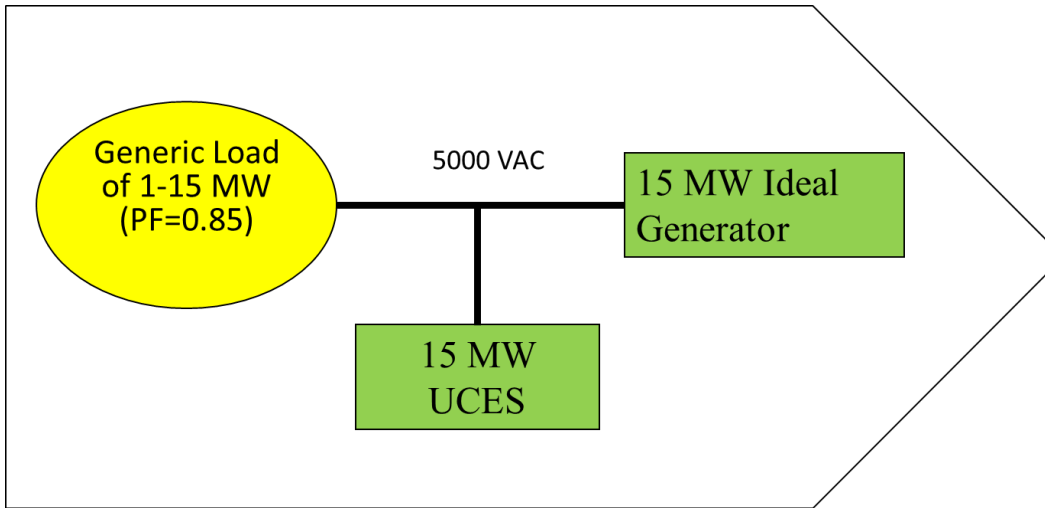


Figure 11 - Model environment for the UCES system

The load in the finalized model environment above was also capped at 15MW, even though ship full power is expected to be around 30MW. This load cap was a result of difficulties in modelling UCES operation in parallel with the ship's generator for any significant length of time. As the model operated with either 15MW power source, but not both concurrently, there was no need to incur loading in excess of the generator and UCES's individual power outputs.

3.2 : Size Limitations of the UCES

Due to the moderate energy capacity of ultracapacitors, the size limitation granted to a UCES must be generous in order for such a system to be capable of sustaining power in the MW range. Section 3.3 discusses specific ultracapacitor bank selection; however, the size limitation proposed here set the standard for that selection.

Given that the specific gravity of ultracapacitors can also be assumed to be just a little heavier than water at 1.4-1.5 kg/L [21], a 100 ton capacity is reasonable for warship use. This translates to a volumetric capacity of 66-72 cubic meters. This volume is a mere fraction of the fuel capacity of Halifax class frigate [9], which is approximately 670 m³ for diesel plus many hundreds of cubic meters more for other fuels and lubricants.

Finally the overall mass of 100 tons would be advantageous to a future warship, as the module could be placed centreline along the keel to increase ship stability. Further proving the need for weight low down in the hull, the Halifax class recently saw the addition of 90 tons of solid ballast to compensate for midlife ship growth [38].

3.3 : The Ultracapacitor Module

As a ship wide UPS, the UCES must be able to maintain power to the ship long enough to emergency start a non-running generator. This normally takes about 2 minutes with a well-trained crew. From that, the goal of the proof of concept was to be capable of providing 15MW of power (the UCES peak output) for 2 min using commercially available components.

Skeleton Technologies, a leading manufacturer, produces some of the highest capacity ultracapacitors currently available; however, they did not produce the highest capacity modules. A literature review found the largest and highest voltage modules were being assembled for an ultracapacitive municipal bus being produced by a Chinese company: Aowei Industries.

3.3.1: The Aowei Industries ultracapacitor bus

The Aowei industries bus was designed for short duration trips with rapid recharging during stops. Of interest to this thesis was the relatively high voltage ultracapacitive energy storage module used in [31], [32], [33]. Table 3 shows the pertinent technical information of that module.

Table 3 - Aowei Industries High voltage ultracapacitor module

Cell Model	UCE15V80000A
Cell No.	400
Nominal Capacitance, F	200
Rated Working Voltage Range	360-600
Maximum Working Voltage(Limit), V	620
Minimum Static Voltage, V	400
Available Energy Stored within Working Voltage Range, Wh	≥6000
ESR, mΩ	≤180
Maximum Charge/Discharge Current, A	300
Volume, m ³	1.5
Weight, kg	≤1450

This module proved promising to this thesis as it was commercially available and at a high enough voltage that could be easily stepped up to 5000 VAC at the main. Initial iterations of the Simulink model used this module for the UCES. Once discharging was modelled, there proved to be a significant drawback to the model.

The problem lay in the Equivalent Series Resistance (ESR). Although 180 mΩ may seem small, it is relatively high resistance for an ultracapacitor module. Examining the currents necessary to produce 15MW at 600V and given that the losses in DC discharge are:

$$P = I^2R \tag{2}$$

where P is power [watts];
 I is current [amps]; and,
 R is the Equivalent Series Resistance [ohms].

The power lost would extreme under maximum discharge. Therefore a significantly improved module had to be found.

3.3.2: Theoretical module based on Skeleton Technologies' components

Although this company does not produce high capacity modules, Skeleton Technologies does produce high energy capacity ultracapacitors that experience a very small ESR. Model SPA2100 details can be found in Table 4 [39] [40].

Table 4 - Skeleton Technologies SPA2100 Details

Cell Model	SPA2100
Number of Cells	1
Volume, L	.283
Weight, kg	.414
Nominal Capacitance, F	2300
Maximum Rated Working Voltage	2.85
Maximum Working Voltage(Limit), V	3
Specific Energy (Wh/kg or kWh/Ton)	6.3
Specific Energy (kW-min/Ton)	378
Specific Power (kW/kg or MW/Ton)	31
ESR, mΩ	.21
Maximum Charge/Discharge Current, A	2400

This thesis assumed that this individual cell could be developed into a module consisting of a number of these cells placed in series and parallel. Creating an array of numerous ultracapacitors has some technical challenges. The module capacitance changes to:

$$C_{module} = C_{cell} \frac{M}{N} \quad (3)$$

where C_{cell} is the capacitance of an individual cell in [Farads];
 M is the number of cells in parallel; and,
 N is the number of cells in series

The modules' ESR changes to:

$$ESR_{module} = ESR_{cell} \frac{N}{M} \quad (4)$$

By applying these and some other simple conversion formulas a theoretical module was developed based upon the SPA2100 cell. This module consisted of 241,546 cells with each individual cell having the properties of the ultracapacitor in Table 4. The arrangement had 210 cells in series to produce a working voltage of 600V.

Although higher voltages would have been ideal to limit losses, the maximum limitations of this theoretical module were uncertain. Since a working voltage of 600V was achieved by Aowei industries in the module discussed in section 3.3.1, the assumption was made that other manufactures could achieve this maximum working voltage ceiling. Assuming this series arrangement was a single string of cells, the theoretical module has 1150 strings in parallel for a total of 241,256 cells. The 1150 strings in parallel provide a large amount of energy storage, while keeping the total mass to less than 100 tons. The details of this theoretical ultracapacitive module are in Table 5.

Table 5 - Theoretical ultracapacitor module used in the simulation

	SPA2100 Cell	Conversion	Theoretical Module
Number of Cells	1	1*210*1150	241,546 cells
Volume	.283 L	.283*241,546	68,358 L
Weight	.414 kg	.414*241,546	100 tons
Nominal Capacitance	2300F	2300/210*1150	12,595 F
Rated Working Voltage Range	2.85 V	2.85*210	600 V
Maximum Working Voltage	3 V	3*210	630 V
Specific Energy	.378 MW-min/Ton	.378*100	37.8 MW-min
ESR	.21 mΩ	.21*210/1150	0.0383 mΩ
Maximum Charge/Discharge Current, A (1s)	2400 A	2400*1150	2,760,000 A

The module above is based upon real components, but is still considered theoretical as it ignores charge balancing. Charge balancing has been overlooked largely because it added another level of technical complexity not required in a proof of concept that is focused on the power system as a whole. Regardless, it should be explained.

3.3.3: Charge balancing – a manufacturers’ problem

During production, it is impossible to ensure that all ultracapacitor cells are perfectly matched. Minor variations during manufacturing can lead to voltage imbalances across these cells. As ultracapacitors need to be connected in long series to develop useful voltages, these imbalances could cause some cells to exceed their recommended voltage levels during charge. As voltage levels should never be exceeded, in order to preserve device lifespan, charge balancing equipment is usually associated with ultracapacitor assemblies.

Charge balancing circuitry normally comprises of one of four designs: passive resistors, switched resistors, DC-to-DC converters, or Zener diodes [41], [42].

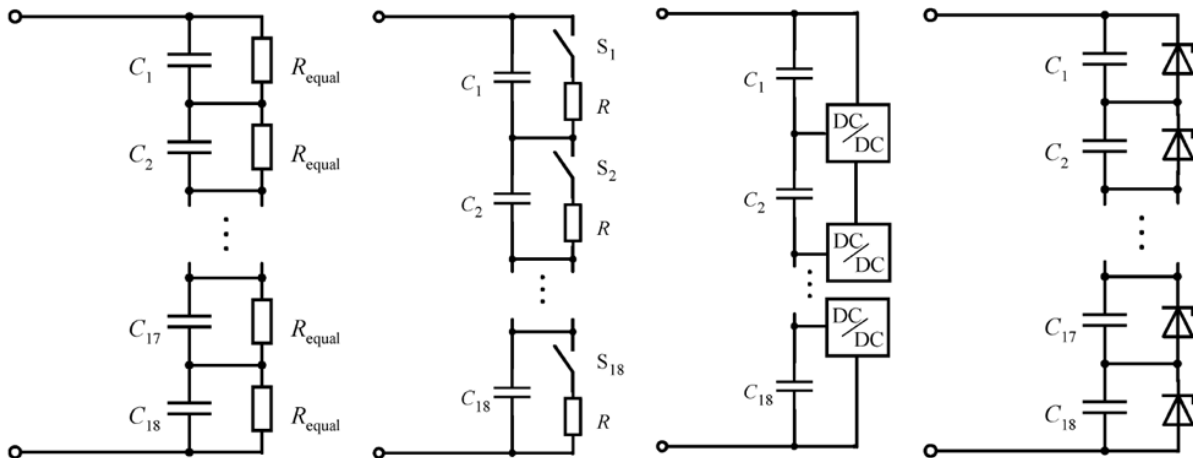


Figure 12 - Charge Balancing Arrangements: Passive resistance, Controlled resistance, DC/DC converters, and Zener diodes [42]

Passive resistors connected in parallel with each cell minimize voltage gradients, but increase losses. While cheap, the energy loss does not make this setup a viable option for high power systems.

Resistors connected in series with a control switch and in parallel to the ultracapacitor can shunt current away from the ultracapacitors when a predetermined voltage level is met. This reduces losses compared to the passive resistor method, but also requires voltage monitoring at each cell.

DC to DC converters can ensure strict voltage control at each cell but increase cost and technical complexity.

Zener diodes shunt current away from the ultracapacitor once a predetermined voltage level has been reached. Although seemingly ideal, the voltage operating point of the Zener diode fluctuates with temperature. In addition, the Zener diode itself experiences some losses.

Regardless of the method being used, cell balancing is absolutely necessary to ensure electrolyte breakdown does not occur within the cell, which would significantly reduce cell capacity and service life.

The problem of charge balancing was outside the scope of the system, as it will ultimately be the manufacturer responsible for producing a suitable ultracapacitor module that will deal with the internal charge issues. However, with a little added complexity and cost, the leading suppliers are more than capable of now delivering modules capable of meeting high power demands.

3.3.4 : Module Construction

While the physical design specifications of the ultracapacitive module are somewhat on the fringes of the scope of this thesis, they can be briefly addressed.

With a total weight of 100 tons, this ultracapacitive module could greatly increase the stability of a warship. By placing the unit centreline along the keel, the module could act as solid ballast, lowering a ship's center of gravity and increasing its metacentric height.

The module should be protected in a watertight grounded steel enclosure, to ensure that there is some separation between it and the ship's bilge. In addition, to increase survivability and redundancy, the module should be divided into submodules, distributed throughout the lower deck spaces.

From a thermal perspective, the module enclosure should be filled with an insulating liquid to provide cooling during charging and discharging operations. Further examination of thermal conditions would be required as a UCES nears development to consider if a pump and a salt water heat exchanges would be required to provide temperature regulation during charging and discharging operations.

Finally, these enclosures should also be fitted with sensors to monitor crucial operating setpoints and to provide condition based analysis to drive reliability centered maintenance regimes.

3.4 : Conclusion

While chapter 1 presented the need for energy storage in an IPS ship, chapter 3 revealed the specific requirements of the model and the UCES. Namely, that the model environment will consist of:

- a) A 15MW ideal generator (unity output and internal losses ignored) producing 3 phase 60Hz power at 5000 VAC (rms phase-to-neutral);
- b) A variable load from 1-15MW at a constant Power Factor (PF) of 0.85 lagging;
- c) A theoretical (charge balancing ignored) ultracapacitor module consisting of commercially available components capable of delivering up to 15MW of power at a PF of 0.85 lagging with the properties outlined in Table 5;

Although there are no specifics that anchor this model to only a marine environment, the ability to deliver 15MW over a duration of a minutes does meet the demand of a future IPS warship. The model specifics will now be discussed.

CHAPTER 4 : MODEL DESCRIPTION

The system was modelled in MATLAB's Simulink software. This simulation tool was chosen as it is widely accepted and known modelling software in the scientific community. In addition, the author's previous experience using Simulink to model power electronics and electric machines proved the software's ability to accurately predict the behaviour of those devices.

4.1 : System Overview

Figure 13 shows the overall system with some of the key components highlighted.

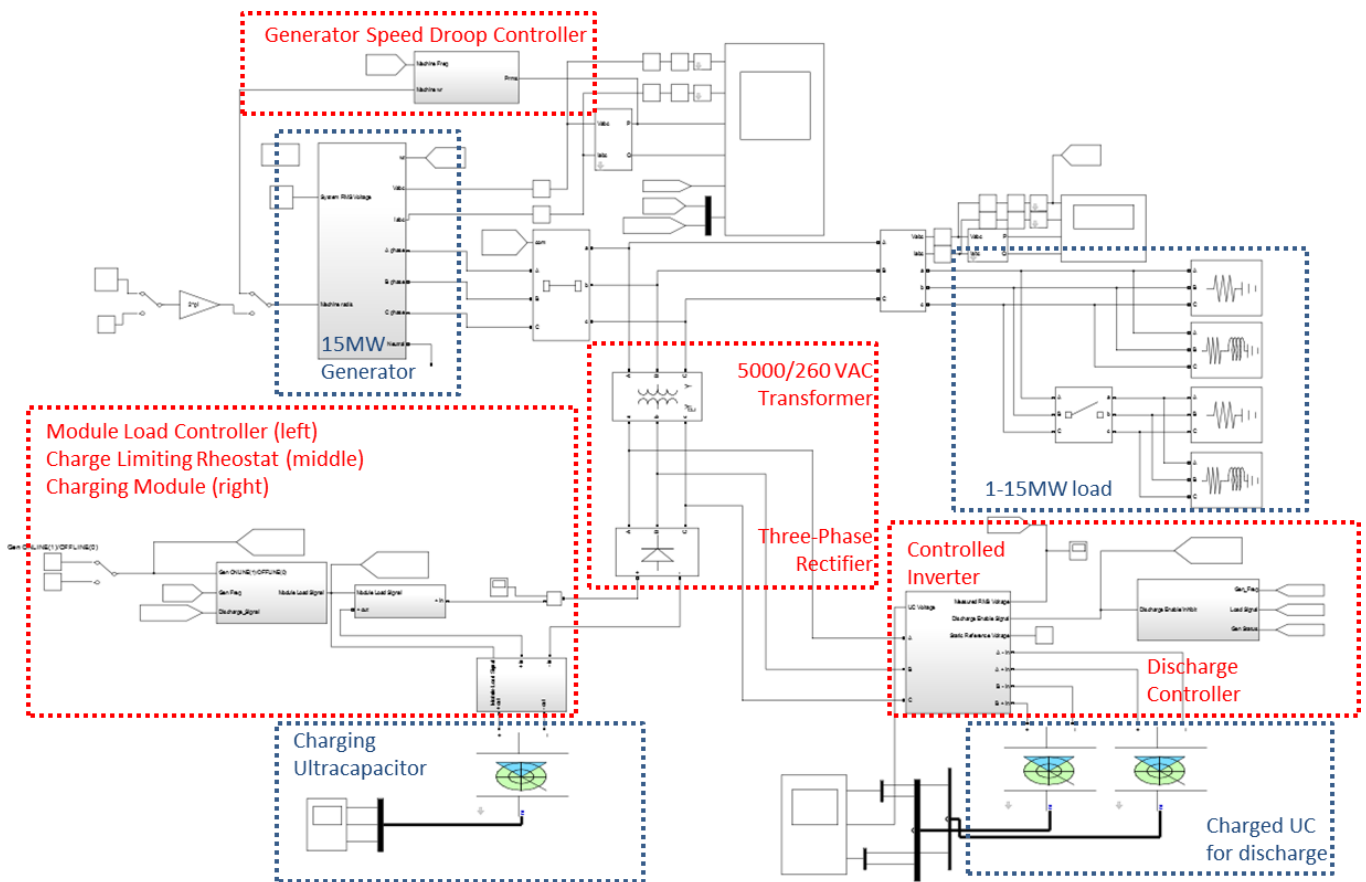


Figure 13 - Top level system model in Simulink

The major components are outlined with blue dotted lines in Figure 13. On the top left is a 15MW synchronous generator which provides stable power to either the ship's load (modeled on the top right) or the ultracapacitor charging system on the bottom left. The generator features speed droop which allows the system to react based upon frequency. If the system detects a drop in frequency or the main generator breaker opens, power is provided automatically to the load from two banks of fully charged ultracapacitors.

The reader should note that the figure shows three separate banks of ultracapacitors. In reality, there would be only one bank; however, for modelling purposes, fully charging the ultracapacitor in each run was not realistic due to computer memory limitations and extraordinarily long run times. As such, a separate non-charged bank of ultracapacitors was modelled on the bottom left while a fully charged bank (split in two) was modelled on the bottom right.

The main system voltage is three-phase, 60 Hz, 5000 VAC (rms voltage phase-to-neutral). Since ultracapacitors are ideally charged at DC voltages, this system's ultracapacitor banks are designed to be charged to a maximum voltage of 600 VDC. To achieve this, system voltage is stepped down through three single phase fixed transformers to 260 VAC and then rectified via a three-phase diode bridge rectifier to 608 VDC. While this DC voltage is later regulated to 600VDC, the two components that perform these operations, the 5000/260 VAC transformer and three-phase rectifier, are located the red outlined block in the middle of Figure 13.

Also present in Figure 13 in the left red outlined block is the Charging Circuitry, which consists of the Module Load Controller (a logic controller), the Charge Limiting Rheostat (a current controller), and the Charging Module (a voltage regulator). Together these components ensure that charging only occurs when system frequency indicates power is available, that charging does not conflict with the UCES providing power back to the system, and that the power going to the charging ultracapacitors is regulated to 600 VDC.

The middle right red outlined block in Figure 13 shows the top level view of the discharge circuitry, which consists of the Discharge Controller and the Controlled Inverter. When required, DC power is provided from the fully charged ultracapacitor banks shown in the bottom right blue block. The split banks have a variable arrangement which allows them to provide their power in series or in parallel. This is pivotal in assuring consistent output from the Pulse-Width Modulation (PWM) controlled ideal switch inverter. Again, a logic controller here ensures there are no discharging conflicts with the charging side. The inverted power is stepped up through the same step down transformer from 260VAC back up to 5000 VAC to drive ship's loads.

4.2 : System Assumptions

The system makes some key assumptions for this first iteration of a UCES back-up power supply model. Many of these assumptions could be factored into later models nearing a prototype stage. However, at this early stage, system voltages both at the power main and ultracapacitors themselves are all estimated values. In the coming years, ultracapacitors will be able to operate at higher voltages with greatly increased capacitance.

First, system losses were largely ignored. No line losses were modelled, and most switching devices were considered ideal or set to $1 \mu\Omega$ resistance if Simulink required a resistance (i.e., when run in discrete mode). The high currents required to provide 15MW at 600VDC would require very specialized high power and low loss switching devices; however, this proof of concept shows that it is possible for an UCES to act in this capacity. Modelling the losses at this stage would be premature as the author expects that a future UCES would operate at significantly higher DC voltages with significantly reduced losses.

Secondly, the ship's loads were considered constant or had a step load added or removed to simulate a load change. A large step load, in the order of MWs, is somewhat unrealistic as a fully developed propulsion control system would gradually increase demand to protect the mechanical systems. If anything though, this step loading proves the dynamic responsive of the system.

Finally, the system was modelled as a wye-connected system.

4.3 : Synchronous Generator

Figure 14 shows the top level view of the generator.

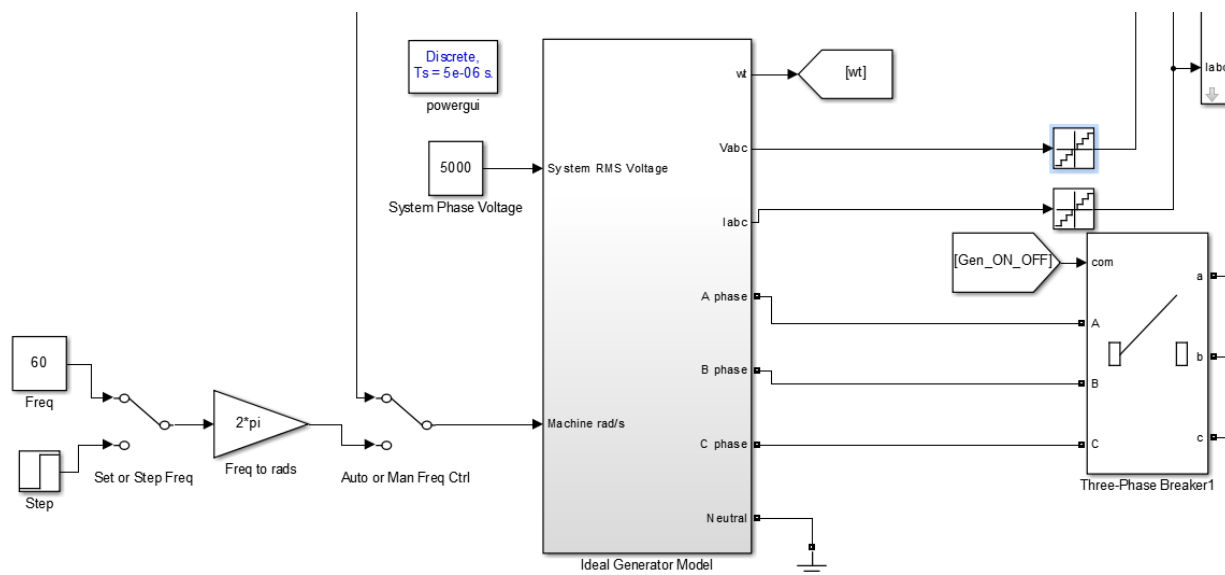


Figure 14 - Top level view of Generator

The generator inputs are the system phase voltage set at 5000V, as well as the mechanical speed of the rotor - listed in the model as Machine rad/s or “wt”. The mechanical speed input has a manual switch to allow fixed speed inputs; however, this is more a troubleshooting tool and not usually used in the simulation. This speed input is normally set by the generator speed controller based upon system loading.

The generator outputs are the phase angle (wt) of phase A; voltage and current sensor outputs of all three phases (V_{abc} and I_{abc}); as well as all three phases' line outputs and the neutral.

Figure 15 shows the bottom level view of the generator.

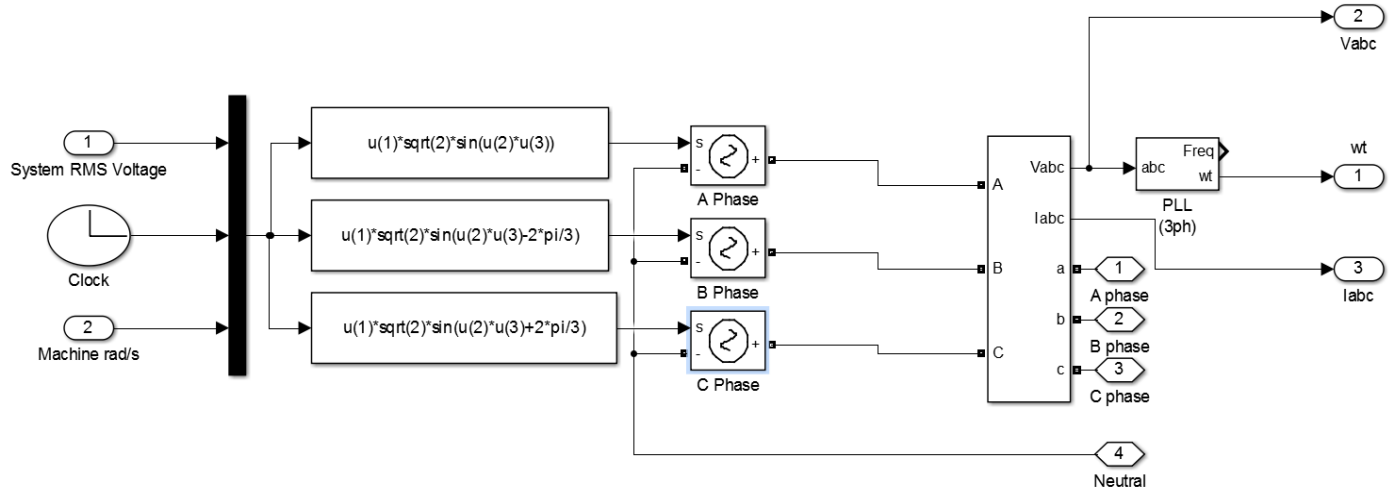


Figure 15 - Bottom level view of the Generator

From the figure above, the equations supplying the input to A, B, and C phase voltage generators represent the ideal sinusoidal voltage equations for a three-phase system [43],

$$\begin{aligned} V_a(t) &= V_{rms}\sqrt{2} \sin(\omega t) \\ V_b(t) &= V_{rms}\sqrt{2} \sin(\omega t - \frac{2\pi}{3}) \\ V_c(t) &= V_{rms}\sqrt{2} \sin(\omega t + \frac{2\pi}{3}) \end{aligned} \quad (5)$$

When relating these equations to Figure 15, the reader should note that the function blocks (the first set of blocks after the inputs) use inputs u(1) as the system rms voltage at 5000V, u(2) as the simulation time, and u(3) as the machine speed.

The outputs of the voltage blocks feed into a three-phase sensor. From the voltage sensor, a phase-locked-loop determines frequency and phase angle. Phase angle was measured to allow the inverted output of the UCES during discharge to parallel with the running generator. However, this paralleling proved unachievable due to the simulation software, so the “wt” output was not used.

For the purpose of the simulation, the generator never stopped running, as there was no need to stop the machine rad/s signal input. If necessary, the generator was removed from system operation by opening its main breaker (“Three-Phase Breaker1” in Figure 14).

4.4 : Generator Speed Droop Controller

Figure 16 shows the top level view of the generator speed droop controller expanded into the bottom level view.

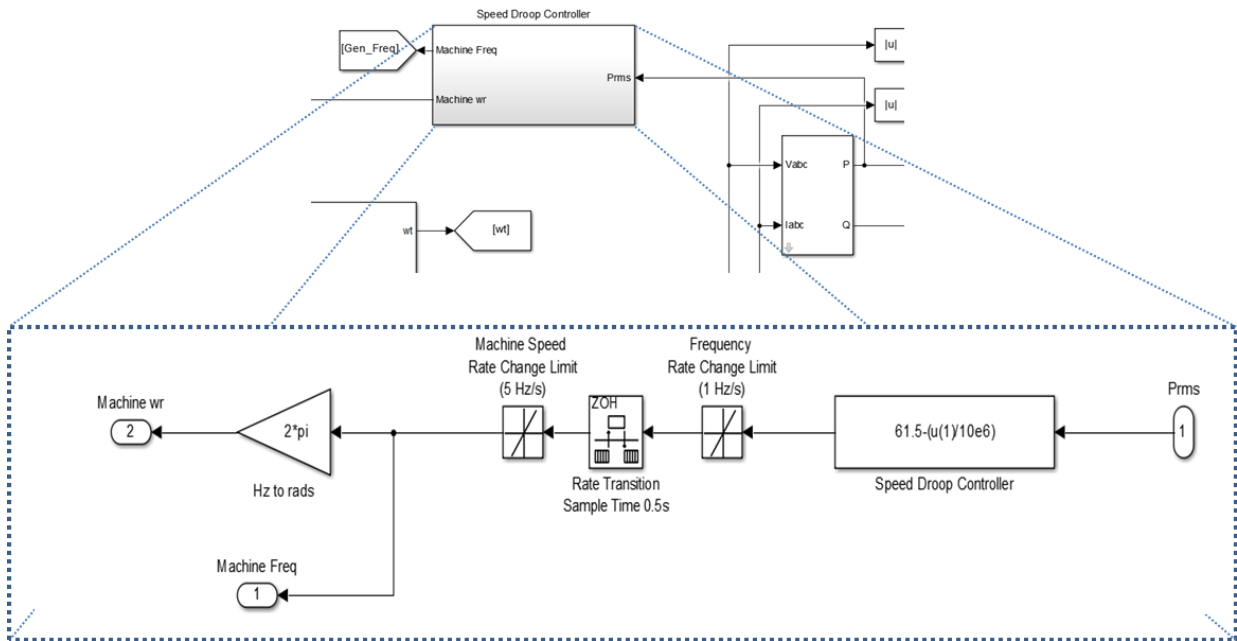


Figure 16 - Generator Speed Droop Controller

The speed droop controller measures the power being developed at the generator. From that, it sets the system frequency by alternating the mechanical speed (w_r) of the generator's rotor. Linear speed droop is a common characteristic given to generators to ensure they can be paralleled properly [44]. The generator frequency is set by the equation:

$$f_{sys} = f_{nl} - \left(\frac{P_{sys}}{S_p} \right) \quad (6)$$

where f_{sys} is the current system frequency;
 f_{nl} is the no load system frequency at 61.5 Hz;
 P_{sys} is the measured system power; and
 S_p is the rate of change (10MW per 1 Hz).

From this equation we can see that at no load the system frequency is 61.5 Hz and when the generator is fully loaded at 15MW its speed is 60Hz. The UCES takes advantage of these changes in speed by using frequency to determine when to charge and discharge the ultracapacitors.

The blocks to the left of the speed droop equation in Figure 16 were implemented to eliminate chatter in the power sensor and provide stability to the controller. The first block labelled "Frequency Rate Change Limit (1 Hz/s)" is a rate limiter block which ensures that the system frequency does not change by more than 1 Hz/s. Given that 1Hz equates to a change in power of 10MW, this was well within tolerances of such a controller.

The second block to the left labelled “Rate Transition Sample Time 0.5s” limits system polling to every half second for a change in frequency. This block was instrumental in providing stability, particularly when the simulation was running in discrete mode which created more pronounced signal chatter. With this chatter, the simulation needed the generator to operate at a constant speed for a short period of time to allow the sensors to achieve stability prior to the next speed change.

The third block to the left labelled “Machine Speed Rate Change Limit (5Hz/s)” simulates machine inertia and the limits how fast the rotor can change speed. In a two-pole pair machine this translates to 300 cycles/s or 150 rpm/s (revolution per minute) at the engine. This is well within reason for a medium- speed industrial diesel engine operating at 1800 rpm.

Finally, the controller provides two similar outputs: the machine speed in rad/s and the machine frequency in Hz/s.

4.5 : Ship’s Load

Figure 17 shows the blocks used to model the ship’s load.

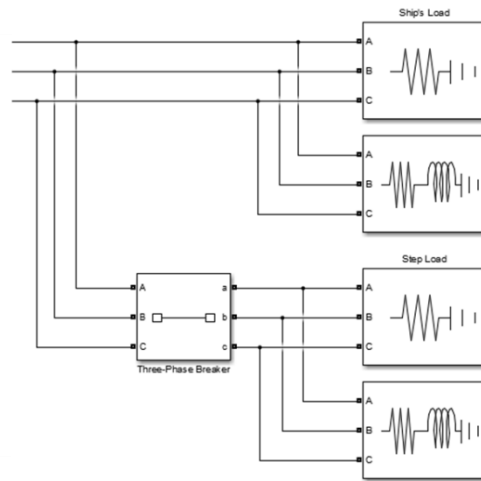


Figure 17 - Ship's loads

The figure above is slightly different from the ship’s load blocks shown in Figure 13, which was reduced for presentation purposes. Ideally, there would be one block that could change its load; however, running the simulation in Simulink created some restrictions. The blocks above are static. They can be manually changed to represent a resistive load in watts and a reactive load in positive or negative Volts Amps Reactive (VAR). In addition, Simulink requires that a reactive load downstream of a current source (a circuit breaker) must have a resistive load in parallel with it.

In order to reduce the number of variables, ship’s loads were assumed to have a constant PF of 0.85 lagging. This is in accordance with a typical warship electrical load due to the high number of (induction) motor driven pumps and the absence of power factor correction equipment [5]. As such, in order to provide a change in ship’s loading, four blocks were required. The blocks labelled “ship’s load,” provide the baseline loading, with the two blocks fed from the circuit breaker providing a step loading through their addition or removal at a predetermined time: manually inputted into the circuit breaker. For the purpose of the simulation, ship’s loading ranged from 1 to 15 MWs.

4.6 : Voltage Transformer and Three Phase Rectifier

The system uses a three-phase wye-wye connected transformer to step the voltage down from 5000VAC at the main to 260VAC. This high current transformer would be a custom build given the power requirements (50 MVA) at relatively low voltages.

The wye-wye connection ensures that there is no phase shift in the voltage signals, eliminating the need for PF correction and making UCES paralleling operations easier.

The system uses a full-bridge, three-phase diode rectifier to convert the 260 VAC (phase-to-neutral) input to a DC voltage charge the ultracapacitors. The conversion from three phase voltage to DC voltage is given by the equation [45],

$$V_o = \frac{3\sqrt{2}}{\pi} V_{3\phi LL} \quad (7)$$

where V_o is the DC voltage [Volts]; and,
 $V_{3\phi LL}$ is the 3 phase line-to-line voltage [Volts].

From this equation, we can see that the 260VAC (phase-to-neutral) produces 608VDC. This slight over voltage is sufficient to allow for some minor fluctuations at the main or losses across the buck chopper and still maintain 600V after a slight DC/DC conversion for ultracapacitor charging.

4.7 : Charging Circuitry

Figure 18 shows the components that provide control and power to the ultracapacitor module for charging purposes.

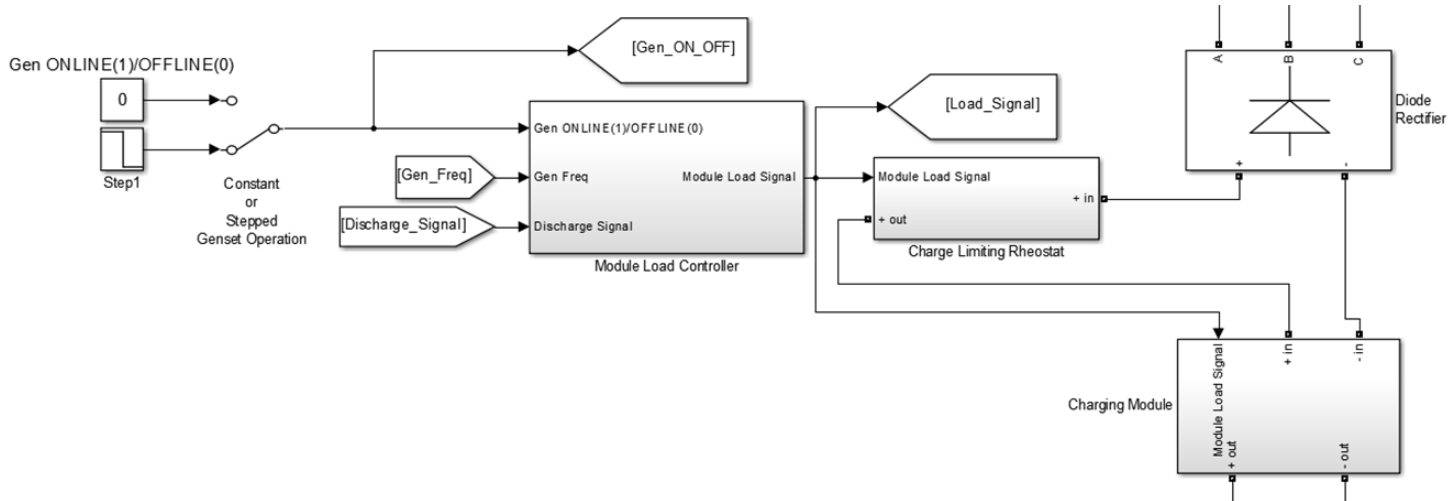


Figure 18 - Top level view of Charging Controller and Power Electronics

The key components from this figure are the Module Load Controller, the Charge Limiting Rheostat, and the Charging Module. These components each provide an essential role. The module load controller provides a control signal that determines the rate of charge. The charge limiting rheostat interprets that signal and electrically limits the current flow to the charging module. Finally, the charging module ensures the voltage across the ultracapacitors does not exceed 600V.

4.7.1: Module Load Controller

The module load controller is a logic controller with three inputs and one output. The primary input is the generator frequency (Gen_Freq) in Hz. The controller's secondary inputs are Gen ONLINE(1)/OFFLINE(0), a binary signal indicating if the generator's main breaker is open or closed, and Discharge_Signal, which is another binary signal indicating if the ultracapacitor banks are discharging.

The bottom level view of the module load controller is provided in Figure 19.

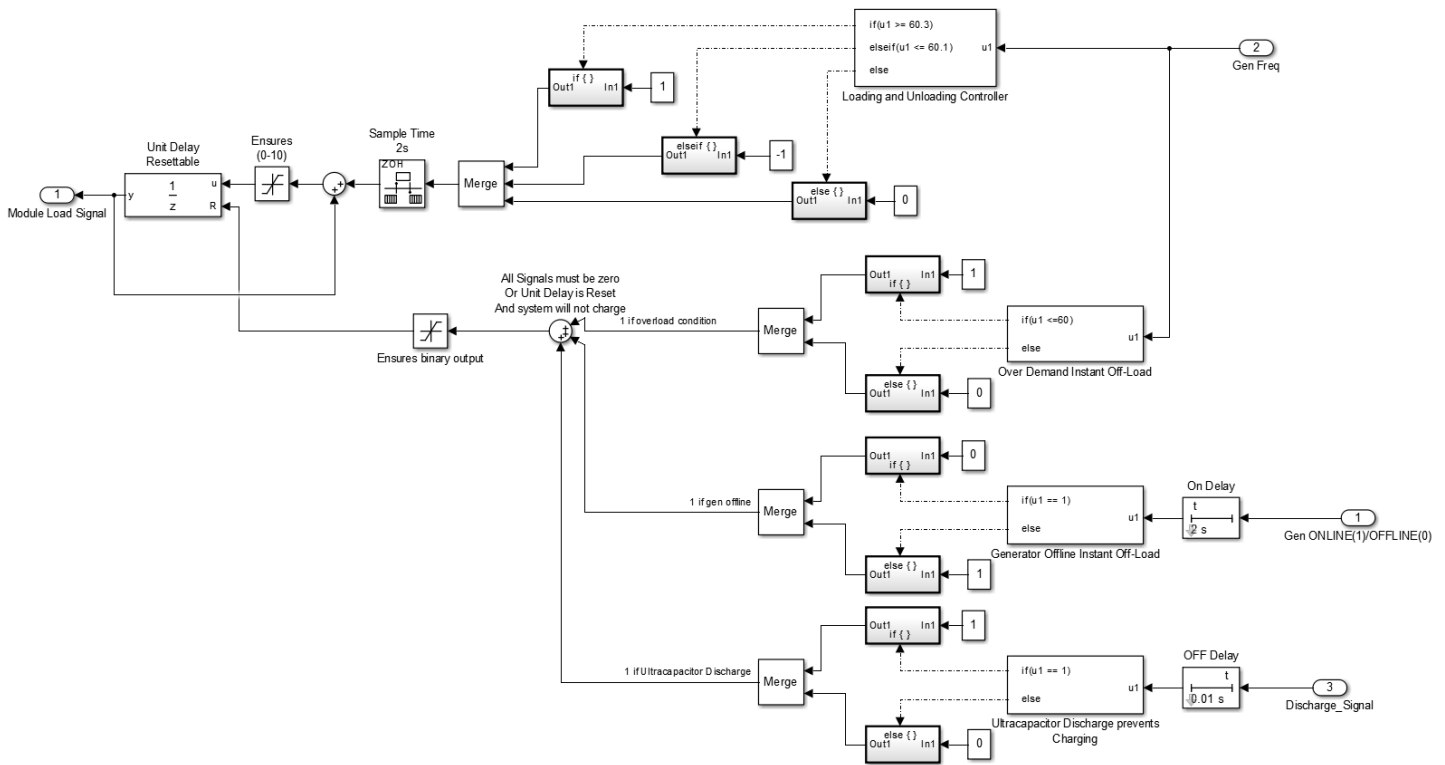


Figure 19 - Bottom Level View of the Module Load Controller

On the right of the figure above, the Gen_Freq signal inputs the speed of the generator in Hz to the controller. The Loading and Unloading Controller block then determines if its input is less than 60.1 Hz, between 60.1 and 60.3 Hz, or greater than 60.3 Hz, and then its associated blocks output a -1,0, or 1 respectively.

This signal of -1,0, or 1, then gets added to a previous iteration of its own signal every 2 seconds. This 2 second polling is provided by the rate transition block labelled, “Sample Time 2s.” A saturation block then limits the signal to a value from 0 to 10. After it passes through a negligible delay, the signal is fed out of the module load controller to the charge limiting rheostat. In section 4.7.2, the reader will see that module load signal of 0 prevents the ultracapacitors from charging, while a signal from 1 to 10 determines a rate of charge, with 1 being the slowest, and 10 the fastest.

The fact that this controller polls, right before the sum block, every 2 seconds is of critical importance. This gives the generator speed droop controller sufficient time to alter the speed of the generator in response to a load change. Keep in mind, the generator speed droop controller itself only polls every half second. Without the delayed 2 second poll, the module load controller would rapidly overload a running generator by quickly creating a full demand signal of 10, allowing nearly unrestricted flow into the ultracapacitors, all of this before the generator could even slow down.

The alternate path of the Gen_Freq input signal leads to the “Over-Demand Instant Off-Load” block. This block, with its downstream components, normally produces an output of 0 unless the generator is overloaded. In the overload condition, system frequency would drop below 60 Hz and the output of these blocks would be a 1. This instantly resets the “Unit Delay Resettable” block, which then outputs a module load signal of 0, and open circuits the charging circuitry. The net effect is that any UCES load is immediately taken off of the generator should the system frequency drop below 60Hz.

The two other inputs signals, Gen ONLINE(1)/OFFLINE(0) and Discharge_Signal, are fed to the module load controller to ensure ultracapacitor charging does not occur at inappropriate times.

If the generator is offline, the Gen ONLINE(1)/OFFLINE(0), signal is zero. In this condition the module load signal is kept at 0 via the “Unit Delay Resettable” block. This prevents the ultracapacitor bank from charging if the generators main breaker is open. In addition, there is a delay block that provides a two second delay when the Gen ONLINE(1)/OFFLINE(0) signal turns on, but not off. This two second delay gives the running generator time to reach steady-state, before the system starts loading the UCES for charging. In a real system, this delay would be significantly longer to allow for engine thermal balancing prior to heavy loading; however, this was not feasible in a simulation environment that can only run for a few hundred seconds.

If the UCES is discharging – providing power to ship’s load – then the ultracapacitors cannot also be charging at the same time. To prevent this conflict, the module load controller also monitors the Discharge_Signal. If the Discharge_Signal indicates the UCES is discharging (binary true (1)), then the module load controller sends an immediate signal to “Unit Delay Resettable” block. The resettable block drives the module load signal to zero, which open circuits both the Charge Limiting Rheostat and the Charging Module in Figure 18.

The Discharge_Signal is also delayed, but only when it switches off. This 0.1s delay provides a brief period of no charging following the end of UCES discharge.

In summary, the module load controller produces a loading signal from 0 to 10 based upon system frequency, with zero being no UCES load, and 1 to 10 being incrementally increasing ultracapacitor charging. The controller also provides system protection by preventing charging if the generator frequency is below 60 Hz, if the UCES is in discharge, or if the main generator breaker is open. This protection is provided by immediately resetting the module load signal to zero if one of these conditions exists.

4.7.2: Charge Limiting Rheostat

The charge limiting rheostat is a necessary device that ensures the current flow to the ultracapacitors is moderated. Without it, the ultracapacitors would essentially short circuit the system. As described in section 4.7.1, the rheostat is controlled by a module load signal varying from 0 to 10. Figure 20 shows the bottom level view of the device.

The rheostat was designed through trial and error to provide approximately 0.2 Hz speed decrease at the generator with each increase in the module load signal. The device works by having 10 resistive elements in series that can each be bypassed by an ideal switch. The main switch shown on the bottom of Figure 20 open circuits the rheostat when the module load signal is at zero: no UCES charging. In fact, with a module load signal of zero, all the switches in the rheostat are open.

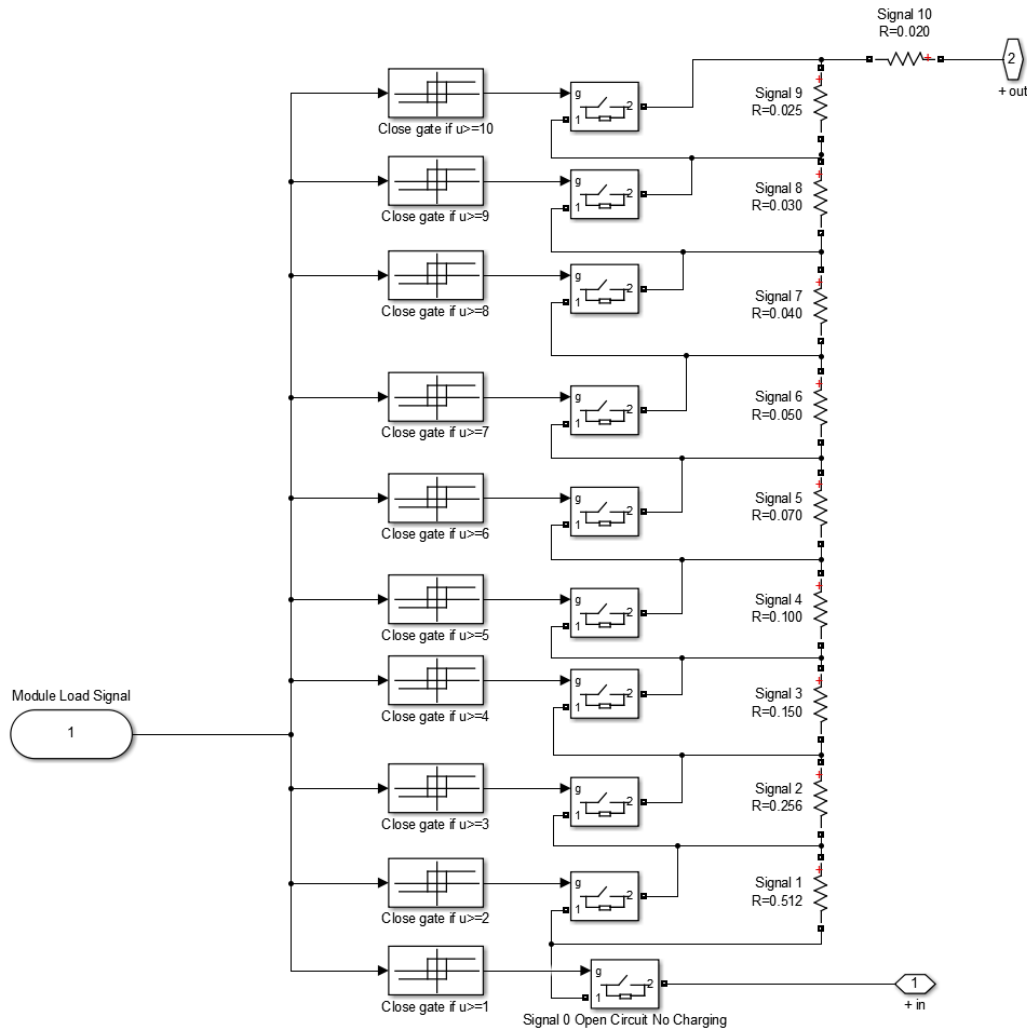


Figure 20 - Bottom Level View of the Charge Limiting Rheostat

When the module load signal increases to 1, the bottom relay closes the bottom switch, completing the rheostat circuit. In this condition, the incoming current must first pass through all ten resistive elements with a total series resistance of 0.512 Ω . This resistance limits the current flow to the UCES and prevents generator overload.

When the module load signal increases to 2, the second from the bottom relay closes, which bypasses the first resistive element labelled “Signal 1 R=0.512.” This first resistive element has a resistance of 0.256Ω. By bypassing this resistor, but no others, the total resistance drops to 0.256Ω. This increases the current flow, rate of charge, and demand on the generator.

With each successive increase in module load signal, another resistor is bypassed until a maximum load signal of 10 is reached and the rheostat imparts a mere 0.015 Ω. Keep in mind, this resistance is still far higher than the ultracapacitor module’s ESR from Table 5.

Table 6 demonstrates the relationship between module load signal and rheostat resistance.

Table 6 - Rheostat Resistance Given the Module Load Signal

Module Load Signal	0	1	2	3	4	5	6	7	8	9	10
Rheostat Resistance (mΩ)	Open Circ.	512	256	150	100	70	50	40	30	25	20

4.7.3: Charging Module

The charging module is designed to maintain the voltage supply to the ultracapacitors at 600V. The device accomplishes this by using a Proportional Integrative (PI) controller to vary the duty cycle of a DC step down converter or buck chopper. Figure 21 shows the mid-level view of the charging module, while Figure 22 shows the buck chopper.

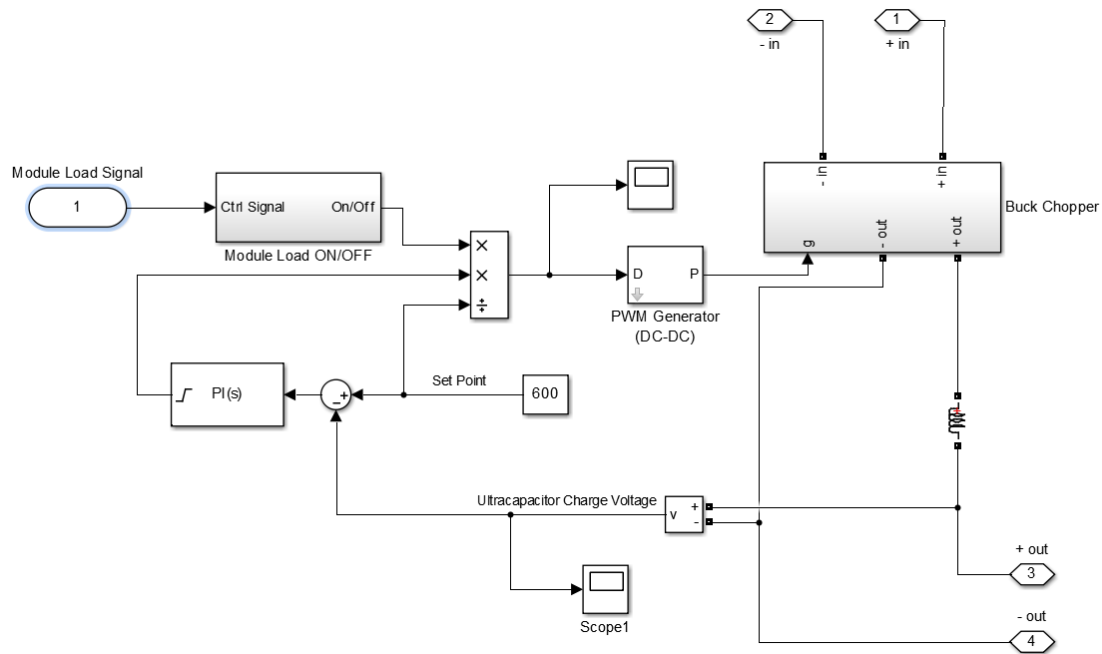


Figure 21 - Mid-level view of the Charging Module

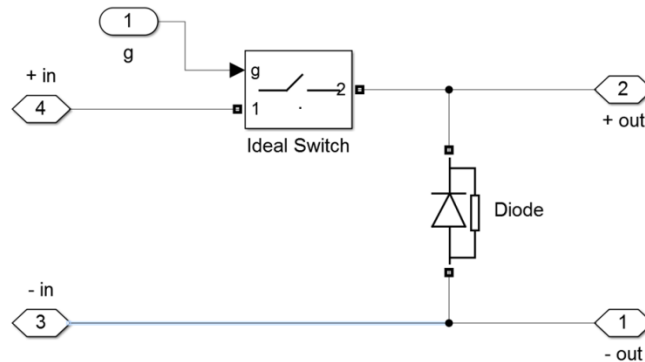


Figure 22 - Buck Chopper

The buck chopper is an elementary power electronic device designed to step down a DC voltage. It functions by using a switching device, modelled as an ideal switch above, to cut flow and provide a voltage drop. The switch is controlled by PWM. This PWM modulates its pulse width based upon a percentage (0 -1) demand from a PI controller known as the duty cycle. There is no voltage reduction at a fully duty cycle of 100%, while at 0% duty there is no current flow across the switch whatsoever.

The voltage output from the buck chopper is given by the equation [46]:

$$V_o = DV_d$$

(8)

where D is the duty cycle [0-1]; and
 V_d is the DC input voltage [volts].

The output of the buck chopper is initially discontinuous however it is smoothed by the inductive filter, consisting of 50 mH, shown in Figure 21 on page 45.

The device is predominantly self-regulated, using an internal set point of 600V as a reference point for the PI controller. Designed to respond quickly to ensure the ultracapacitors are not overcharged, the controller has a proportional gain of 1 and an integrative gain of 100. This PI controller's output is clamped between 0 and 600 with its output then divided by 600. This in turns creates a duty cycle value between 0 and 1 for use by the PWM generator.

The one external input is the module load signal. In the event that the module load signal is zero, the "Module Load ON/OFF" block will zero out any output from the PI controller. If the module load signal is any other value, the "Module Load ON/OFF" block will convert that signal to 1, providing no distortion to the PI controller output through the multiplication block.

The PI controller output, now a duty cycle value after the multiplication block, is then fed into the PWM Generator. The pulse generator, operating at 5000 Hz, creates appropriate width pulses to shut the ideal switch at the correct ratio corresponding to duty cycle value.

The net effect is that the internally set charging module effectively regulates the charge voltage to 600 VDC.

With all three major charging circuitry components working together, the ultracapacitors are kept at the correct Voltage, the generator is not overloaded, and the UCES is never charged at an inappropriate time.

4.8 : Ultracapacitor Module

The ultracapacitor module used in the simulation was the imbedded Simulink object masked as the "Supercapacitor." For ease of simulation, three of these objects were used: one uncharged module to simulate charging, and two fully charged modules to simulate discharge.

Prior to understanding how the block was implemented, the reader should first be cognizant of how Simulink itself models the non-linear capacitance.

4.8.1: Simulink's Supercapacitor Object

The Simulink supercapacitor object models ultracapacitive changes in state using charge in accordance with the equation,

$$Q_T = Q_{init} - \int I_{uc} \cdot dt \quad (9)$$

where Q_T is the current total charge [Coulombs]; and,
 I_{uc} is the current flow, into or out of the ultracapacitor [Amps].

This is required to provide accuracy as an ultracapacitor does not behave linearly due to voltage dependence capacitance. Knowing that the ultracapacitor has an electrostatic component and a diffused layer effect, Simulink translates this into a total voltage equation of two terms respectively:

$$V_T = \frac{Q_T}{C_e} + \frac{2RT}{F} \sinh^{-1} \left(\frac{Q_T}{A_i \sqrt{8RT \epsilon_o \epsilon c}} \right) \quad (10)$$

Where C_e is the electrostatic capacitance [Farads];
 R is the ideal gas constant [8.314 J·mol⁻¹·K⁻¹];
 T is temperature in Kelvin [298.15 K];
 F is the faraday constant [96,845 J·V⁻¹·g⁻¹];
 A_i is the interfacial area between electrodes and electrolyte [m²];
 ϵ_o is permittivity of the material [6.0208e-10 F·m⁻¹];
 ϵ is the permittivity of free space [8.854×10⁻¹² F·m⁻¹]; and,
 c is the molar concentration.

Finally the electrostatic capacitance is given by the equation:

$$C_e = \epsilon_o \epsilon \frac{A_i}{d} \quad (11)$$

where d is the separation between the plates [metres].

Despite the many terms in Equations 9 and 10, Simulink automatically derives most of these values from the rated capacitance using predetermined parameters with Mathworks claiming they are accurate within 2% [47].

This internal total voltage (V_T) sets the output of a DC voltage source, which simulates ultracapacitor discharge. The current flow from this source (I_{uc}) is dependent upon system load, with the actual ultracapacitors voltage output determined after calculating ESR losses as follows:

$$V_{uc} = V_T - I_{uc} R_{ESR} \quad (12)$$

where I_{uc} is the current flow out [A]; and
 R_{ESR} is the equivalent series resistance [ohms].

With each time step, the system repeats itself by integrating the current flow to determine the new Q_T (via Equation 8); updating the total voltage V_T (via Equation 9) and producing a new output current I_{uc} ; and finally calculating the new ultracapacitor voltage output V_{uc} (Equation 11).

The measurements of the discharge ultracapacitor bank are shown in FIGURE 23. The charge bank is similar but combines both modules measurement into one scope (set of figures).

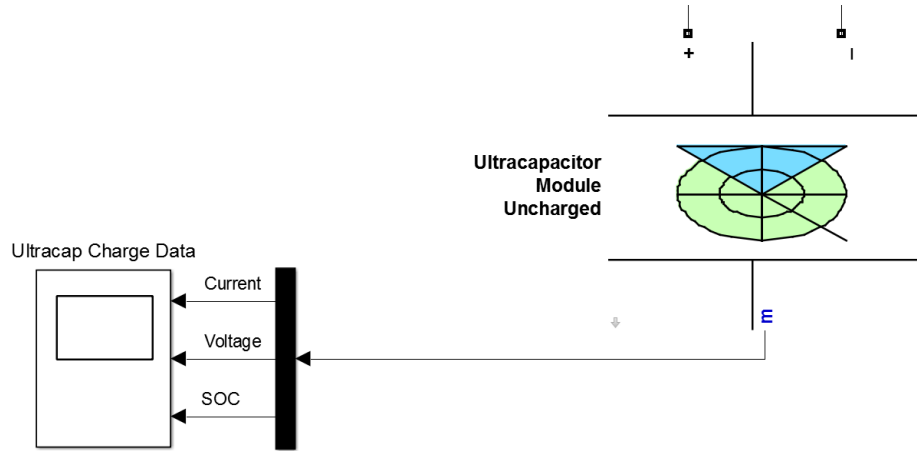


Figure 23 - Ultracapacitor Measurements

As seen in the figure above, the current and voltage data come from traditional sensors within the block. The State Of Charge (SOC) of the bank is determined again based upon charge in accordance with the equation,

$$SOC = \frac{Q_T}{Q_{max}} \times 100\% \quad (13)$$

where Q_{max} is the total possible charge based upon the rated voltage.

4.8.2: Ultracapacitor Module Implementation

In order to increase the speed of simulation, the three ultracapacitors blocks used were initially treated as single cell units with the specifications from Table 5: capacitance of 12595F; ESR of 38.3 $\mu\Omega$; and, an operating voltage of 600V. However, it became necessary to further reduce the capacitance to one tenth the value to shorten run times. As such the single module on the charging side had a capacitance of 1259.5 F, and the two discharge modules that provide power to the system each had a capacitance of 629.75 F or a combined value of 1259.5F.

The ultracapacitor module on the charge side has an initial voltage of zero volts. Charged by the charging circuitry, it serves as a means to estimate total charge time. With its capacitance representing 10% of the overall system capacitance, total system charge times were assumed to be approximately ten fold the time or projected time it took to bring this uncharged ultracapacitor bank to full charge.

On the discharge side are two fully charged modules that serve to power the ship's load in the event of generator failure. Combined, they represent 10% of overall capacitance. Like the charging bank, total system discharge times were also assumed to be tenfold longer than this smaller module could provide.

As the modules discharge, their overall voltage drops. The discharge modules were split into two 5% modules to provide a more uniform input voltage into the inverter. By splitting the modules, they were able to be rearranged as required into a series configuration to double their voltage. This allowed the system to be able to draw more power from the modules, prior to failing on under voltage. This varying parallel series arrangement is further explained in the following section.

4.9 : Discharge Circuitry

The purpose of the discharge circuitry is to invert the DC output of the fully charged ultracapacitive modules to provide three phase power at 260VAC. This power is then stepped back to system voltage through the main transformer bank.

Figure 24 shows the top level view of the discharge circuitry with its major components: the Discharge Controller and the Controlled Inverter. The two banks of ultracapacitors are also included in the figure for reference but they are part of the discharge circuitry itself.

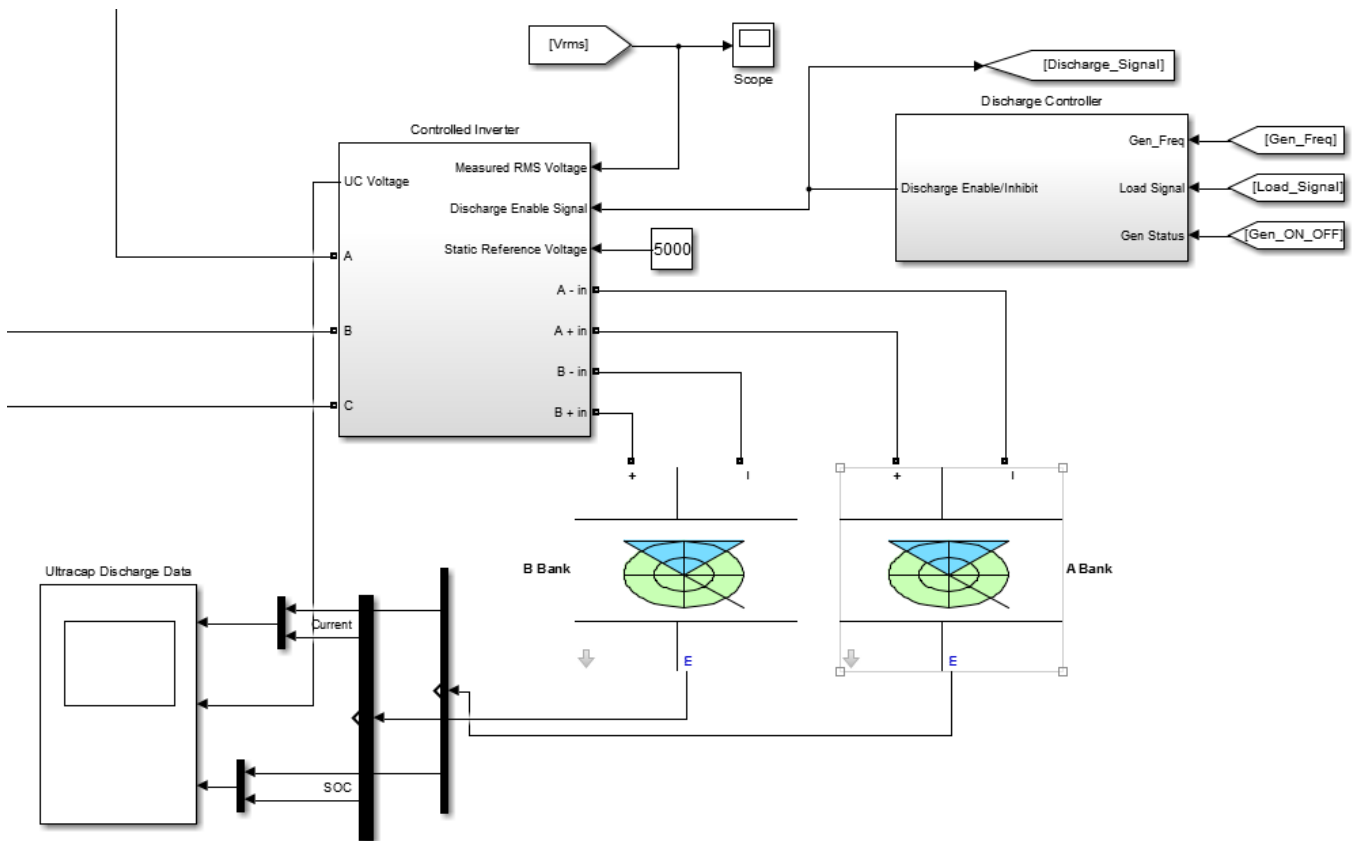


Figure 24 - Top level view of Discharge Circuitry

These two components each provide an essential role. Similar in function to the module load controller, the Discharge Controller provides a binary signal to begin or terminate ultracapacitor discharge. The controlled inverter assembly provides two functions: to place the ultracapacitive modules in series or parallel arrangement and to invert that output into an AC waveform.

4.9.1: Discharge Controller

The discharge controller is a logic controller with three inputs: Gen_Freq, (Module) Load_Signal, and Gen_ON_OFF. By monitoring these inputs, the device can successfully determine when discharging operations should occur.

Figure 25 shows the bottom view of the Discharge Controller's components.

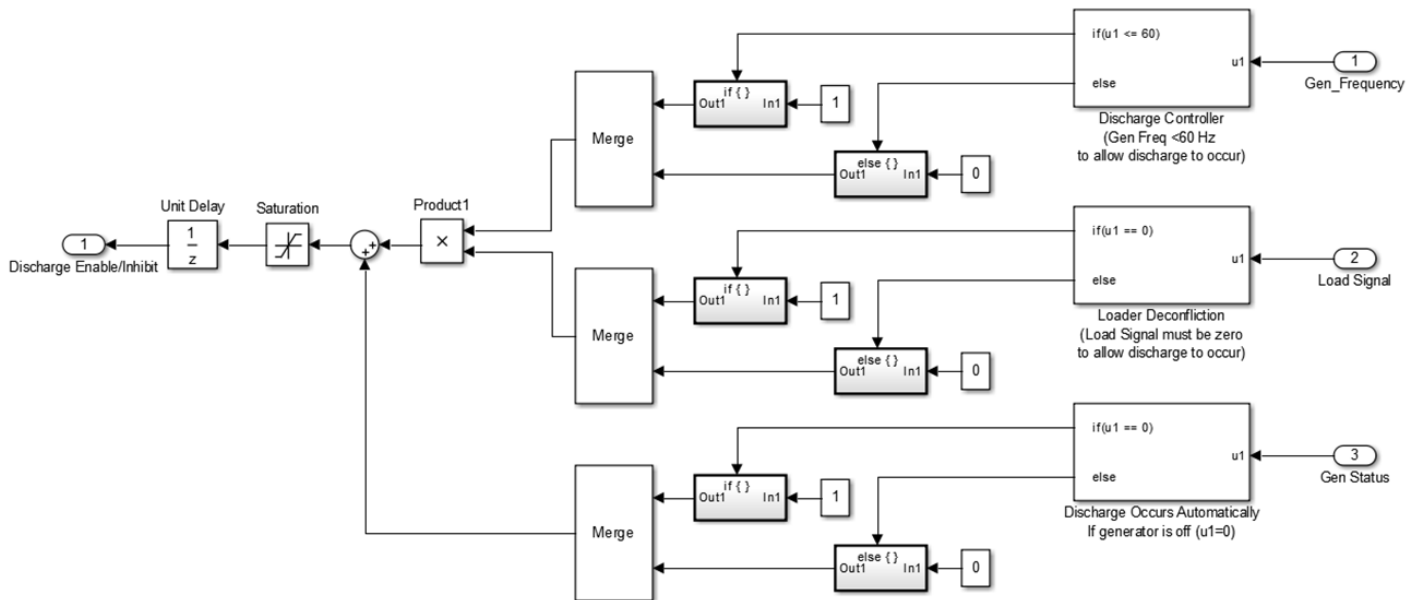


Figure 25 - Bottom Level View of Discharge Controller

Under paralleling conditions the discharge controller engages when two conditions are both met. First, the Gen Frequency signal must be less than 60Hz; and, secondly, the (Module) Load Signal must also be zero. These functions are performed by the logic blocks on the right of Figure 25.

These two conditions must be met for the following reasons. If the Module Load Signal is greater than zero, than charging operations are occurring and discharge should not be occurring. If the generator speed is greater than 60Hz, than the generator is not being overloaded and discharge should not be occurring. These conditions imply that discharge can occur when the generator is running. This is because the UCES model was originally designed with generator paralleling but it was not successfully simulated.

Under the operations that the simulation was able to achieve, the UCES acts as a UPS: a sole source power provider. The bottom logic block, and its associated sub blocks, labelled “Discharge Occurs Automatically...” provides a binary true signal if the Gen Status input is zero. This signal indicates if the generator main breaker is open, and if it is, the UCES should be discharging to provide power to the ship’s load.

The single output on the left of Figure 25 delivers the result from this logical analysis: a binary signal that allows ultracapacitor bank discharge to occur if the output is 1, or prevents discharging from occurring if the signal is 0. This Discharge Signal is then fed to the Module Load Controller to inhibit charging operations should they be occurring and to the Controlled Inverter for discharge to begin.

4.9.2: Controlled Inverter

Figure 26 shows the mid-level view of the controlled inverter.

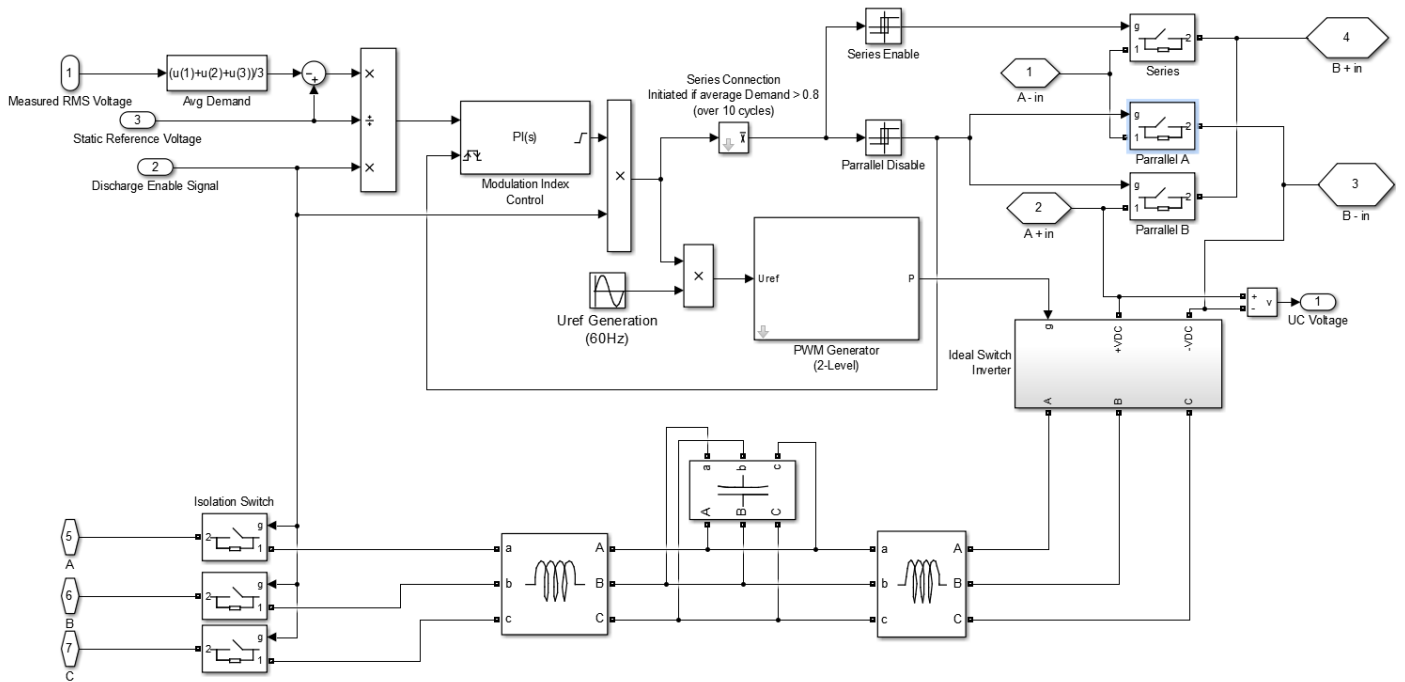


Figure 26 – Mid-Level View of the Controlled Inverter

The main purpose of this device is to invert the DC voltage provided by the charged ultracapacitor banks to 260 VAC. With most other UCES, a DC/DC converter regulates the output of the ultracapacitors, which is then inverted. This device above is able to do so without the need for DC/DC regulation as the DC/AC converter is able to provide a stable output despite the dropping voltage from the ultracapacitors.

The regulation is provided by a PI controller controlling the modulation index of the PWM generator. The details of which we be explained in the paragraphs to follow.

The top right of Figure 26 show the physical inputs from the two banks of charged ultracapacitors defined as A bank and B bank. These inputs are labelled “A + in, A - in, B + in, and B - in.” These physical lines are run through a set of switches that allows their arrangement to be changed from parallel to series.

Under the parallel arrangement, the ideal switches labelled “Parallel A” and “Parallel B” are both closed, while the “series” switch is open. When in the series configuration, both parallel switches are open, while the series switch is closed. After which point, the DC power flows through the ideal switch inverter shown in Figure 27.

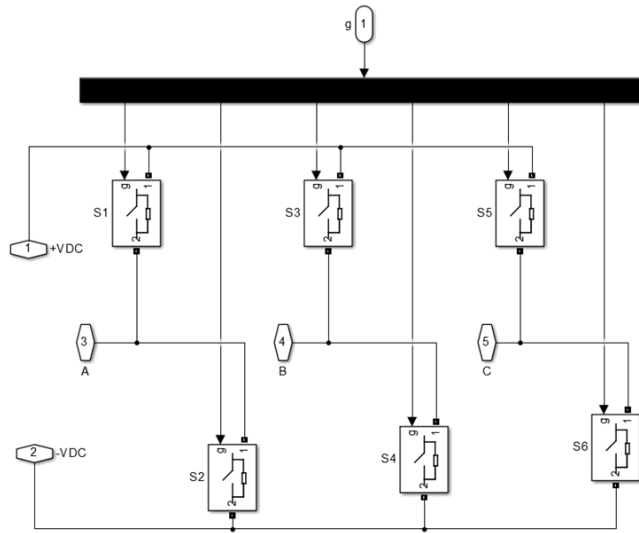


Figure 27 - Bottom Level View of Ideal Switch Inverter

The inverter is controlled by the PWM generator. The PWM provides gate controlling pulses into the inverter in the correct sequence to generate a piecemeal sine wave. The switches S1 and S2 from Figure 27 create the positive and negative sequence of phase A respectively, while S3 and S4 create phase B's sine wave, and S5 and S6 create phase C's wave.

Turning back to Figure 26, this piece meal sign wave output is then smoothed by the LCL filter consisting of two 20 μ H inline inductive elements and three large 110 mF capacitors running between each phase. The rapid switching of the PWM at 6 kHz also provides boosting through the LCL filter similar in nature to a DC/DC boost converter. This produces a smooth output in accordance with the equation [48],

$$V_{ao}(t) = km_i \frac{V_d}{2} \sin(\omega t) \quad (14)$$

Where V_{ao} is the A phase voltage at the fundamental frequency [volts];

m_i is the modulation index [0-1];

V_d is the DC voltage input [volts];

ω is the angular speed derived from the voltage reference signal [rad/s]; and,

k is the author derived constant from LCL filter boosting [a constant of value 4.55].

From this equation, the controllable variable presents itself. The DC voltage (V_d) cannot be controlled as it is a function of the decaying voltage during ultracapacitor discharge. In addition, the angular speed must be set at 60Hz to match system frequency. That leaves only the modulation index that can provide linear gain at values from 0 to 1. (A modulation index above 1 creates an over modulated and distorted output). With only one real control variable, the PI controller was implemented to adjust the modulation index into the PWM generator.

As seen on the top left of Figure 26, there are three sensor inputs. The first is the measured rms value, with its sub block taking the average of all three phases of the system main. The PI controller, using a proportional gain of 0.5 and an integrative gain of 2, varies the m_i to maintain 5000 VAC at the main.

The next input is the static reference voltage of 5000V. Through a multiplication block this turns the error signal ($V_{ref} - V_{rms}$) into a per unit value. Also in this multiplication block is the discharge enable signal that zeroes the error signal if the system is not in discharge. This leaves the PI controller at its last known position, but does not reset it.

The discharge enable signal provides isolation on multiple fronts when its value is zero. Isolation is provided through the inverter, where the zero input into the PWM forces all inverter switches open, as well as a set of isolation switches a set of isolation switches located in the bottom left of Figure 26.

During discharge operation, the PI filter continually changes the modulation index to ensure a voltage of 5000V is achieved at the main. The block labelled “Uref Generation” produces the 60Hz reference signal that is multiplied with the modulation index and fed into the PWM generator. From this, the inverter is switched in the correct order to produce a piecemeal sine wave at 60Hz, which is then smoothed to produce a near ideal sinusoidal output.

As the ultracapacitors discharge, the DC voltage at the inverter drops. The PI controller increases the modulation index to compensate, but it cannot be increased above 1 without distortion. In fact the PI controller’s output is clamped between 0 and 1. As the system approaches high demand, a set of relays monitors the output of the PI controller. When the modulation index is increased above 0.8 for 10 cycles, the relays at the top of Figure 26 change the parallel and series switches to a series connection. This effectively doubles the input voltage, and allows the inverter to maintain power at the desired output voltage (260V) for a longer period of time.

The series connection has no risk of damaging the ultracapacitors as it only engages during discharge when the input voltage is inadequate: the ultracapacitors are already partially depleted. During the switch over, the PI controller continues almost seamlessly. This is because the change in the parallel/series switches also triggers a controller reset to a modulation index of 0.4

In summary, on high inverter demand where the modulation index is greater than 0.8, the ultracapacitors are reconfigured to a series connection, doubling the input voltage, and the modulation index is reset by the PI controller to 0.4. If the demand were to suddenly fall and the modulation index falls below 0.2, the system reverts the ultracapacitors to a parallel connection, halving the input voltage, and the modulation index is reset to 0.4.

Through this arrangement, the model showed that it could continue to draw power out of the ultracapacitors for increased durations, even to the point where the SOC was below 10% under some loads.

As this section has shown, the controlled inverter effectively changes the variable DC input voltage from the ultracapacitors to a regulated output voltage of 260VAC. This waveform is then stepped up through the main transformer to 5000VAC. Through the use of the discharge controller, the UCES model also knows when to engage and disengage.

This concludes the system description. This chapter has demonstrated how the system model works. Although complex, the system can be summarized as follows.

When the 15MW speed droop controlled generator is in operation, the UCES siphons available power for ultracapacitor bank charging. The Module Load Controller determines how much power is available for charging, based upon changes in system frequency, and sets the Charge Limiting Rheostat appropriately. During this process, power is converted from 5000VAC to 260VAC over the main transformer; rectified through the three phase diode rectifier assembly; and, then regulated to 600VDC through the Charging Module. This effectively charges the discharged bank of ultracapacitors which represent 10% of the total module capacitance.

Discharge occurs when the generator's main breaker is open, and the generator is unable to power the ship's load. When this occurs, the Discharge Controller initiates the logic sequence allowing power to be drawn from the two banks of charged ultracapacitors that collectively represent 10% of the total module capacitance. The output from these two ultracapacitive banks produces a decaying DC voltage that can be doubled by rearranging the banks in series. This variable DC voltage is then inverted and regulated through Controlled Inverter that produces a steady 260VAC output. This 260VAC power is then stepped up to 5000V, through the main transformer to power the ship's load.

Now that the reader is familiar with how the system works, it is time to examine the results obtained.

CHAPTER 5 : METHOD AND RESULTS

5.1 : Introduction

The ship's system model presented in the previous chapter contains many variables and thus presents many ways in which the simulation of the model could be presented. In addition to the model, the Simulink simulation software itself presents many different ways in which to run an electrical simulation. This chapter will discuss the software parameters used to simulate the system and then present the various testing methods and their results.

5.2 : Simulink Simulation Parameters

Electrical system modelling in Simulink is performed with one of two different simulation time step modes: discrete or continuous. These features are accessed through the "Power GUI" block. This block must be present for Simulink to simulate an electrical system.

In discrete mode, the user sets a defined time step. For the purposes of these simulations, this was generally in the range of 1 ms to 10 μ s. Discrete mode offers a faster response time over continuous mode, but creates more system chatter, and does not simulate ideal switching devices. Snubbers must be present in diodes and switches.

In continuous mode, Simulink takes variable steps sizes as required by the system to preserve accuracy. This mode produces much more accurate results, with considerably less system chatter. Despite these advantages, the author was often unable to simulate the system in this mode, and did so only when discrete mode proved otherwise unsuccessful. Due to the complexity of the model, simulations conducted in continuous mode often took extremely small step sizes in the order of $1e-9$. This small step size not only created extremely long run times, but also created a large number of data points. These data points, and quite possibly the simulation itself, overloaded available computer system memory (RAM) and caused the simulation to terminate unexpectedly.

Figure 28 displays the results of a 15MW discharging under discrete mode, while Figure 29 shows the same simulation under continuous mode. Both figures display 6 seconds of simulation time. The discrete mode took just a few minutes to run, while the continuous mode took over 3 hours.

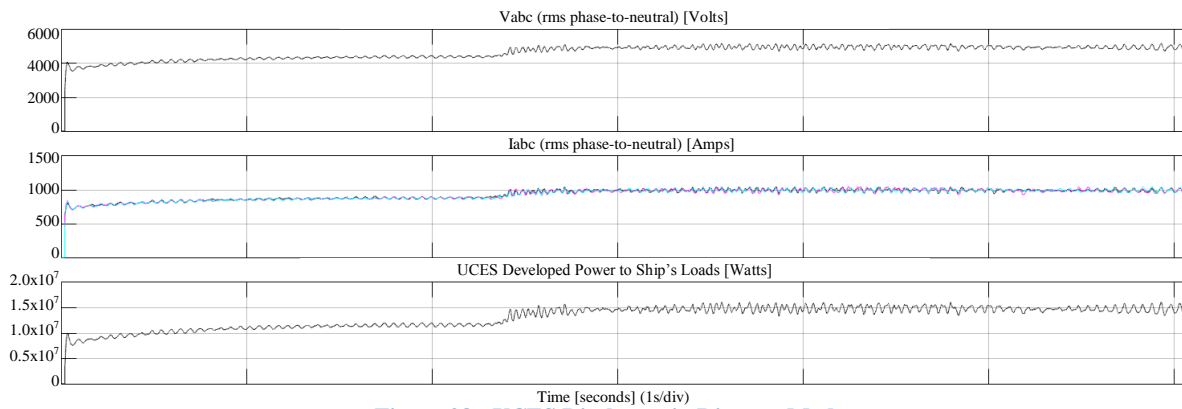


Figure 28 - UCES Discharge in Discrete Mode

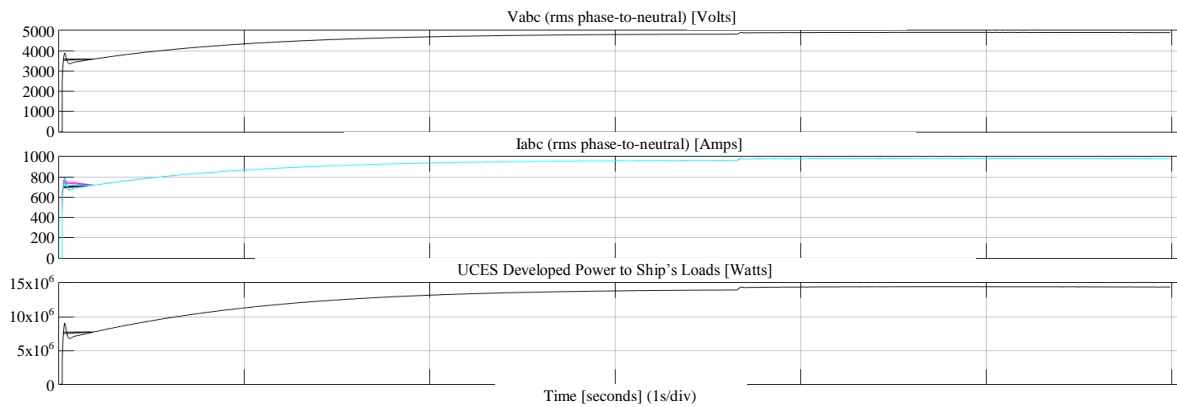


Figure 29 - UCES Discharge in Continuous Mode

As the system grew in size, discrete mode became increasingly unstable. Not only was significant system chatter present, such as the 1MW power fluctuation in Figure 28, but simulations would often halt due to infinite or zero value errors. These errors often occurred under steady-state conditions and were not the result of a system event. Changing system parameters such as the load or time step would alter when these errors occurred; however, the only way to eliminate them entirely was to run the simulation in continuous mode.

This phenomenon created a dilemma. Under some conditions the system could not be modelled in discrete mode, yet continuous mode overloaded available computer resources before producing useful results. These errors ultimately led to the abandonment of UCES with generator paralleling as a thesis objective.

As continuous mode simulation was generally unachievable, most simulations were conducted in discrete mode. When examining the results, the reader should be cognizant of the extreme chatter created by the discrete simulation of the model. This chatter is not a result of system design, but of simulation methods. The pertinent information displayed in the figures located within this chapter and the thesis annexes are the trend lines.

In addition to discrete versus continuous mode, Simulink also offers different methods of executing a simulation. Accelerator and Rapid Accelerator generate executable code to allow for faster run times. These modes can only be run with the Ordinary Differential Equation 45 (ODE45) solver and are unable to provide error and warning messages [49]. As such, a problem encountered during an accelerated simulation often required a system rerun in the longer normal mode. Nevertheless, with a normal-mode single-simulation run time sometimes exceeding an hour, the rapid accelerator and accelerator modes were often used to run longer simulations.

5.3 : System Simulation Methods and Results

The model provided many different ways in which the simulation and its results could be shown. The following sections will present the results of the UCES charging and discharging under static loads, and also provide a discussion on load changes during charging operations and Generator to UCES transitions.

As stated previously, all loads were kept a constant PF of 0.85 lagging. As such, the reactive component matched any changes in the resistive load to preserve this balance. The results are as follows.

5.3.1: Module Charging under a Static Load

Charging of the ultracapacitors was initially done under conditions of static load. Without a change in loading, the time it would take to charge the ultracapacitor can be well projected. In order to reduce simulation time the UCES discharge components were “commented out,” a Simulink term for disabled, during these charging operations.

Figure 30 shows the generator data during charging operations at a static 1 MW load. The top graph in the figure is the rms voltage produced at the generator. As the simulation was run in discrete mode with a step time of 1ms, there is significant chatter in these rms values, yet the voltage remains at a constant 5000V rms. The second from the top graph shows rms current separation consistent with an unbalanced load. This is not accurate, as all loads are balanced. The large step time in discrete mode consistently showed current separation.

The middle two graphs show the active and reactive powers respectively. These graphs again reveal a large amount of chatter in these values attributed to poor rms block output during frequency changes. The chatter occurs predominantly at half second intervals, which coincides with a generator speed change. In addition, there are more pronounced voltage, current, and power spikes that occur at each change in the module load signal.

Despite this interference, the generator is accurately powering the 1MW and 0.6 MVAR load prior to UCES system charging.

The second from the bottom graphs shows generator frequency. If only the static load of 1MW was present, the generator would have achieved a steady state speed of 61.4 Hz. After two seconds of operation, however, UCES charging begins. The module load signal on the bottom graphs provides an indication of UCES load. As each successive rheostat element is removed, more and more current flow into the ultracapacitor module is permitted.

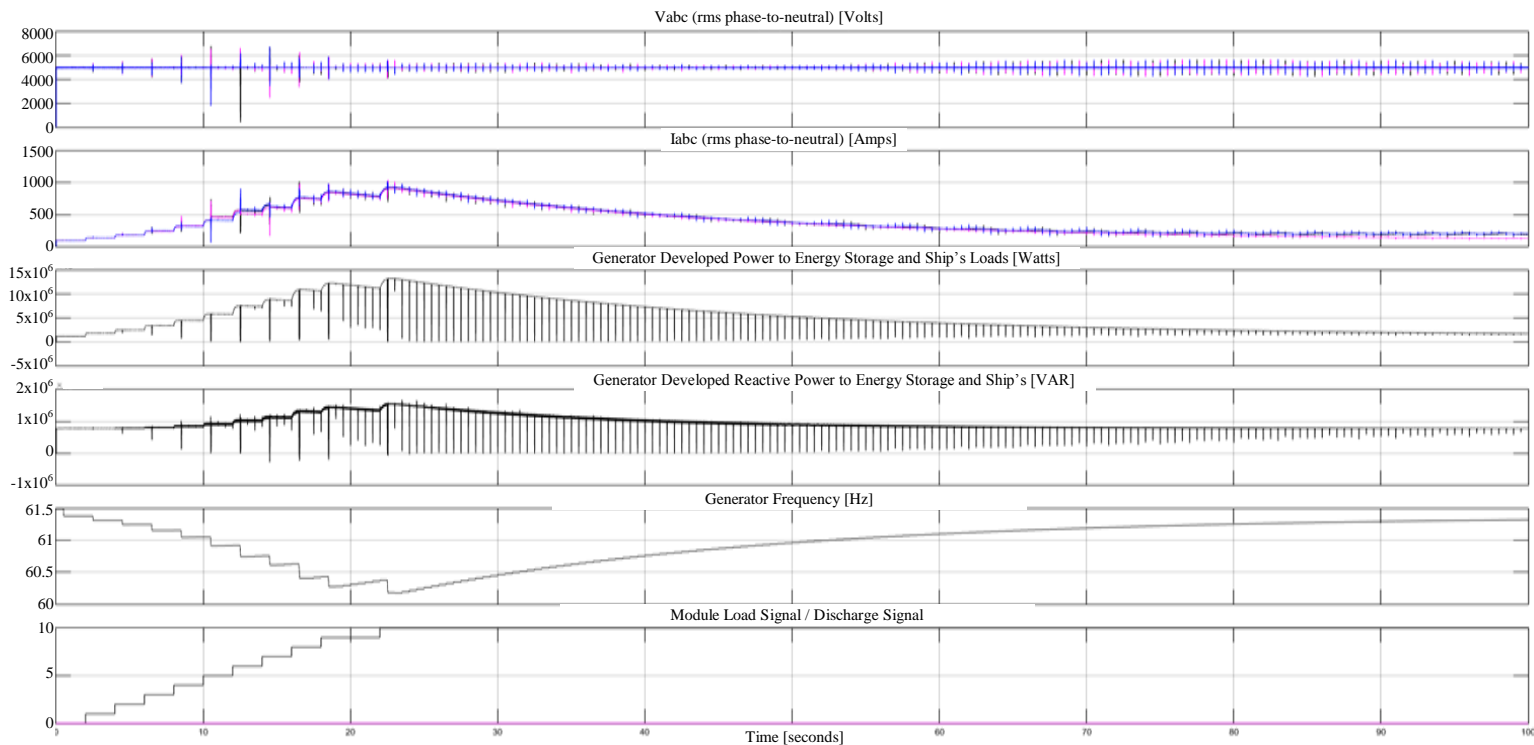


Figure 30 - Generator Data for UCES Charging at 1 MW Load

Figure 31 reveals what is occurring at the ultracapacitor bank itself. With each successive increase in module load signal the current flow, shown in the top graph, increases. The bypassing of successive resistors in the Charge Limiting Rheostat allows for the step increases in current seen in the top graph.

As the charge accumulates, the voltage in the second graph gradually increases from 0 to a little less than 600V. As the voltage builds, the current flow would decrease under steady state conditions; however, this is compensated for by bypassing successive resistive elements in the charge limiting rheostat.

After 100s of operation the ultracapacitor module is nearly fully charged at 92%. This SOC is revealed in the bottom graph. From this, a linear approximation projects that a real module of 12595F capacity could be charged using available generator power in approximately 18 minutes.

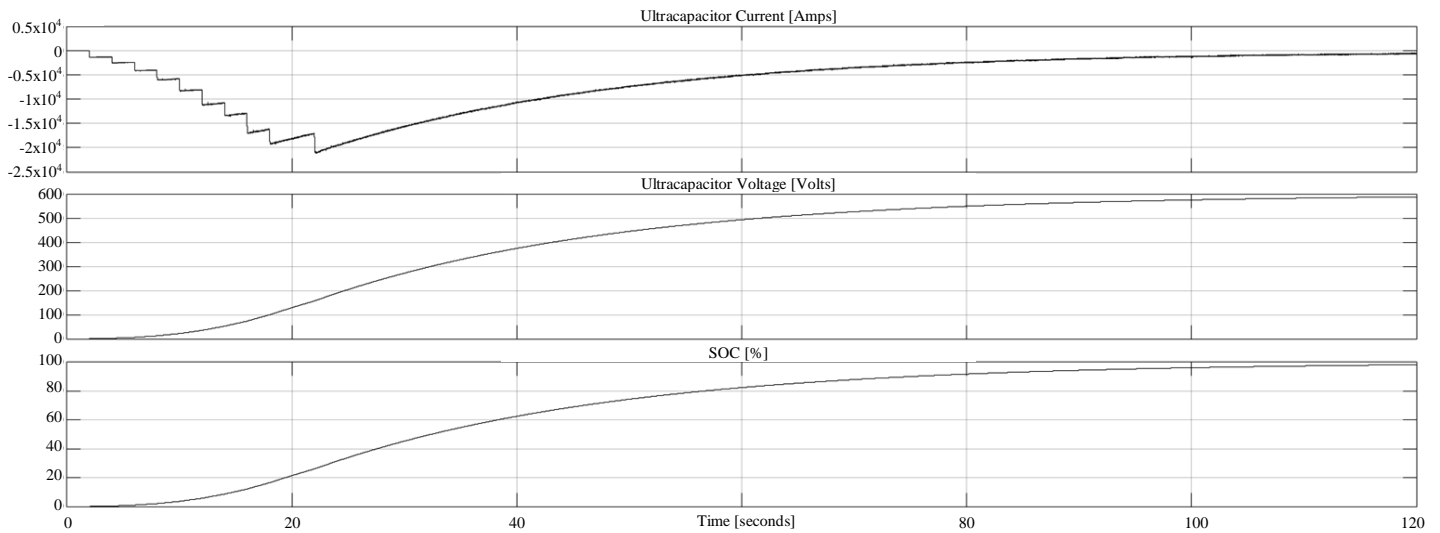


Figure 31 - Ultracapacitor Charge Data at 1 MW Load

The dominant trend that the above graphs reveal is that the ultracapacitor banks can experience fast charging initially and decrease their rate of charge as they approach full charge. A closer examination of the top graph reveals what is happening with the current flow.

Initially, there is no charging of the ultracapacitors and as such no current. This is because the Module Load Controller only polls every two seconds. After two seconds, the module load signal is increased to 1, allowing some flow through the Charge Limiting Rheostat and into the ultracapacitor banks. This flow is increased every two seconds until the Module Load Signal reaches a value of 9 at 18 seconds.

With a Module Load Signal of 9, there is little restriction on current flow into the ultracapacitors. This puts significant demand on the generator and the system frequency drops below 60.3 Hz. As such, there is no increase in Module Load Signal at the next polling interval (20 seconds) because the system frequency is too low. However, the current flow into the ultracapacitor between 18 and 22 seconds steadily decreases as the ultracapacitor builds charge. This is because the difference between the DC charging voltage and the ultracapacitor internal voltage is decreasing.

At 22 seconds, the Module Load Controller polls the system frequency. As the system frequency is now above 60.3 Hz, thanks to the decrease in current flow into the ultracapacitors, the module load signal is increase to 10. This drops the resistance of the Charge Limiting Rheostat to its minimum value of 20mΩ. As such, there is sharp increase in current, which then again begins decreasing as the ultracapacitors continue to charge.

At 30 seconds, the system frequency, shown in Figure 30, is approximately 60.5Hz. This value correlates to a generator loading of about 10MW. Although the 15MW generator is fully capable of providing extra charging to the ultracapacitors, it is unable to do so as the Charge Limiting Rheostat is already at its minimum resistance. This reveals that a redesign with more rheostat settings would allow for faster ultracapacitor charge times.

Similar graphs to Figure 30 and Figure 31 were produced for a static load at each 1MW interval up to 12 MW load. Loads in excess of 12MW result in a generator frequency of 60.3Hz, preventing the module load controller from initiating charging operations. As such, there was no purpose in generating data for loads above 12 MW. All of these graphs can be found in Appendix A, but for brevity they were not all included for the discussion in this chapter.

Table 7 provides a summary of the results for each of the loading conditions and a linear approximation of how long a full bank of ultracapacitors would take to charge – as opposed to the 10% capacity module used in the model.

Table 7 - UCES Charging Under Static Load Conditions

Ship's Loads (MW)	Ship's Loads (MVAR)	Power Factor	SOC Achieved in Model's Ultracapacitive Bank(%)	Run Time (s)	Discrete Mode Step Time (μs)	Simulation Method	Rough Time Estimate to Charge a 12595F Bank of Ultracapacitors (min)
1	0.6	0.85	92	100	100	Rapid Accelerator	18.1
2	1.2	0.85	100	60	10	Accelerator	10.0
3	1.9	0.85	100	67	1000	Rapid Accelerator	11.2
4	2.5	0.85	100	55	1000	Rapid Accelerator	9.2
5	3.1	0.85	92	150	500	Accelerator	27.2
6	3.7	0.85	94	150	500	Accelerator	26.6
7	4.3	0.85	100	136	50	Rapid Accelerator	22.7
8	5.0	0.85	98.5	140	1000	Accelerator	23.7
9	5.6	0.85	100	111	1000	Rapid Accelerator	18.5
10	6.2	0.85	82	150	1000	Rapid Accelerator	30.5
11	6.8	0.85	45	150	500	Rapid Accelerator	55.6

The author fully expected that at lower ship's loads the generator would have more power available to charge the ultracapacitive bank. Thus, one would expect a linear increase in expected charge time as the load increases. The table above shows a wide dispersion of results, with estimated charge times varying from those logical expectations.

There are many reasons for this non-uniform change in charge times with static load. The control system within the model produced a wide range of results as did the simulation environment itself. As an example, Figure 32 shows the generator data for charging operations at a load of 2MW.

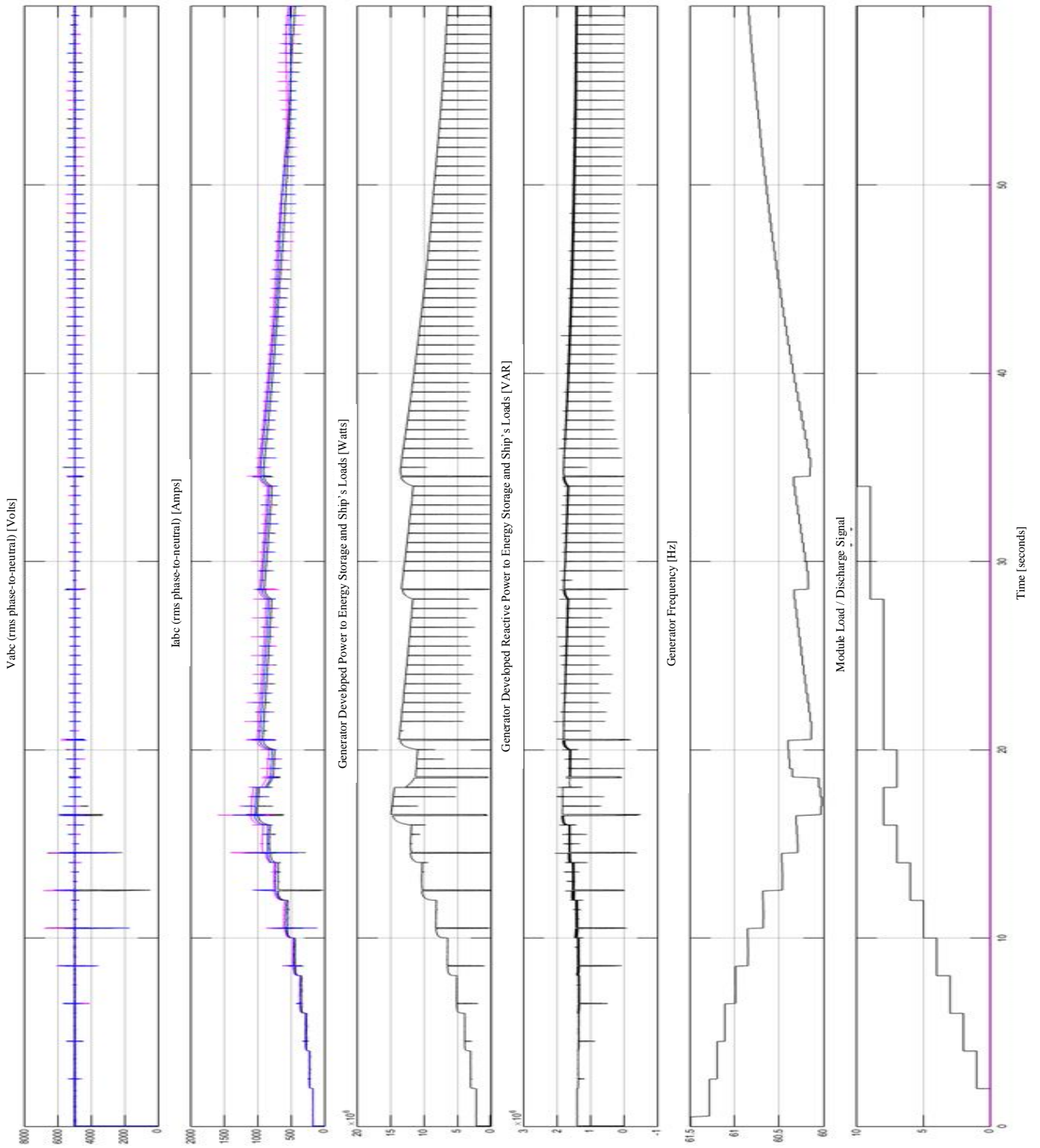


Figure 32 - Generator Data for UCES Charging at 2 MW Load

This run was produced using a discrete time step of 10 μ s under the rapid accelerator mode. As mentioned previously, different time steps were used if the model failed to simulate under a previous time step. Yet, using different time steps produced varying results. For instance charging the ultracapacitors with a 2MW load under a time step of 1 ms, found that even after 150s the system was not charged. Meanwhile, charging the ultracapacitors with the same ship's load but with a time step of 10 μ s fully charged the UCESS in 60 seconds.

Figure 33 shows the results for ultracapacitive charging at 2MW ship's load with a discrete step time of 10 μ s, while Figure 34 shows the same results with a step time of 10 ms.

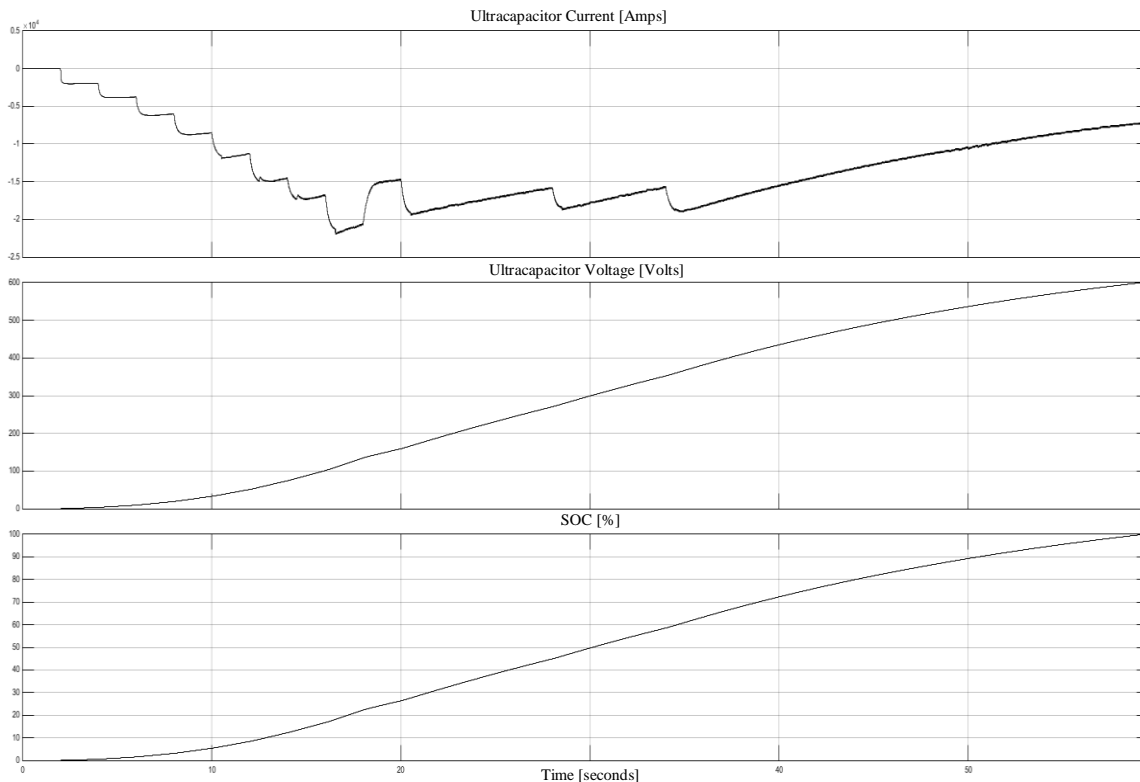


Figure 33 - Ultracapacitor Charge Data at 2 MW Load Step Time 10 μ s

The above figure shows the fastest ultracapacitor charge time. In this simulation there is an inrush current of over 20 kA. This high current was of course in response to a rapid increase of Module Load Signal. At 16 seconds, the Module Load Signal increased to 8, which drove the system frequency below 60.1 Hz. As the generator was now close to being overloaded, the system responded correctly by reducing the Module Load Signal to 7 at the next polling cycle.

At 18 seconds, the system decreases UCES charging load and protects the generator by increasing the resistance imparted by the Charge Limiting Rheostat and thus decreases the current. As the simulation doesn't model component overload, some consideration must be given to how much current the ultracapacitors can handle.

Even with an inrush current significantly higher than the one shown above, there is no risk of overloading the ultracapacitors themselves as they are designed for just that. Assuming a current of 30 kA each of the 1150 strings would be subjected to an average peak current of 26 amps, well within the design tolerance of 2.4 kA per cell [39].

Figure 34 is presented below to return to the comparison of the same simulations being executed under different discrete step times.

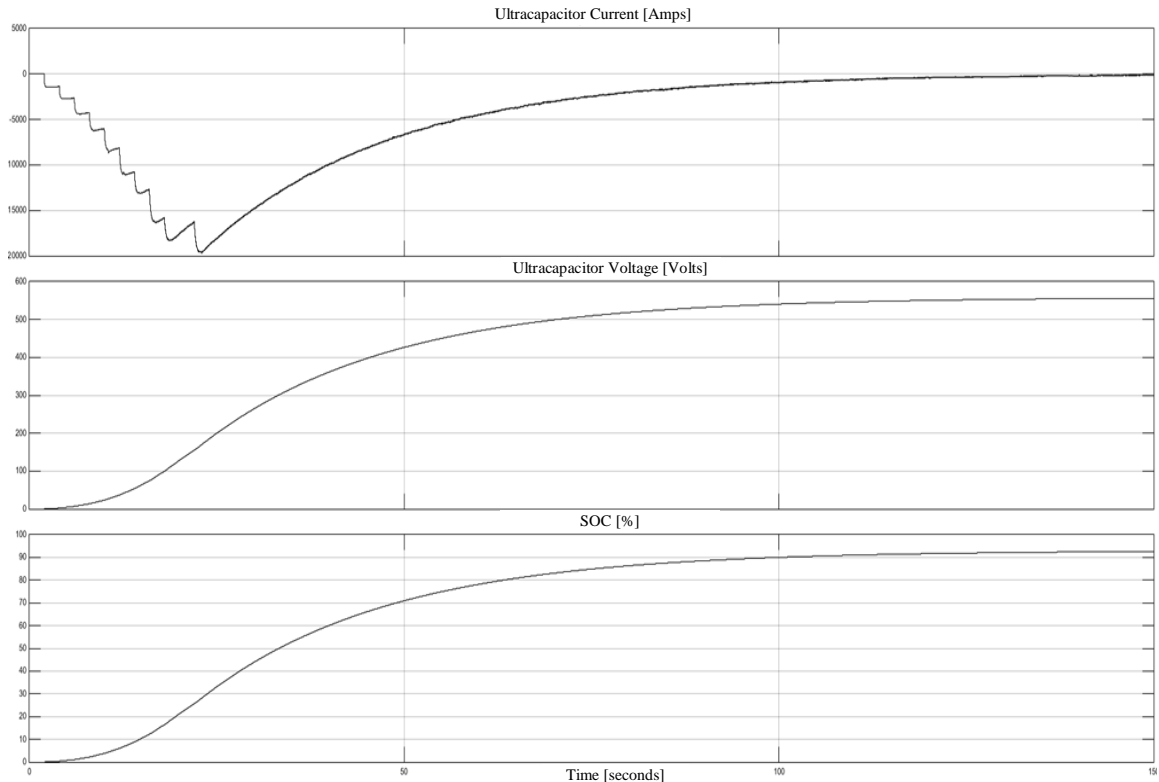


Figure 34 - Ultracapacitor Charge Data at 2 MW Load Step Time 10 ms

The above figure reveals that the ultracapacitor voltage reaches an upper limit of around 550V at 150 seconds; yet, there is little current flow at this point, and the ultracapacitors have only reached 92% charge. The large step times consistently produced widely different results from PI controllers. In this case, the PI controller controlled buck chopper is stifling current flow even though the ultracapacitor is not fully charged.

Yet with a step time of 10 μ s, Figure 33 shows high current flow into the ultracapacitive bank right up until the UCES is fully charged at 60 seconds. The end result was a significantly faster charge time with no changes in any of the system parameters.

This wide dispersity in results that was produced by simply changing step times was significant. Ideally, all simulations should have been conducted under the same step time. In addition, that step time should have been as small as hardware limitations allowed for; however, some simulations would not execute correctly at some step times.

As there is a wide dispersity in the information provided for the charging system, the pertinent result from Table 7 is the order of charge time. A system using a full bank of ultracapacitor (12595F) can be charged from a 15MW generator in approximately 10 to 30 minutes.

This four page discussion concludes the results of UCES charging under static load conditions. What this section has shown is the charging scenario using the 1MW load as an example; a summary of ultracapacitive charging under static loads in Table 7; an analysis showing the ultracapacitors ability to handle high current; a demonstration of correct operation of frequency responsive protection via the Module Load Controller to high power demand; and, finally, a discussion upon some of the difficulties experienced during model simulation using the 2MW run as an example. Again, the full spectrum of results can be found in Appendix A.

5.3.2: Module Discharging to a Static Load

The static load discharge provides a reliable method to project ultracapacitor endurance for a given power setting. Just as in the previous section, ultracapacitors were discharged at each 1MW interval for loads from 1 to 15 MW. Again, discrete mode created significant artificial chatter but was the only viable option in producing simulations greater than a few seconds.

Figure 35 shows the UCES under discharge to a 9MW load at 5000V and 60Hz. This figure will be used as an orientation to the results of these runs.

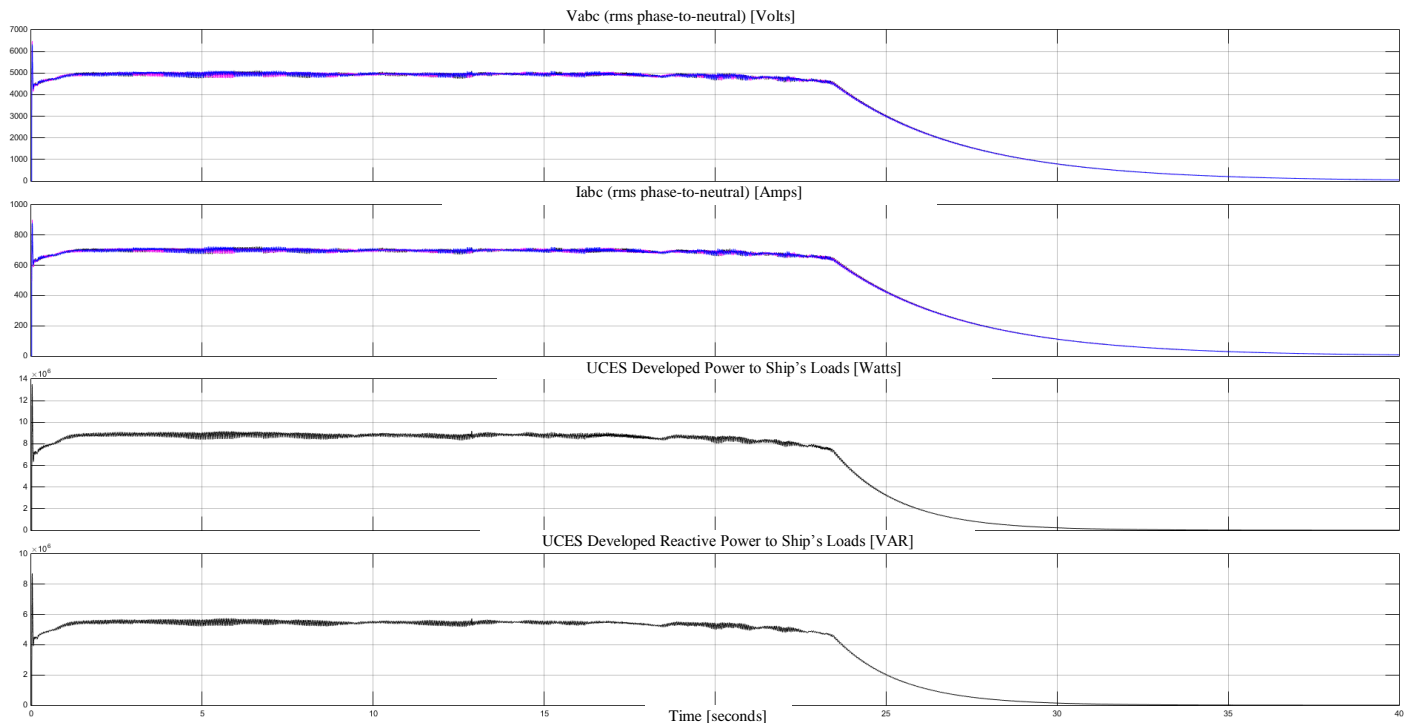


Figure 35 - UCES Discharge to a 9 MW Load

The figure above shows four graphs all pertaining to the system main: the three phase rms voltages, the three phase rms currents, the active power being provided to the load, and the reactive power being provided to the load.

The system shows a slight under voltage; this is mainly a product of a slower PI controller than ideal. Unfortunately a more responsive controller significantly increased chatter and even created instability in discrete mode simulations. As such, the system suffered from a slight under voltage at increasing loads, particularly those above 9MWs. These translated into 0.5 to 1 MW under delivery of power during UCES discharge for those high demand loads.

Another pertinent observation is the power fall off. Unlike a traditional generator, the UCES currents fall off with voltage. This is because there simply is no power left. The advantage here is that the system can be run in an emergency until all power is lost. The damaging “brown out” phenomenon, where current surges to compensate for falling voltages, does not occur as the UCES runs out of stored energy.

After 23.5 seconds, the ultracapacitors are obviously depleted and the system voltage starts to fall. To create a baseline a point of failure must be determined to establish system endurance. Reference [50] defines voltage sag as drop to between 0.1 to 0.9 per-unit (pu) for a short duration. This thesis assumes a point of failure once the voltage falls below 0.9 pu or 4500V. In the figure above this sag or failure point is reached after 23.5 seconds of UCES operation.

This failure point also coincides with what is happening at the ultracapacitor banks. Figure 36 shows the output current, voltage, and SOC respectively from the fully charged ultracapacitors.

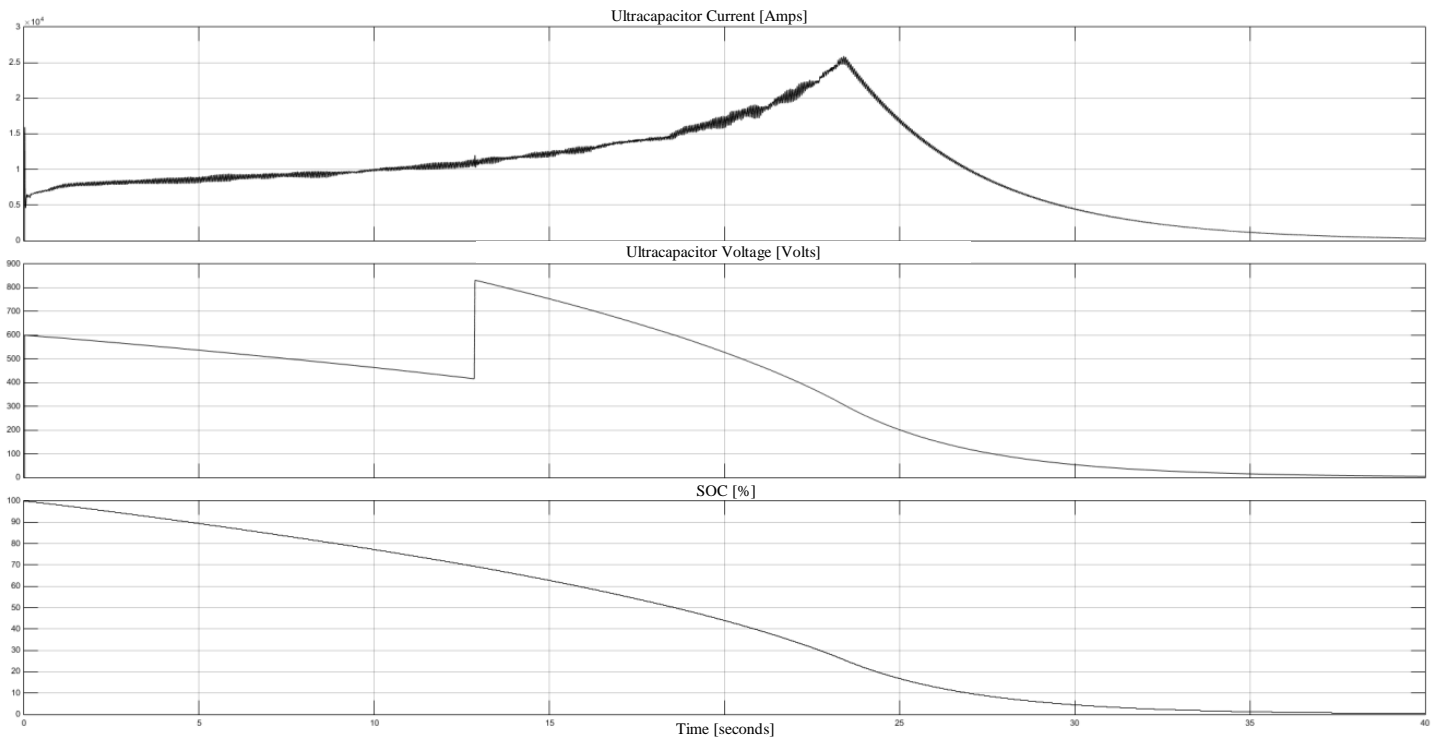


Figure 36 - UCES Discharge Data to a 9 MW Load

The top graph shows a clear peak at 23.5 seconds in current output. As the current increases to compensate for the falling voltages during discharge, this demonstrates that the ultracapacitor has reached its peak power output given the charge remaining. This peak also occurs at 41% SOC. Future runs will reveal that this peak can be delayed to lower SOC's with lower power demands.

Finally, the voltage output of the ultracapacitors is doubled relatively early on at 1.5 seconds to compensate for the high demand out of the inverter. This voltage doubling is created by the series parallel switches placing the two banks of ultracapacitor into a series configuration in response to a high demand (modulation index).

One of the challenges faced when running these simulations was finding a balance between load blocks that would allow the simulation software to run correctly. Although the load blocks appear equal, the simulation become highly unstable unless the purely resistive load block was very small in power demand in comparison to the resistive inductive load block in parallel with it. As an example, to achieve stability for the 9MW static load run, the loads were split at 0.3 MW resistive with 8.7 MW/5.6 MVAR complex loads in parallel.

The summary of results is provided in Table 8, with all graphical results being presented in appendix b. As a note, all simulations were run in the rapid accelerator mode.

Table 8 - UCES Discharge Endurance

Ship's Loads (MW)	Ship's Loads (MVAR)	Power Factor	SOC Remaining at Voltage Sag (%)	Discharge Time until Voltage Sag (s)	SOC Remaining at Current Peak (%)	Ultracapacitor Current Peak at (s)	Discrete Mode Step Time (μs)	Estimated Endurance with a fully charged 12595F Ultracapacitor Bank (min)	Estimated Ship's Speed Attained During Discharge (kts)
1	0.6	0.85	15	130.0	7	133.0	50	21.7	0
2	1.2	0.85	10	85.0	10	85.0	50	14.2	5
3	1.9	0.85	11	61.0	11	61.0	50	10.2	10
4	2.5	0.85	13	47.0	12	48.0	50	7.8	12
5	3.1	0.85	13	43.0	13	43.0	10	7.2	14
6	3.7	0.85	17	35.5	17	35.5	10	5.9	15
7	4.3	0.85	20	30.5	20	30.5	10	5.1	16
8	5.0	0.85	22	26.5	22	26.5	10	4.4	17
9	5.6	0.85	25	23.5	25	23.5	10	3.9	18
10	6.2	0.85	28	22.0	28	22.0	10	3.7	19
11	6.8	0.85	31	19.0	28	20.0	10	3.2	20
12	7.4	0.85	32	18.5	32	18.5	10	3.1	20
13	8.1	0.85	35	17.0	35	17.0	5	2.8	20
14	8.7	0.85	40	15.0	40	15.0	10	2.5	21
15	9.3	0.85	41	14.0	41	14.0	10	2.3	21

The results of the table show that the UCES can provide ample reserve power at low to moderate demands. In all cases, the estimated endurance was based upon a failure point given by the voltage sag as opposed to the peak ultracapacitor current; however, the differences between voltage sag and ultracapacitor peak current are significant. This difference provides an indication of available stored energy that was not fully utilised due to slow controllers. The author believes that all available energy could have been harvested up to the peak current with a faster PI controller in a simulation environment that can properly model its response. In addition, a faster controller would also alleviate the under voltages at higher demands.

The final two columns in the table show the expected endurance of a fully system consisting of a bank of 12595 F capacitance. The second from the right column shows the expected endurance in minutes of the UCES during a blackout. Interpolating from Figure 9, the far right column projects the speed an IPS warship would be able to achieve while maintaining 1MW of other non-propulsion related loads while operating on that UCES at that power level.

The results are significant. At a one MW demand, this thesis' UCES can keep a ship's non-propulsion loads fully operational for 20 mins in the event of a black out. The impact of this capability is significant when putting this in respect to the naval damage control priorities of "float, move, and fight." This means communications, sensors, and even weapons could remain operational during the loss of power generation capability allowing the ship to continue to "float and fight" for an extended period of time.

This being said, it would be relatively difficult to fight a warship without propulsion. With this UCES, a ship can maintain power during a blackout for over 5 minutes at 7MW. This translates to ship speed of 16 or more knots even with maintaining all other electrical loads. Those minutes are more than ample for crews to start and parallel an offline engine.

This section has demonstrated the ability of the UCES to provide stored power back to the system during the loss of power generation equipment. Now that the reader has an appreciation of how the system charges and discharges under static loads, it is time to present the pertinent results from changing loads.

5.3.3: Load Changes during charging operations

While it is easy to provide an appreciation for how fast the system can be charged or discharged under static loading conditions, it is significantly more difficult to show the UCES capabilities under changing conditions. Even limiting load changes to one addition or removal at 1MW increments creates 900 different scenarios to show both charging and discharging changes.

For brevity, only two scenarios will be presented in the next two sections. The first will demonstrate an unloading of charging operations due to a change in ship's load. The second will demonstrate a change in the parallel series configuration during discharge.

Figure 32 has already demonstrated the overload protection provided by the Module Load Controller when it load shed ultracapacitor charging. Figure 37 shows an event that causes the Module Load Controller to reduce demand on the generator. A chronological analysis of these results provides a good delineation of charging operations with frequency control. Due to the short time frame of the load change, the ultracapacitor data is not included in this analysis, as it did not contribute to the discussion.

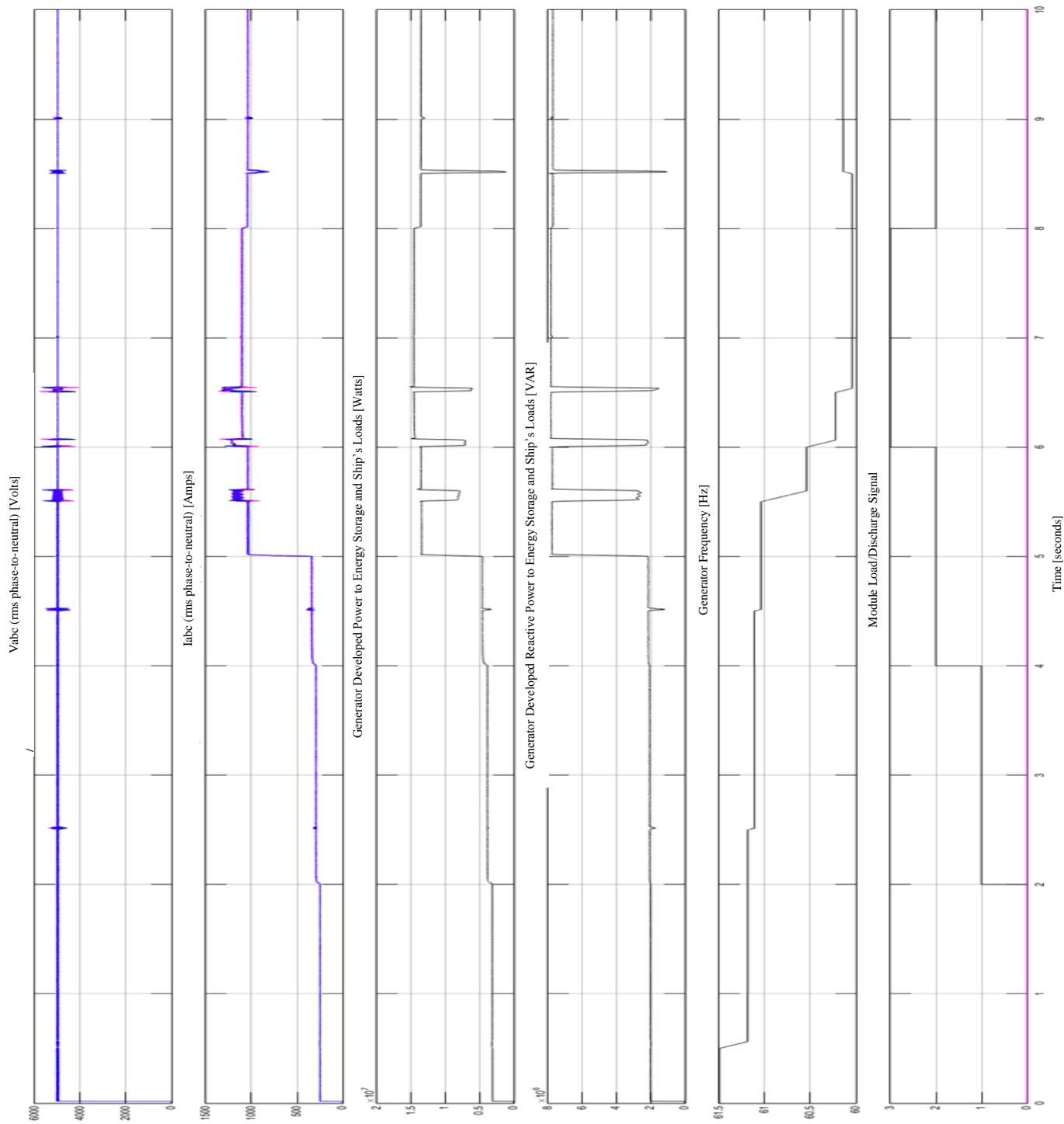


Figure 37 - Charging Operations with a 3MW to 12 MW increase at 5 seconds

As seen in the figure above, the load is initially set at 3MW. At 0.5s, the Speed Droop Controller polls the system load and adjusts generator speed from 61.5 Hz to 61.2 Hz. At 2 seconds, the Module Load Controller polls the generator frequency. Since it is above the threshold of 60.3Hz, this controller increases the Module Load Signal to 1. This allows current to flow into the ultracapacitor banks via the Charge Limiting Rheostat.

With some charging now occurring, the current and power demands also increase. At 2.5 seconds, the Speed Droop Controller again polls the system load and performs a minor generator speed adjustment. A small blip in current and voltage is noted. This occurs whenever the system experiences a speed change and is a product of the simulation environment. In reality, generators adjust their speed constantly with little consequence on the distribution system.

At 4 seconds, the Module Load Controller polls the generator frequency. As frequency is above 60.3Hz, the Module Load Signal is increased to 2, and the first resistor in the Charge Limiting Rheostat is bypassed. A subsequent current and power increase to the ultracapacitors is observed and the generator responds by slowing its speed at 4.5 seconds.

At 5 seconds, the ship's load is increased to 12MW and again the generator responds by slowing down at the next half-second polling cycle. At 5.5 seconds, the generator slows down but only by 0.5 Hz. Although a load increase of 9MW should translate to a speed decrease of 0.9 Hz, the Speed Controller does not allow changes in excess of 1Hz/s or 0.5Hz/polling cycle. As such, the generator undergoes a second speed decrease at 6 seconds to achieve its new steady state speed.

Meanwhile the Module Load Controller performs its 3rd polling cycle at 6 seconds. As the system frequency is still above 60.3 Hz, the Module Load Signal is increased to 3. This bypasses another resistor in the Charge Limiting Rheostat, allowing more current and power to flow into the ultracapacitors.

At 6.5 seconds, the generator speed is further reduced in response to additional ultracapacitor charging demand. Steady state is maintained until 8 seconds, when the Module Load Controller performs its 4th poll and discovers that system frequency is below 60.1Hz. This means the generator is providing over 14MW of power and is near its rated 15MW. As such, the Module Load Controller decreases the module load signal to 2. This increases the resistance imparted by the Charge Limiting Rheostat, and reduces current and power flow.

The last speed change occurs at 8.5 seconds when the speed droop controller increases the generator frequency in response to the now lower power requirement. Although right at the end of Figure 32, there is no change in Module Load Signal at 10 seconds as the generator frequency is between 60.1 and 60.3 Hz.

The analysis of this loading operation does present one potential problem. The Module Load Controller performs its 2 second poll at the same time as the Generator Speed Droop Controller's half-second poll. As such, the Speed Droop Controller may be changing speed while the Module Load Controller is determining whether or not to increase load based upon that speed. These polling cycles should be made distinct in future models.

5.3.4: Load Changes during Discharging Operations

Discharge operations are somewhat easier to describe compared to charging. The boost provided by the PWM inverter via an LCL filter did create some issues. Despite restricting the modulation index to a value between 0 and 1, the control system still suffered when regulating the output voltage at extremely low or extremely high demands. This was exacerbated by the decaying input voltage from the ultracapacitors.

In a fixed arrangement the decaying 600V input from the ultracapacitors would quickly result in the system being unable to maintain a 15MW output. In a strict series arrangement, the output voltage of 1200V caused clipping in the control system. Namely, the modulation index drove to zero and created surges of power in a futile attempt to maintain the required 260VAC output out of the inverter.

By making the output of the ultracapacitors variable through the parallel and series switches, the system was effectively able to regulate low and high power demands. This removed the need for an additional DC/DC converter. This arrangement also had the secondary effect of allowing more charge to be drawn out of the ultracapacitors, particularly at lower demands.

Figure 38 provides a good example of the effectiveness of parallel switching operation during a load change from 15 to 1 MW. These graphs are similar to those in 5.3.2 but contain some additional data. The top graph measures system rms voltage and should be regulated to 5000V. The second graph shows system rms current, the third system active power, and the fourth reactive power. The fifth graph shows the modulation index with y-axis values from 0 to 1. The final graphs shows ultracapacitor output voltage. The switching into parallel or series is apparent by the doubling or halving of the ultracapacitor voltage. Due to the short time frame of the load change, the ultracapacitor data is not included in this analysis, as it did not contribute to the discussion.

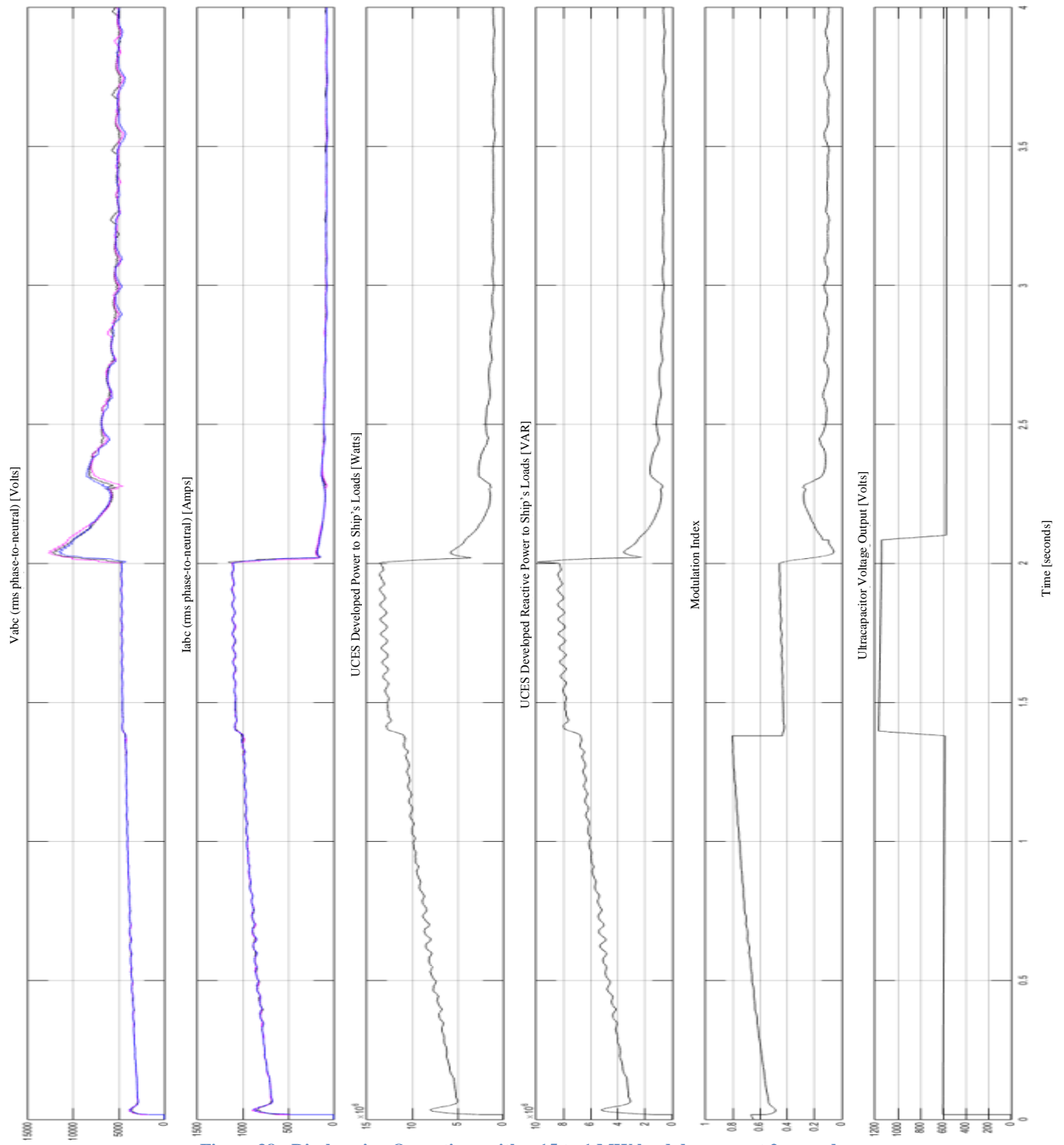


Figure 38 - Discharging Operations with a 15 to 1 MW load decrease at 2 seconds

With an initial demand of 15MW, the PI controller increases the modulation index to drive up the output voltage to meet the system value of 5000V. At approximately 1.35 seconds, the modulation index reaches 0.8 (for 1/6 second), and the system places the ultracapacitor into a series configuration. As this happens, the PI controller is reset to a modulation index of 0.4, and there is a noticeable spike in system voltage, current, and powers.

At 2 seconds, the load is changed to 1MW. A considerable voltage spike is observed as a result of the large instant load change. Again, a step load like this is unrealistic as a propulsion plant would apply gradual load changes. Current and powers decrease to compensate. As the modulation index drives towards zero the system is likely to display clipping; however, the reversion to a parallel configuration protects the system.

At approximately 2.2 seconds the modulation index falls below 0.2 and the system changes the configuration to halve the inverter input voltage from the ultracapacitors. As such, clipping is prevented as the system reaches a steady-state modulation index of 0.1 with time.

These two sections have described how charging and discharging operations occur. Namely, how the system can absorb power and provide power. But to act as an emergency power source, the system must be able to react to a loss of generation capability as well.

5.3.5: Generator to UCES handovers

The ability of the system to supply power the moment generation capability is lost is pivotal to preventing an interruption in ship operations. With most sensors and weapons being computer controlled, a power interruption, however brief, could be disastrous during combat.

In order to successfully simulate generator to UCES handovers, the model was simulated in discrete mode with the rapid accelerator and an extremely small step size of 10^{-7} seconds. In addition, the generators' frequency was held constant at 61.2 Hz so that there was no speed change during this short duration simulation. Figure 39 demonstrates the 0.2 seconds of data capture that show this handover. Due to the short time frame of the handover, the ultracapacitor data is not included in this analysis, as it did not contribute to the discussion.

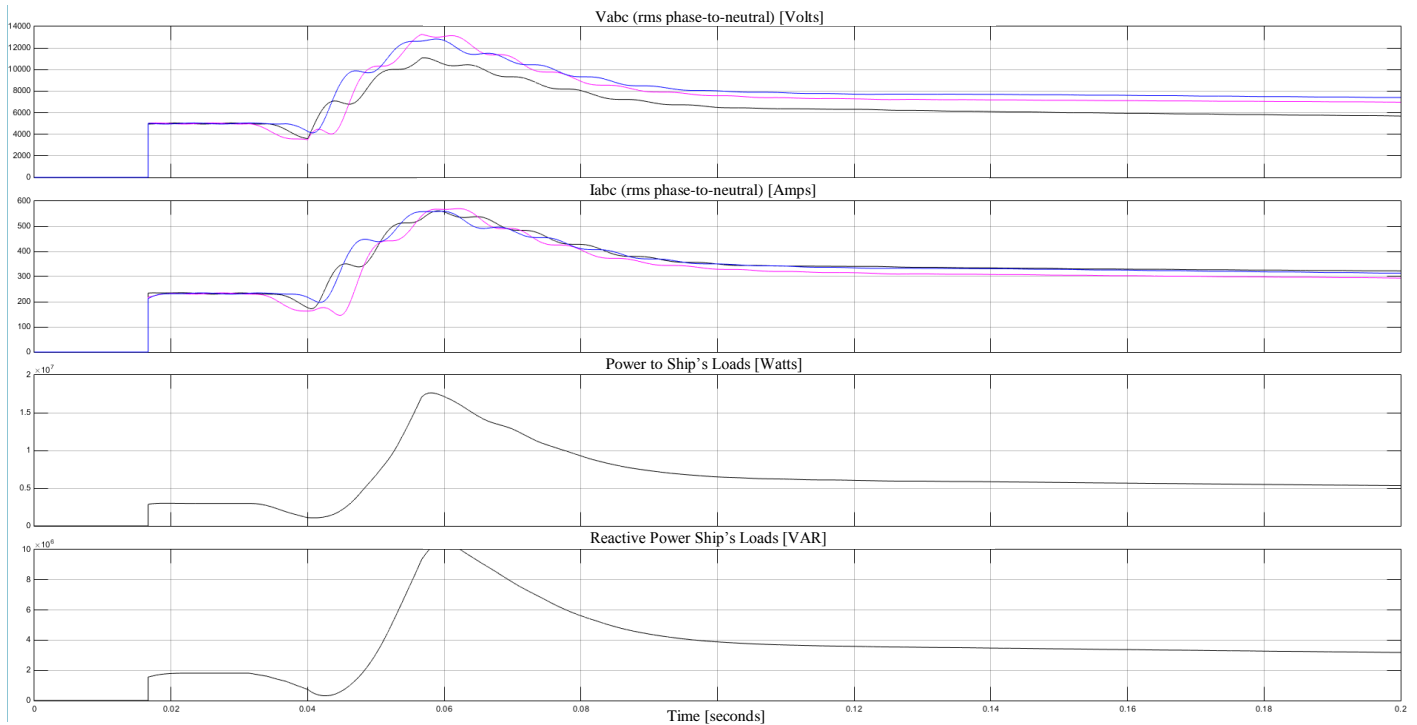


Figure 39 - Generator to UCES Handover at 3MW Demand

The simulation above shows the voltages, currents, and powers flowing to a ship's load of 3MW. Although the generator is running at the start of the simulation, the sensors that provide this information did not provide an output until 1 cycle at 60Hz has been completed. At 0.0167 seconds, the generator can be seen providing power to the load at 3MWs.

At 0.03 seconds the generator main breaker is opened and begins to de-energize. At 0.04 seconds the Discharge Controller responds to the indication of the open generator breaker and enables ultracapacitor discharge. For graphical clarity, these control signals are not shown in the figure above.

Almost immediately after the signal to discharge the ultracapacitors is generated, the power begins increasing and briefly surges as the Controlled Inverter PIs control starts to compensate. By 0.2 seconds, the system is shown a controlled recovery with a projected return to 1MW of load demand within 1 second.

A key factor supporting UCES integration into a ship is the response time. The figure above shows the ability to return power to the system before the main breaker has fully de-energized.

The power surge is caused by the initial condition of the PI controller to initialize the modulation index at 0.4. This initial condition is required to accurately reset the PI controller during series/parallel re-arrangement of the ultracapacitors. Unfortunately, the PI controller cannot distinguish between an initial condition and reset.

Figure 40 illustrates the reversion back to generator power after UCES discharge. The graphs in the figure are the same as those in Figure 39. Respectively, they demonstrate the rms voltage, rms current, and powers flowing to the ship's loads. These graphs were also generated in discrete time but with a more reasonable time step of 10^{-5} s. Due to the short time frame of the handover, the ultracapacitor data is not included in this analysis, as it did not contribute to the discussion.

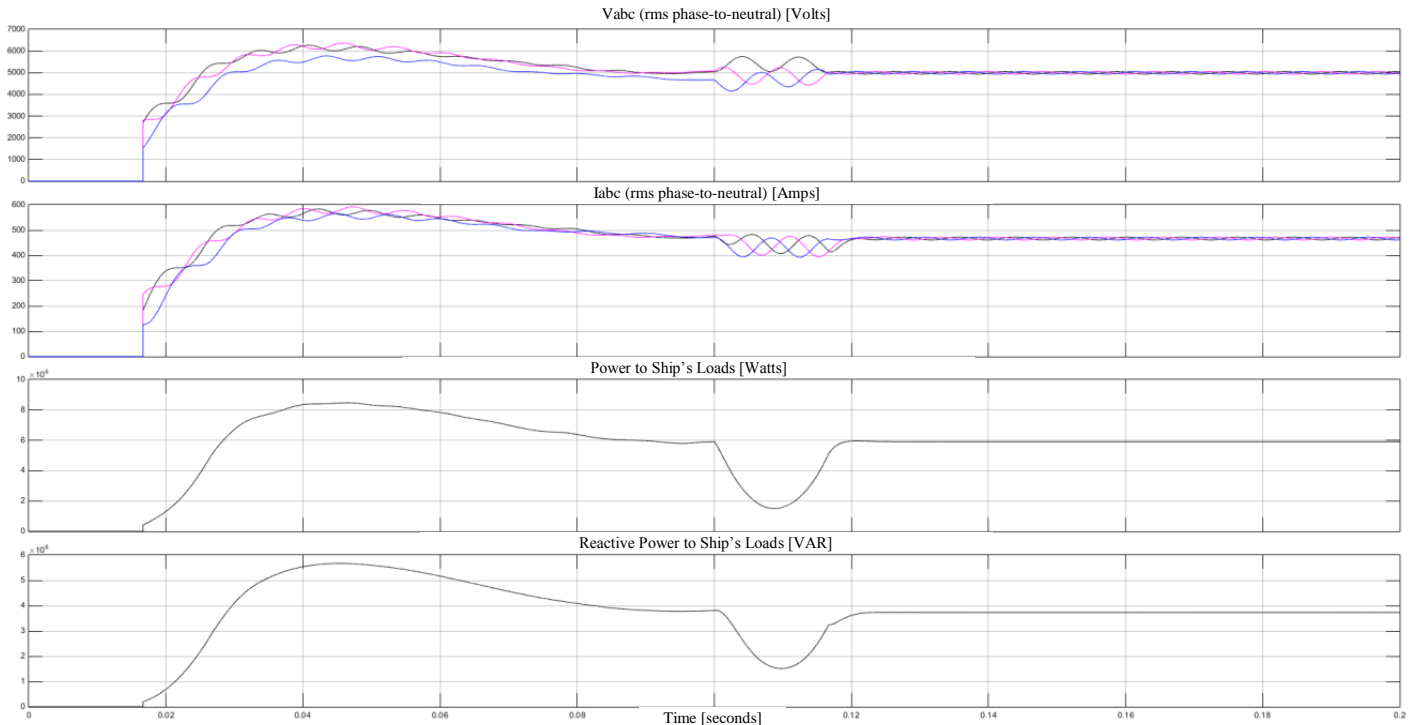


Figure 40 - UCES to Generator Handover at 6MW Demand

Just as in the generator to UCES transition, the data above is not provided by the sensors until 1 cycle at 60Hz has been completed. Regardless, the UCES is providing power from the start of the simulation. By 0.08 seconds, the power output of the UCES is nearing steady state and providing power to the ship's loads. At 0.1 seconds, the generator's main breaker is closed and normal power generation capability is restored. A slight power dip is observed as the voltage and current transition; however, steady state is re-achieved within two cycles at 0.12 seconds.

This concludes both this section and this chapter. This section has successfully demonstrated the speed in which a changeover from UCES to generator and more importantly generator to UCES can occur. Not only does the UCES benefit from speed of response, but the ultracapacitors ability to rapidly charge means the system would almost always be fully charged whenever required. Even with loads approaching 10MW, the system is achieving maximum charge from a depleted state in less than ten minutes. Finally, the endurance shown provides ship's crews ample time to emergency start another generator and bring it online before electrical power is lost.

The capabilities shown in the simulation environment have successfully demonstrated the UCES proof of concept. This system will always be fully charged, provide ample time to restore power generation, and can effectively maintain electrical power to a ship during a generator failure with only a minor dip in the distribution system power flow. This makes a UCES an ideal choice as an emergency power system for an IPS warship.

CHAPTER 6 : CONCLUSION

The thesis has demonstrated the ability of a UCES to act as a source of emergency power in an IPS warship. Using many zero loss components and an ideal arrangement of commercially available ultracapacitors, it may only be considered as a proof of concept. Nevertheless, by demonstrating the ability for ultracapacitors to be integrated into a medium voltage alternating current isolated power system, this simulated UCES may act as a starting point for future modelling.

Yet this thesis is only a starting point and still more work needs to be done. As such, this chapter addresses some recommendations for future modelling and closes with a brief discussion on IPS warships.

6.1 : Future Modelling Recommendations

Many insights were gained into the operations of ultracapacitors in a power storage context throughout the completion of this thesis, some of which could not be included in this initial proof of context for various reasons. Should others progress this work, they should take into consideration the following recommendations.

6.1.1: Simulation Software

Using MATLAB's Simulink was an obvious choice since it is widely accepted and known modelling software in the scientific community. However, early on there were difficulties faced when using Simulink with a variable frequency model. The pronounced spikes from the rms blocks associated with each speed change provided data that was difficult to use. There may be ways within Simulink to generate reliable data from an rms block under changing conditions, but there may also be other simulation software that can generate smoother rms data during frequency changes.

In addition, as the model grew more and more complex the simulation became increasingly difficult to operate. Simulation accuracy could often only be maintained with small time steps. But to do so created a plethora of data that overload computer memory. In addition, showing UCES endurance became extremely difficult at lower power demands requiring extended run times. This was due to both simulation length and the amount of data stored in RAM.

Future modelling needs to be done in simulation software that can handle a large power system model. This software needs to be able to accurately run simulations that span minutes or even hours. Simulink may be able to do this, but other software should also be examined to determine a best fit before a second iteration of this model is attempted.

6.1.2: Polling Distinction

There were many controllers involved in this model, all of which would have been unstable or generated instability had they been constantly responding to their sensory inputs. As such, controllers were designed to poll the system at set periods. As discussed in 5.3.3, there are certain controllers such as the Speed Droop Controller and Module Load Control that should not be polling at the same time.

6.1.3: Charge Limiting Rheostat

Even with ten different settings, the variable resistance imparted by the charge limiting rheostat was insufficient. Although the generator was often initially heavily loaded by the UCES charging system, the ultracapacitors natural rate of charge decreased throughout the charging process. Thus more current flow could have been provided as the SOC increased. A rheostat with more low resistance options would have allowed for faster charging with fewer resistive losses. That being said the charge limiting rheostat, and its associated losses, may not even be required if the rate of charge could be controlled by other means.

6.1.4: Improved Buck Chopper performance

The voltage regulation provided by the buck chopper was negligible in the Simulink model. With a static set point of 600V, the buck chopper's associated PI controller maintained a 100% duty cycle until 600V was achieved. Once the full voltage was achieved the PI controller rapidly drove the duty cycle to 0% to stop UCES charging. This function could have been performed by the Charge Limiting Rheostat, making the buck chopper superfluous.

However if the buck chopper could regulate the power flow into the UCES, then the Charge Limiting Rheostat, and its associated losses, could be eliminated. This could be achieved if the converter's PI controller's reference point was variable. In the current setup, the buck chopper limits the charge voltage to 600V regardless of the ultracapacitor voltage. This in effect allows a massive rush of current into the ultracapacitors when they have no charge, which is the reason the charge limiting rheostat was required.

But if the buck chopper provided power to the ultracapacitors at only a few volts greater than the ultracapacitor voltage then that could limit the inrush currents without the need for the Rheostat. By using the Module Load Controller to set a voltage difference between the PI controller's reference point and the ultracapacitor's actual voltage, generator loading could still be achieved by other means. Of course, this variable voltage reference point would need to be capped at the ultracapacitor module's maximum operating voltage to avoid overcharging the cells.

6.1.5: Commercial Components

This proof of concept used a theoretical ultracapacitor module based upon commercial available cells. From this, charge balancing and any other inter-cell regulatory components were ignored. This was necessary as no commercially produced ultracapacitor module met the low ESR and high voltage requirements to be efficient at 15MW output. Yet the environment of commercially available ultracapacitors is rapidly changing. Proving this, Skeleton Technologies recently released a cell capable of being charged in series up to 1360V [51].

An ultracapacitive module operating at this voltage range would have far fewer losses than the 600V theoretical module used in this thesis. Future work could easily use the top commercially available modules, which already have integrated cell balancing, to create a more credible high voltage and low loss UCES.

6.1.6: Component Realism

The predictive accuracy of future models can also be increased by incorporating resistive losses and impedances throughout the system. Line and switching losses for instances, might have little impact during charging, but could have a significant impact during UCES discharge where the stored energy is finite. To accomplish, ideal switching devices should be replaced by the appropriate semiconductor switch.

In addition, if model speed was improved a single set of ultracapacitors that could be fully charged and discharged during a single simulation would increase confidence in the system as whole.

6.1.7: Paralleling

Future models should be able to parallel with running generators. To do so would allow a UCES to provide a sprint capability to a ship. Essentially, the ship could draw upon its reserve power to achieve speeds above what a single generator could provide. This would allow for a short duration sprint. With this capability there would be no need to start an engine ahead of time. Unplanned sprints could be immediately initiated and then sustained, provided another engine was ready to assume load by the time the UCES was depleted.

Finally, paralleling the UCES provides an early intervention option in the event of pending generator failure without having to wait for the generator's main breaker to open. A UCES that can parallel with the system main at the first sign of a problem would further mitigate the blackout risk of future IPS warships.

6.2 : IPS Warships are the Future

The future of marine propulsion is electric. The technological benefits IPS ships offer are and will continue to be increasingly overwhelming. Major car manufacturers have delayed full electric integration by offering hybrid models that have essentially made the car considerably more complicated with some increases to fuel economy. But the number of drivers who will see a return on investment is slim when comparing the higher initial equipment cost to projected fuel savings.

The same is true for warships. The hybrid concept offers one possible future for warship design, but that is a future that sees little savings in initial equipment cost and provides many geographical restrictions associated with shaft lines, gearing, and ancillary equipment.

Tesla is affecting a revolution that the major auto manufacturers have resisted for years. Their electric cars have the range and the infrastructure to maintain electric charging stations is easier than that of fossil fuels to maintain. The only advantage the latter has really is that they have been in place for a century.

Just like a well-designed electric car, IPS warships offer significant advantages over their hybrid counterparts. Less equipment means fewer parts and less maintenance. The redundancies provided in a hybrid ship through a separate conventional propulsion system create an enormous additional cost, a cost that could be better invested in simple electrical redundancy: a UCES.

Even at their currently moderate energy capacity, today's ultracapacitors are able to meet the demand of providing reserve power to an IPS warship. This thesis has proven it.

In addition, this system can provide considerable fuel savings by eliminating risk and allowing navies to cease the running of redundant engines during hazardous scenarios. This proof of concept has shown that a UCES can restore power before the ship's power system has even fully de-energized. And, an IPS warship can achieve this redundancy in a UCES package the size of a single fuel tank. With this UCES we can use science to mitigate the blackout risk created by electric ships and see the real future IPS warships have to offer.

CHAPTER 7 : REFERENCES

- [1] BAE Systems, "Global Combat Ship," [Online]. Available: <http://www.baesystems.com/en/product/global-combat-ship>. [Accessed 10 August 2016].
- [2] J. North, "Driven to Destruction," *IEEE Power Engineer*, pp. 28-33, Aug/Sep. 2005.
- [3] X. Vavasseur, "Q&A with BAE Systems on Type 26 Frigate Design Update at Euronaval 2012," 10 January 2013. [Online]. Available: http://www.navyrecognition.com/index.php?option=com_content&task=view&id=828. [Accessed 19 March 2015].
- [4] R. Thorne, E. Bowles and M. Reed, "Integration of Electromagnetic Technologies Into Shipboard Applications," *IEEE Transactions on Applied Superconductivity*, vol. 16, no. 2, pp. 1074-1079.
- [5] Canadian Forces Technical Order C-26-320-000/MS-001, "Primary Electrical Power Generation and Distribution System manual applicable to Halifax class," Jun. 1997.
- [6] M. R. Patel, Shipboard Electrical Power Systems, Boca Raton, FL: CRC Press, 2012.
- [7] Canadian Forces Technical Order C-27-783-000/MS-001, "High Pressure Compressed Air System Manual for the CPF," Jan. 2004.
- [8] Canadian Forces Technical Order C-27-784-000/MS-001, "System Manual Low Pressure Compressed Air applicable to Halifax class," Oct. 2007.
- [9] Canadian Forces Technical Order C-25-509-000/MS-001, "Technical Manual Fuel Oil Service applicable to Halifax class," Aug. 2008.
- [10] Canadian Forces Technical Order C-24-559-000/MS-001, "Operation and Maintenance Instructions with a parts identification list Controllable Reversible Pitch Propellers and Propeller Shafting applicable to Halifax class," Jul. 2011.
- [11] Canadian Forces Technical Order C-24-486-000/MP-001, "Repair and Overhaul specification sea water service system (F/M)," Aug. 1998.
- [12] F. Kanellos, "Optimal Demand-Side Management and Power Generation Scheduling in an All-Electric Ship," *IEEE Transactions on Sustainable Energy*, vol. 5, no. 4, pp. 1166-1175, Oct. 2014.
- [13] P. Mitra and G. K. Venayagamoorthy, "Implementation of an Intelligent Reconfiguration Algorithm for an Electric Ship's Power System," *IEEE Transactions on Industry Applications*, vol. 47, no. 5, pp. 2292-2300, Sep. 2011.
- [14] S. McCulloch, "Confusion on Fishing Boat Cited in Esquimalt Harbour Collsion," *Times Colonist*, 2 April 2014. [Online]. Available: <http://www.timescolonist.com/news/local/confusion-on-fishing-boat-cited-in-esquimalt-harbour-collision-1.938411>. [Accessed 18 March 2015].
- [15] R. Lasseter, "Smart Distribution: Coupled Microgrids," *Proceedings of the IEEE*, vol. 99, no. 6, pp. 1074-1082, Jun. 2011.
- [16] V. Boicea, "Energy Storage Technologies: The Past and the Present," *Proceedings of the IEEE*, vol. 102, no. 11, pp. 1777-1794, Nov. 2014.
- [17] S. Vazquez, "Energy Storage Systems for Transport and Grid Applications," *IEEE*

- Transactions on Industrial Electronics*, vol. 57, no. 12, pp. 3881-3895, Dec. 2010.
- [18] G. Grazzini and A. Milazzo, "A Thermodynamic Analysis of Multistage Adiabatic CAES," *Proceedings of the IEEE*, vol. 100, no. 2, pp. 461-472, Feb. 2012.
- [19] M. Ali, B. Wu and R. Dougal, "An overview of SMES Applications in Power and Energy Systems," *IEEE Transactions on Sustainable Energy*, vol. 1, no. 1, pp. 38-47, Apr. 2010.
- [20] P. Grbovic, *Ultra-Capacitors in Power Conversion Systems*, Chichester, West Sussex, UK: John Wiley & Sand Ltd., 2014.
- [21] "Skelcap high energy ultracapacitor SCHE3500 Data Sheet," [Online]. Available: Internet: <http://skeletontech.com/datasheets/skelcap-energy-en.pdf>. [Accessed 29 October 2015].
- [22] P. Tamilarasan and S. Ramaprabhu, "Graphene based all-solid-state supercapacitors with ionic liquid incorporated polyacrylonitrile electrolyte," *Energy*, vol. 51, pp. 374-381, Jan. 2013.
- [23] R. Signorelli, D. Ku, J. Kassakian and J. Schindall, "Electrochemical Double-Layer Capacitors Using Carbon Nanotube Electrode Structures," *Proceedings of the IEEE*, vol. 97, no. 11, pp. 1837-1847, Nov. 2009.
- [24] N. Jha, E. Bekyarova, P. Ramesh, M. Itkis and R. Haddon, "Ruthenium Oxide – Single Walled Carbon Nanotube Composite Based High Energy Supercapacitor," in *International Conference on Advanced Nanomaterials & Emerging Engineering Technologies (ICANMEET)*, Chennai, India, 2013.
- [25] C. Fu, Y. Kuang, Z. Huang, X. Wang, Y. Yin, J. Chen and H. Zhou, "Supercapacitor based on graphene and ionic liquid electrolyte," *Journal of Solid State Electrochemistry*, vol. 15, pp. 2581-2585, Nov. 2010.
- [26] C. Abbey and G. Joos, "Supercapacitor Energy Storage for Wind Energy Applications," *IEEE Transactions on Industrial Applications*, vol. 43, no. 3, pp. 769-776, May/June 2007.
- [27] "Maxwell ultracapacitors enabling the future," [Online]. Available: <http://www.maxwell.com/products/ultracapacitors/>. [Accessed 5 November 2015].
- [28] O. Abdel-baqi and A. Nasiri, "Dynamic Performance Improvement and Peak Power Limiting Using Ultracapacitor Storage System for Hydraulic Mining Shovel," *IEEE Transactions on Industrial Engineering*, vol. 62, no. 5, pp. 3173-3181, May 2015.
- [29] J. Lee, S. Lee and S. Sul, "Variable Speed Engine-Generator with Supercapacitor Isolated Power Generation System and Fuel Efficiency," *IEEE Transactions on Industrial Engineering*, vol. 45, no. 6, pp. 2130-2135, Nov/Dec 2009.
- [30] P. Clarke, T. Muneer and K. Cullinane, "Cutting vehicle emissions with regenerative braking," *Transportation Research Part D*, no. 15, pp. 160-167, 2010.
- [31] "Ultracapacitor Buses, Sep. 18, 2009, [Oct. 20, 2015]," 18 September 2009. [Online]. Available: <https://www.youtube.com/watch?v=LYL6NyU1g3k>. [Accessed 20 October 2015].
- [32] "Ultracapacitor City Bus [Oct. 20, 2015]," [Online]. Available: http://www.aowei.com/en/case_view.php?typeid=1&id=4. [Accessed 20 October 2015].
- [33] "Chariot E-Bus," [Online]. Available: <http://www.chariot-electricbus.com/products/chariot-e-bus/>. [Accessed 20 October 2015].
- [34] A. Ostodi and M. Kazerani, "A Comparative Analysis of Optimal Sizing of Battery-Only, Ultracapacitor-Only, and Battery-Ultracapacitor Hybrid Energy Storage Systems for a City Bus," *IEEE Transactions on Vehicular Technology*, vol. 64, no. 10, pp. 4449-4460, Oct.

2015.

- [35] S. Balathandayuthapani, C. Edrington and S. Henry, "Study on Converter Topologies for Capacitive Pulse Forming Network and Energy Storage Units in Electric Ship," *IEEE serial number 978-1-4244-9273-2/11*, pp. 459-462, 2011.
- [36] D. Somayajula and M. Crow, "An Integrated Dynamic Voltage Restorer-Ultracapacitor Design for Improving Power Quality of the Distribution Grid," *IEEE Transactions on Sustainable Energy*, vol. 6, no. 2, pp. 616-624, April 2015.
- [37] J. Mandy, Interviewee, *Electrical Engineering Manager - Arctic Offshore Patrol Vessel Project Management Office*. [Interview]. 24 March 2015.
- [38] "Halifax-Class Modernization (HCM) / Frigate Life Extension (FELEX)," National Defence and the Canadian Armed Forces, 24 November 2014. [Online]. Available: <http://www.forces.gc.ca/en/news/article.page?doc=halifax-class-modernization-hcm-frigate-life-extension-felex/hkm9beb0>. [Accessed 2 July 2016].
- [39] "Skeleton Technologies SkelCap High Power SPA2100 Data Sheet," [Online]. Available: <http://www.skeletontech.com/industrial-ultracapacitor-modules>. [Accessed 6 April 2016].
- [40] "Safety Data Sheet - Skelcap High Power SPA," Skeleton Technologies, [Online]. Available: http://cdn2.hubspot.net/hubfs/1188159/Material_Safety_Data_Sheets/. [Accessed 5 July 2016].
- [41] S. Smith and P. Sen, "Ultracapacitors and Energy Storage: Application in Electrical Power System," in *Power Symposium, NAPS*, 2008.
- [42] D. Linzen, S. Buller, E. Karden and R. De Doncker, "Analysis and Evaluation of Charge-Balancing Circuits on Performance, Reliability, and Lifetime of Supercapacitor Systems," *IEEE Transactions on Industrial Applications*, vol. 45, no. 5, pp. 1135-1141, Sep./Oct. 2005.
- [43] N. Mohan, T. Undeland and W. Robbins, "Review of Basic Electrical and Magnetic Circuit Concepts," in *Power Electronics: Converters, Applications, and Design*, 3 ed., Hoboken, NJ, John Wiley & Sons, Inc., 2003, p. 40.
- [44] C. Hubert, "Synchronous Generators (Alternators)," in *Electric Machines: Theory, Operation, Applications, Adjustment, and Control*, 2 ed., Upper Saddle River, Pearson Education, Inc., 2002, pp. 350-363.
- [45] N. Mohan, T. Undeland and W. Robbins, "Line-Frequency Phase-Controlled Rectifiers and Inverters," in *Power Electronics: Converters, Applications, and Design*, 3 ed., Hoboken, NJ, Wiley & Sons, Inc., 2003, p. 139.
- [46] N. Mohan, T. Undeland and W. Robbins, "dc - dc Switch Mode Converters," in *Power Electronics: Converters, Applications, and Design*, 3 ed., Hoboken, NJ, John Wiley & Sons, Inc., 2003, p. 167.
- [47] "Simulink Supercapacitor Help Documentation," MATLAB, [Online]. Available: <http://www.mathworks.com/help/physmod/sps/powersys/ref/supercapacitor.html>. [Accessed 17 July 2016].
- [48] N. Mohan, T. Undeland and W. Robbins, "Switch-Mode: dc-ac Inverters: dc-sinusoidal," in *Power Electronics: Converters, Applications, and Design*, 3 ed., Hoboken, NJ, John Wiley & Sons, Inc., 2003, p. 206.
- [49] "How Acceleration Mode Works," Mathworks, [Online]. Available: <http://www.mathworks.com/help/simulink/ug/how-the-acceleration-modes-work.html>.

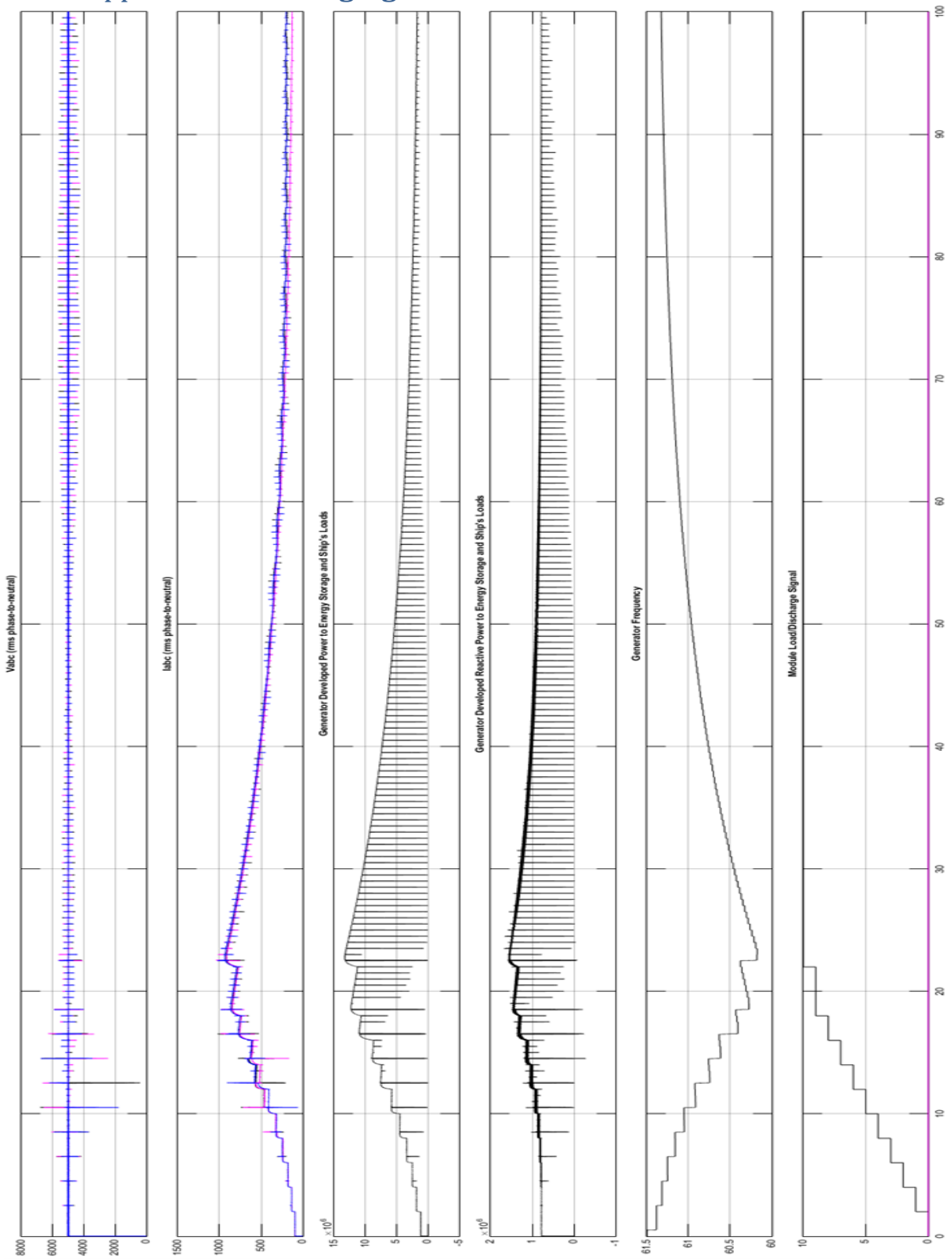
[Accessed 22 July 2016].

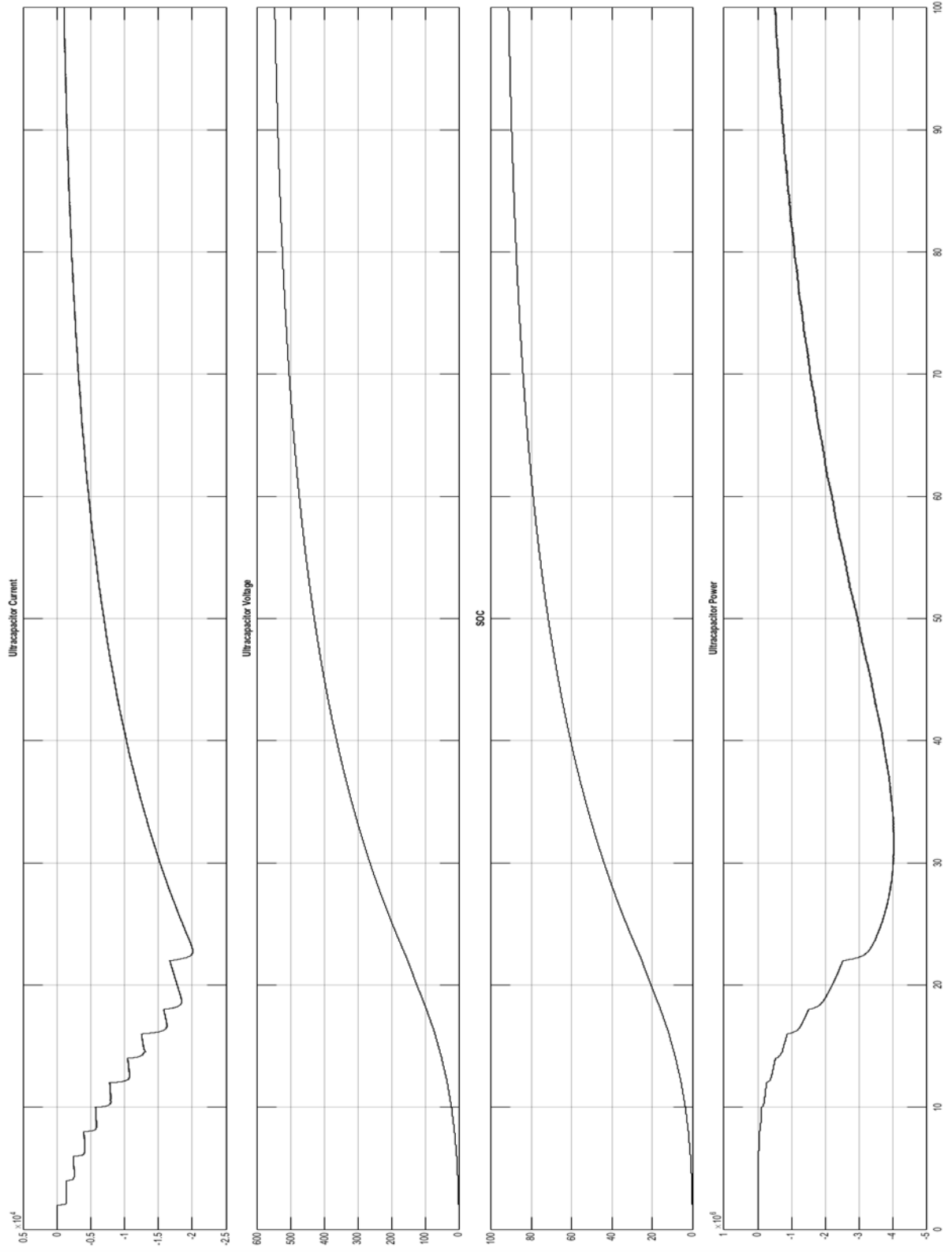
- [50] R. Dugan, M. McGranaghan, S. Santoso and H. Wayne Beaty, *Electrical Power Systems Quality*, 3 ed., New York: McGraw-Hill, 2012.
- [51] "Industrial Ultracapacitor Modules - 170V75F Data Sheet," Skeleton Technologies, [Online]. Available: <http://www.skeletontech.com/industrial-ultracapacitor-modules>. [Accessed 5 July 2016].

APPENDIX A : ADDITIONAL CHARGING SYSTEM RESULTS

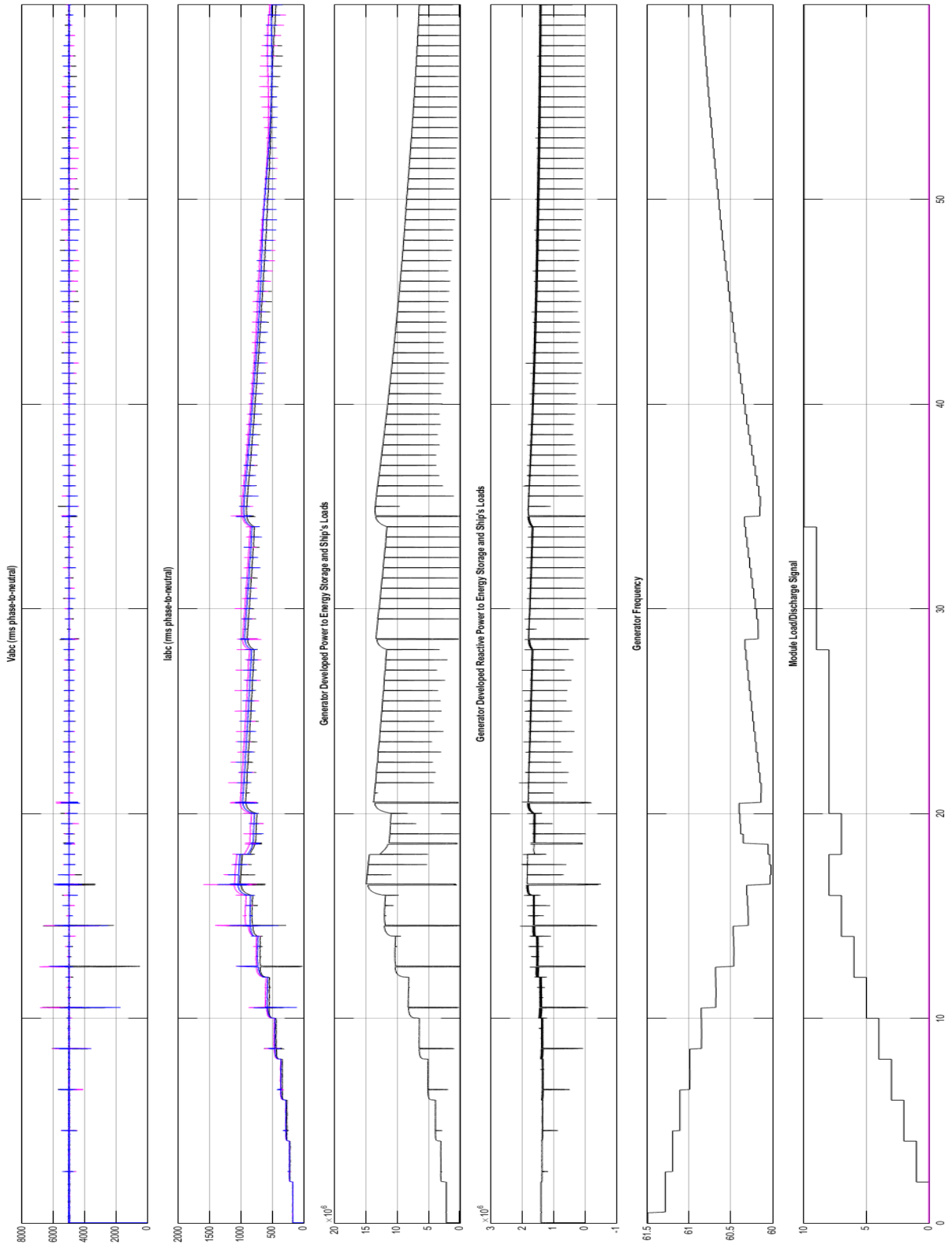
For all the graphical data appearing in the Annexes, the graph title implies the unit of the Y-axis. In addition, all units are in base units. For example, the graph labelled “ V_{abc} (rms phase-to-neutral)” would indicate that the Y-axis corresponding to that graph has its divisions in Volts. The graph labelled SOC, or State of Charge, indicates % charge of the ultracapacitors. The module load signal and discharge signals have no units. All X-axis values are in seconds.

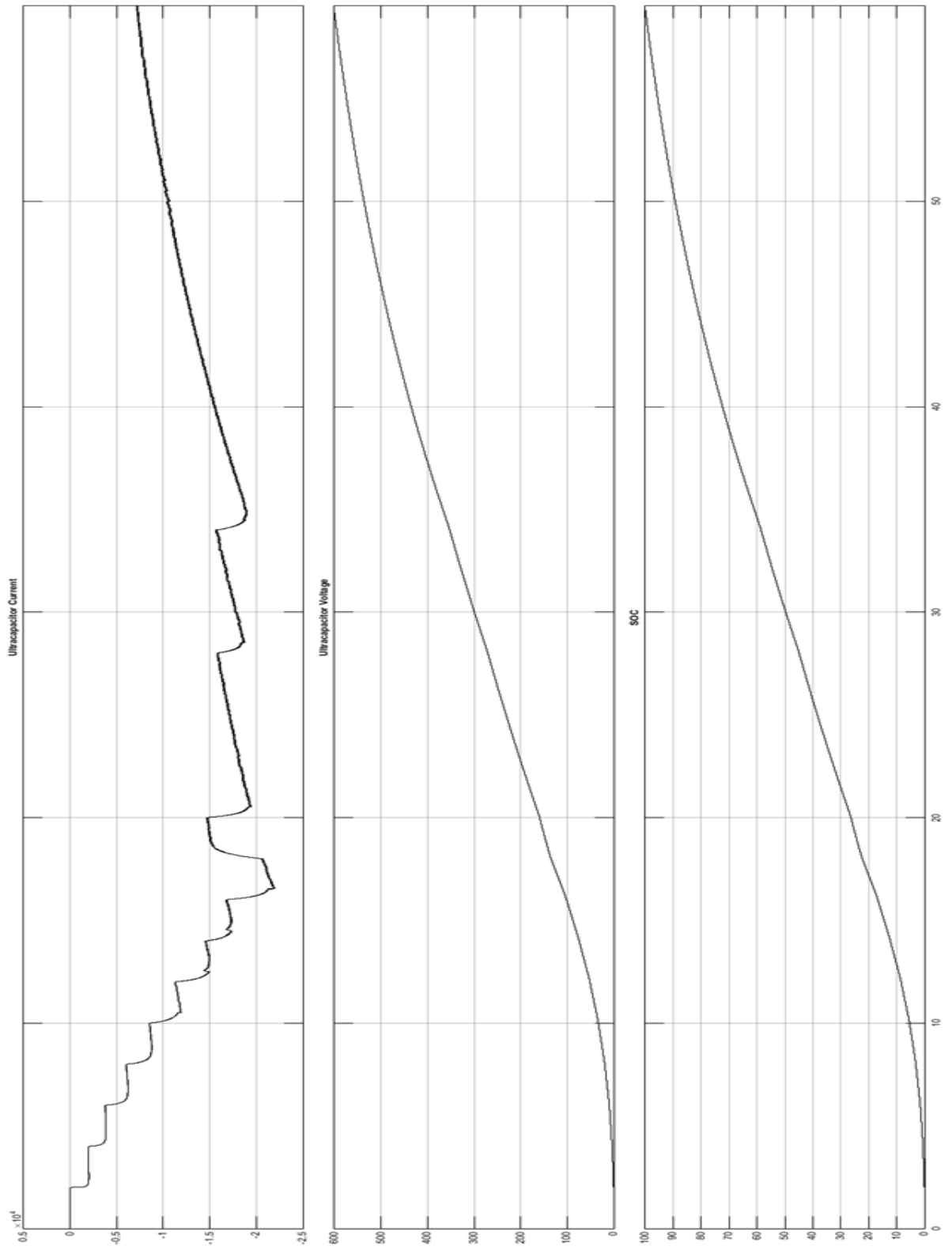
Appendix A.1 : Charging Results with a 1 MW Static Load



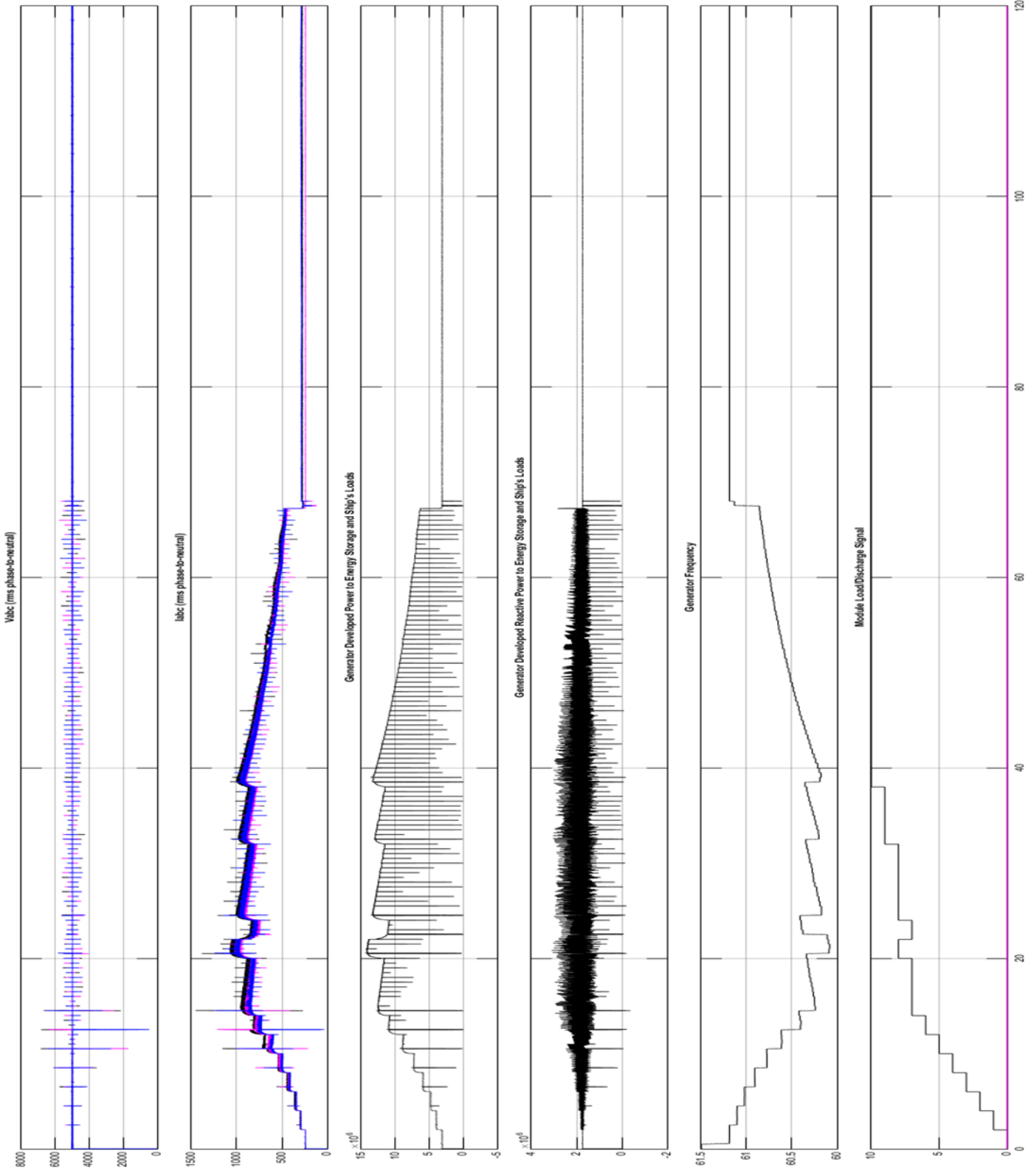


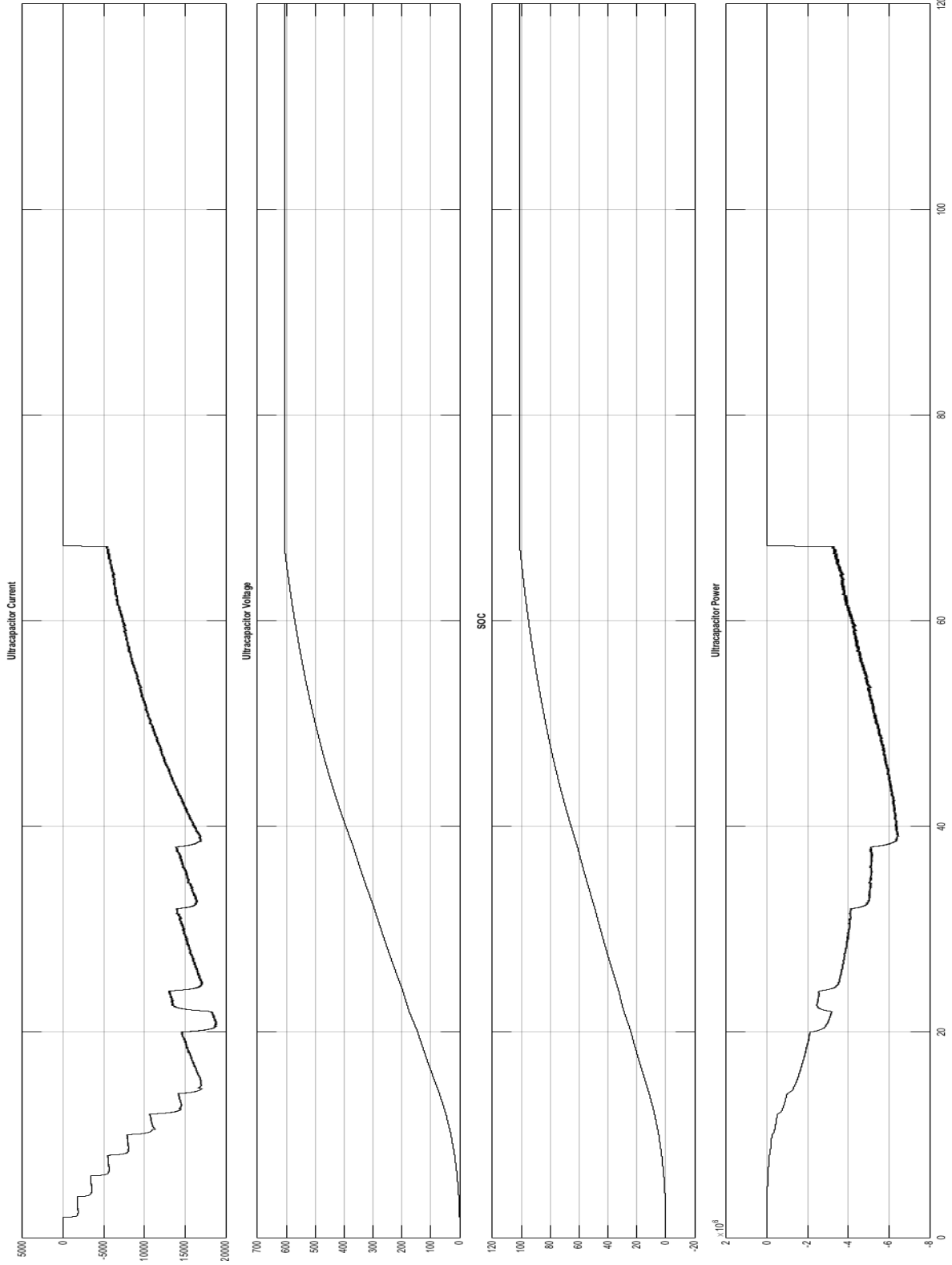
Appendix A.2 : Charging Results with a 2 MW Static Load



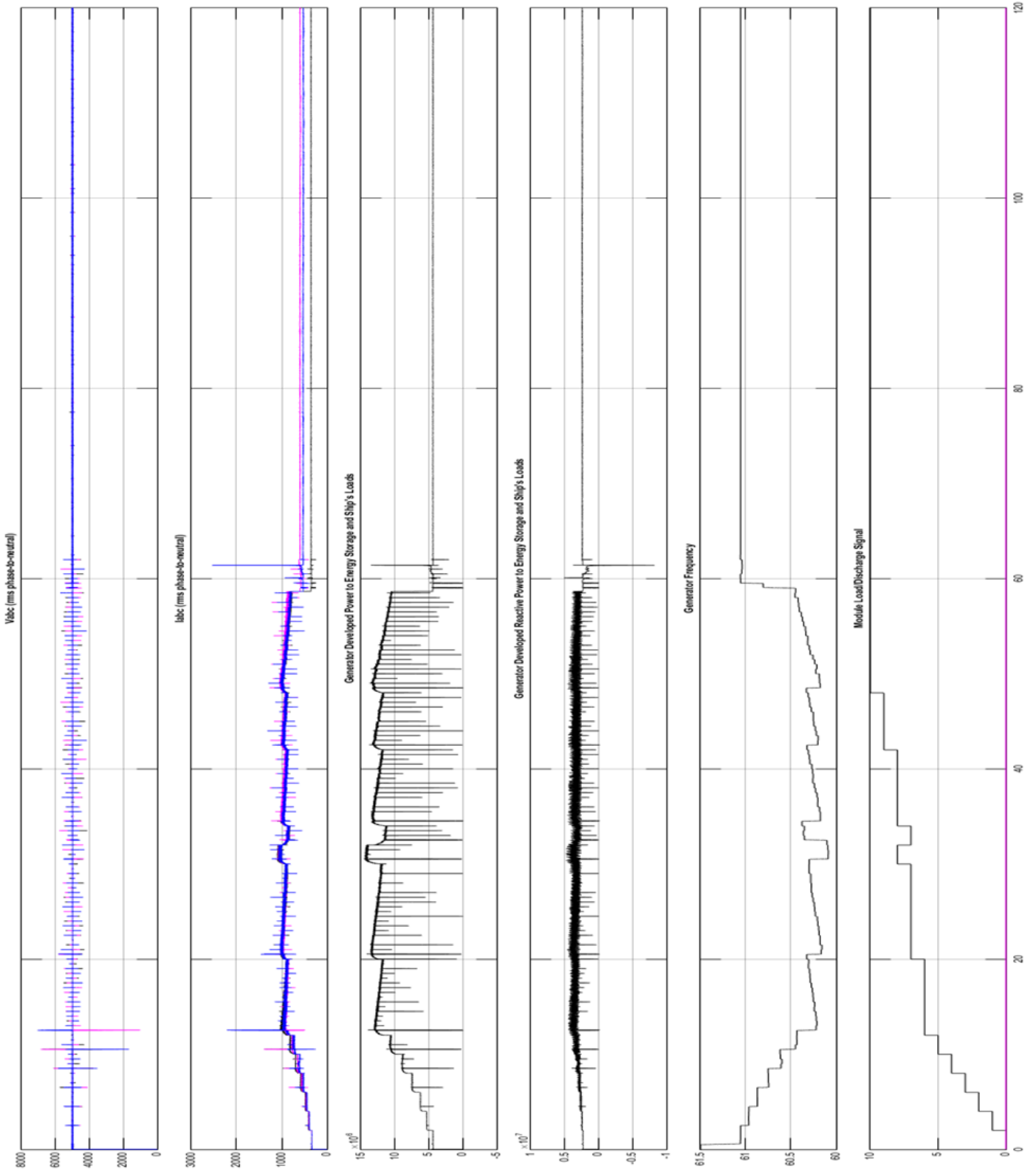


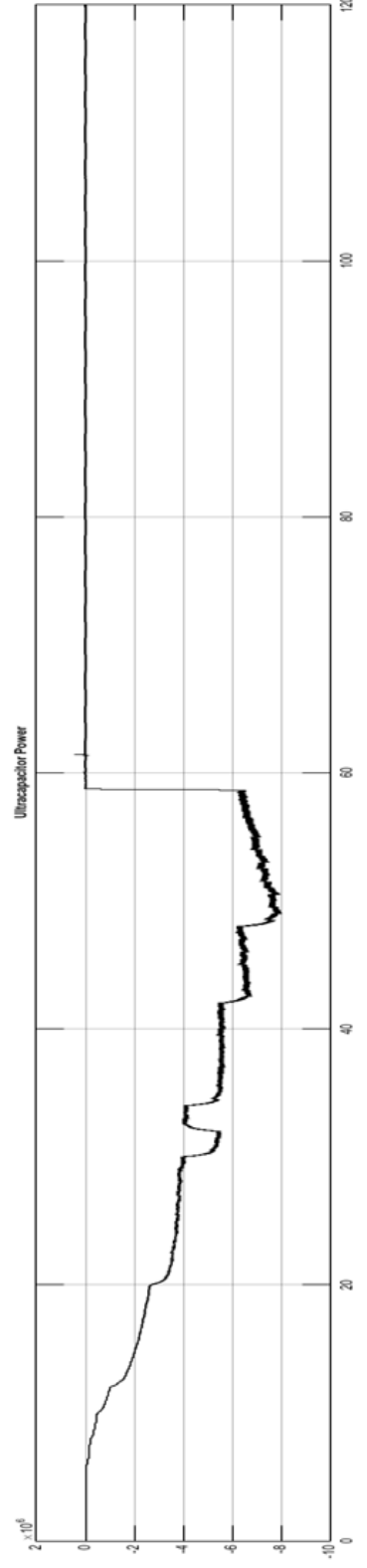
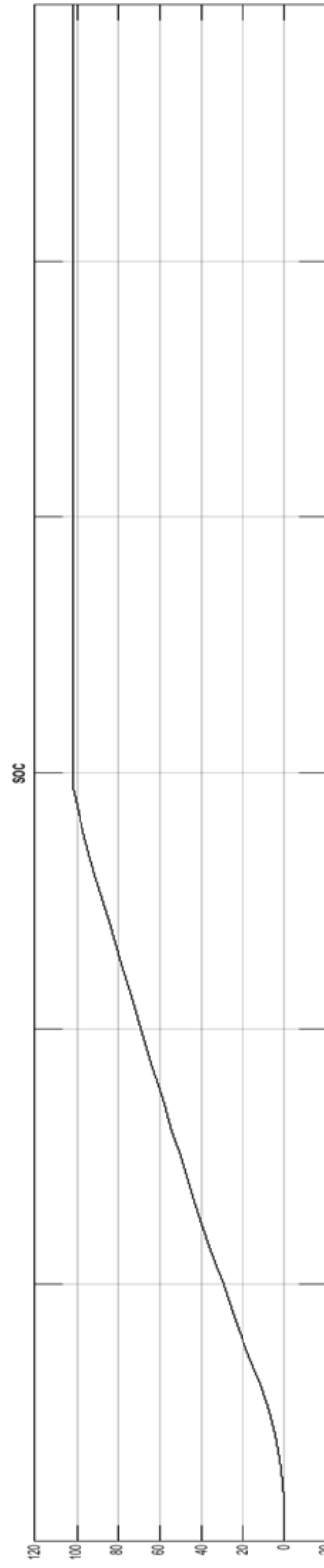
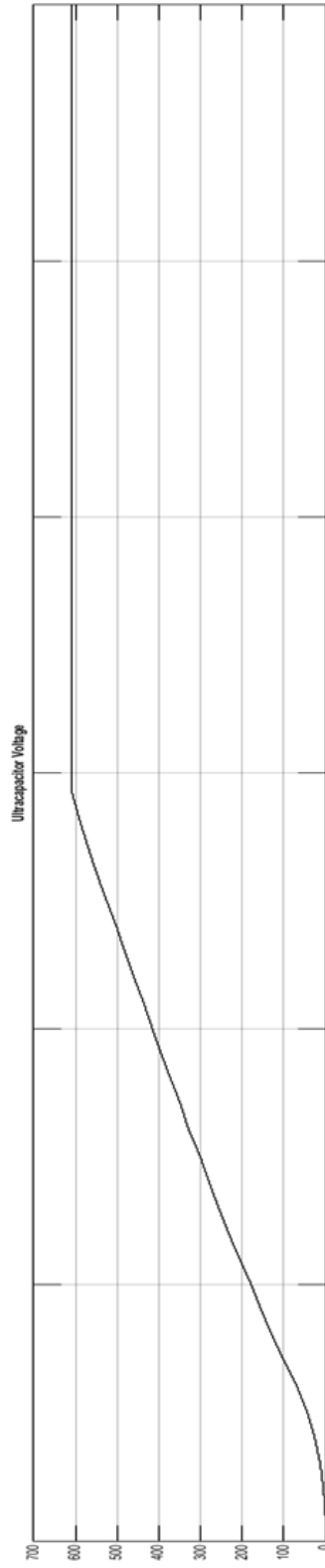
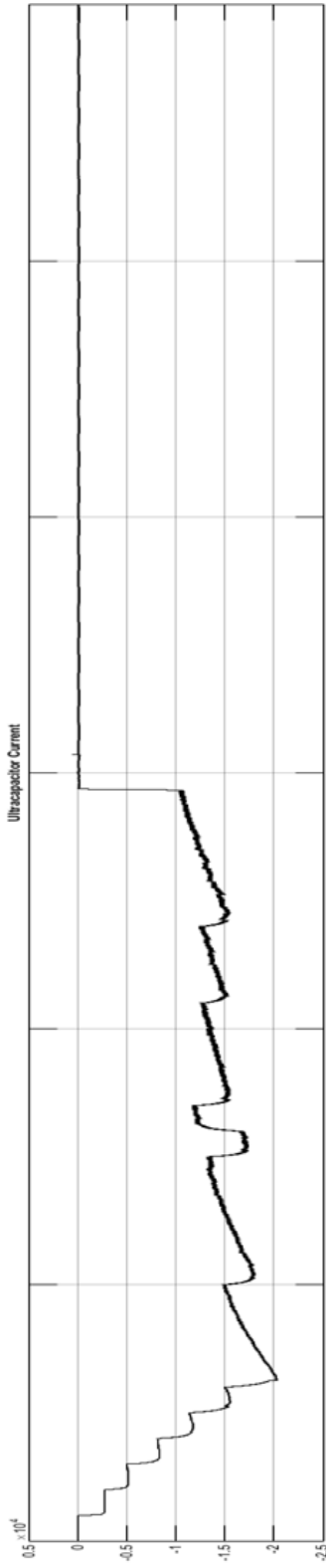
Appendix A.3 : Charging Results with a 3 MW Static Load



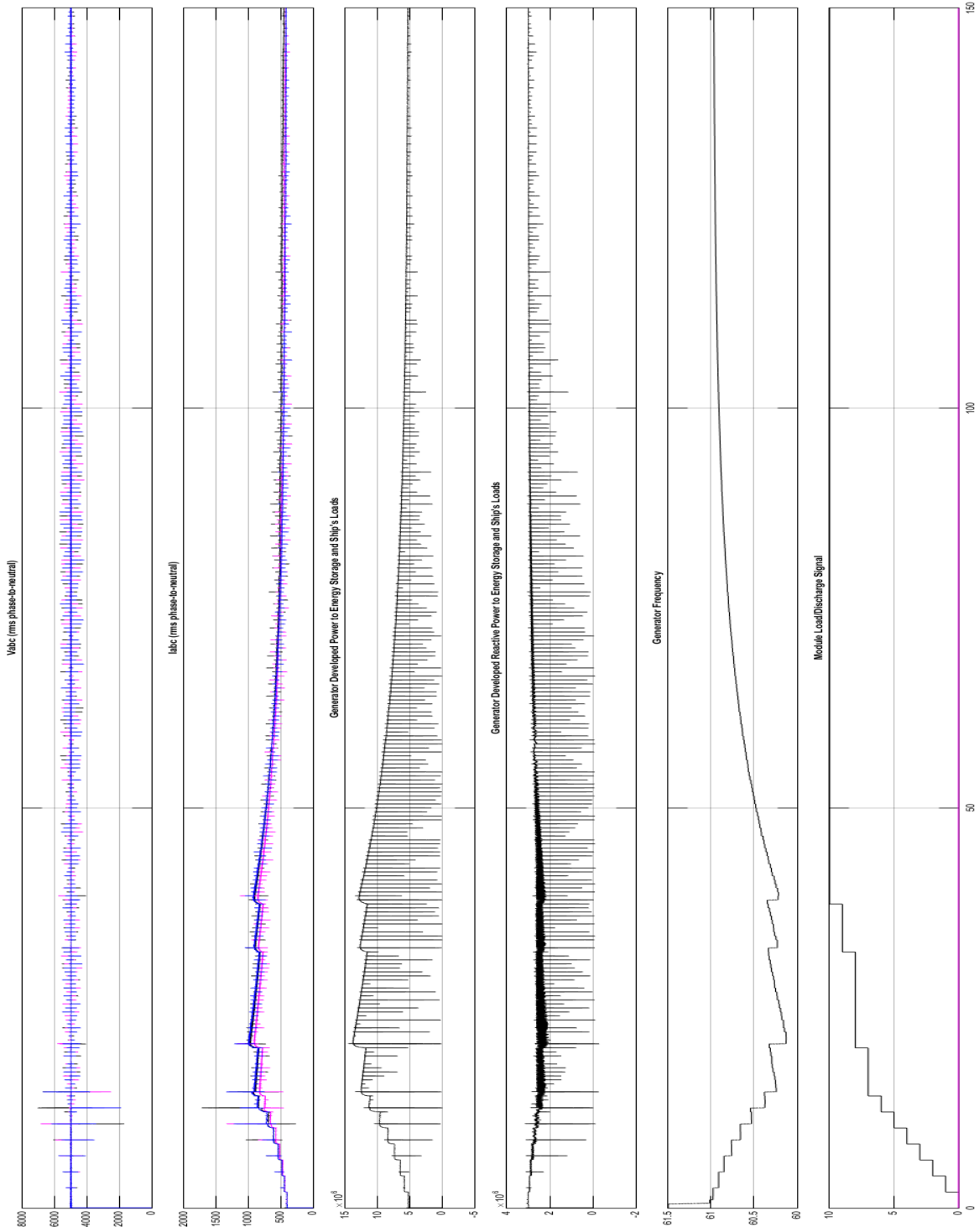


Appendix A.4 : Charging Results with a 4 MW Static Load



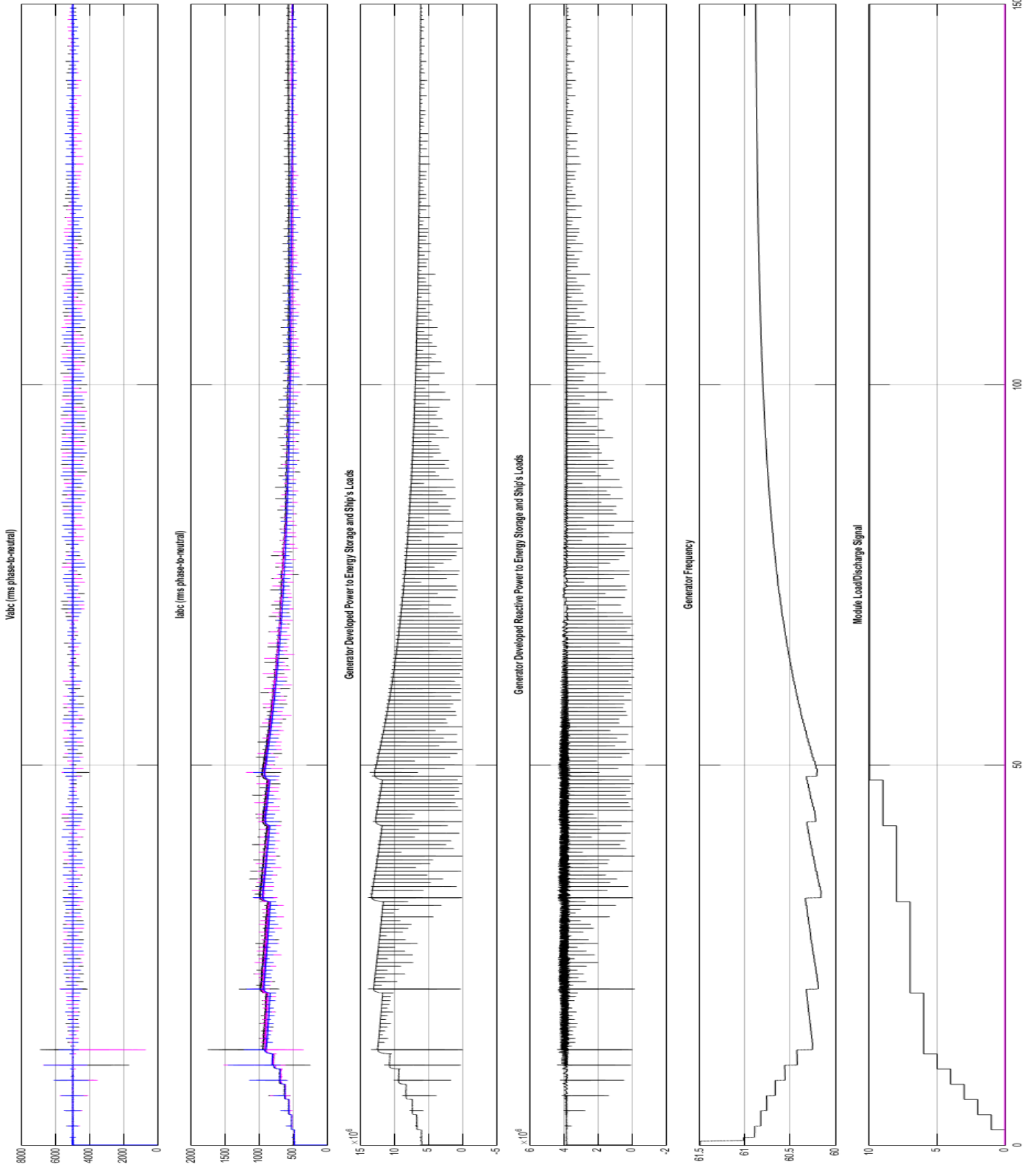


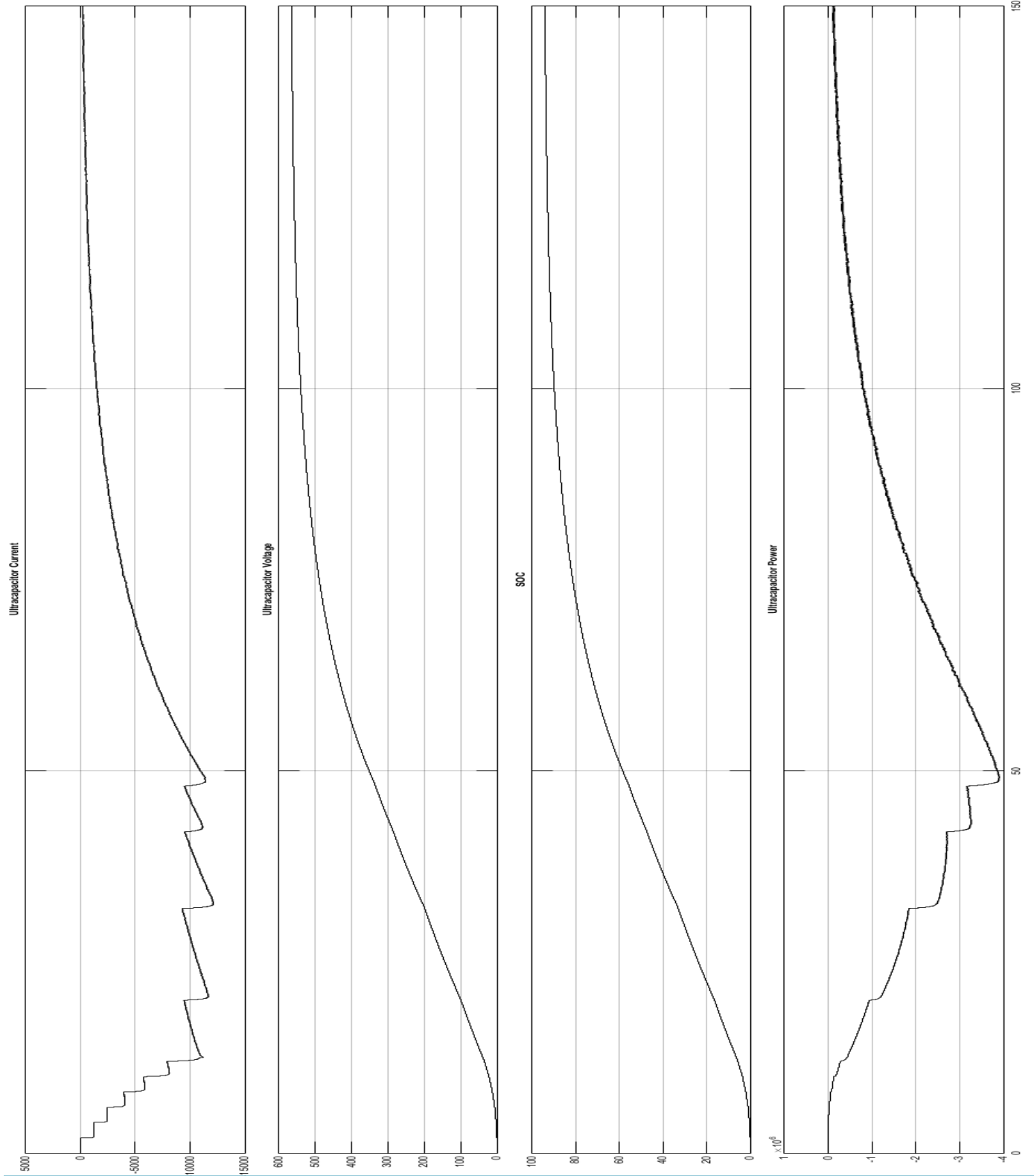
Appendix A.5 : Charging Results with a 5 MW Static Load



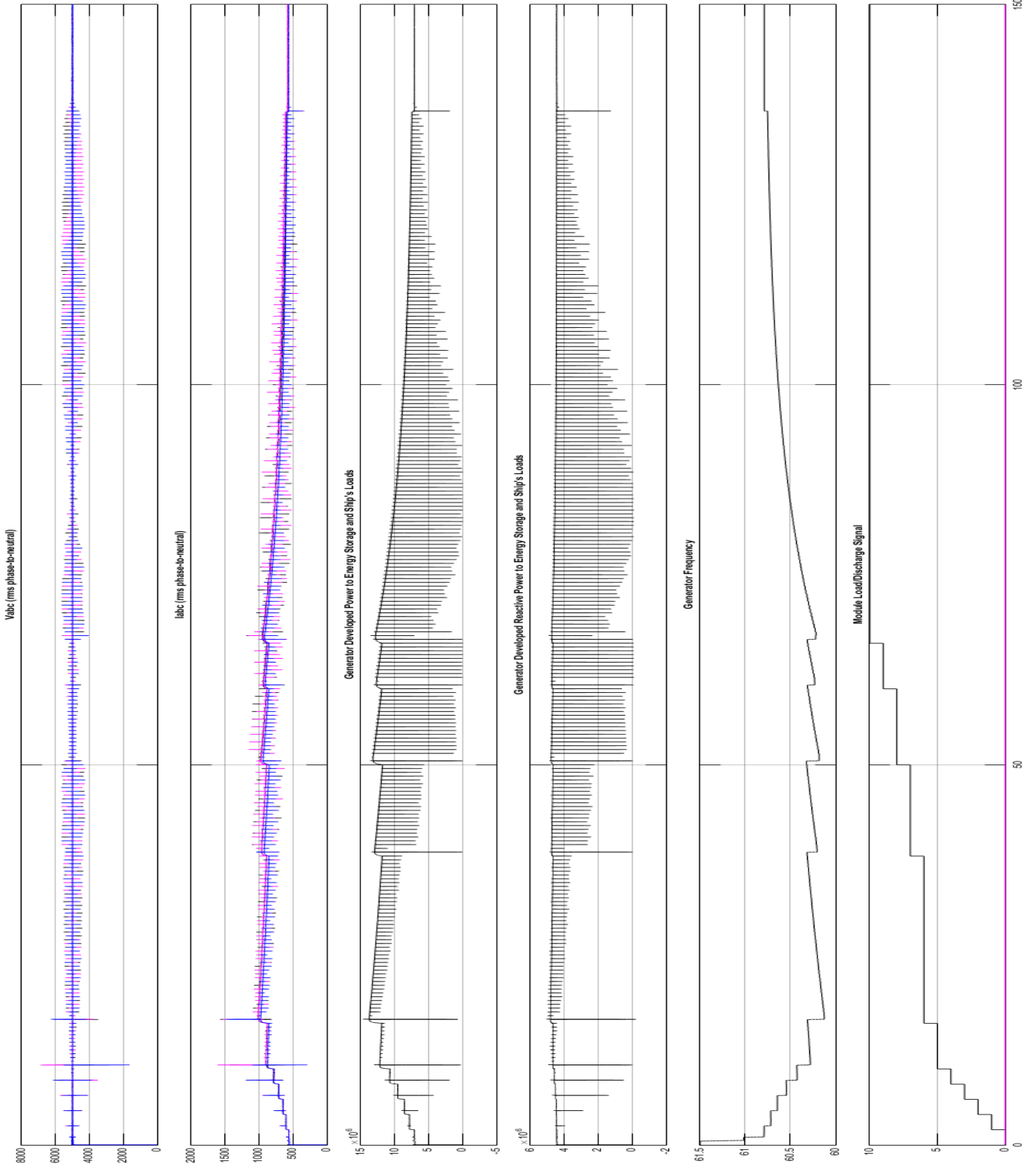


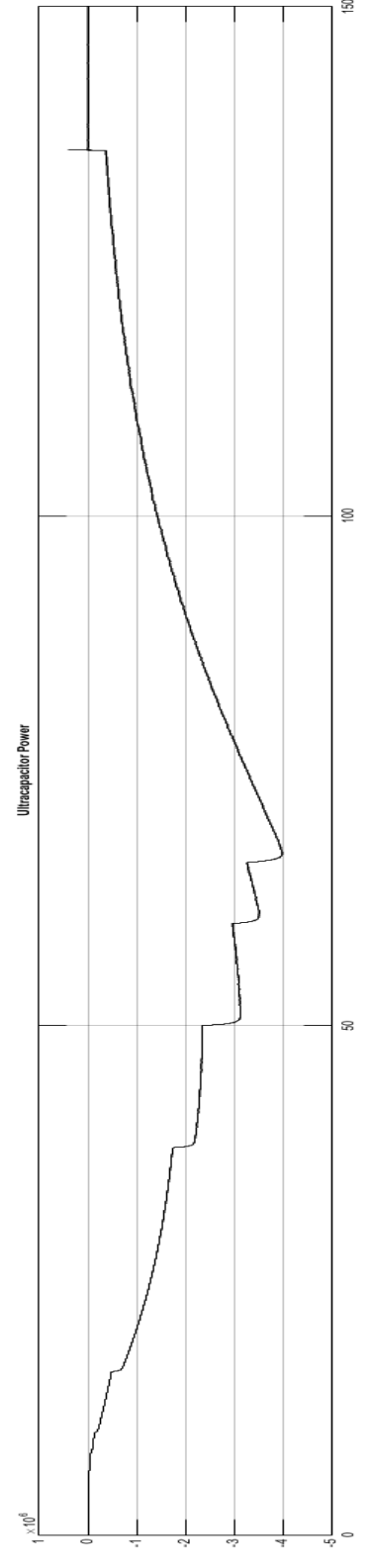
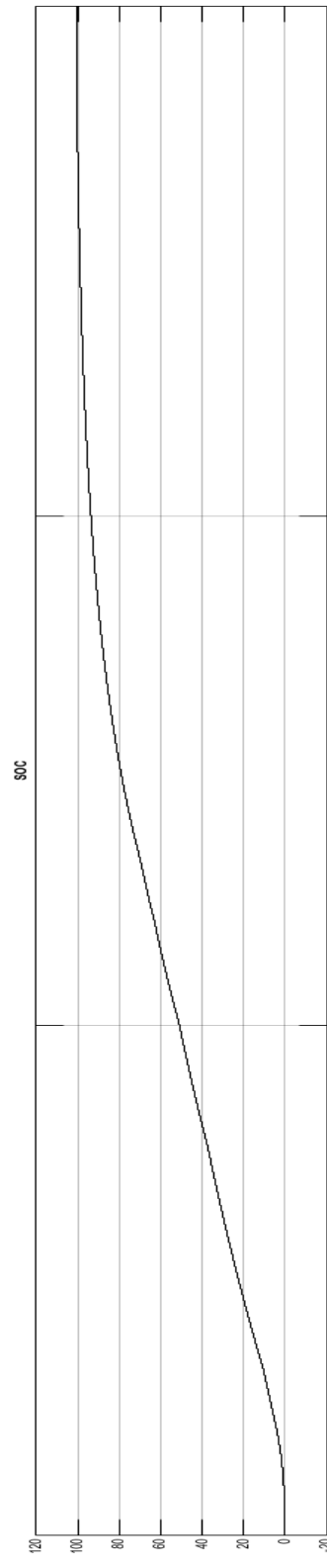
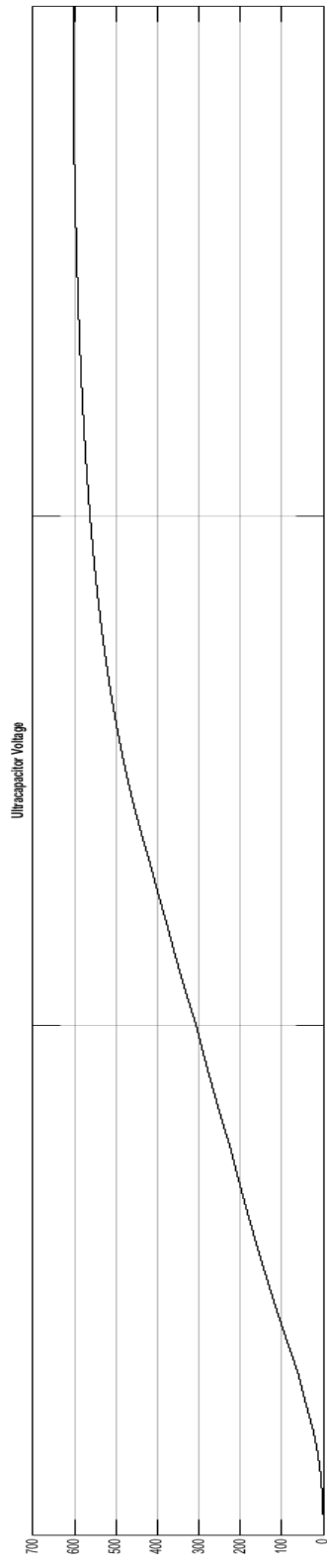
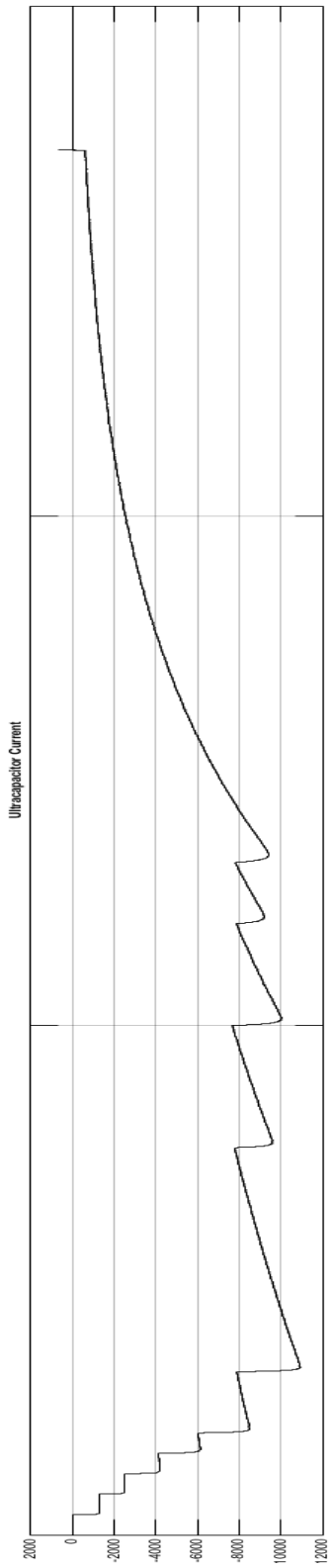
Appendix A.6 : Charging Results with a 6 MW Static Load



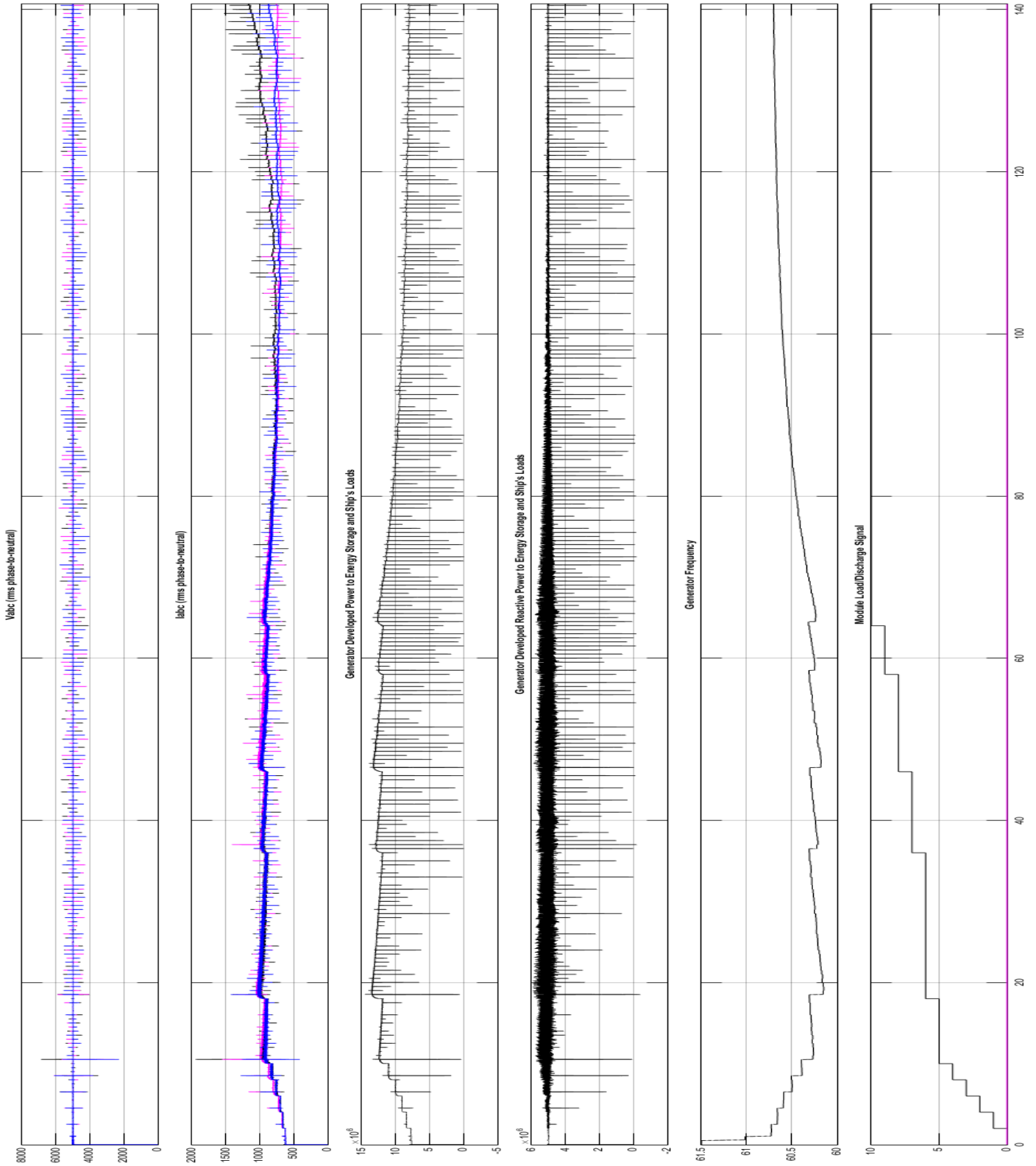


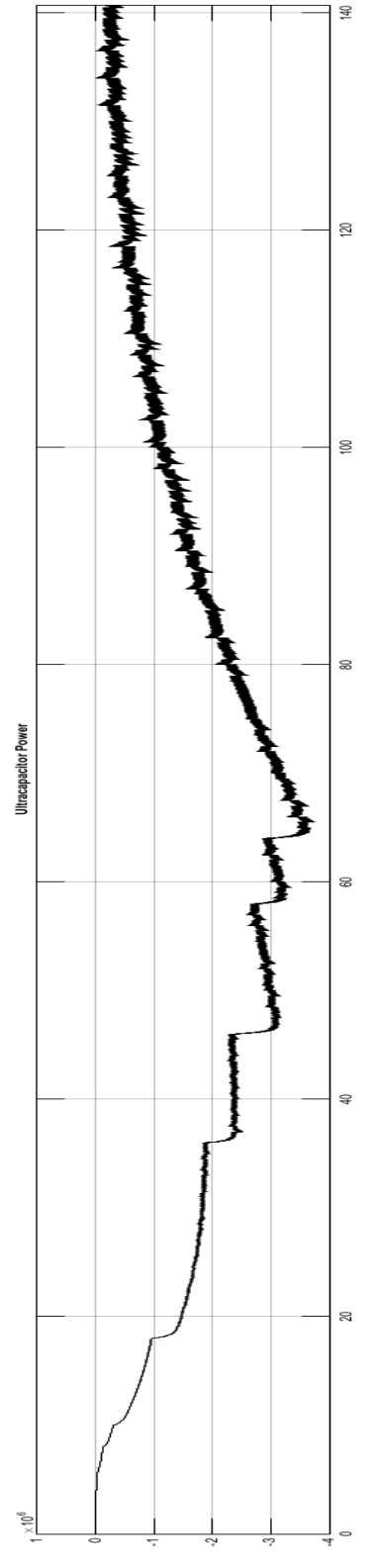
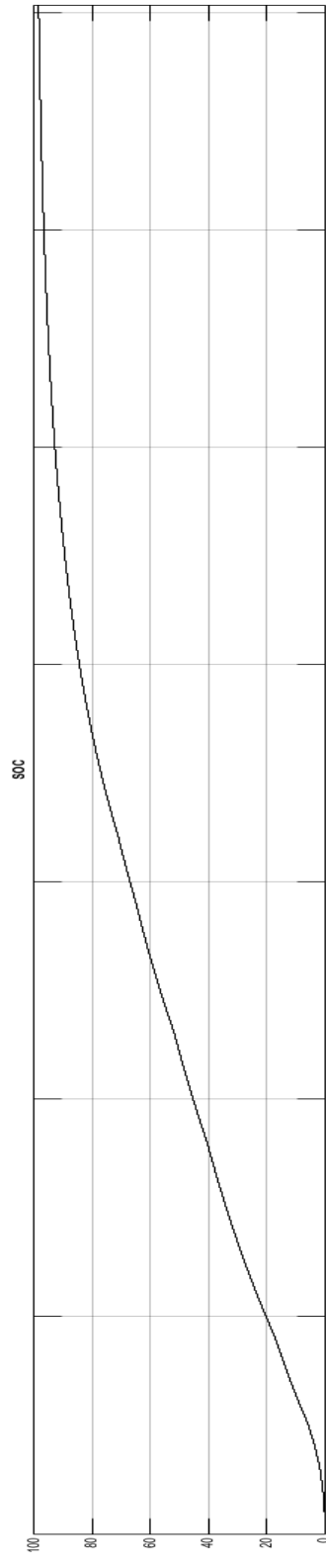
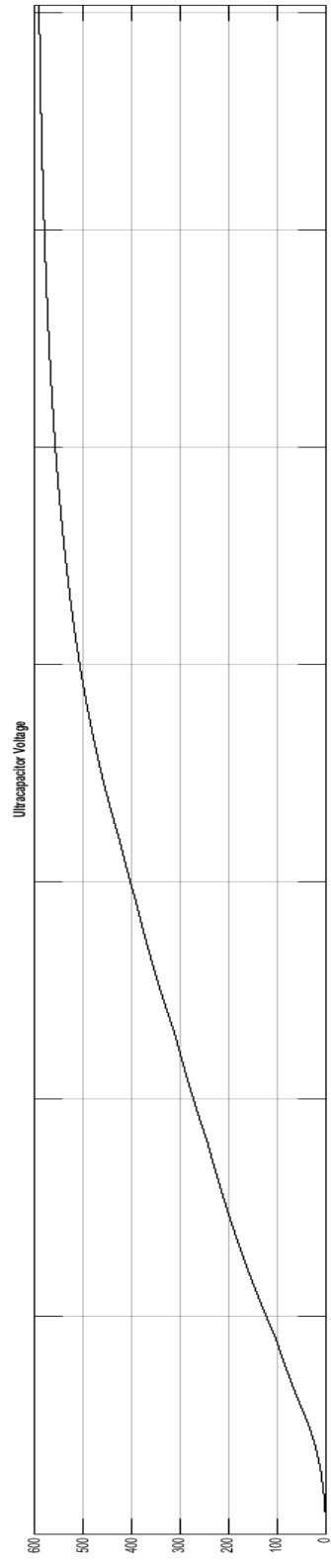
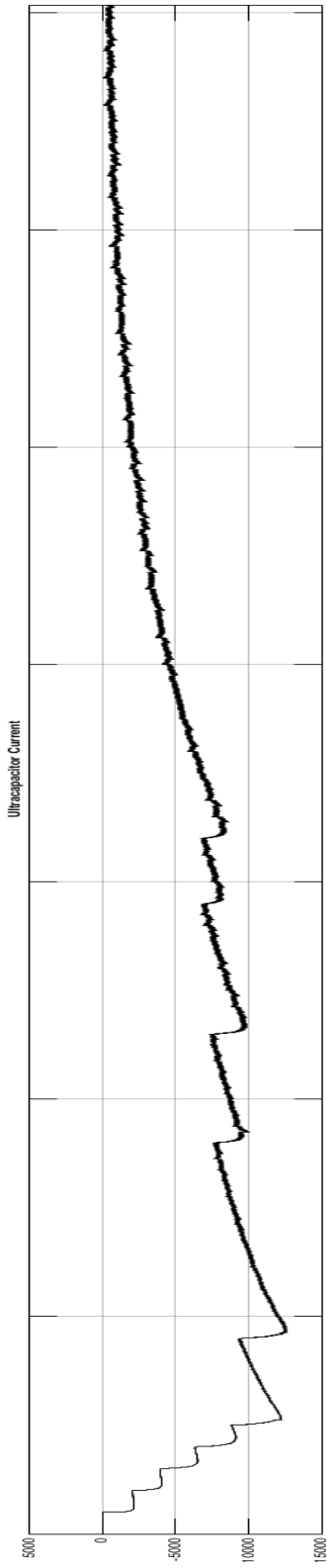
Appendix A.7 : Charging Results with a 7 MW Static Load



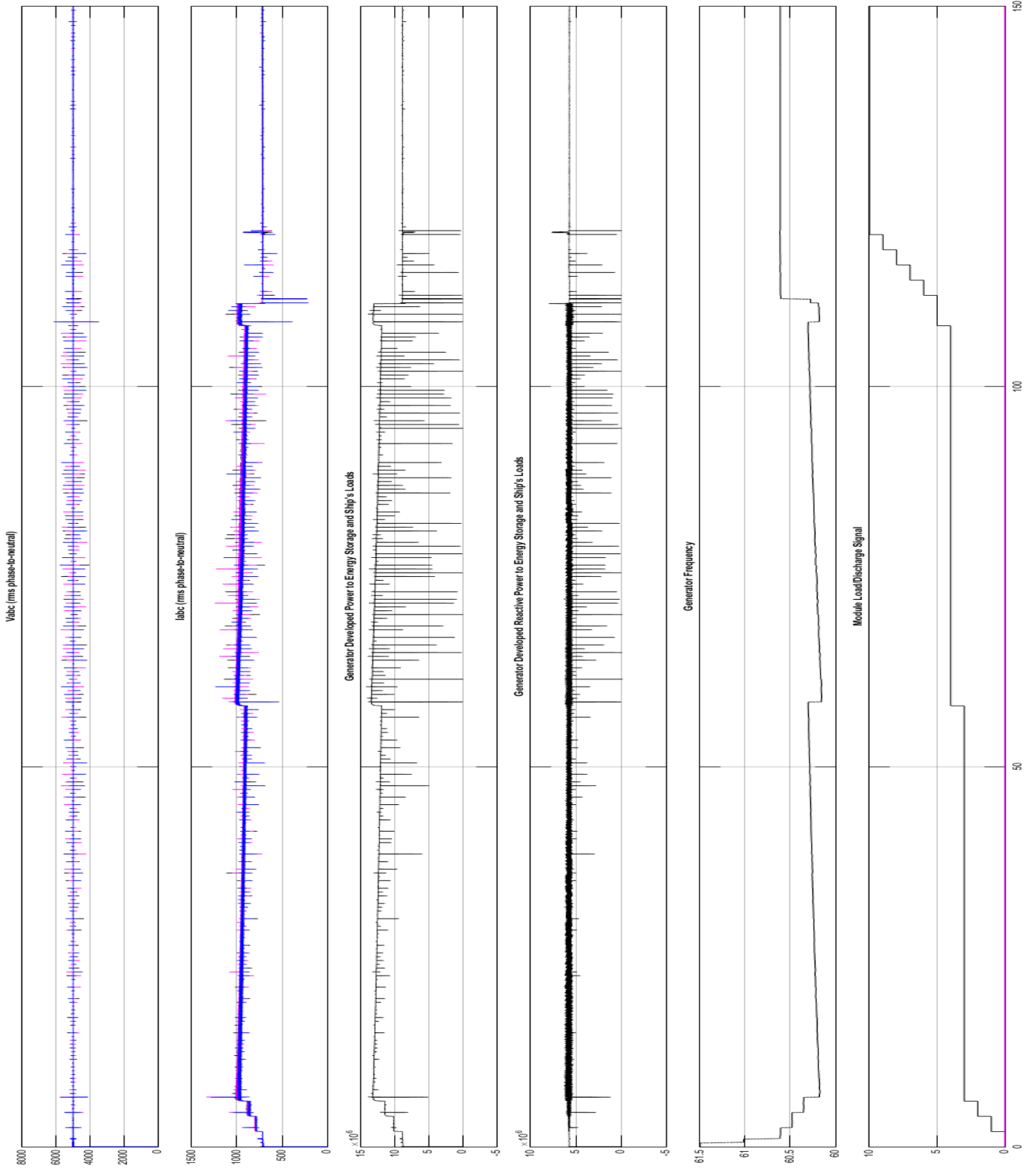


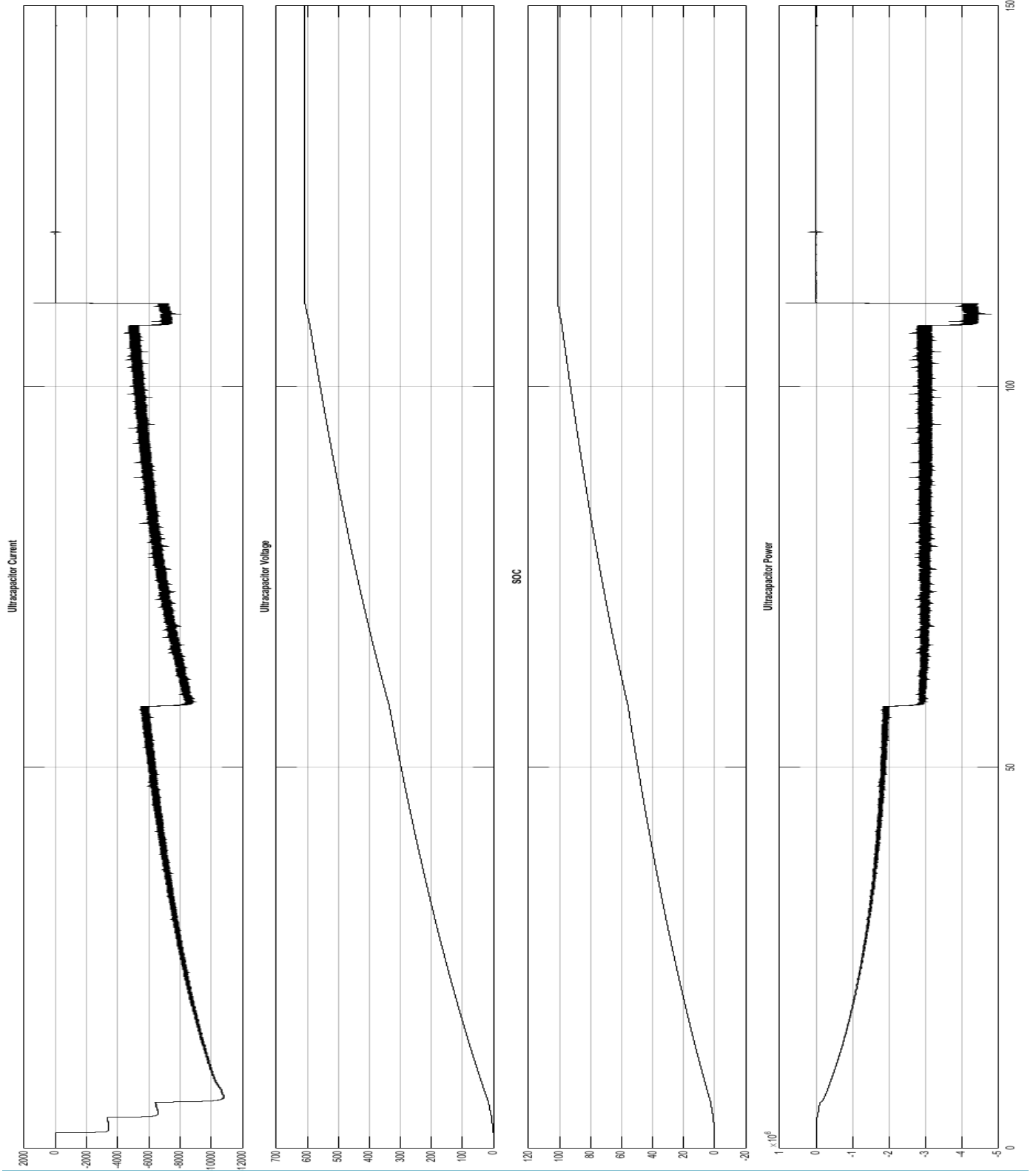
Appendix A.8 : Charging Results with an 8 MW Static Load



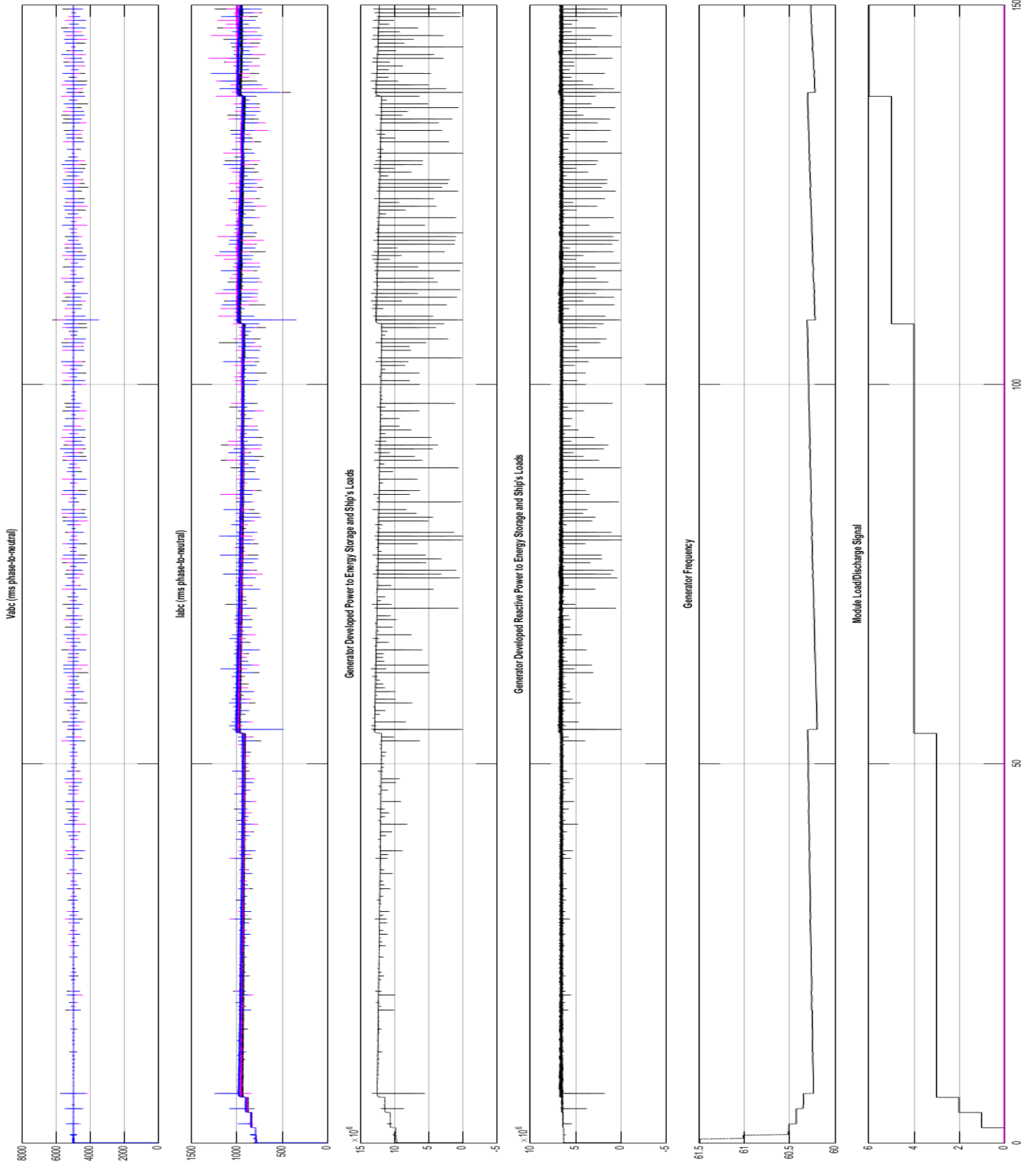


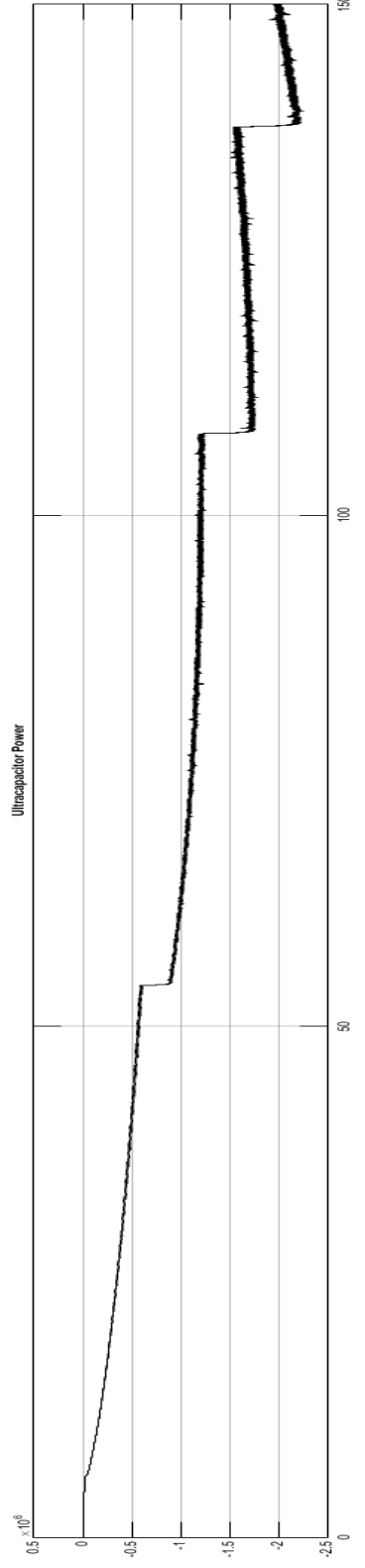
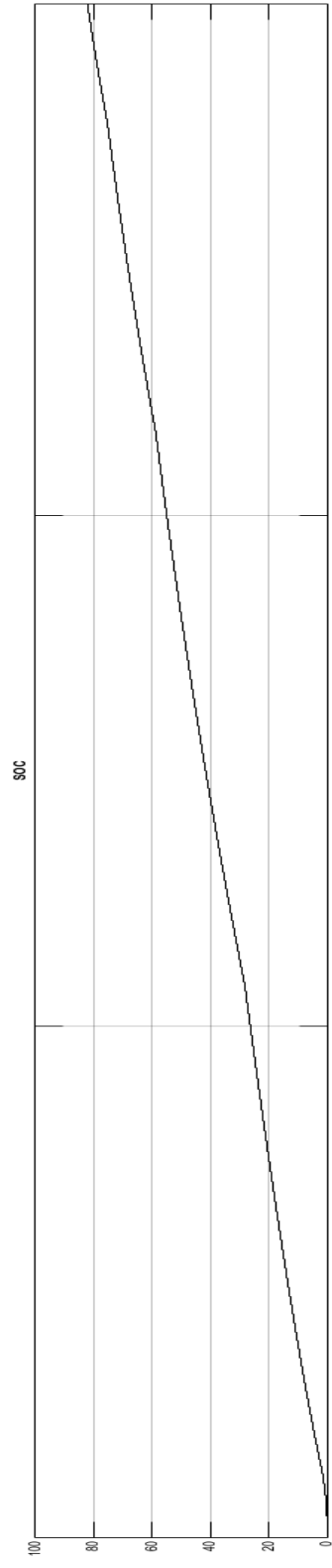
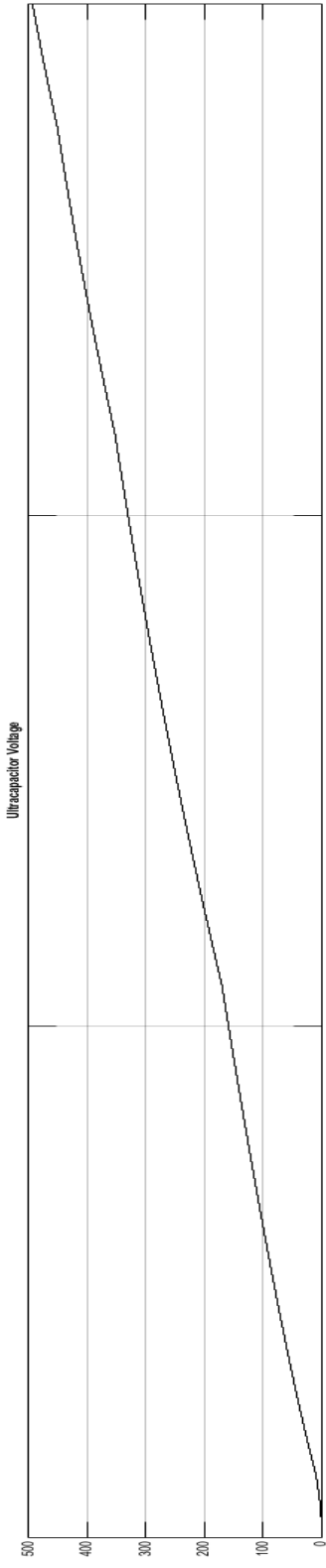
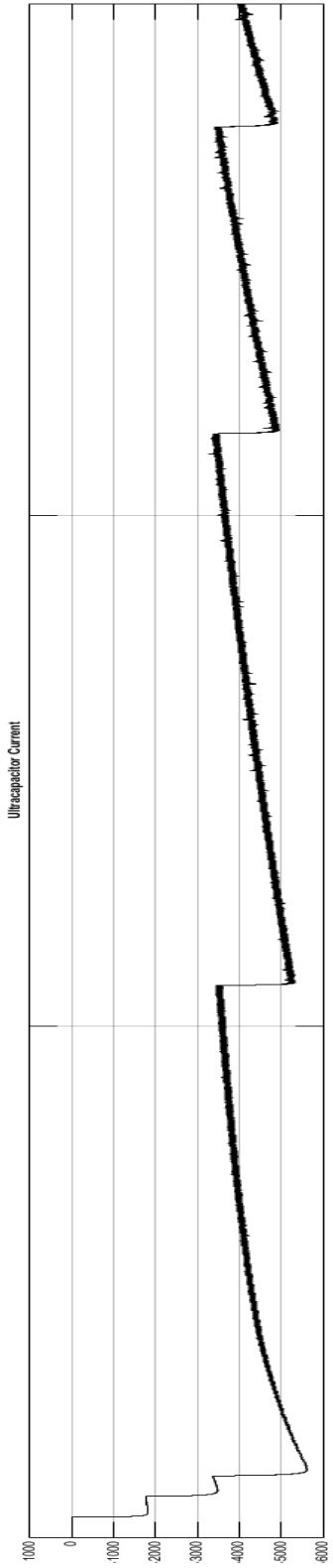
Appendix A.9 : Charging Results with a 9 MW Static Load



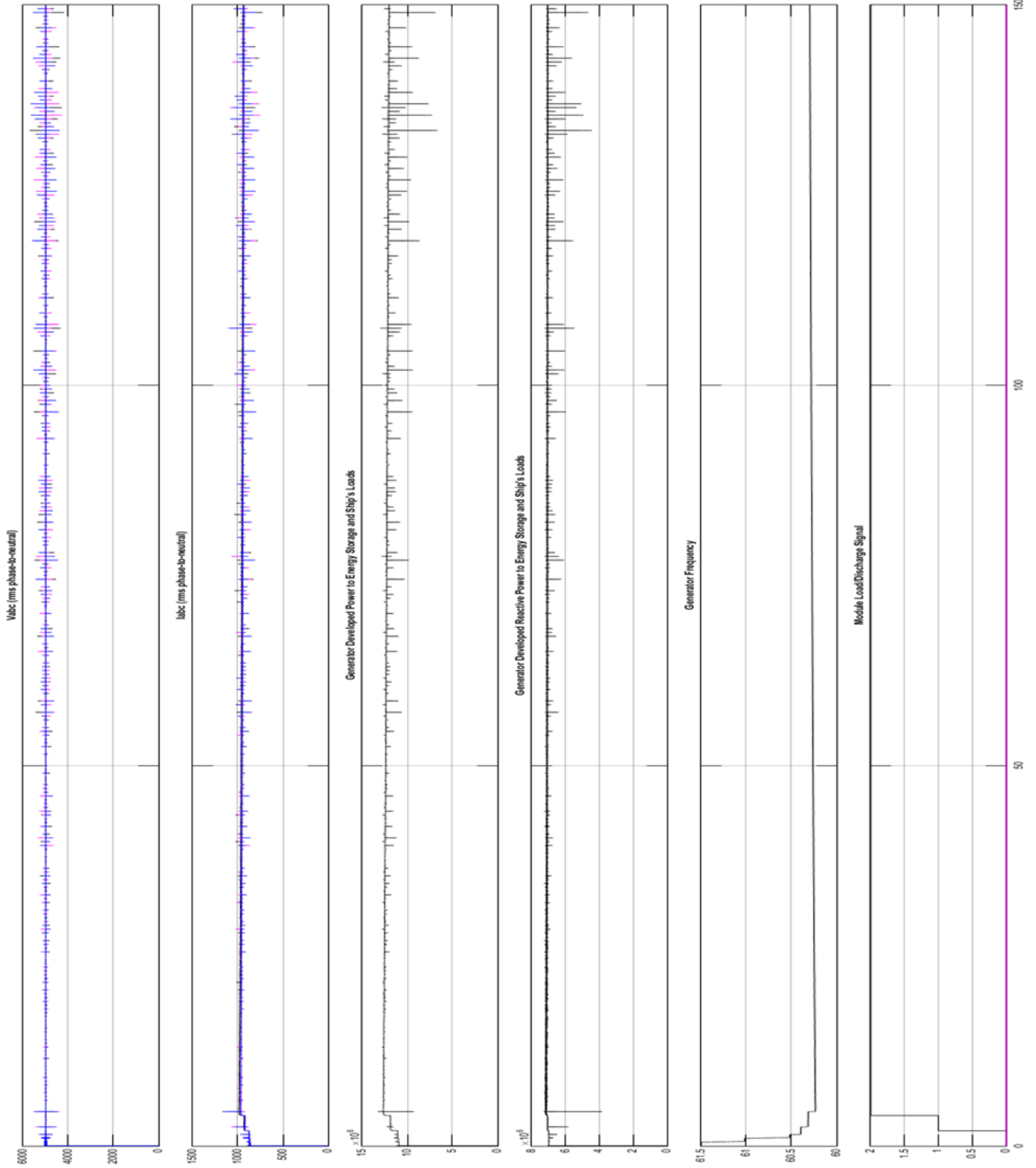


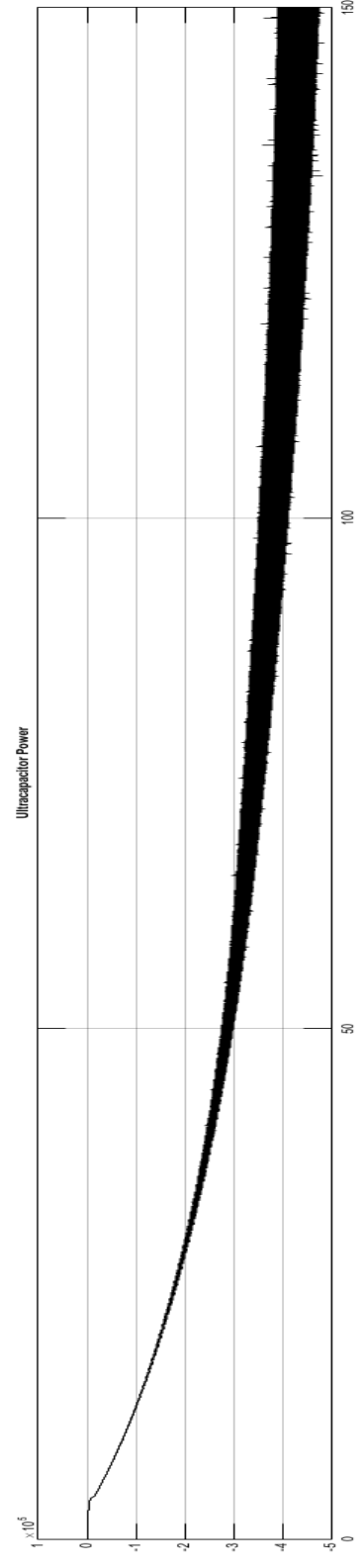
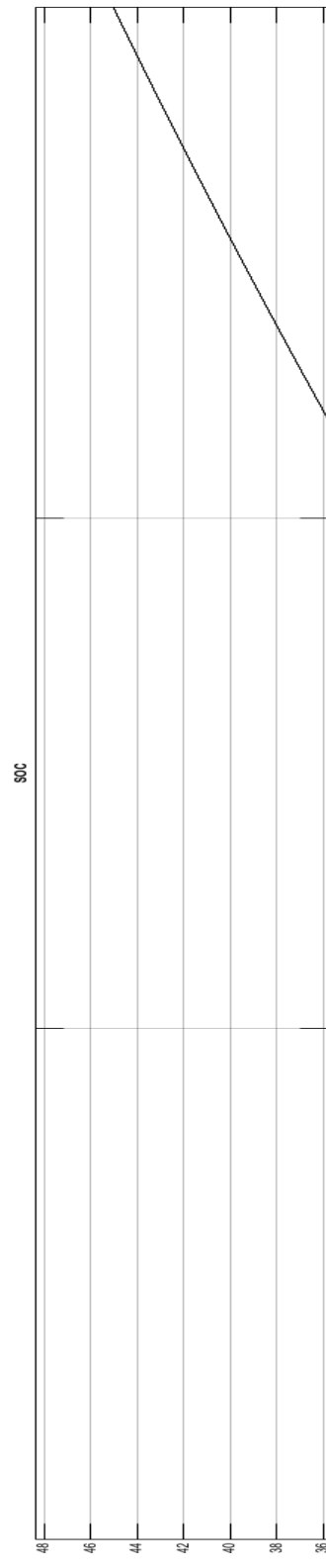
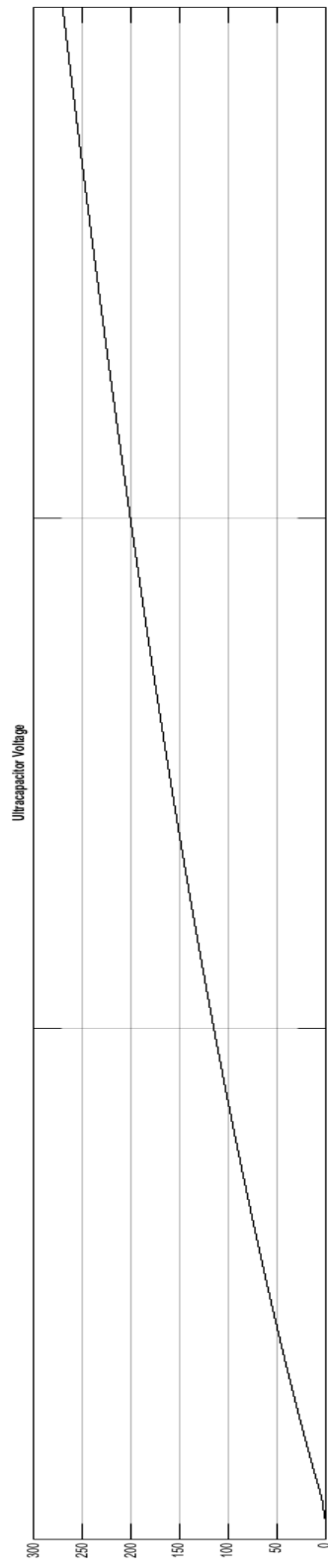
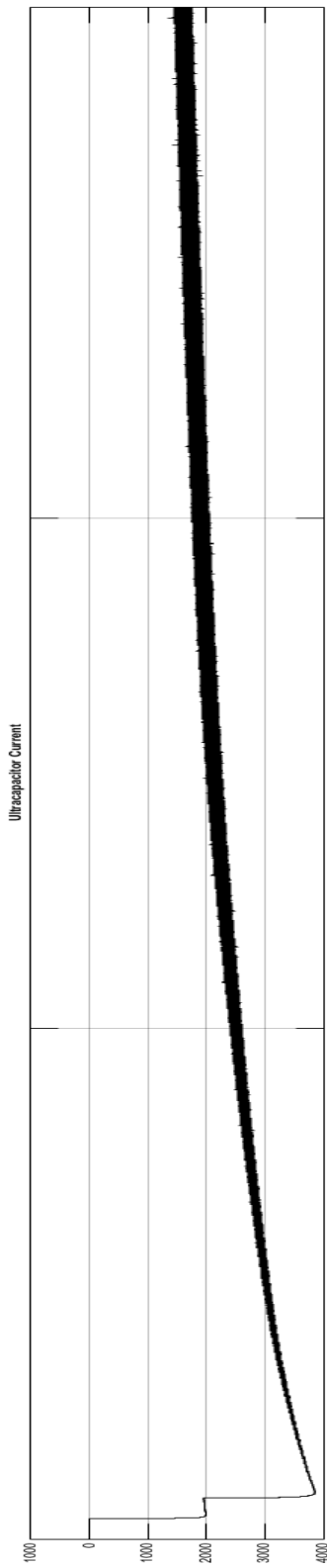
Appendix A.10 : Charging Results with a 10 MW Static Load





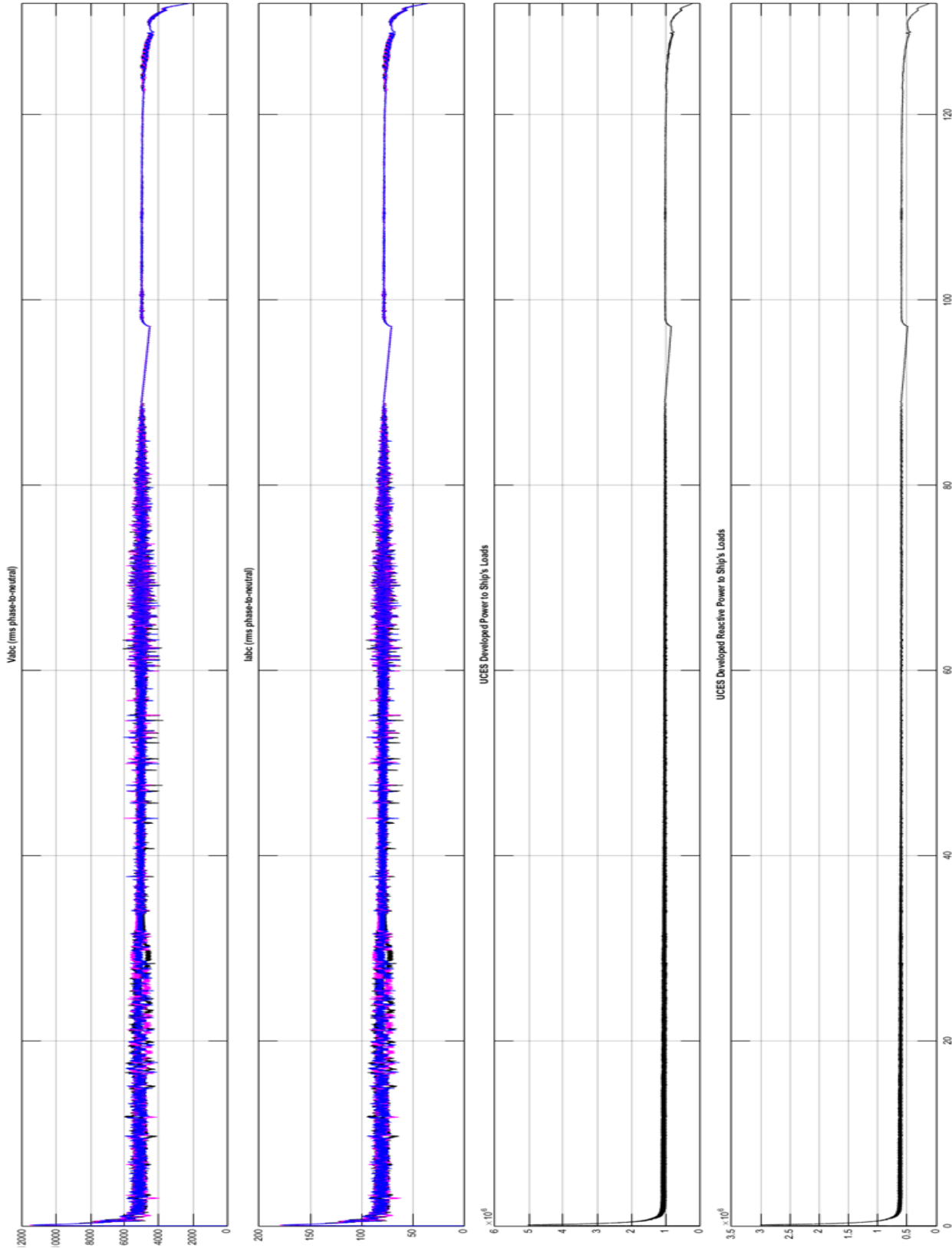
Appendix A.11 : Charging Results with an 11 MW Static Load

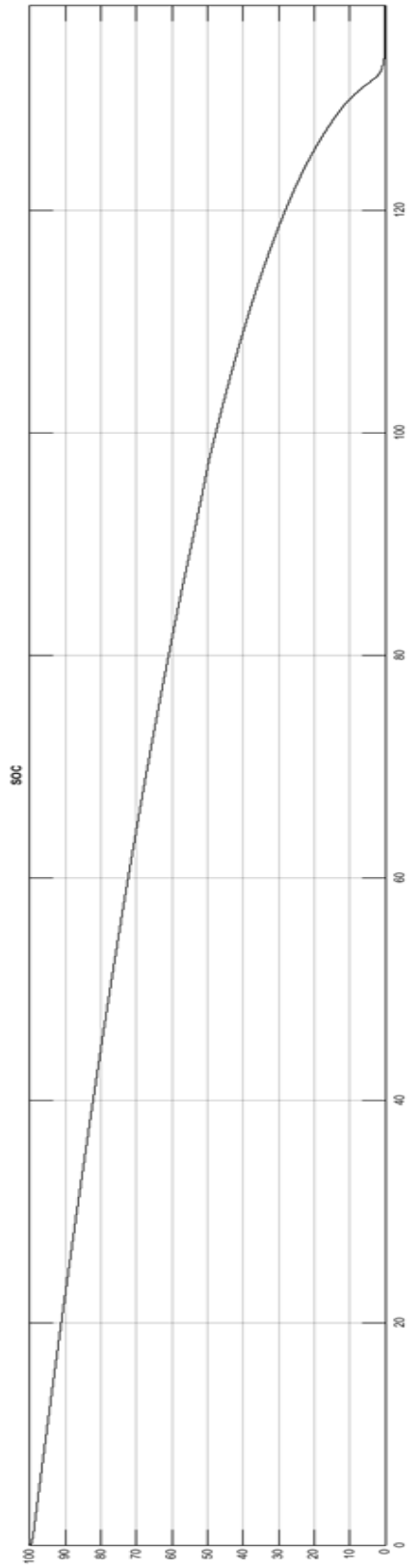
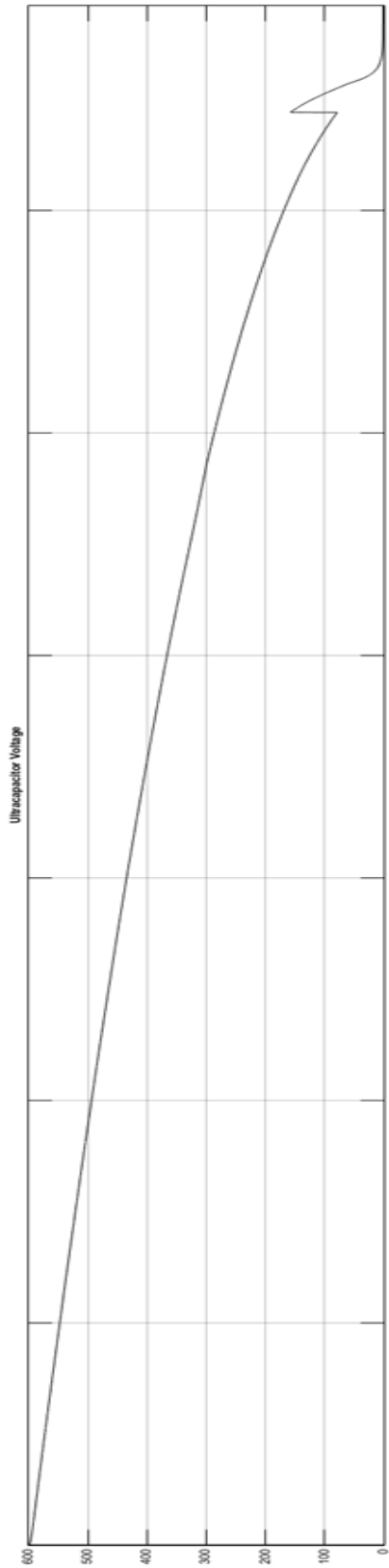
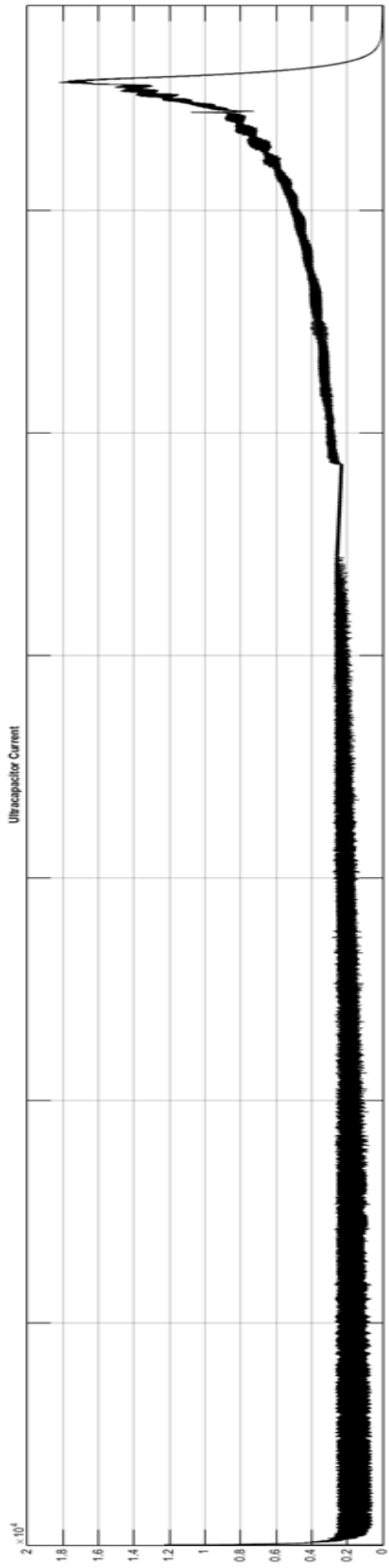




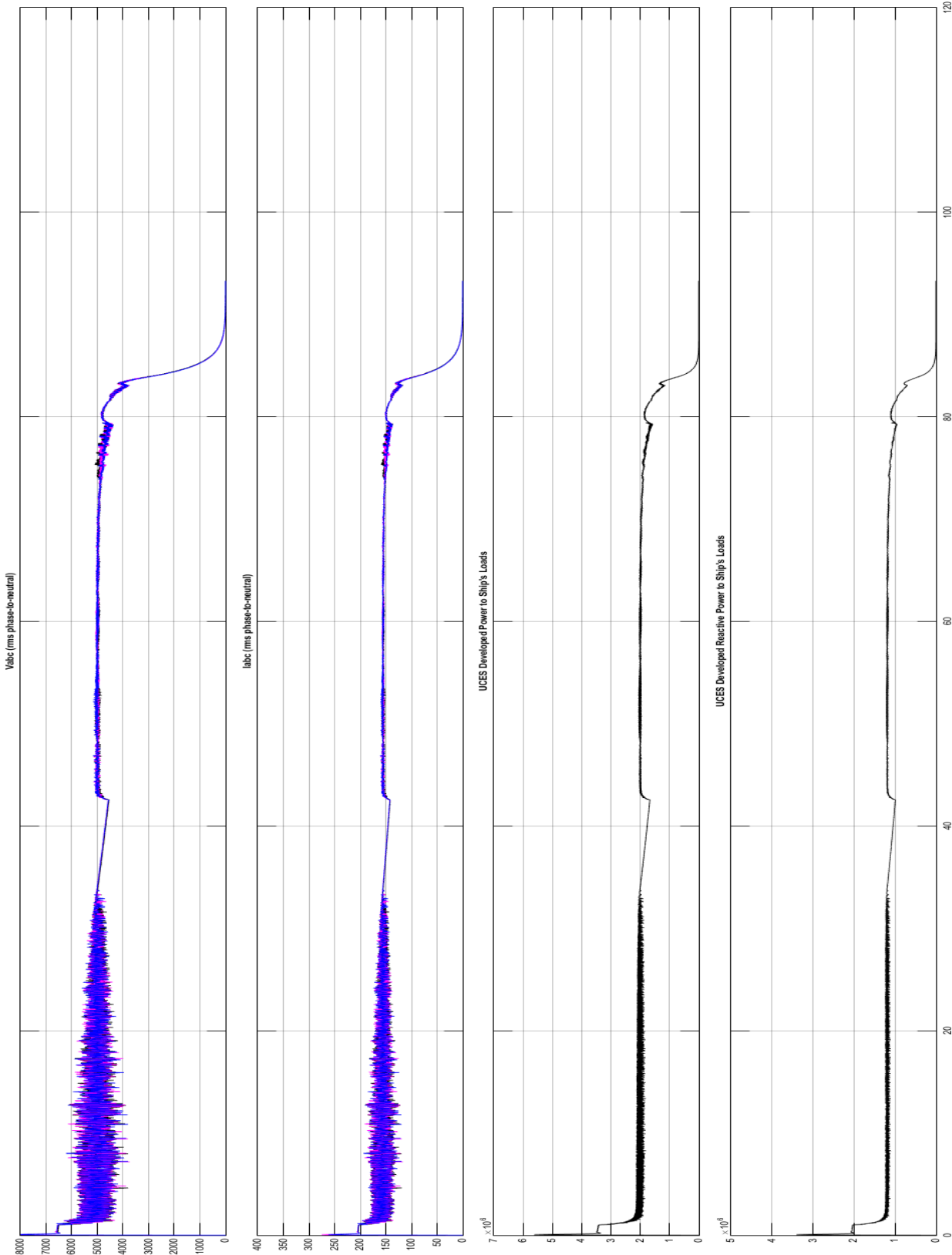
Appendix B : Additional Discharge System Results

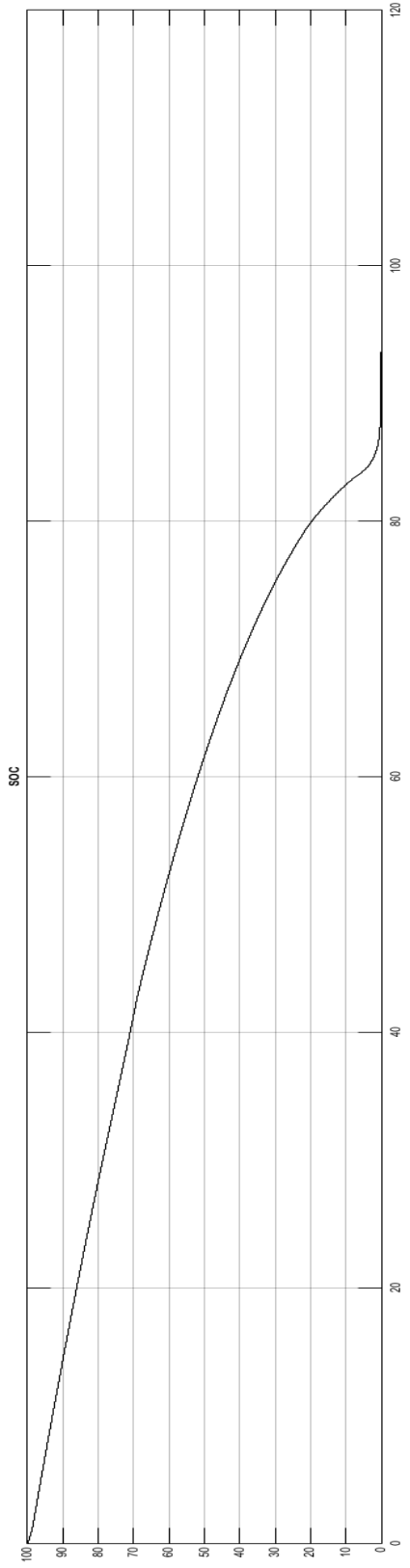
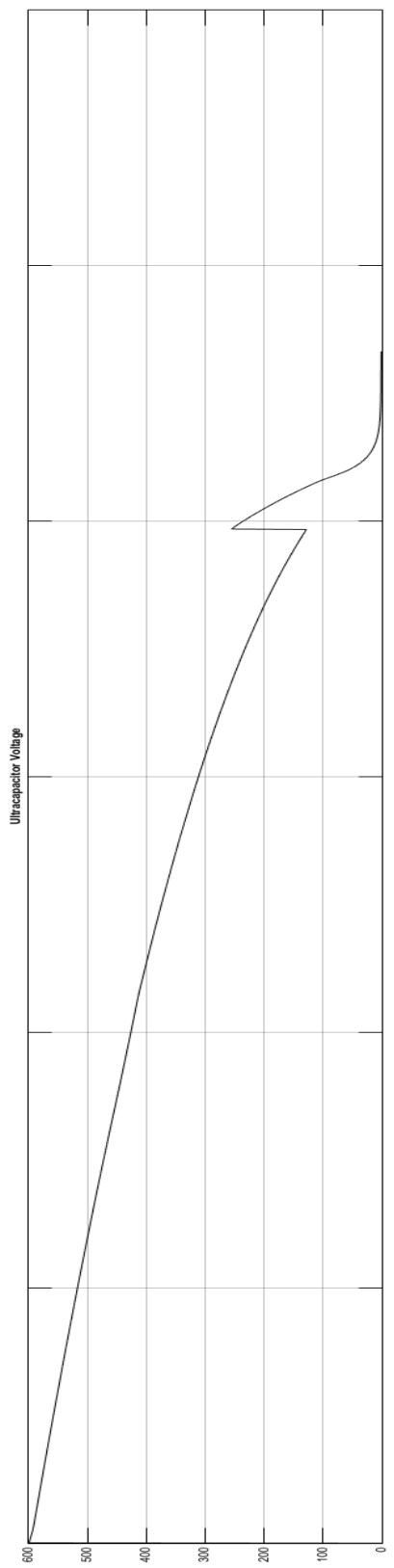
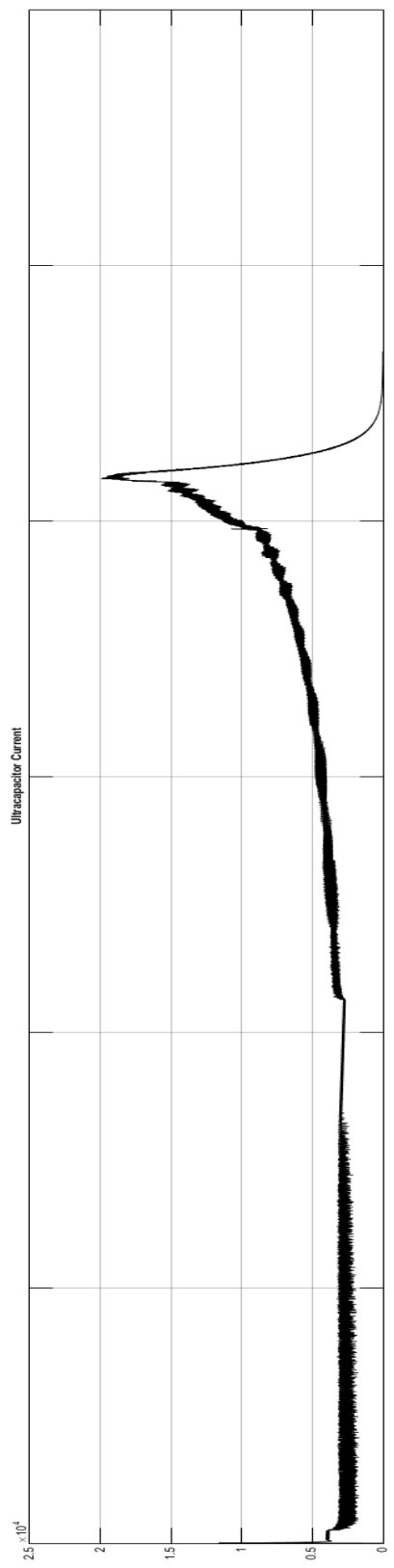
Appendix B.1: Discharge Results Powering a 1MW Static Load



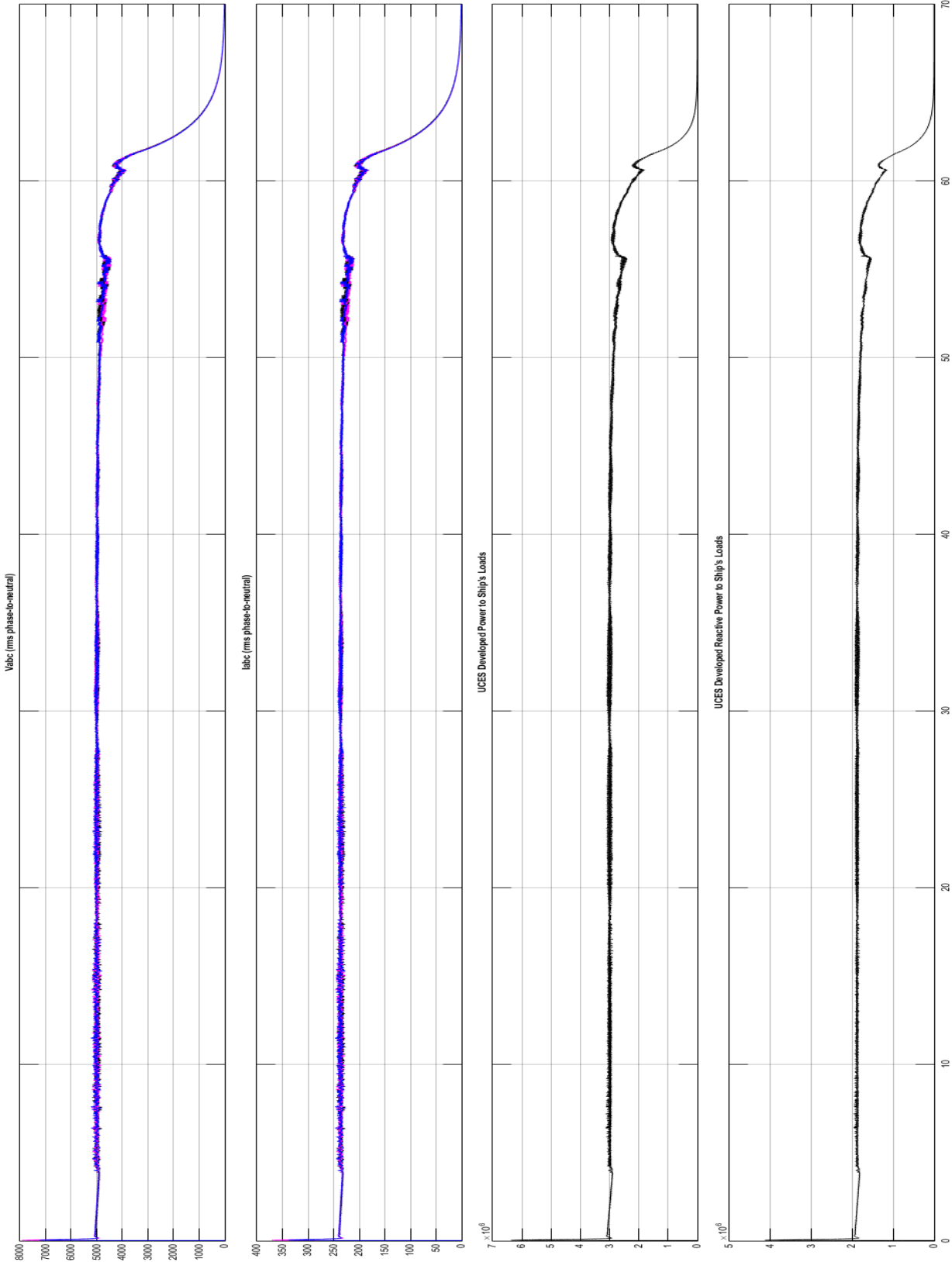


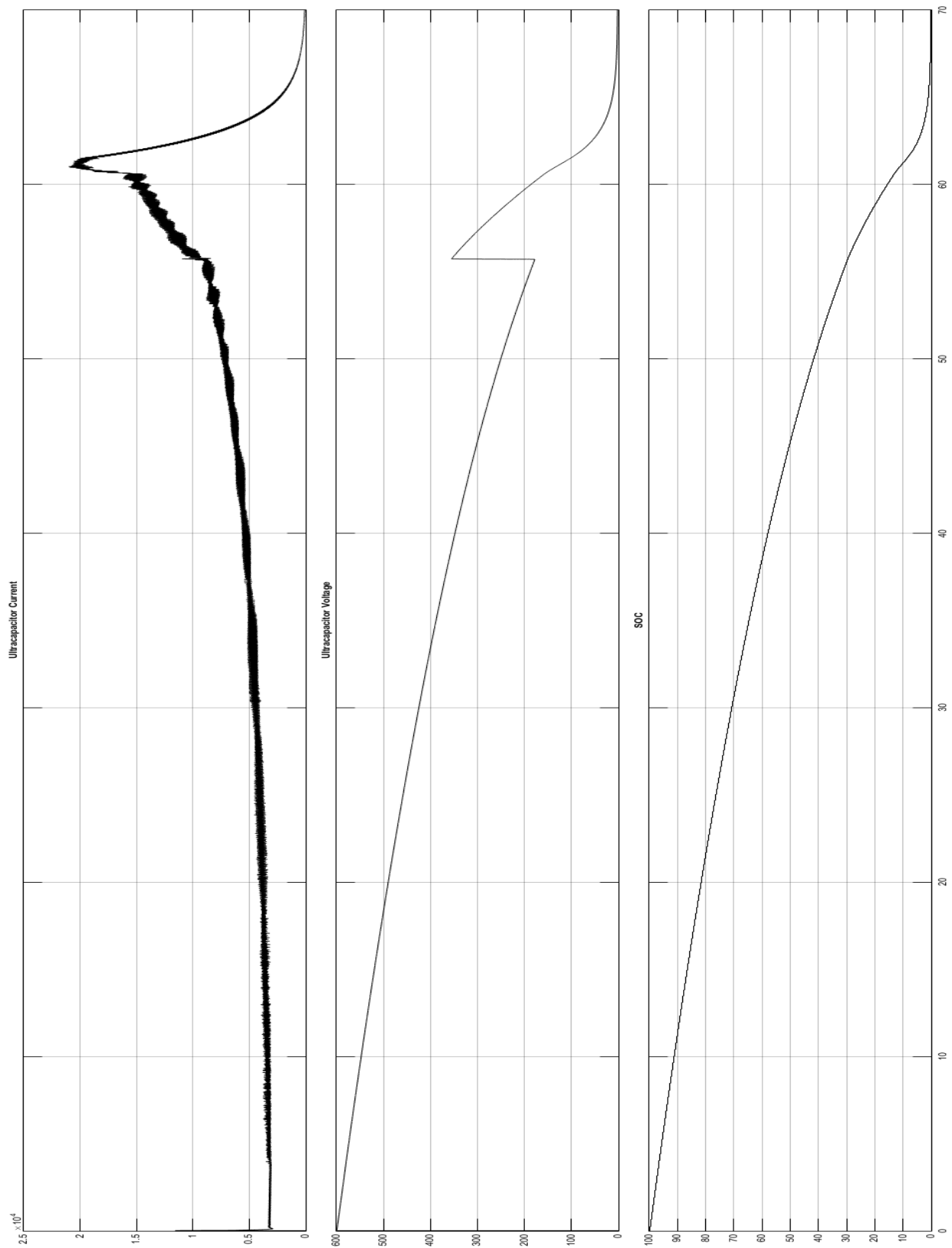
Appendix B.2: Discharge Results Powering a 2MW Static Load



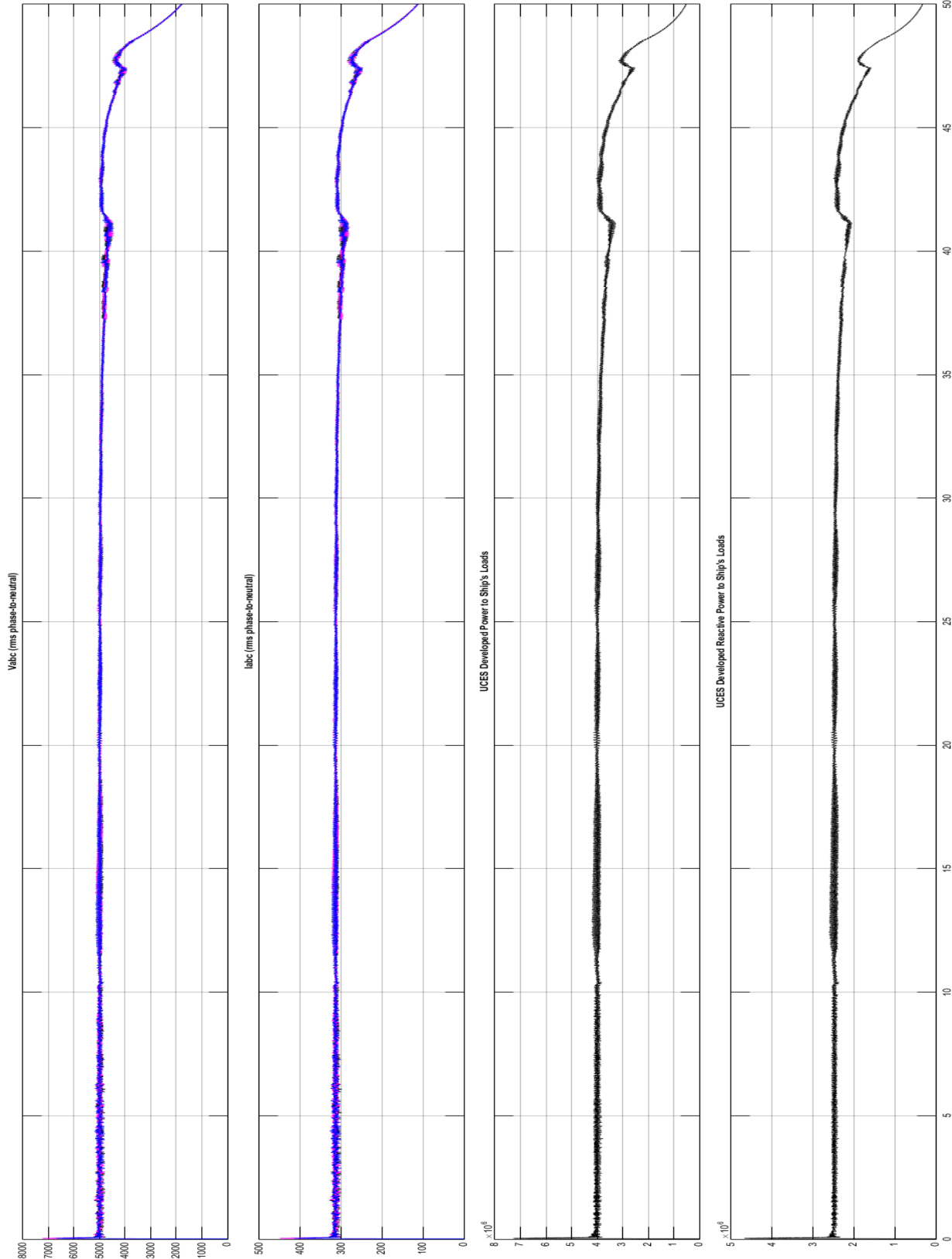


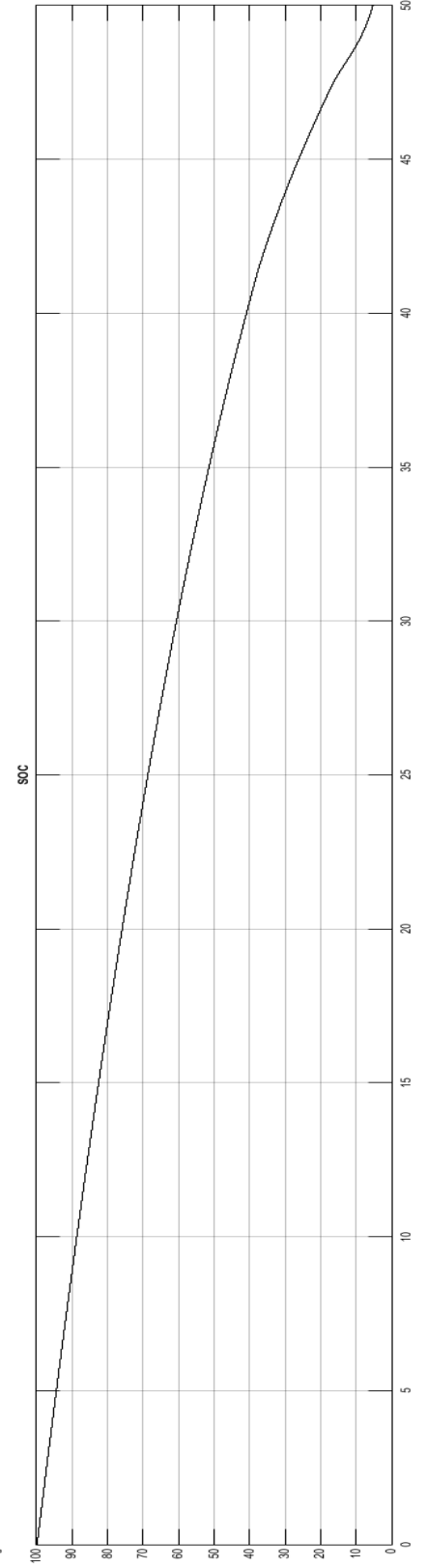
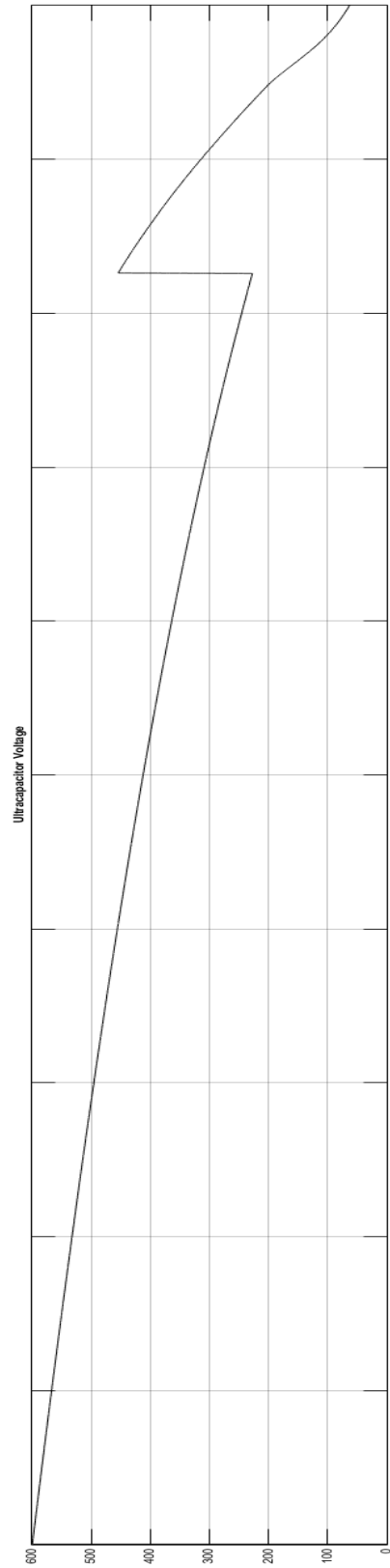
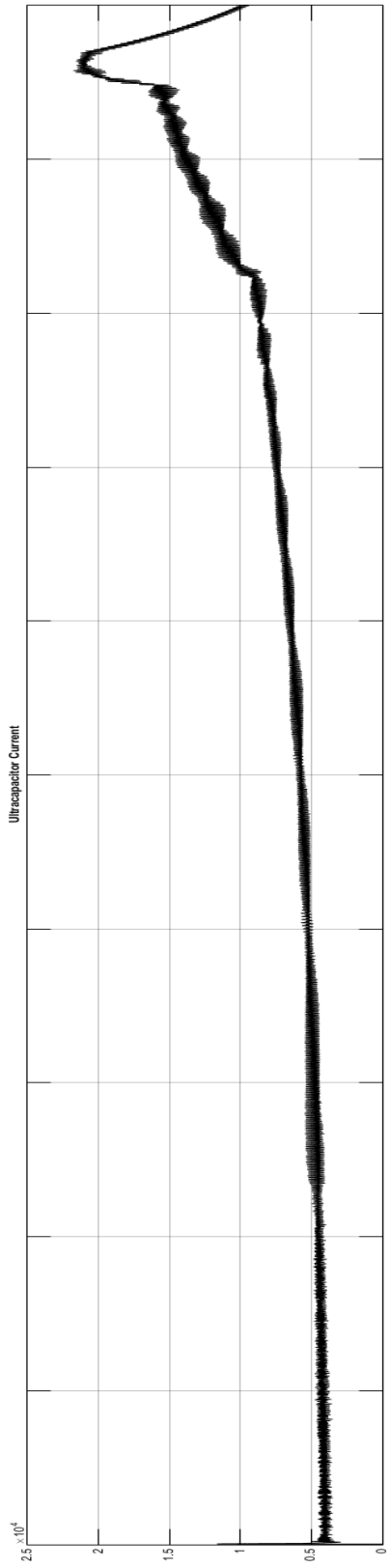
Appendix B.3: Discharge Results Powering a 3MW Static Load



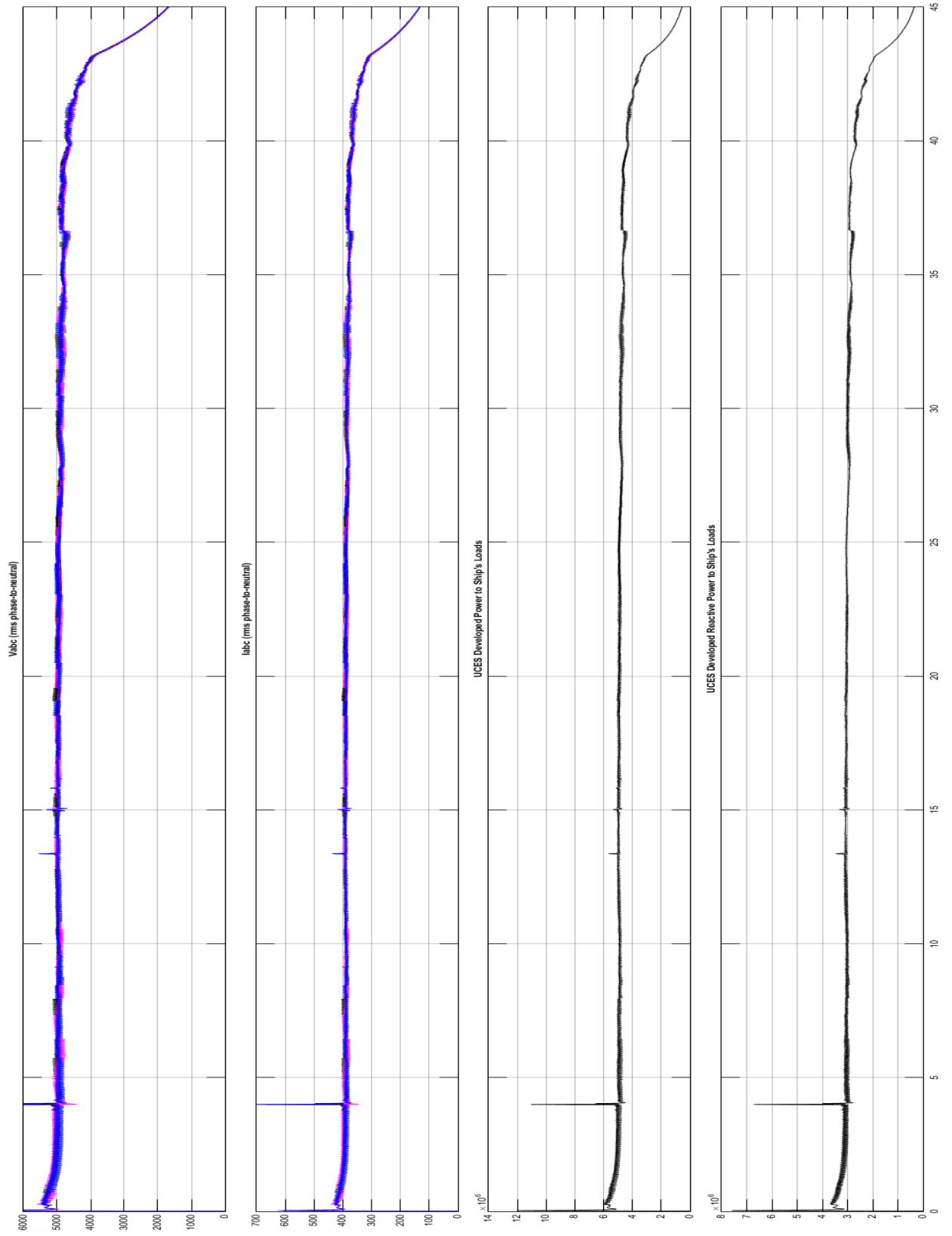


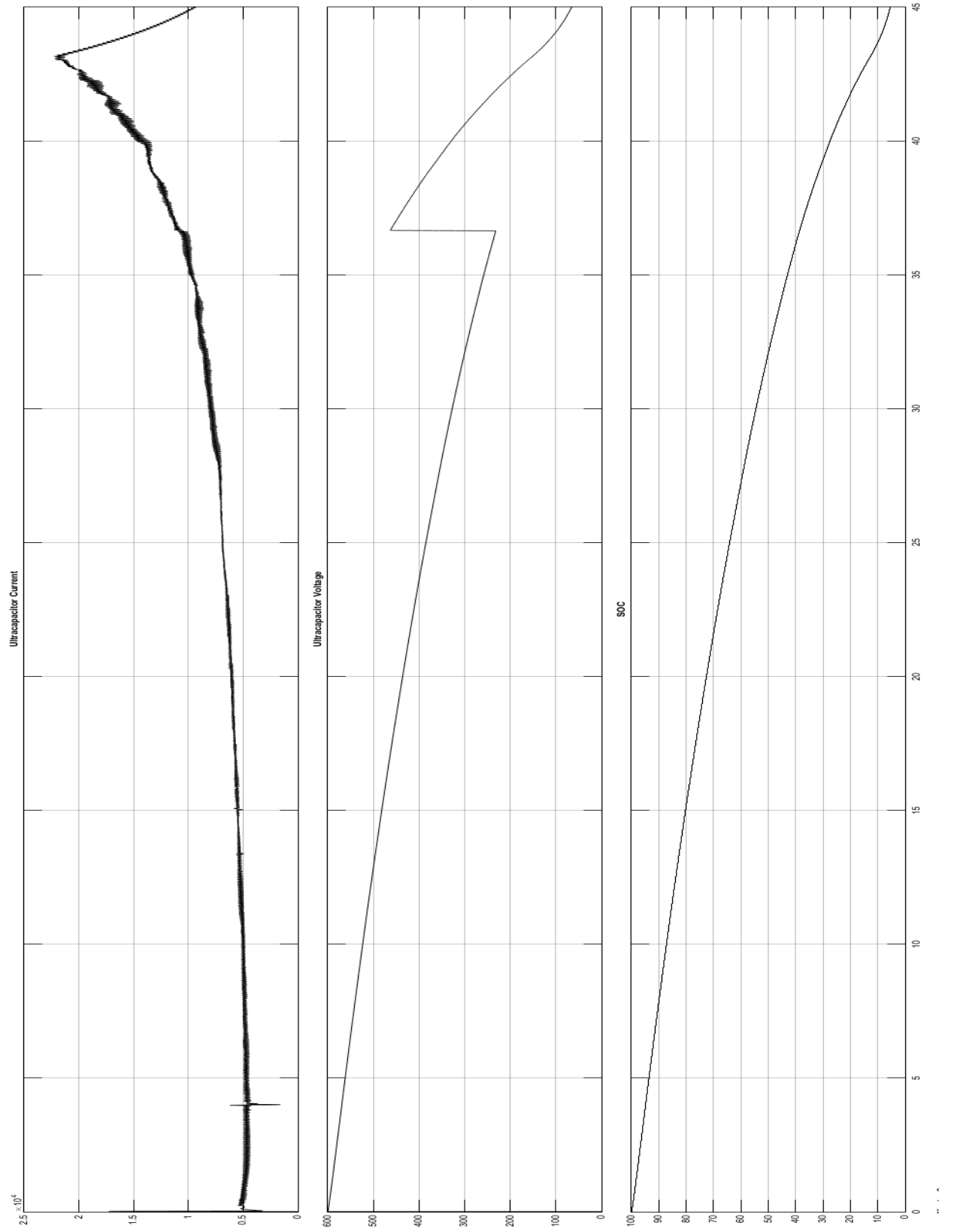
Appendix B.4: Discharge Results Powering a 4MW Static Load



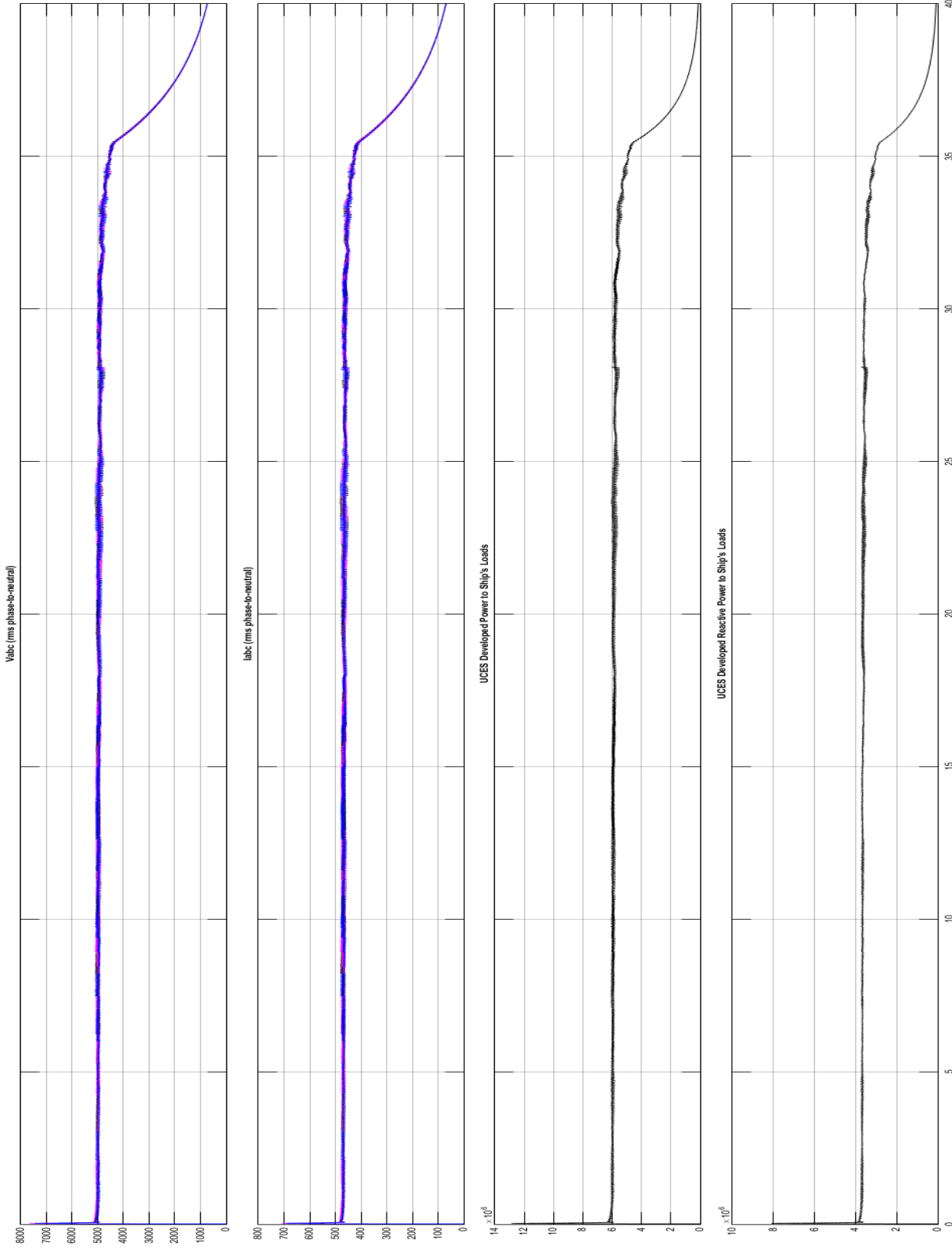


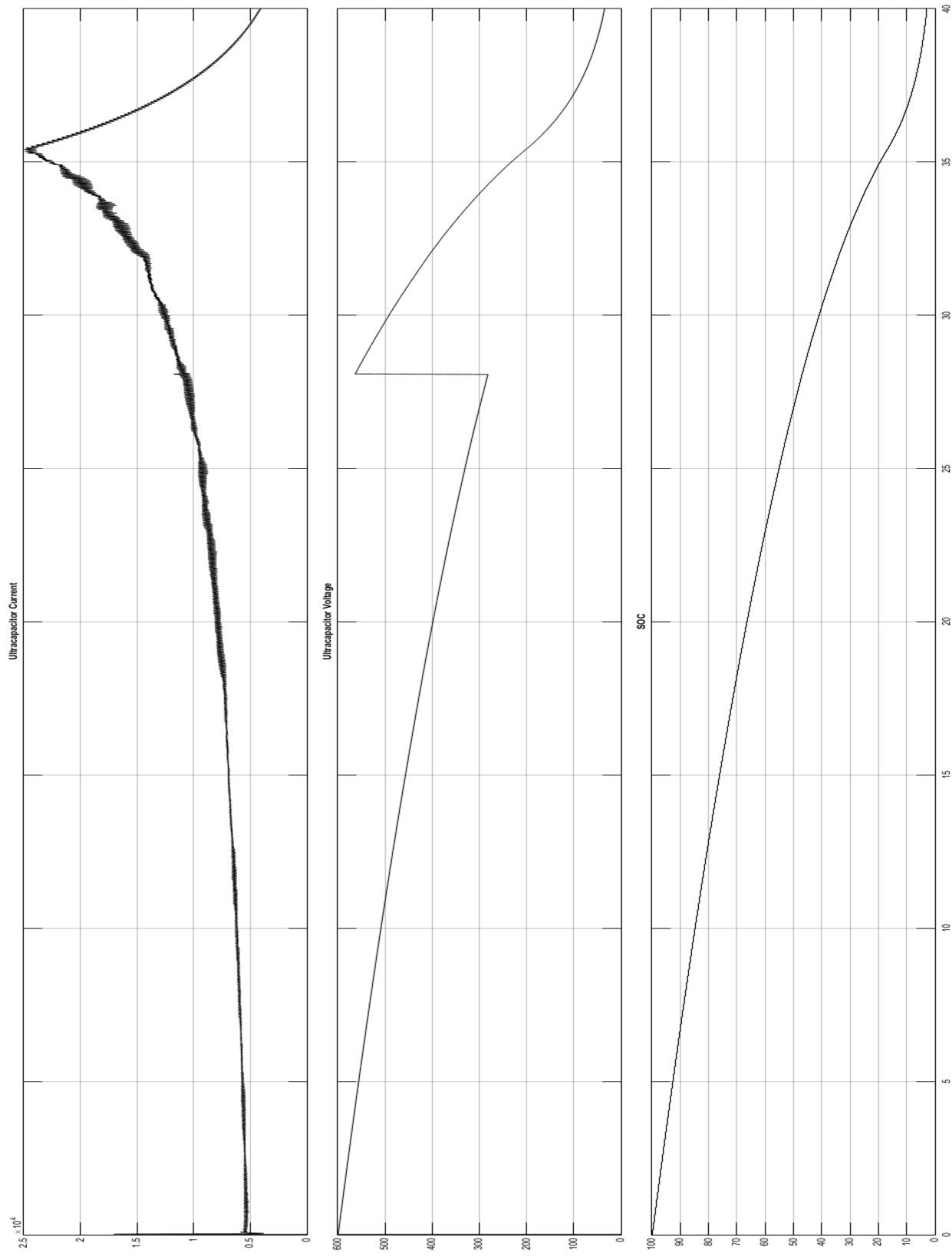
Appendix B.5: Discharge Results Powering a 5MW Static Load



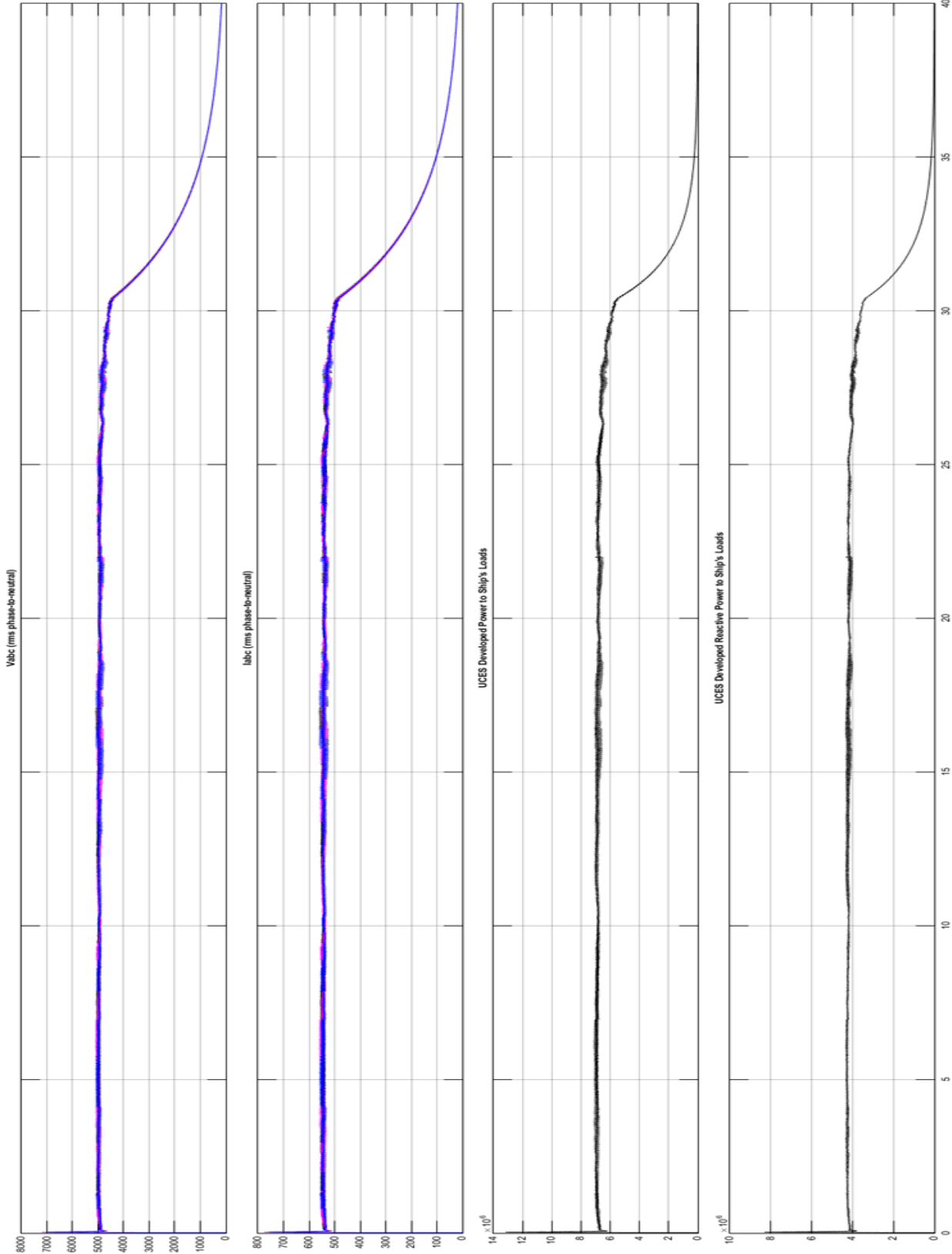


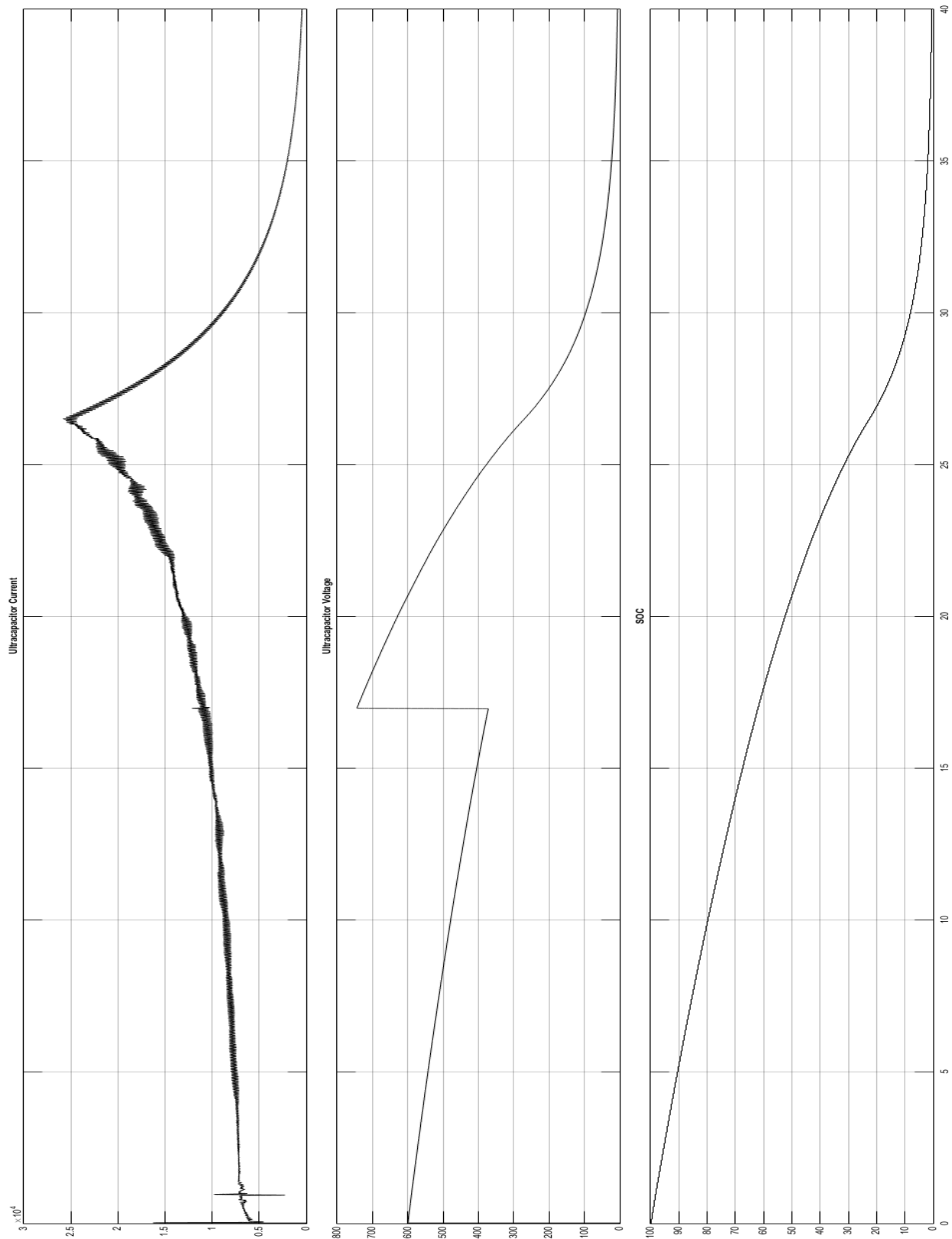
Appendix B.6: Discharge Results Powering a 6MW Static Load



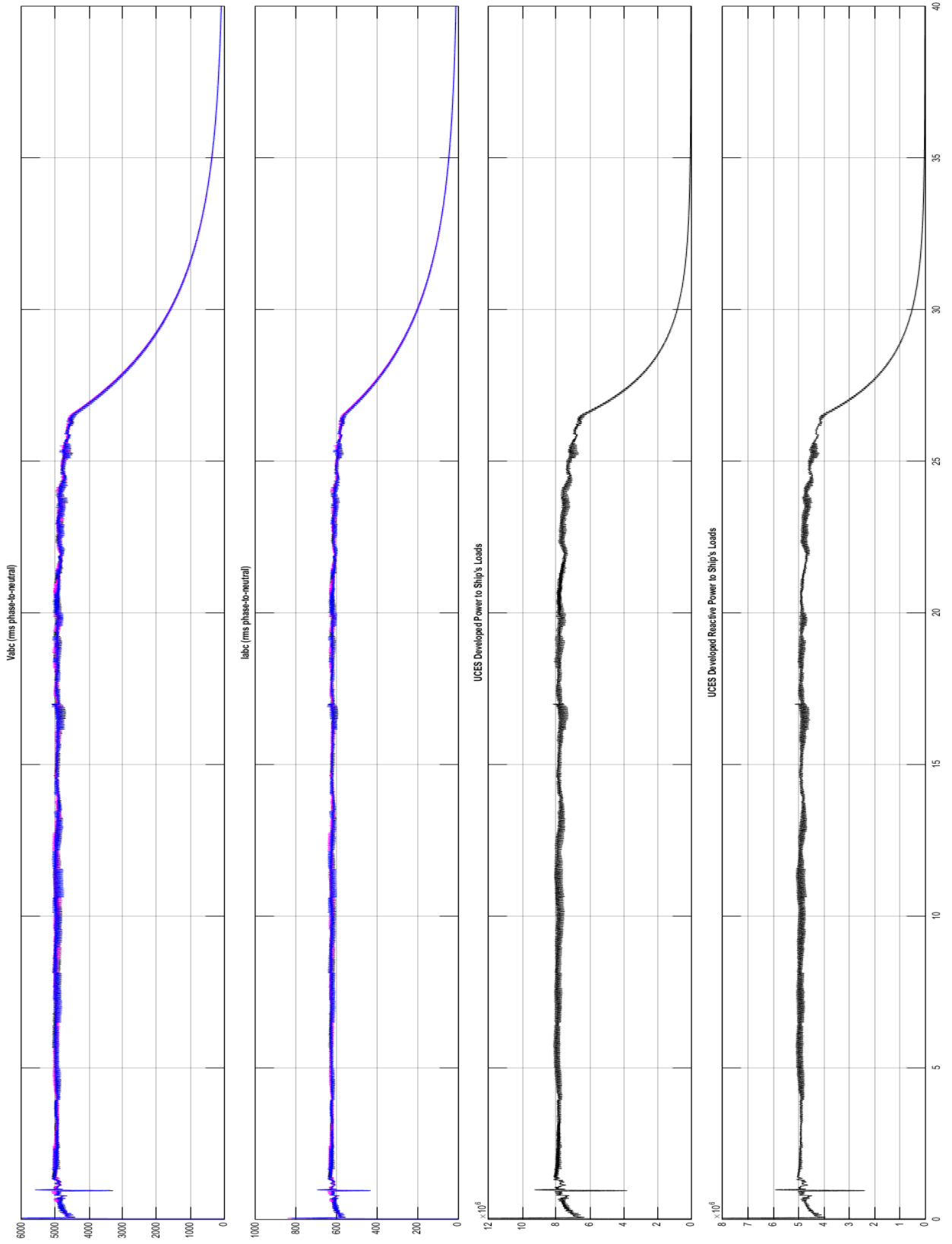


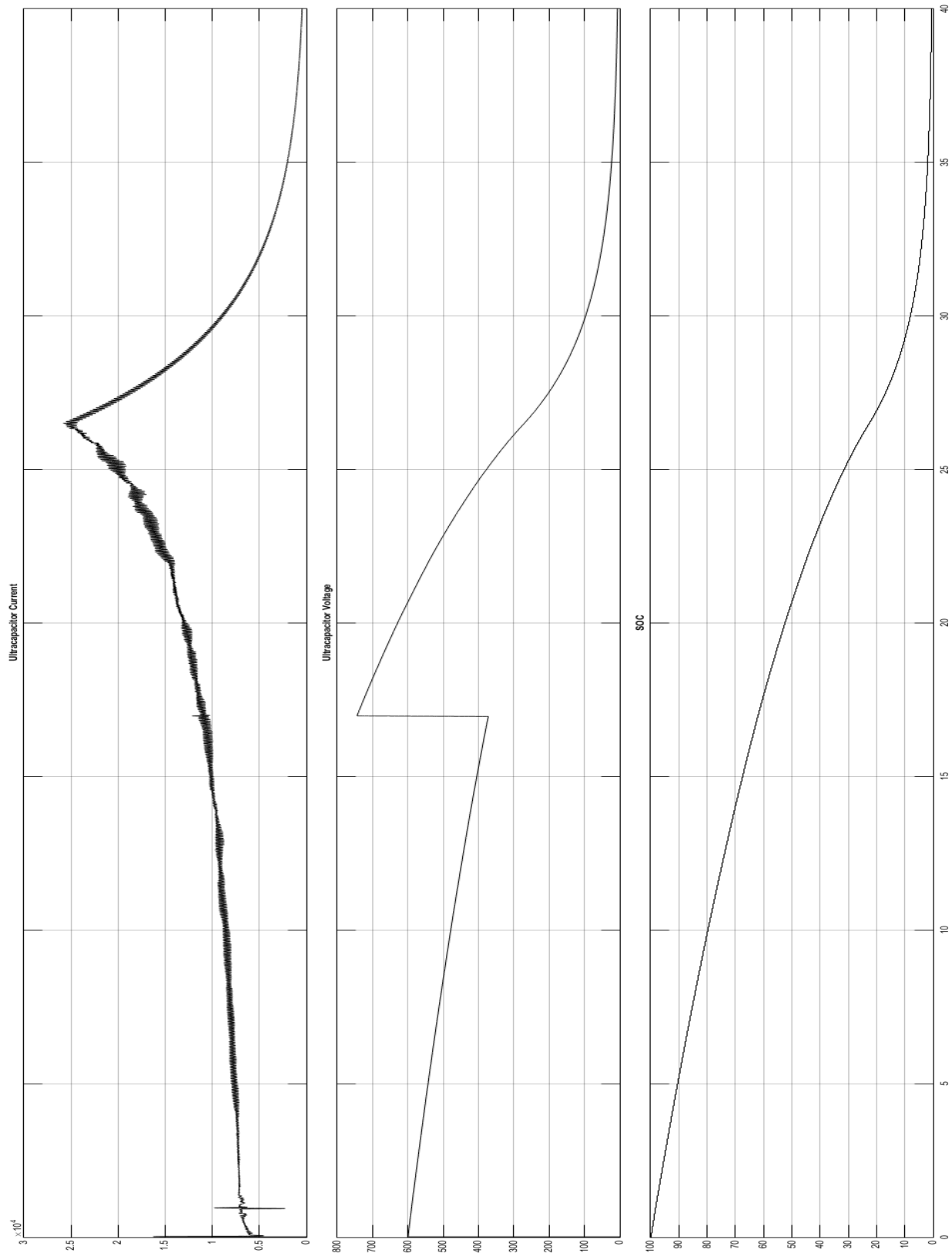
Appendix B.7: Discharge Results Powering a 7MW Static Load



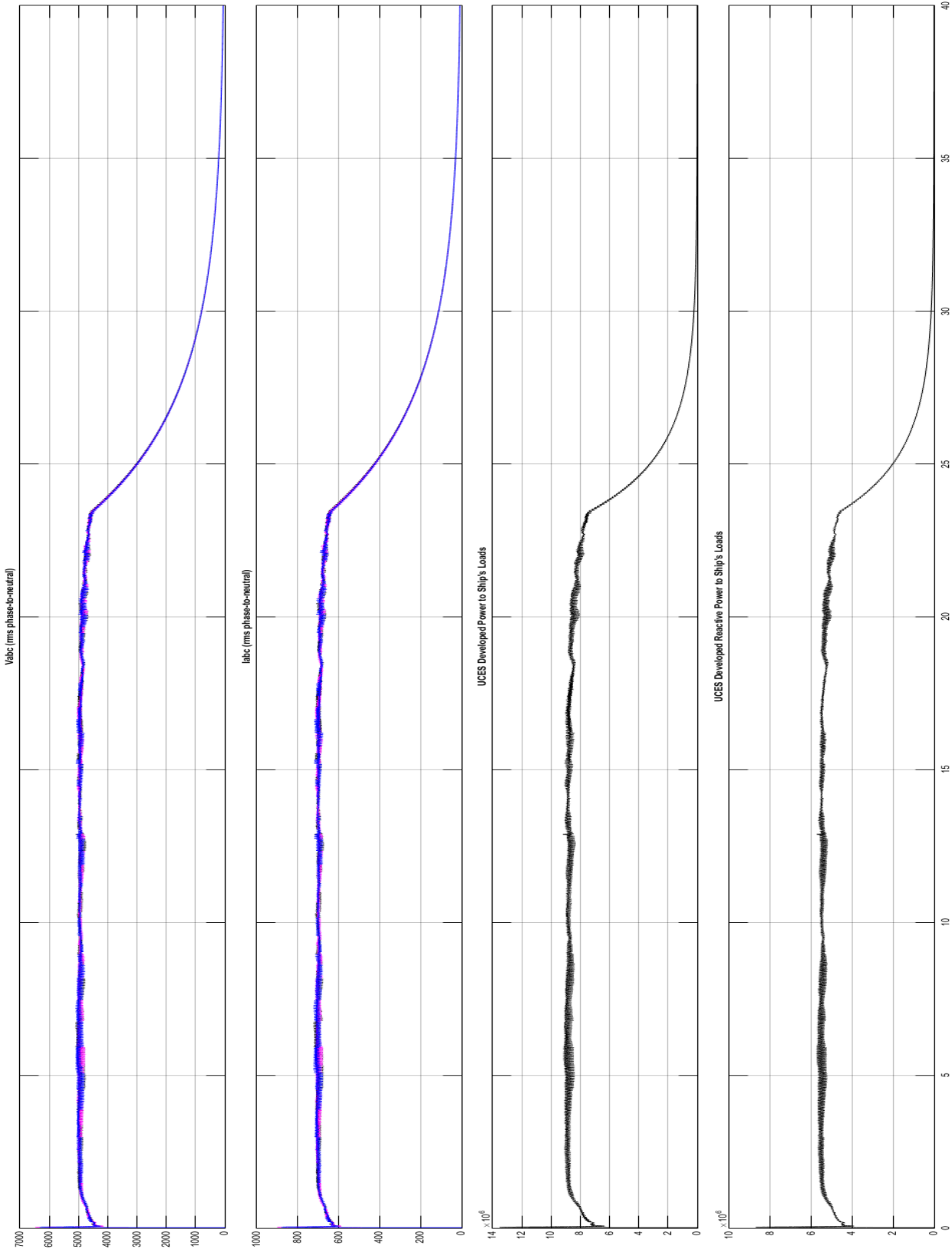


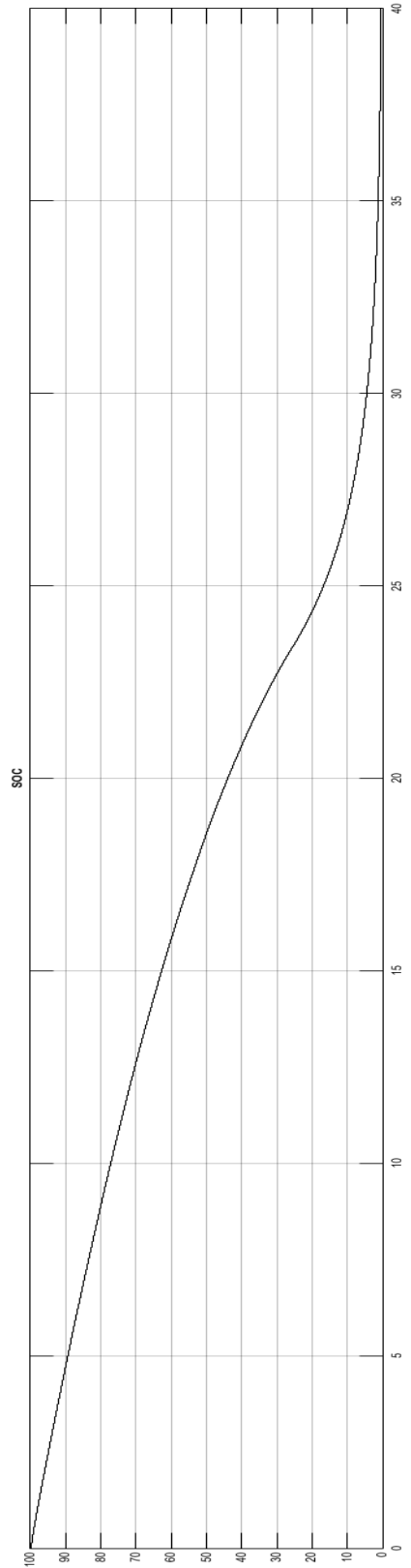
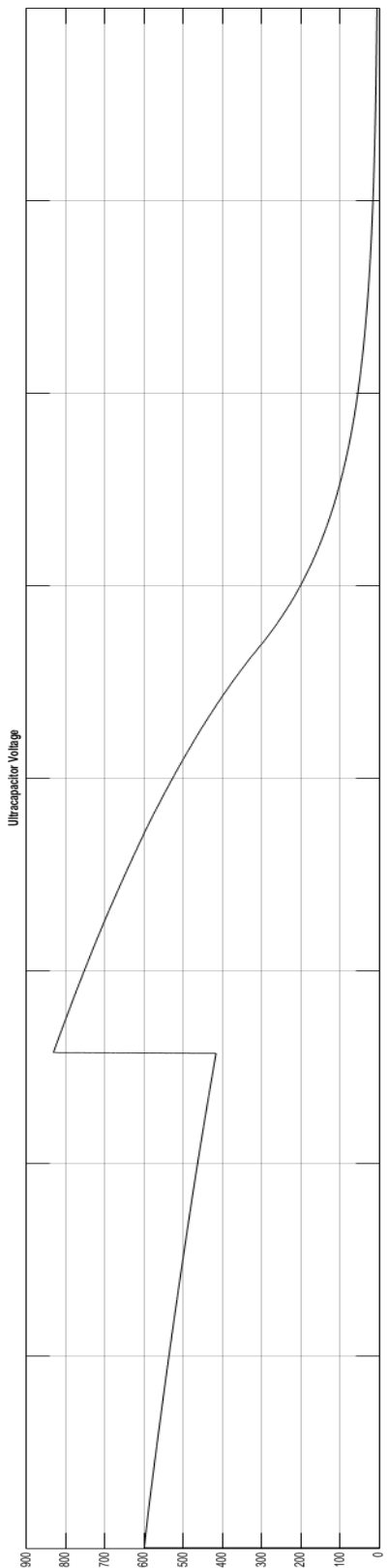
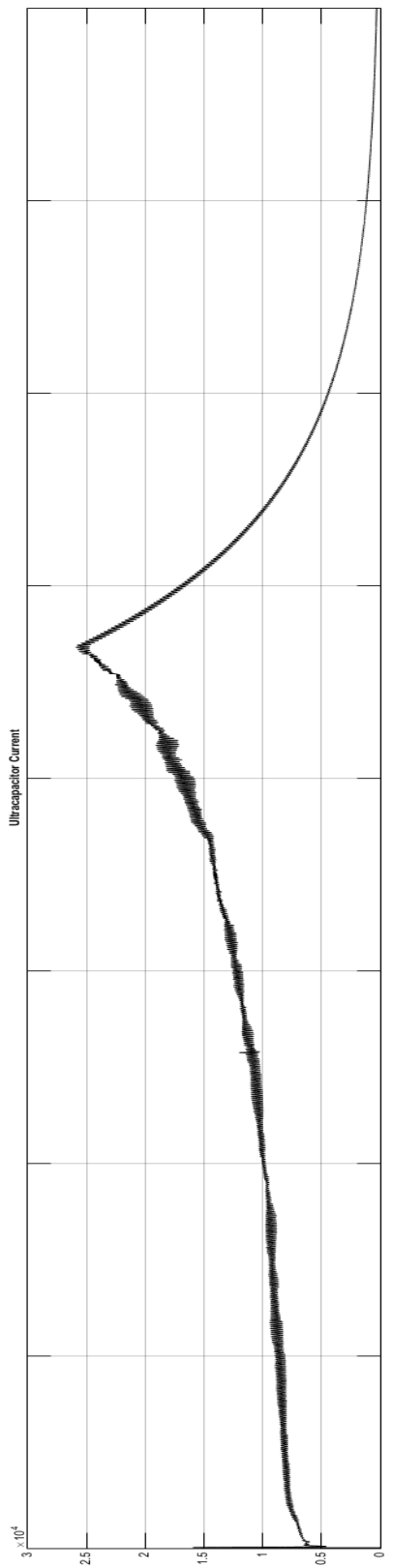
Appendix B.8: Discharge Results Powering an 8MW Static Load



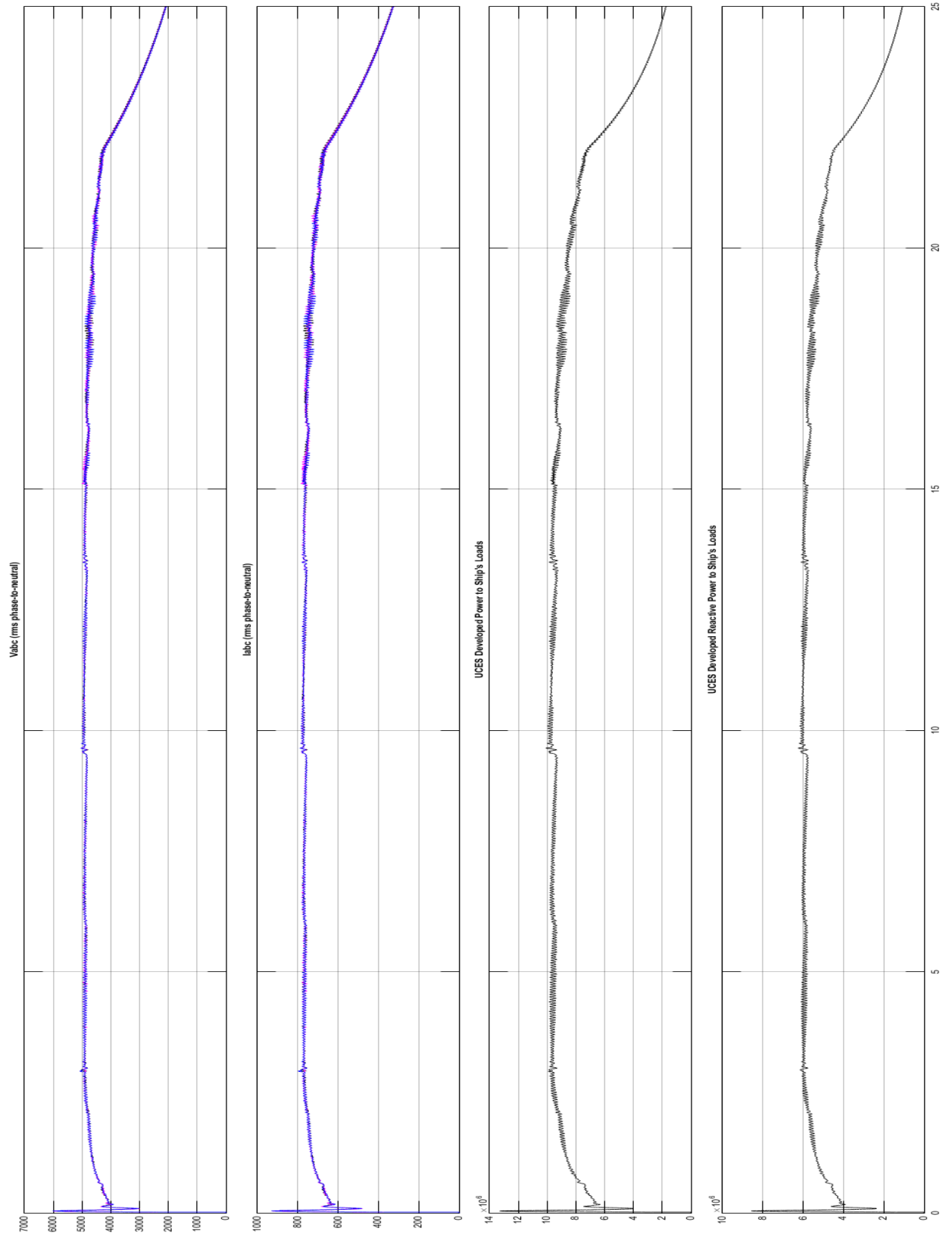


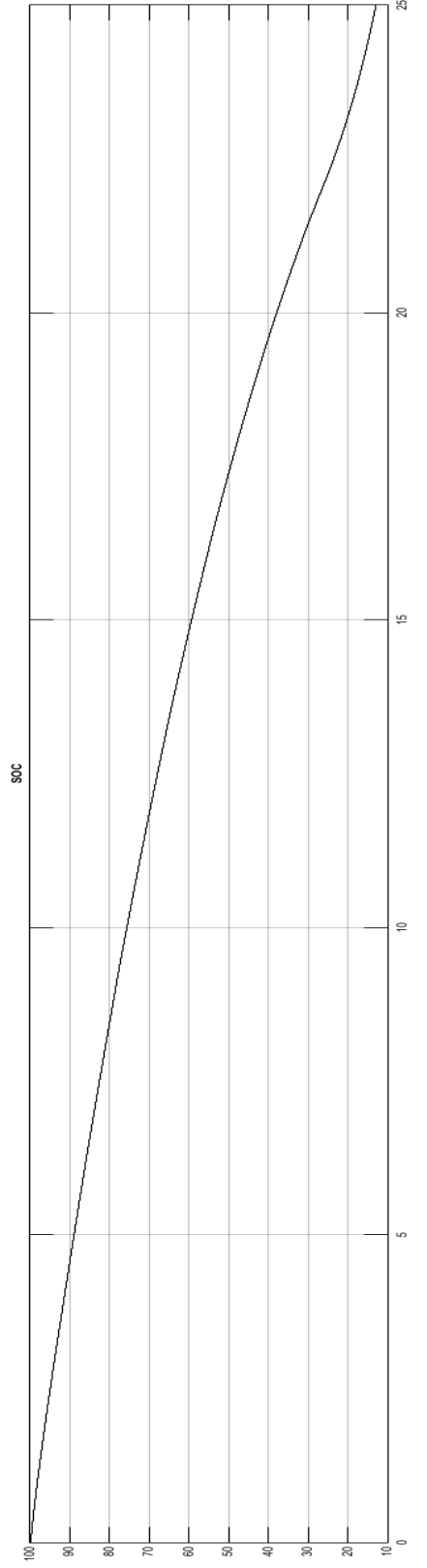
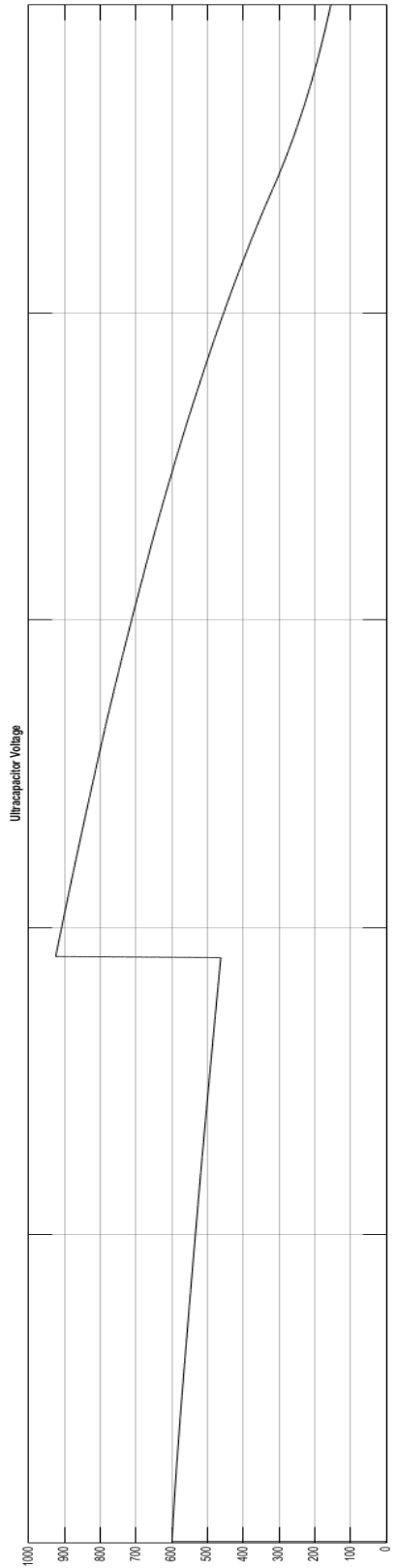
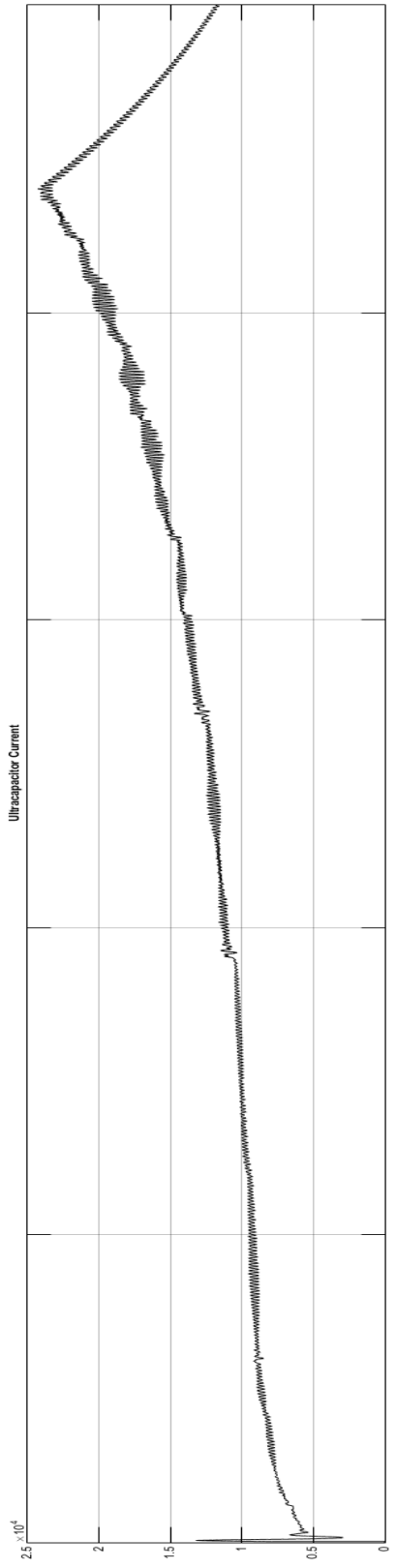
Appendix B.9: Discharge Results Powering a 9MW Static Load



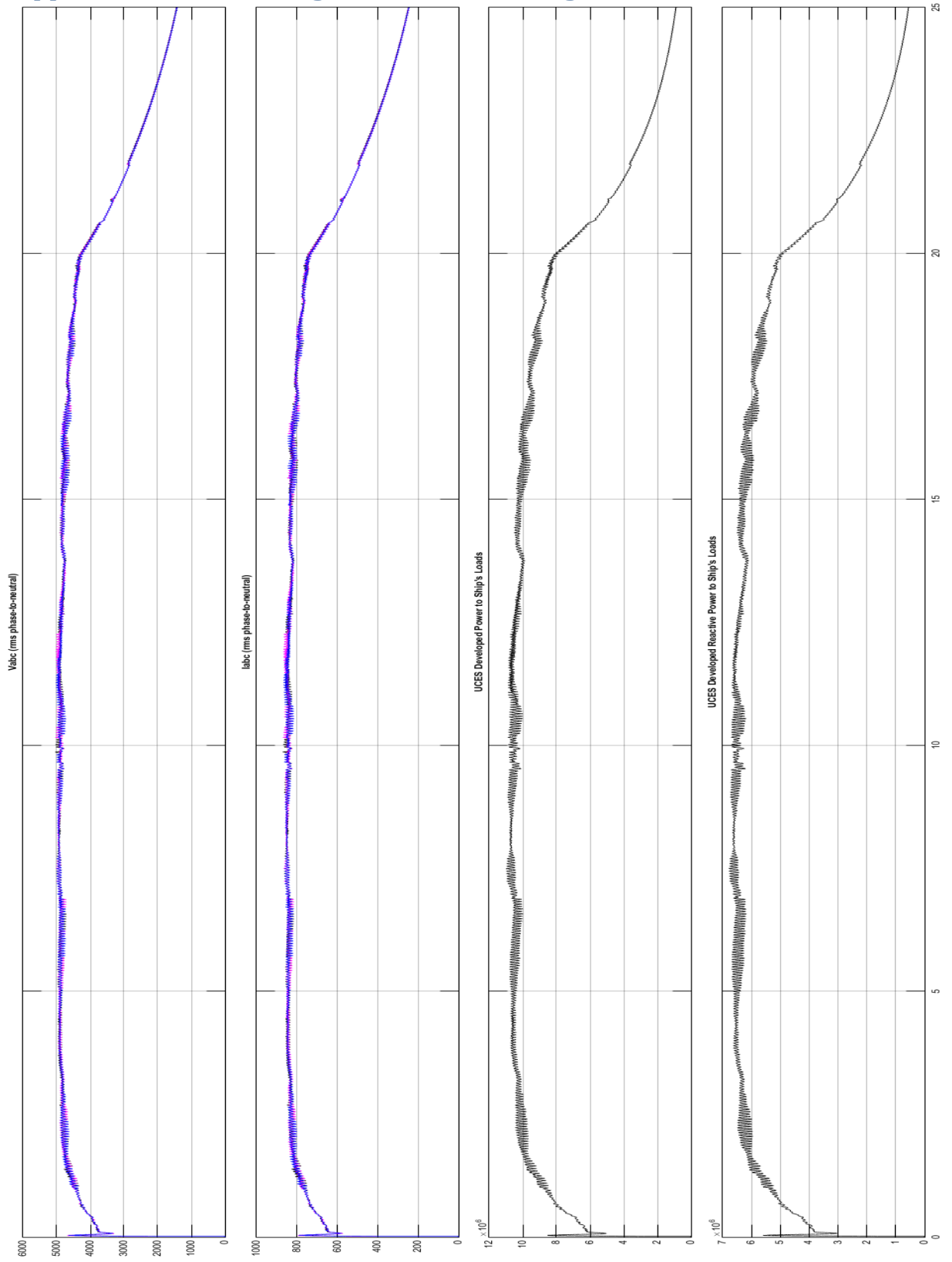


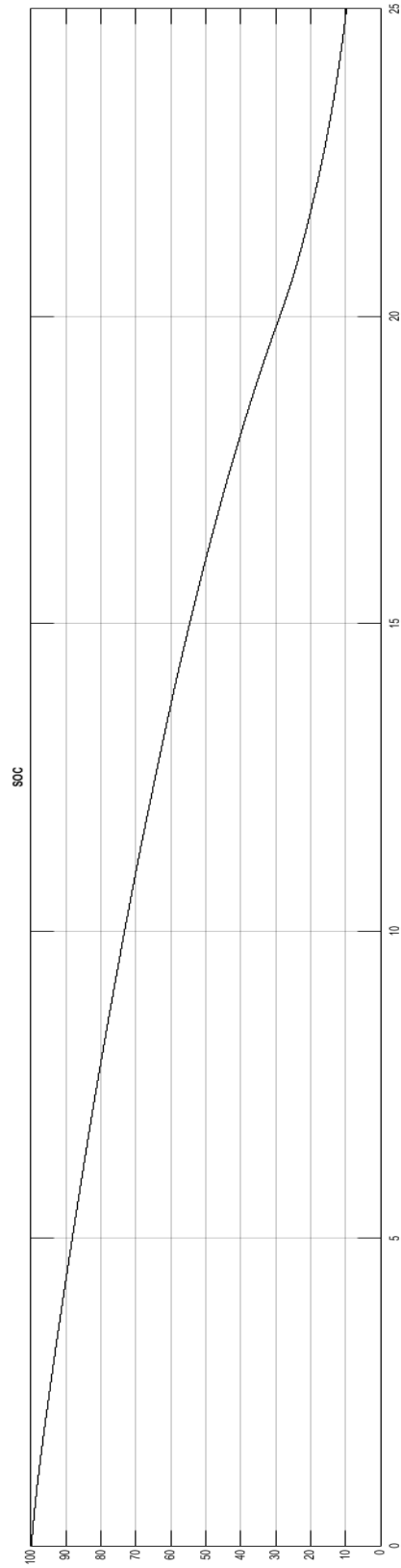
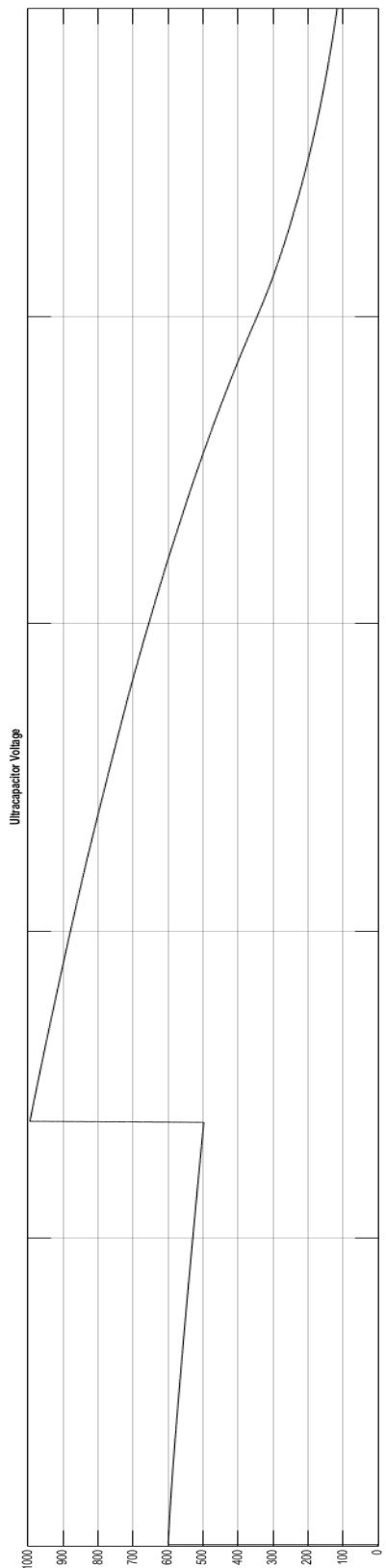
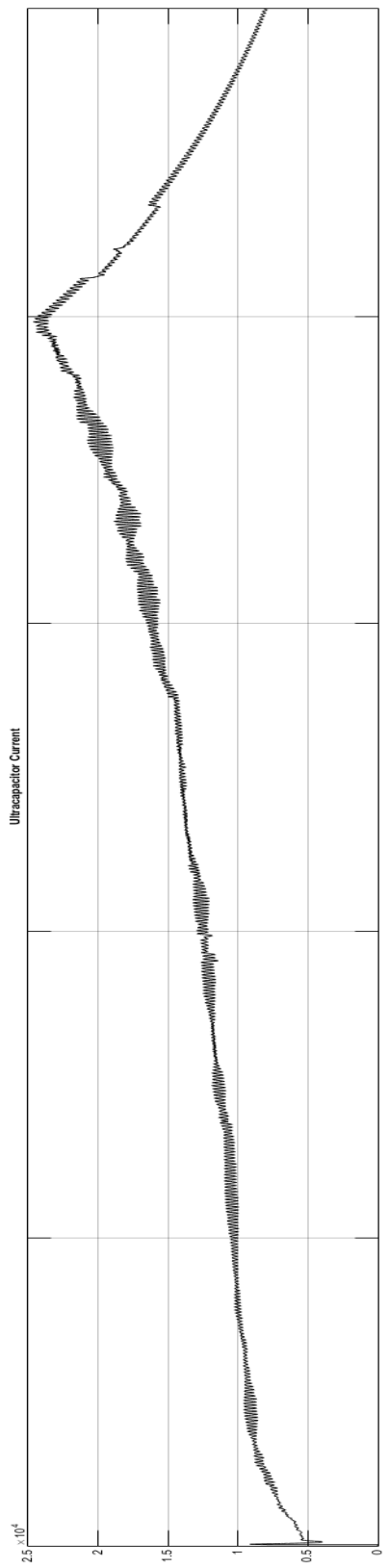
Appendix B.10: Discharge Results Powering a 10MW Static Load



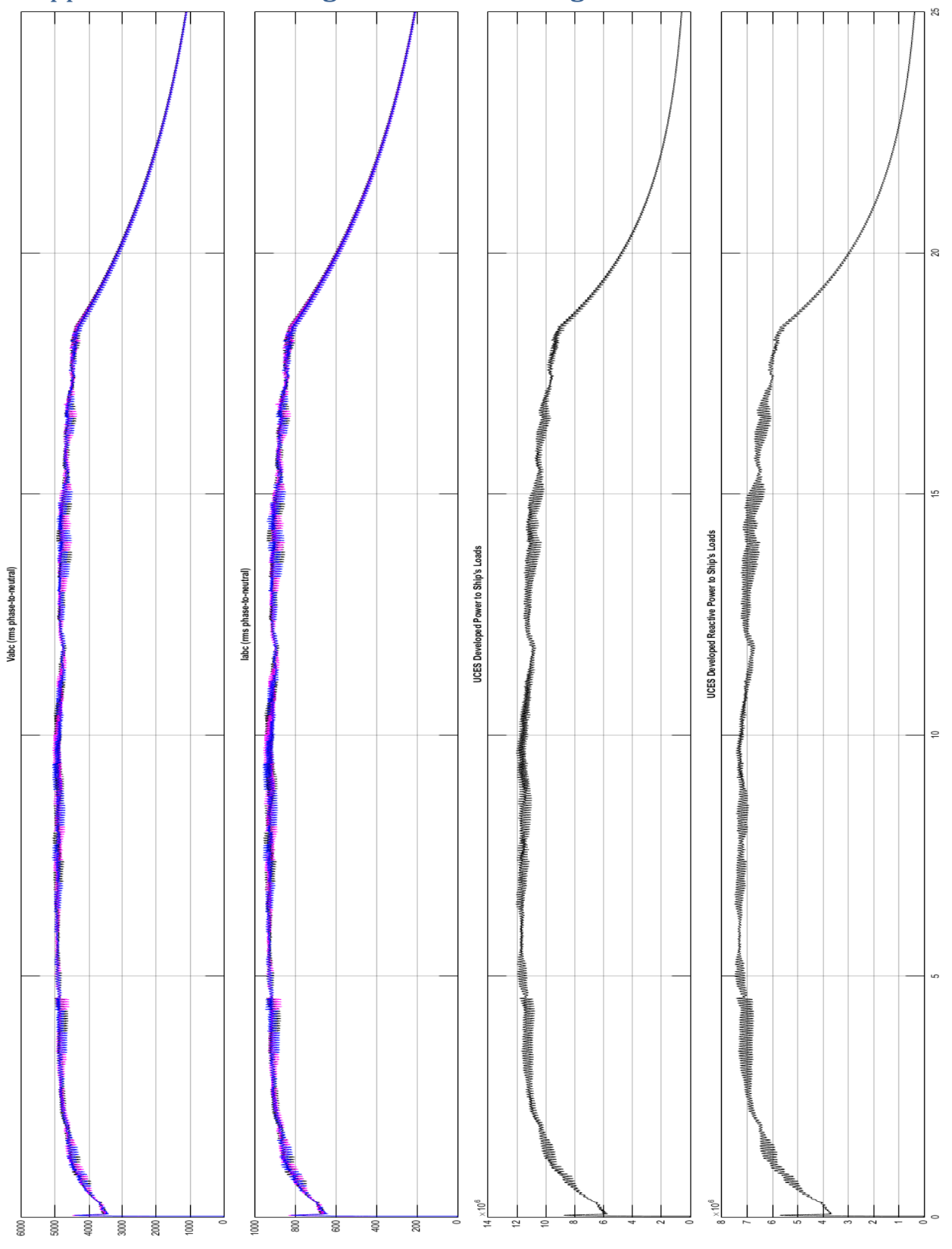


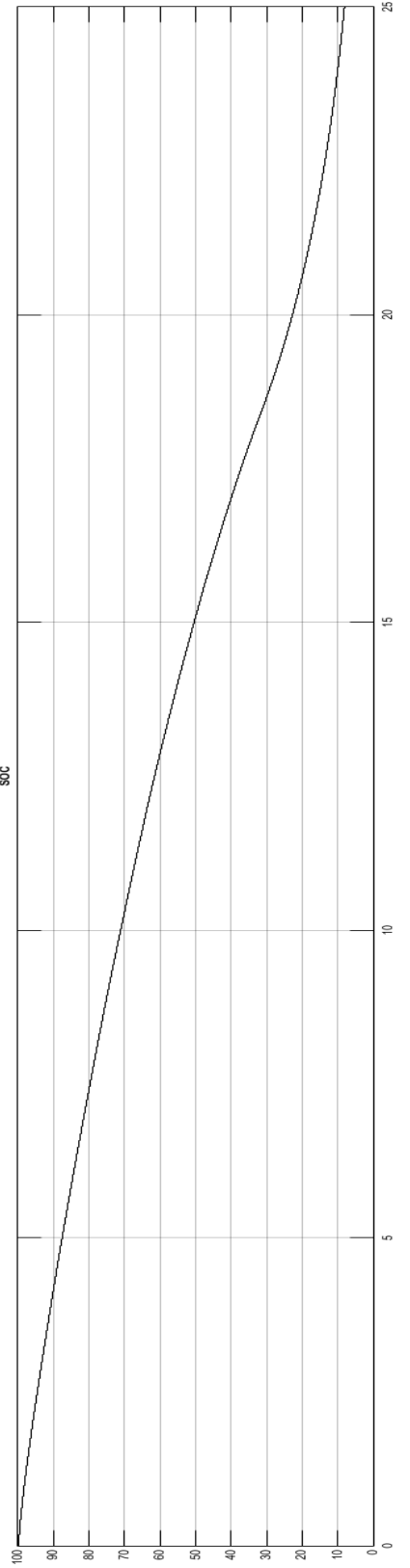
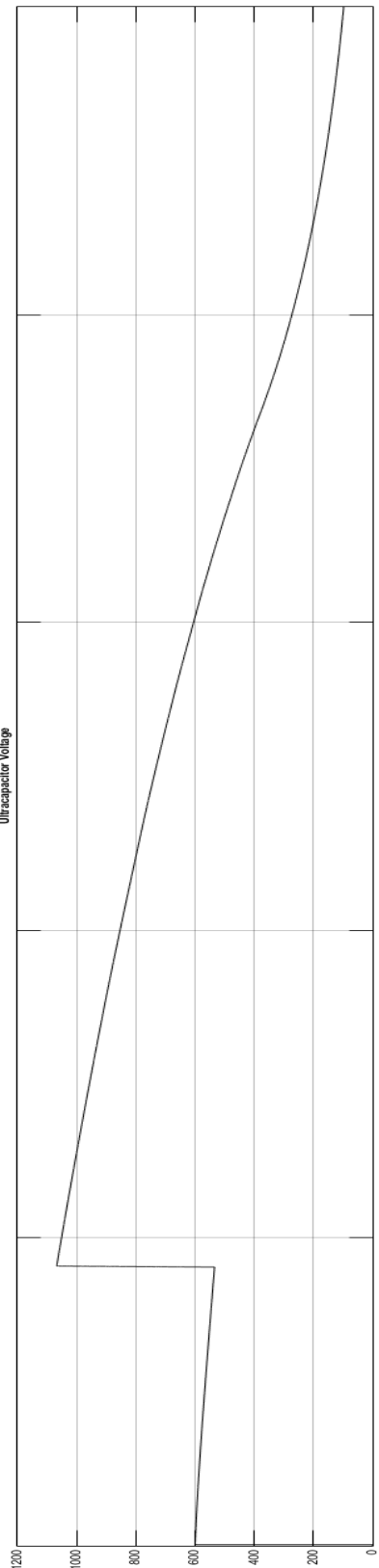
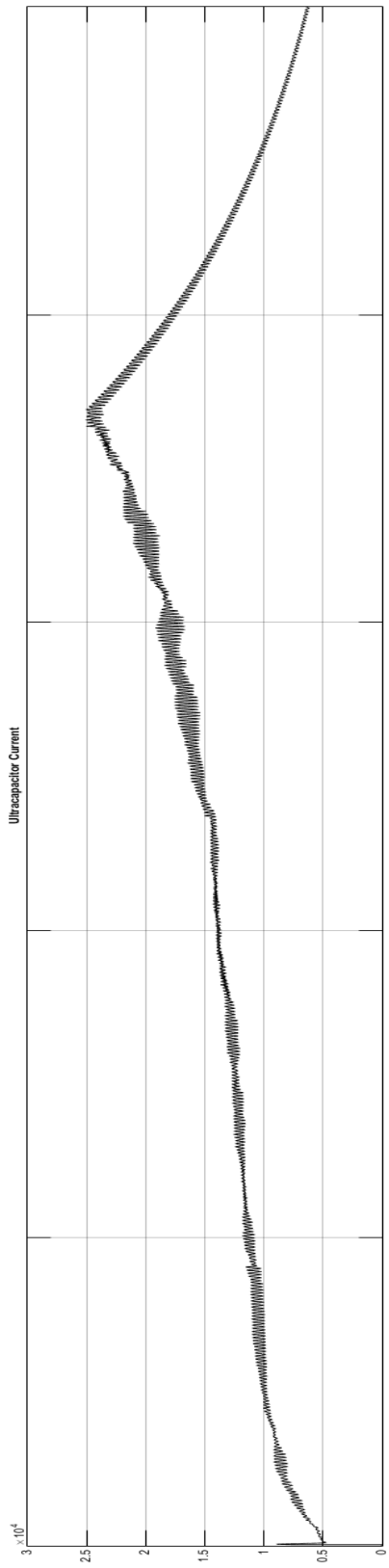
Appendix B.11: Discharge Results Powering an 11MW Static Load



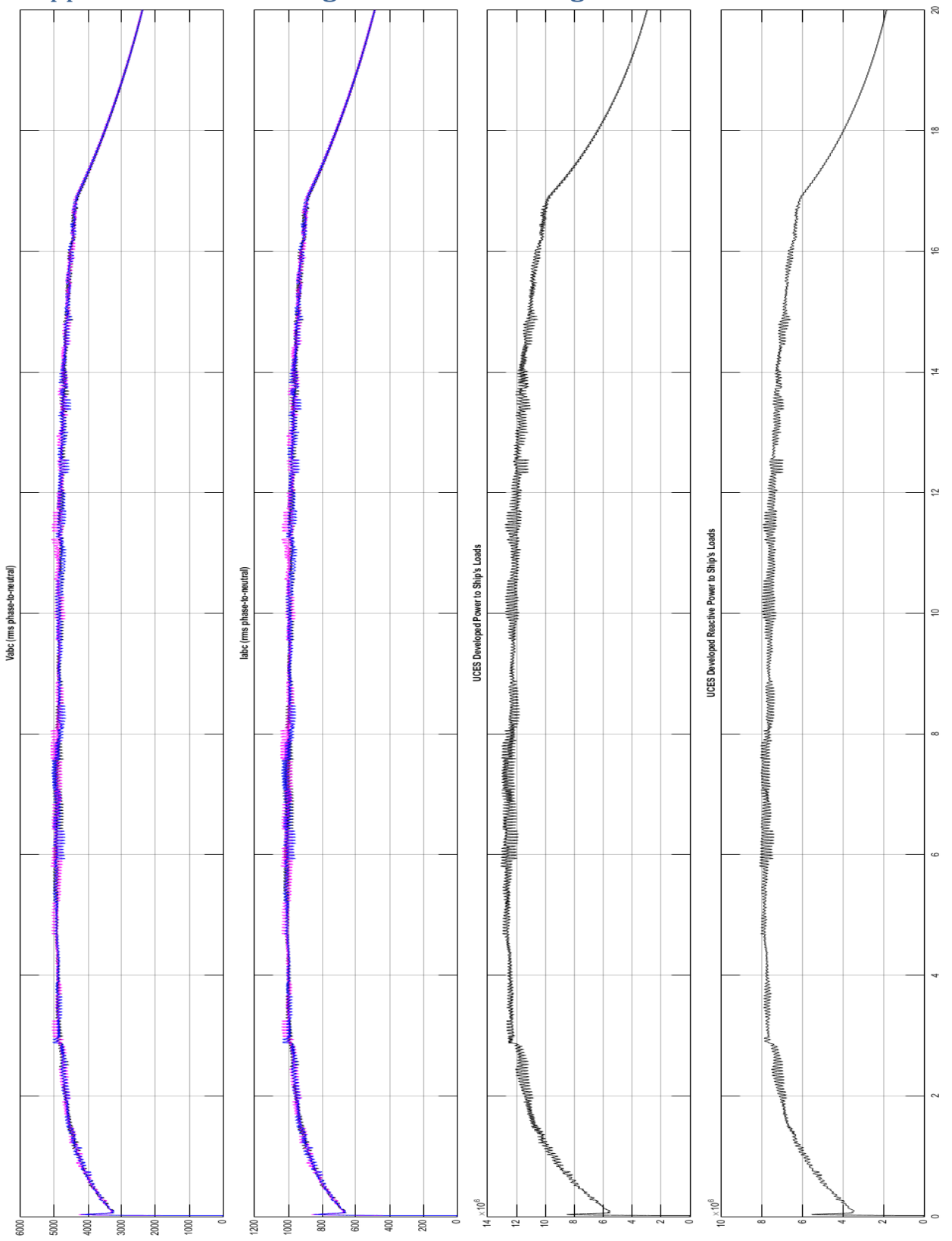


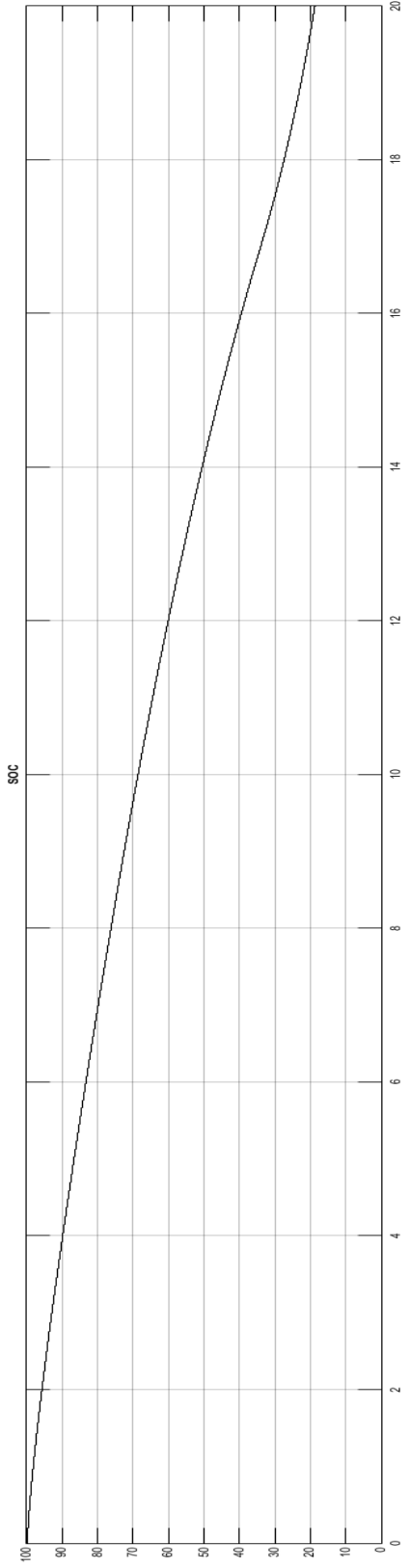
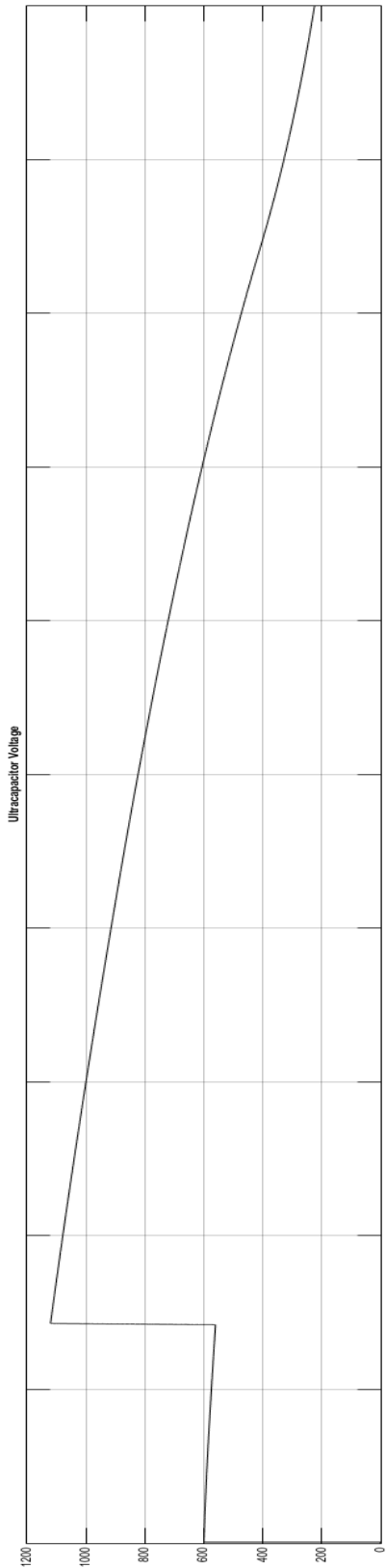
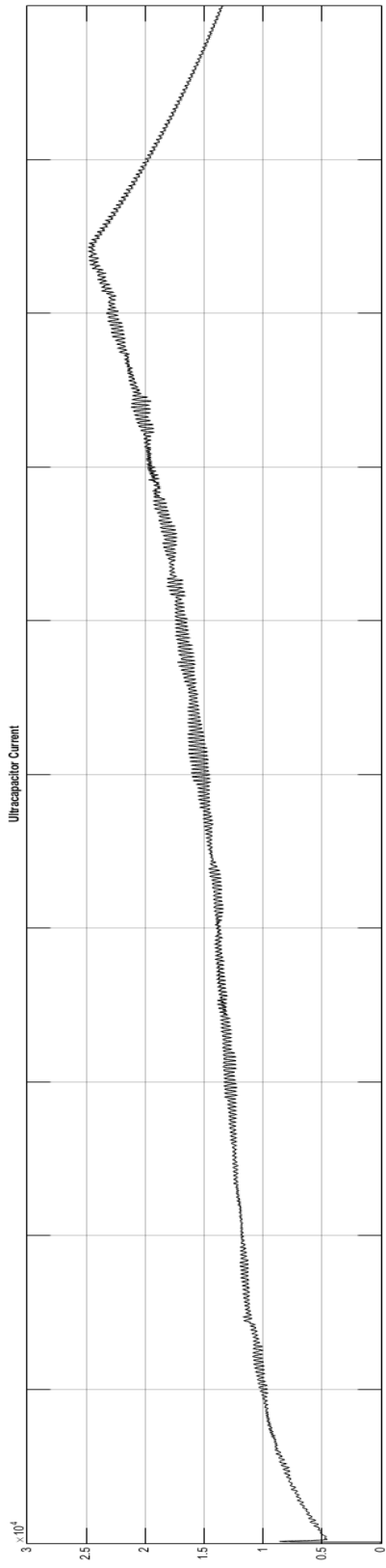
Appendix B.12: Discharge Results Powering a 12MW Static Load



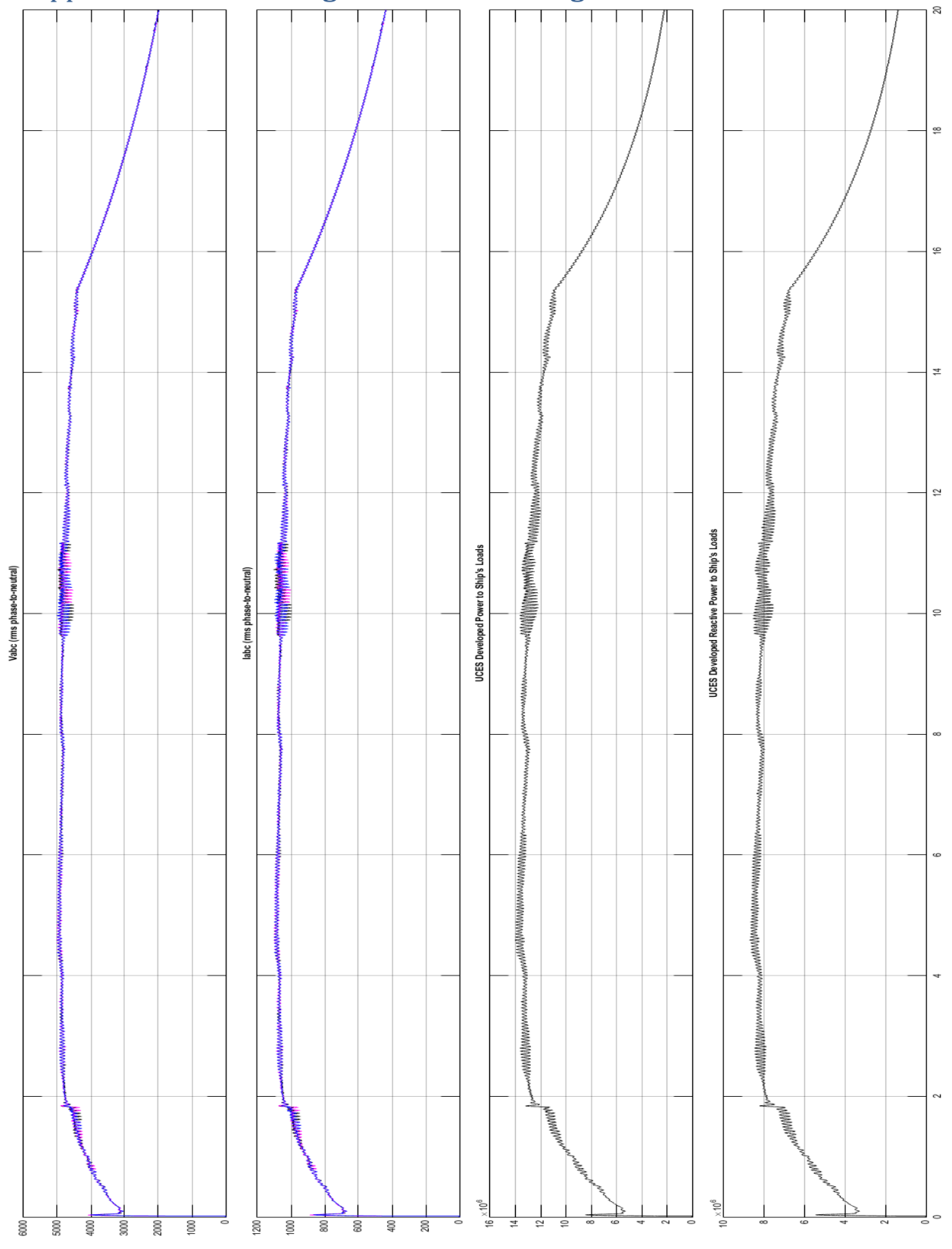


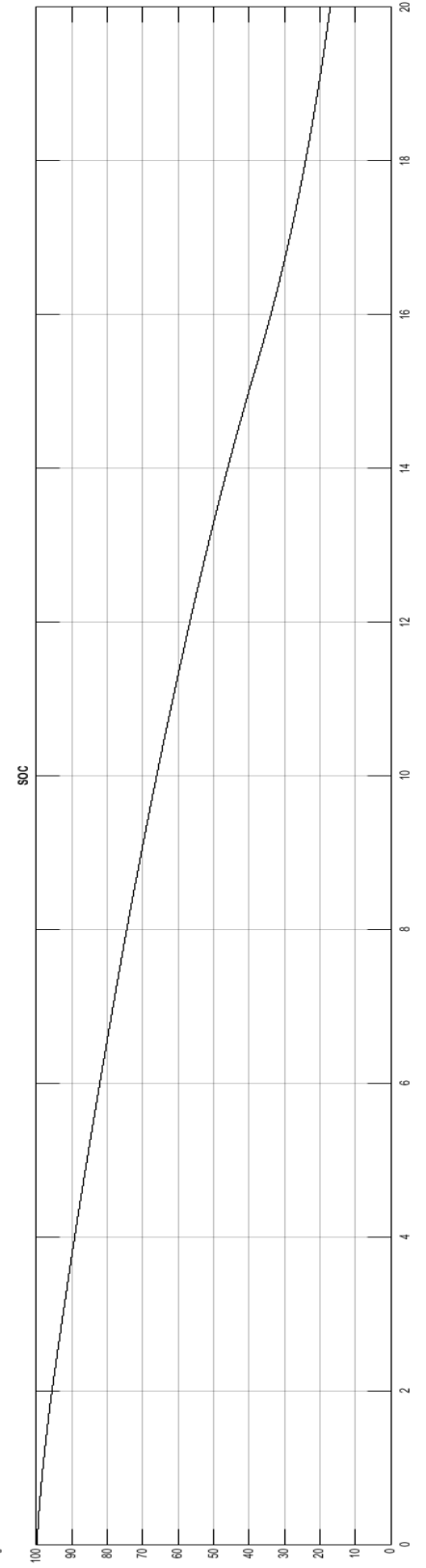
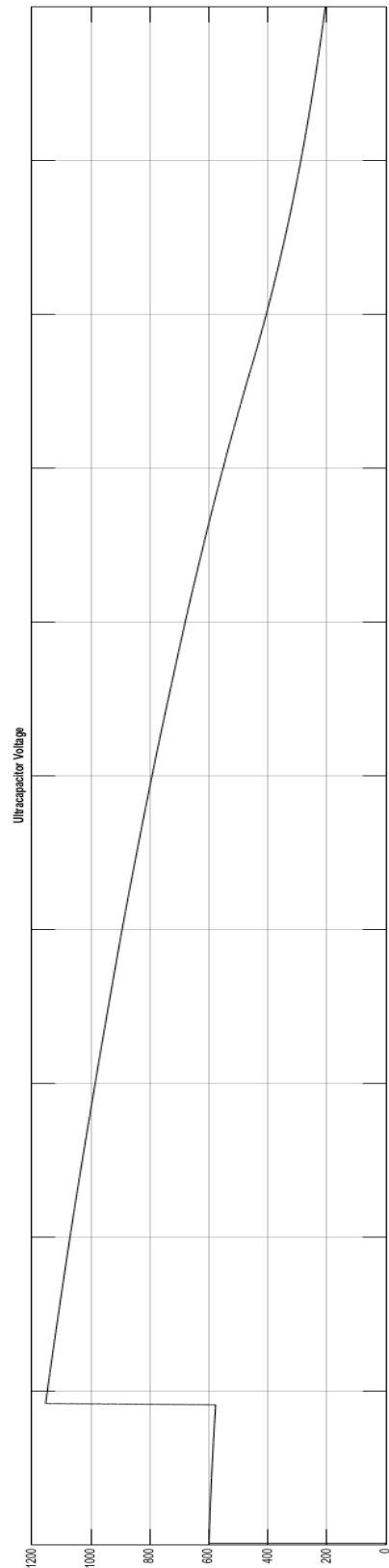
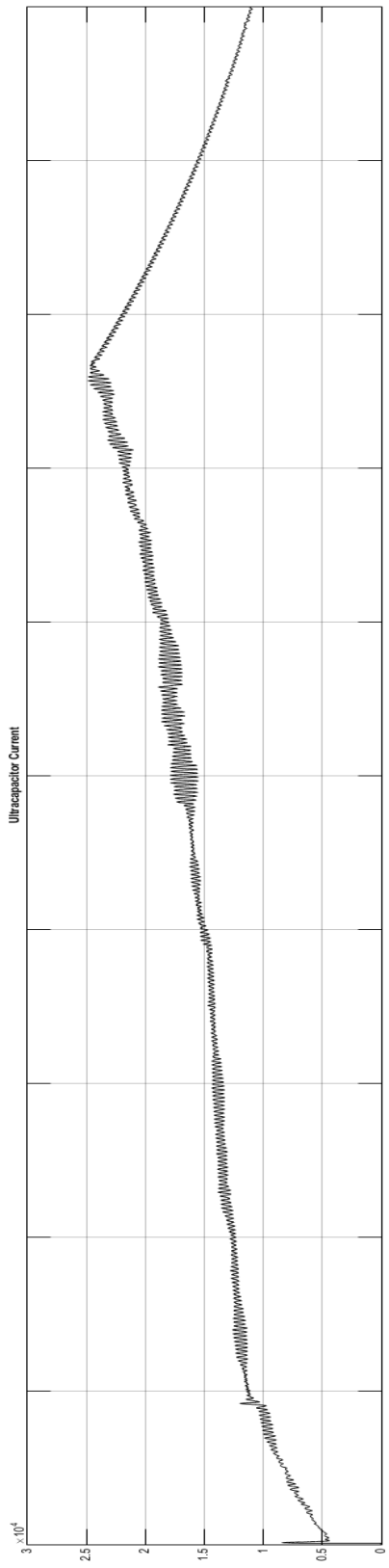
Appendix B.13: Discharge Results Powering a 13MW Static Load





Appendix B.14: Discharge Results Powering a 14MW Static Load





Appendix B.15: Discharge Results Powering a 15MW Static Load

